

**Energy-efficient low-temperature drying using  
adsorbents: a Process Systems Engineering approach**

**James Chibuzo Atuonwu**

## **Thesis committee**

### **Promotor**

Prof. Dr. Ir. G. van Straten  
Emeritus Professor of Systems and Control  
Wageningen University

### **Co-promotor**

Dr. Ir. A.J.B. van Boxtel  
Associate Professor, Biomass Refinery and Process Dynamics Group  
Wageningen University

### **Other members**

Prof. Dr. Ir. J.G.A.J. van der Vorst, Wageningen University  
Prof. Em. Ir. J. Grievink, Delft University of Technology  
Prof. Dr. Ir. A.C.P.M. Backx, Eindhoven University of Technology  
Prof. Dr. Ing. M. Peglow, Otto von Guericke University, Magdeburg, Germany

This research was conducted under the auspices of the Graduate School VLAG (Advanced studies in Food Technology, Agrobiotechnology, Nutrition and Health Sciences).

# **Energy-efficient low-temperature drying using adsorbents: a Process Systems Engineering approach**

**James Chibuzo Atuonwu**

## **Thesis**

submitted in fulfillment of the requirements for the degree of doctor  
at Wageningen University  
by the authority of the Rector Magnificus  
Prof. dr. M.J. Kropff,  
in the presence of the  
Thesis Committee appointed by the Academic Board  
to be defended in public  
on Friday 1 March 2013  
at 4 p.m. in the Aula.

**Energy-efficient low-temperature drying using adsorbents: a Process Systems Engineering approach**

James Chibuzo Atuonwu

PhD Thesis, Wageningen University, the Netherlands, 2013  
With summaries in English, Dutch and Nigerian Pidgin

ISBN: 978-94-6173-461-7

## **Dedication**

To the dream of my father

Albert Einstein: "Education is what remains after you have forgotten all you learnt in school"  
James Atuonwu: "What you learn, you may forget, but not what you do. Education is what you do!"

## **Preface**

This thesis is the result of my PhD research work at the Systems and Control Group, Wageningen University in the period January 2009 to February 2013. The work is funded by the Dutch Ministry of Economic Affairs under its Energy Research Program, Project EOSLT07043 and is part of a broader project “Energy-efficient Drying of Healthy Food Products”. Primarily concerned with developing energy-efficient drying systems using adsorbents, the thesis is divided into ten chapters with seven of them either published or submitted for publication in international journals. The main body of the thesis is divided into two broad themes: improving dryer energy efficiency (covered in Chapters 2 – 6), and analyzing controllability issues and how they affect energy efficiency (Chapters 7 – 9). Chapter 1 gives a detailed introduction to the study while Chapter 10 reflects on the major accomplishments while projecting into the future of energy-efficient drying research. The work will be useful to students, academic researchers and industrial practitioners of drying technology, energy management and systems approaches to problem solving. It is also my hope that the general public, particularly those with little technical background will find this publication useful in getting some ideas on general issues like problem solving and reporting research results without losing sight of the advances made in energy management as it relates to drying technology.

Lateral thinking is a mental superstructure optimization procedure that screens out obvious solutions



## Abstract

Drying consumes much energy due to the low energy-efficiencies of conventional dryers particularly at low temperatures required for heat-sensitive products. In this work, we aim to develop viable alternative strategies for energy-efficient low-temperature drying using adsorbents. A Process Systems Engineering approach is employed which essentially is divided in two: process optimization on the one hand and controllability analysis in relation to energy efficiency on the other. Process optimization is further divided in two: sequential, in which the drying process is first optimized independent of heat recovery possibilities and the heat recovery options explored in a second step; and simultaneous in which the process and heat recovery optimization is carried out in a single step. Both optimizations are done for single stage systems with zeolite as adsorbent and multistage systems in which adsorbent choice is not fixed but determined from a superstructure of alternatives. With the optimal one-stage system, we perform controllability analysis using classical set-point tracking and disturbance rejection controllability measures. Thereafter, a relationship is established between dryer controllability and energy efficiency by system analysis. An experimental system is then developed and tested to prove some of the concepts.

Overall, energy performance improvements of up to 65% are recorded compared to equivalent conventional systems at the same drying temperatures, representing a significant step ahead in process sustainability. In addition, various design and operational insights are deduced from the work. They include optimal operational strategies in single and multistage systems, adsorbent sequencing in multistage systems, optimal adsorbent properties for selection in energy-efficient drying applications and new process control input options as compared to conventional dryers. Other achievements are the establishment of a relationship between dryer energy efficiency and controllability, analysis of the effects of the adsorbent system on this relationship, derivation of a condition for energy efficiency improvement by incorporating desiccant dehumidifiers, and the assessment of effects of heat losses.

In view of the demonstrated potential of Process Systems Engineering approaches in improving system performance while providing useful insights, we recommend that the same be applied to the general class of drying systems known as “hybrid dryers” of which multistage adsorption dehumidification drying is just one representative.

Problem solving essentially involves designing appropriate control actions to minimize the difference between currently observed or predicted future realities and desired goals

## Table of Contents

Dedication .....	v
Preface.....	vii
Abstract.....	ix
<b>Chapter 1</b> Energy-efficient low-temperature drying: a challenge for innovative process design .....	1
<b>Chapter 2</b> Model-based energy efficiency optimization of a low-temperature adsorption dryer .....	9
<b>Chapter 3</b> Improving adsorption dryer energy efficiency by simultaneous optimization and heat integration.....	27
<b>Chapter 4</b> A mixed integer formulation for energy efficient multistage adsorption dryer design.....	47
<b>Chapter 5</b> Simultaneous superstructure optimization and heat integration of multi-stage adsorption dryers .....	65
<b>Chapter 6</b> Synergistic process design: reducing drying energy consumption by optimal adsorbent selection.....	71
<b>Chapter 7</b> On the controllability and energy sensitivity of heat-integrated desiccant adsorption dryers.....	87
<b>Chapter 8</b> Improving dryer controllability and energy efficiency simultaneously by process modification .....	111
<b>Chapter 9</b> On dryer controllability and energy performance: generalized modeling and experimental validation.....	125
<b>Chapter 10</b> Reducing drying energy consumption using adsorbents: reflections and outlook .....	141
References.....	147
Nomenclature .....	157
Appendices.....	159
Summary .....	165
Samenvatting.....	169
Tori sharp sharp for dis akada work .....	173
Acknowledgements.....	177
About the author .....	179
List of Publications .....	181
Overview of Completed Training Activities.....	183



# Chapter 1

## **Energy-efficient low-temperature drying: a challenge for innovative process design**

### **1.1. Energy efficient low-temperature drying: the need for innovative design and operation**

Foods in their natural state generally contain water which promotes microbial growth and spoilage over time. The same goes for other raw materials and semi-finished products in various application domains like the pharmaceuticals, chemicals, pulp and paper, textiles, wood, just to mention but a few. Drying, the process of removing excess water is thus an important preservation technique which at present is gaining increasing relevance. In the food industry for instance, a market survey covering about 62 countries of the world and conducted between 2004-2009 reveals an annual global dried food market growth rate of about 3.6% (MarketResearch.com, 2012). This trend is expected to be maintained or even accelerated in the coming years.

Apart from improved shelf-life, dried products are characterized by reduced weight for easier packaging and transportation, improved consumer convenience, and in some cases like in the food industry, enhanced flavour and appearance compared to their fresh counterparts. These products are usually heat-sensitive. Hence, drying, which in most cases involves thermal treatment, is characterized by a wide variety of degradation reactions which affect quality attributes like sensory characteristics and nutritional value. The requirement to supply the latent heat of evaporation of water, heat losses and product heating make the process energy-intensive. As a result, drying contributes about 15% of industrial energy consumption in general (Kemp, 2005) and 10% of energy used in the food industry (Mujumdar, 1997), significantly affecting operating costs and environmental impact. For process sustainability therefore, drying systems must be designed and operated to satisfy quality requirements with reduced energy consumption per unit mass of water evaporated. This becomes more necessary with the rising energy costs, demand for energy with increasing global population and more stringent environmental regulations. Little wonder, energy efficiency and product quality have been identified as the main research and development drivers in drying technology as a result of which over 400 dryer types have been developed (Mujumdar, 2004). In spite of these developments, the energy efficiency of most dryers in operation is still low especially when drying conditions are made mild to reduce the effects of thermal degradation. Typically, dryer energy efficiencies range from 20-60% (Mujumdar, 2007a) where energy efficiency is defined as the ratio of the latent heat of evaporated water to the total heat input to the drying system. With the rising energy prices, more stringent environmental regulations and increasing consumer demand for quality products, the question arises: “how can the energy

efficiency of existing dryers be improved while satisfying product quality requirements?”. A related question is “what novel system design configurations and drying operational strategies can be introduced for improved energy efficiency while satisfying product quality requirements?”. Broadly speaking, this thesis aims at answering these questions using dehumidification technology based on zeolite and other adsorbents, process integration, optimization and control as tools.

## **1.2. Historical developments and research gaps**

Drying, as a unit operation of pre-historic origins has undergone many developments over time. An exhaustive review is beyond the scope of this work. However, comprehensive reviews of more recent developments can be found elsewhere (Mujumdar, 2007b; Kudra and Mujumdar, 2009). In terms of energy efficiency and obtaining good product quality, developments have been largely evolutionary in nature (Mujumdar, 2004). Ground-breaking solutions in energy efficient drying have been relatively scarce and improvements tend to approach a saturation level (Djaeni et al., 2007a). In general, for drying processes, the use of low-grade, low-cost primary energy sources is encouraged. For any given energy source, the effectiveness of energy utilization holds the key to improving system performance. This work focuses on improving the efficiency of energy utilization in drying for any appropriate primary energy source while satisfying drying requirements. In terms of product quality, freeze drying which has existed for quite some time is still the industry-standard. Minor developments in this technology have occurred since the first related US patent was issued nearly nine decades ago (Tival, 1927). Radio-frequency drying and the closely-related microwave drying whose first application dates back to the 1930s (Puschner, 1964) are also widely regarded as good techniques for high-value products since they ensure volumetric heating and fast drying while limiting product shrinkage. However, the energy costs are high and overall efficiencies low. A relatively recent development, superheated steam drying has high energy saving potentials especially when the exhaust steam is reused and integrated with surrounding processes (van Deventer and Heijmans, 2001). For product quality, the absence of oxygen makes the technology promising but it is unsuitable for heat-sensitive products since the temperatures involved are high. Moreover, it is a complex process. Due to the limitations described in the foregoing, most non-convective air dryers are yet to make significant inroads in industry.

At present, convective air dryers make up over 85% of industrial dryers (Mujumdar, 2007a). This dominance is expected to remain so, far into the foreseeable future. Hence, any technology that reduces the energy consumption of existing and would-be convective dryers would impact significantly on overall drying energy consumption reduction. However, compared to technologies like freeze drying, convective air dryers usually are characterized by inferior quality attributes due to thermal degradation (Ratti, 2001). The main strategy for reducing thermal degradation is to

limit drying temperatures. However, low-temperature drying is also synonymous with low energy efficiency for systems with high throughput per unit volume (excluding systems like open air solar dryers). Hence, the search for improved technologies that yield energy efficient performance at low drying temperatures becomes an interesting challenge. Heat integration by recycling portions of dryer exhaust heat and/or using the exhaust air to preheat the inlet via heat exchangers have been shown to improve energy performance of convective dryers (Strumillo et al., 1995; Moraitis and Akiritidis, 1997; Krokida and Bisharat, 2004; Laurijssen, 2010; Atkins and Walmsley, 2010). However, since the drying process in itself is limited by a thermodynamic barrier - the requirement to supply at least the latent heat of vaporization of the water evaporated and due to limitations in heat recovery particularly for low temperature drying, improvements might not be significant. Kemp (2005) by pinch analysis showed the heat-recovery limitations of low-temperature dryers. Usually, only a small portion of the exhaust air sensible heat can be economically recovered while all the latent heat is lost. In view of these issues, the use of process integration to reduce energy consumption is gaining increasing prominence. In its broadest form, this usually involves combining the basic conventional dryer with complementary unit operation(s) or some other dryer type(s) and then performing heat integration where possible. The technique forms part of an active research field known as hybrid drying which is foreseen to make significant progress in industrial drying this decade (Mujumdar, 2007b).

Various hybrid drying technologies are currently in different stages of development. Examples include the infra-red, radio-frequency and microwave-assisted convective dryers (reviewed in Raghavan, et al., 2005) with microwave-assisted freeze dryers (Duan et al., 2010) and infra-red-assisted freeze dryers (Chakraborty et al., 2011) developed mainly to enhance drying speed and quality. Others are the dehumidification-based strategies like heat pump drying, a variant of which is the chemical heat pump drying (Ogura and Mujumdar, 2000; Ogura et al., 2003), and desiccant adsorption dehumidified air drying (Djaeni et al., 2007a; Djaeni et al., 2007b). There is also multistage drying using either the same or different dryer types per-stage (Spets and Ahtilla, 2004; Menshutina et al., 2004; Namsanguan et al., 2004; Djaeni et al., 2009a). Intermittent drying involving time-varying process conditions for batch drying or different drying conditions per stage or pass of a multistage or multi-pass continuous system (Islam et al., 2003) could also be seen as an example of a hybrid system capable of improving energy performance and quality. Here, although the equipment is uniform, the system is hybrid in operation. Combining heating modes like conductive-convective-radiative drying is another hybrid drying method currently in use. In some cases, some of the hybrid dryer types are again combined to form new hybrid systems. Instances include heat pump-assisted microwave drying (Jia, 1993), multistage heat pump drying (Alves-Filho et al., 2008), adsorbent-assisted atmospheric freeze drying with multimode heat input (Rahman and Mujumdar, 2008), desiccant wheel-assisted heat pump drying (Wang et al., 2011) and a host of others. More detailed discussions on some of these and other hybrid drying systems are

available in the review (Kudra and Mujumdar, 2009). There is evidently much room for improvement since many dryer combinations are yet to be well-investigated.

For the afore-mentioned hybrid systems, design (e.g. choice and sequencing of dryer types) and choice of operating conditions remains largely an art, guided by intuition. However, it is generally agreed (Chou and Chua, 2001; Mujumdar, 2007b; Kudra and Mujumdar, 2009) that an “intelligent” combination of dryer types is critical to fully harnessing the potential benefits of hybrid drying. With the advent of sophisticated modeling and optimization tools with high computing power in the market today, the possibility of increasing the design and operational “intelligence” has increased more than ever before. Drying technology is in dire need of exploiting these developments in optimal drying system design for energy efficiency and quality. Also, an interesting but often overlooked fact about hybrid dryers is that the addition of more system components opens more opportunities for beneficial heat integration than would be possible for stand-alone dryers with limited number of process streams. Another is the fact that while on the one hand, there is increased complexity which might limit operability, extra control inputs are also introduced which increase process flexibility potentials. These imply new process controllability issues which in turn affect energy performance and product quality under operational conditions. These issues need to be investigated further for each existing and would-be hybrid system.

The objective of this research is to fill the afore-mentioned research gaps for a class of hybrid dryers that uses desiccant (i.e. adsorbent) systems (e.g. zeolite wheel or bed) coupled to a basic convective dryer, either in a single or multistage arrangement. The desiccant adsorption system lends itself easily to incorporation to existing convective dryers (both batch and continuous) which as mentioned earlier make up an overwhelming majority of all industrial dryers. The drying air is dehumidified by passing through the adsorbent such that it gains drying capacity and hot air, used to regenerate wet adsorbents to ensure continuous usage. The overall system is suitable for low-temperature drying with possibilities for heat integration. In this thesis, modeling and optimization are used as tools to minimize overall dryer specific energy consumption while satisfying drying requirements such as final moisture content under constrained temperatures to limit thermal degradation. Issues like the optimal operating conditions, routing of heat recovery streams for heat integration, choice and sequencing of adsorbent types in multistage systems, controllability analysis and controllability integration in energy-efficient system design are investigated.

### **1.3. Dehumidified air drying by adsorbents: the potential of intelligent process, energy and controllability integration**

The need to produce dehumidified air for various applications like air conditioning and refrigeration has long been recognized. Literature studies on the use of adsorbents for this purpose date back to as far as the 1960s (Getty and Armstrong, 1964; Plachenov, 1965; Roubinet, 1969; Kritsula, 1969; Chi and Wasan, 1970).



Applications in solids drying, for instance in food products came much later with mainly “proof of concept” studies (Tutova and Fel’dman, 1976; Milner, 1979) a modern schematic of which is shown in Fig. 1.1. Since then, many more studies, some experimental and a few model-based, have appeared in the literature with various research themes as chronicled in Table 1.1. Apart from using adsorbent-dehumidified air for drying, the approach used in most works is the so-called contact-sorption drying which involves direct contact between the adsorbents and dried solids (van Boxtel et al., 2012). Drying with adsorbent-dehumidified air introduces a number of advantages. There is wide applicability as the adsorbent system lends itself to easy incorporation in existing convective dryers regardless of the type. In terms of energy performance, the drying capacity of the drying air is increased by adsorbent dehumidification and the corresponding sorption heat release. All these can be achieved while drying at low temperatures, which is beneficial from a product quality perspective. Although much energy is consumed for adsorbent regeneration which typically occurs at high temperatures, the additional process streams provide more alternative pathways for beneficial heat integration than stand-alone dryers. These alternatives increase in multistage systems where the exhaust air from each drying stage is passed through adsorbent systems to recover sensible and latent heat with

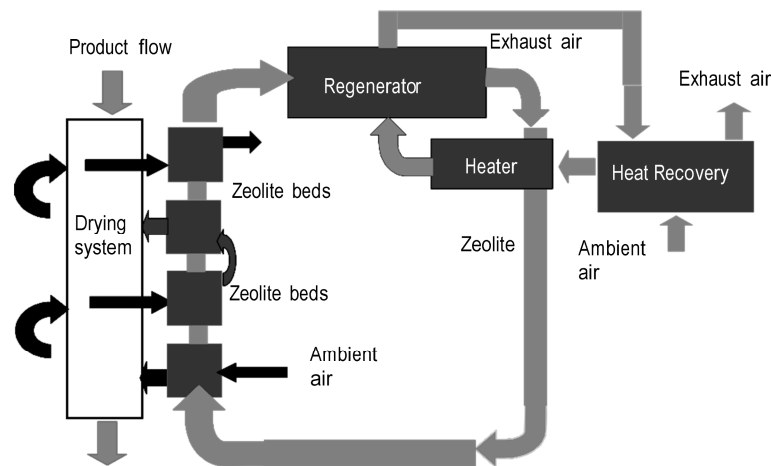


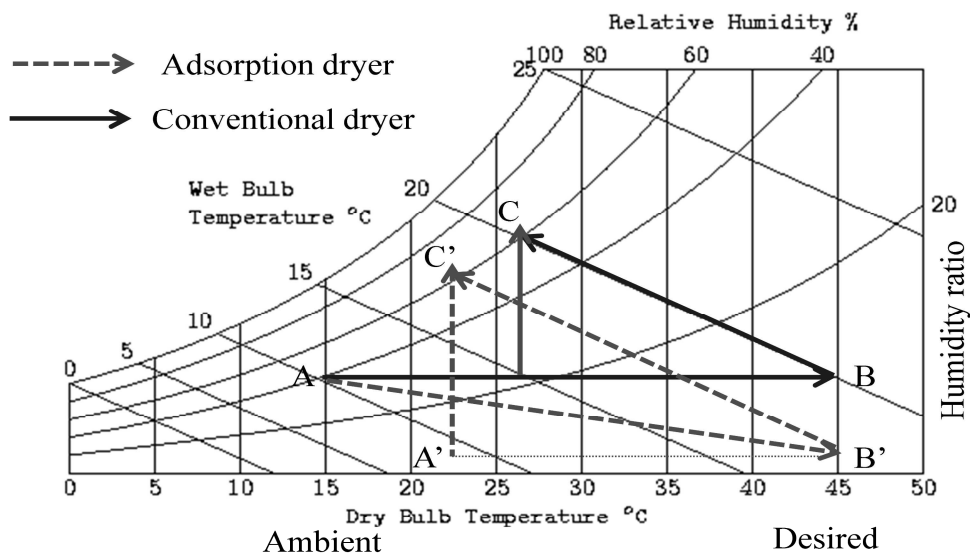
Fig. 1.1. Adsorption dryer system (Adapted from Djaeni et al., 2009b): Ambient air is dehumidified and passed through a multistage drying system to contact the wet product. Spent adsorbent is regenerated by hot air.

Table 1.1. Selected literature review on desiccant-based drying on various research themes

<i>Research Theme</i>	<i>References</i>
Product quality	Tutova et al., 1988; Strumillo et al., 1995; Tadayyon et al., 1997; Seyhan and Evranuz, 2000; Nagaya et al., 2006
Drying kinetics in various adsorbents	Pinaga et al., 1984; Watts et al., 1987; Falabella et al., 1991; Alikhani et al., 1992, Li et al., 2002; Osorio-Revilla, et al., 2006; Yang et al., 2006; Wachiraphansakul and Devahastin, 2007; Madhiyanon et al., 2007
Development and use of novel adsorbents	Ertas, et al., 1997; Thoruwa et al., 2000; Tirawanichakul et al., 2008; Witinantakit, et al., 2009; An et al., 2010
Energy issues	Milner, 1983; Ülku et al., 1991; Lazzarin et al., 1992; Djaeni et al., 2007a, b; Djaeni et al., 2009a, b; Antonellis et al., 2011

more possibilities for heat exchange. Again, the introduction of the adsorption system decouples energy expenditure from the drying process itself. In conventional dryers where the drying air is heated up by utility energy from ambient to desired temperature before drying (see point A to B in the psychrometric chart of Fig. 1.2), the air faces thermodynamic barriers. As the product dries, the air humidity rises from the dryer inlet B to the outlet C. Drying capacity represented by the vertical line terminating at C is therefore limited, restricting energy efficiency. The problem is more when drying at low temperatures to limit product quality degradation. For the adsorption dryer, the dehumidification process (from A to B') increases the drying capacity of the air (represented by the vertical line from A' to C') under the same exit relative humidity conditions as the conventional dryer. The dehumidification is also accompanied by sorption heat release which causes the temperature to rise (from A to B'), thus supplying energy for drying without utility. The main utility energy is thus not spent on drying but on regenerating the spent adsorbent. The operating conditions that determine regeneration energy consumption (e.g. flows and temperatures) can in principle be manipulated independent of the drying process itself thus shifting the thermodynamic barrier on the conventional system. More manipulated inputs are also introduced by the sorption system for controlling the dried product-based output variables. The desiccant adsorption dehumidification system thus increases the performance potentials of convective dryers from the point of view of energy efficiency, controllability and low-temperature operation for product quality.

However, exploiting the potentials depends on establishing synergy among component parts and determining optimal operating conditions. This requires a Process Systems Engineering approach which so far is lacking in the open literature.



57

Fig. 1.2. Psychrometric chart comparing drying capacities of adsorption and conventional dryers

In this thesis, available knowledge from systems modeling, optimization and control theory is utilized to extend the energy performance of adsorption dryers while drying at low temperatures. For this purpose, the following research questions are posed:

1. How best should the adsorbent-based dehumidification dryer be operated energy-wise while drying at low temperatures?
2. What is the optimal energy recovery routing among process streams?
3. How can process and energy integration techniques be applied to optimize synergy among components in multi-pass or multi-stage systems?
4. What key adsorbent properties should guide selection in adsorbent dryers as far as energy efficiency is concerned?
5. How can such a system be controlled?
6. What are the disturbance rejection capabilities?
7. How can controllability be integrated within energy-efficient dryer design and how does the adsorbent system affect this?
8. Are there any practically-relevant theoretical insights from the developments?

The discussion that follows outlines the steps taken to realize solutions to the above issues which can broadly be classified in finding optimal operating conditions for a given process structure (1, 2 and 3), finding optimal process structures (2, 3 and 4), process controllability (5-7) and scientific advancement (8).

#### **1.4. Research methodology and thesis structure**

The methodology employed in this work is represented in Fig. 1.3. It involves a survey of relevant literature, mathematical model development which comprises the development of models of the process units, integration of the models to form systems and formulation of various levels of energy-related optimization problems based on different process scenarios. As part of the overall model development, controllability assessment-relevant models are also developed and integrated into the energy-efficient design problem. Finally experimental work is done to prove some parts of the earlier developed concepts while extending the frontiers of the study. On the basis of the foregoing, the thesis is structured as follows. After the general introduction which is the subject of the current chapter, a mathematical model of a zeolite adsorption dryer is developed in **chapter 2** and an energy efficiency optimization procedure formulated to determine the optimal operating condition before and after heat recovery. In **chapter 3**, sensible and latent heat recovery are considered an integral part of drying system design and a one-step pinch location-based optimization problem formulated to determine simultaneously, the optimal operating conditions of the drying process and heat recovery. **Chapter 4** details the formulation of a superstructure of adsorbent alternatives in a multistage drying system to find the optimal adsorbent per-stage in terms of energy performance while optimizing operating conditions. Heat recovery is considered as a second step. In **chapter 5**, heat recovery is considered simultaneously with the drying process in a one-step optimization while the derivation of some optimal adsorbent properties that promote

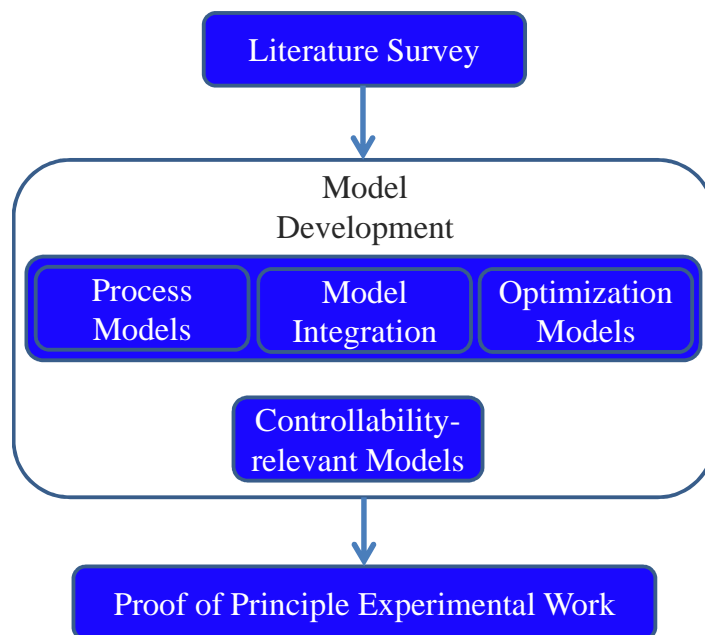


Fig. 1.3. Block diagram showing research methodology: arrows show the chronological order of starting (for instance, literature survey starts before model development).

process synergy and energy efficiency using a generalized superstructure forms the basis for **Chapter 6**. Controllability assessment of single-stage adsorption dryers with heat recovery is the focus of **chapter 7**, along with the sensitivity of energy performance to disturbances. In **chapter 8**, a relationship is established between dryer controllability and energy efficiency which permits the integration of controllability concepts into the design phase. The role of the adsorbent system in this regard is examined in detail. In **Chapter 9**, the methods used in chapter 8 are extended to practical systems involving significant heat losses. Two case studies are considered with the first involving a continuous fluidized bed dryer taken from literature. In the second case study, a lab-scale drying system with a detachable zeolite-filled rotary wheel is designed and coupled to a batch tray dryer. By means of this system, proof of principle experiments on the relationship between dryer energy efficiency and the process gain matrix are carried out. The drying behavior of constant-drying rate materials is used as case studies with and without the desiccant dehumidifier to demonstrate the level of improvement derivable from the dehumidifier. The work is concluded in **chapter 10** which takes a retrospective view of the work, details the main contributions and examines future perspectives and challenges for further development in energy efficient drying system design. **Chapters 2 – 6** pertain to research questions 1 – 3 while **Chapters 7 – 9** address questions 4 – 6. **Chapters 2 – 9** address question 7 while **Chapter 10** concludes the entire study. The main body of this thesis is therefore divided into two broad themes: improving dryer energy efficiency (covered in **Chapters 2 – 6**), and analyzing controllability issues and how they affect energy efficiency (**Chapters 7 – 9**).

### Model-based energy efficiency optimization of a low-temperature adsorption dryer

Published as Atuonwu, J.C., Straten, G. van., Deventer, H.C. van., Boxtel, A.J.B. van (2011). Model-based energy efficiency optimization of a low-temperature adsorption dryer, *Chemical Engineering and Technology*, 34, 1723-1732.

#### Abstract

Low-temperature drying is important for heat-sensitive products, but at these temperatures conventional convective dryers have low energy efficiencies. To overcome this challenge, an energy efficiency optimization procedure is applied to a zeolite adsorption dryer subject to product quality. The procedure finds a trade-off between the improved drying capacity due to dehumidification and energy expenditure due to regeneration while incorporating product drying properties. By optimizing the regeneration air inlet temperature, drying air, adsorbent, and regeneration air flow rates as well as sensible and latent heat recovery from the regenerator exhausts, the energy consumption is reduced by up to 45% compared to the state-of-the-art. The high mass transfer effect of high temperatures is utilized in the regenerator to boost dehumidification while isolating the heat-sensitive dried product from the quality-degrading effect.

*Keywords:* Adsorption drying, energy consumption, heat recovery, process optimization

#### 2.1. Introduction

Drying is an important unit operation applied in a wide variety of processes such as in food, pharmaceuticals and chemicals. It is an energy intensive process that accounts for about 15% of industrial energy consumption (Kemp, 2005) and as such, contributes significantly to industrial operating costs and environmental impact. With increasing energy costs and more stringent environmental legislations world over, reducing dryer energy consumption becomes more important. Usually one of the last steps in many processing operations, drying conditions have significant effects on product quality. The development of energy efficient and product friendly dryers is thus an important issue in industry.

Thermal efficiency ( $\eta$ ), the most important index of dryer energy performance, is defined as the ratio of the energy ( $Q_{evap}$ ) required to evaporate water from the product to the total energy input of the dryer ( $Q_{in}$ ):

$$\eta = \frac{Q_{evap}}{Q_{in}} \quad (2.1)$$

Hence, for convective dryers which constitute over 85% of all industrial dryers (Mujumdar, 2007a), the drying capacity, essentially  $Q_{evap}$ , is improved by increasing the amount of moisture evaporated by raising drying air temperature, reducing its absolute humidity or a combination of both (Djaeni et al., 2007a). For the same drying capacity, efficiency can be improved by recovering a part  $Q_{rec}$  of the exhaust stream energy such that net efficiency becomes

$$\eta_{eff} = \frac{Q_{evap}}{Q_{in} - Q_{rec}} \quad (2.2)$$

Due to the limiting effect of high drying temperatures on quality retention, low and medium temperature drying have been proposed for heat sensitive products. However, low temperature drying suffers from very low energy efficiencies (Djaeni et al., 2007a). Drying air dehumidification using adsorbents leads to a reduction in absolute humidity accompanied by the release of adsorption heat (Djaeni et al., 2007a). The combined effect increases the capacity of the air to dry more efficiently without raising the temperatures to undesirable high values. The limitation however lies in the energy required for regeneration. For instance, Madhiyanon et al. (2007) in an experimental study on a silica gel adsorption dryer report a 30-35% improvement in drying capacity but with a 40-80% increase in energy usage by regenerating at 101°C. Djaeni et al. (2007a) simulated a zeolite system at a regeneration temperature of 300°C. Although an improvement in drying capacity was recorded, the high regeneration temperatures used for the chosen zeolite, air and product flows negated the improvement. The result for a one-stage system without heat recovery was an efficiency of 48.6%. In these studies, the possibility of improving system performance before heat recovery by optimal choice of operating conditions was not explored. The free parameters of the system such as regeneration air temperature, flowrate, drying air and adsorbent flowrates were determined based on engineering judgment alone.

Process optimization provides a means of driving processes to operate at the best possible point with regard to specific objective(s) while respecting defined constraints. To achieve this, models capable of reliable sensitivity analysis of the objective function with respect to the decision variables are required. Many mathematical models e.g. (Beccali et al., 2003; Harshe et al., 2005; Sander and Kardum, 2009) are available in literature for simulating various categories of adsorbent and drying systems, each considered in isolation. Although both processes are reasonably understood, very few models are available that show systematically the interactions between them and how system energy efficiency is affected. Those available are either too complex for fast online optimization as in the case of the CFD formulation proposed by Djaeni et al. (2008) or lack the necessary level of detail for

reliable optimization. In the latter case, simplifying assumptions infeasible in actual operational situations are usually made. For instance zero moisture content of sorbent at adsorber inlet and saturation at outlet without considering sorption equilibria and kinetics, 90% moisture removal from air at adsorber, 40% relative humidity of air at dryer exit are assumed in Djaeni et al. (2007a). This limits the freedom of the system to respond to changes in free variables. Moreover, product drying kinetics was not considered even though this has strong effects on drying rate and hence efficiency as well as product heating which ultimately will affect quality. A modeling scheme without these assumptions is required, and is developed in this work.

Few studies on performance optimization of adsorption systems are available in literature with the moisture removal capacity (from the wet ambient air) as the usual performance measure (Chung et al., 2009; Chung and Lee, 2009). More recently, Antonelis et al. (2010), included regeneration energy in the objective function, but the primary purpose was air dehumidification and heat recovery was not investigated. Optimization studies on various kinds of stand-alone dryers are also available in literature. When the adsorption/regeneration and drying systems are linked, the interactions among them and the effect on product properties make the system more complex and interesting for investigation. For drying of heat-sensitive products, quality constraints are essential and they have implications on the adsorption system performance limits. Moreover, the moisture removal capacity for the system is now in terms of how much water can be removed from the dried product as opposed to how much can be removed from the air. Most previous studies on adsorption drying (Yang et al., 2000; Ye et al., 2008; Li et al., 2002) have focused on the effect of different types of adsorbents on drying kinetics and quality of different products without any attempt to optimize energy efficiency subject to product quality. The objective of this work is to formulate an optimization paradigm for maximizing the energy efficiency of the overall adsorption drying system taking into consideration the quality of the product in the dryer. To facilitate this, an energy sensitivity-relevant generalized model of a zeolite adsorption dryer is developed. A unique feature of the model is the unified manner in which the adsorber, regenerator and dryer equations are presented in matrix form. The model which considers the drying properties of specific food products with pumpkin as a case study (Krokida et al., 2003) is simple but detailed enough for reliable optimization. The energy efficiency of the system is optimized subject to temperature and moisture constraints on the product which indicate quality. Given the optimization results, the sensible and latent heat recovery potentials of the process exhaust streams are investigated to further improve energy efficiency.

## **2.2. Process Description**

The process consists of the dryer, heat sources and a zeolite adsorption/regeneration system (Fig. 2.1). Ambient air is passed through a zeolite adsorber bed where it is dehumidified and then used for drying the wet product. The spent zeolite is regenerated using hot air obtained by passing ambient air through a heater.

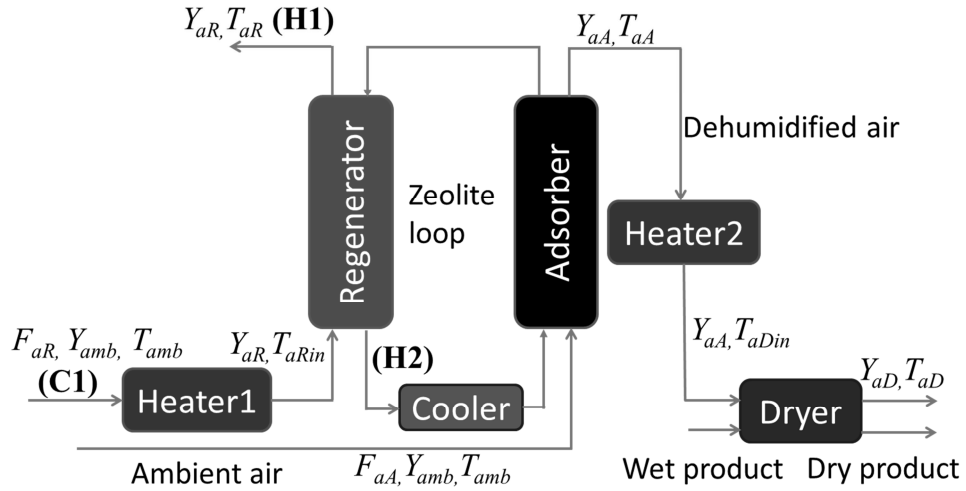


Fig. 2.1. Drying system process configuration with adsorber-regenerator subsystem

The zeolite circulates alternately between the adsorber and the regenerator. To regain adsorption capacity after regeneration, the hot zeolite is cooled. For practical implementation, the adsorption-regeneration system is usually fitted as an add-on to the dryer. For continuous operation, available configurations include rotary wheels with adsorption, regeneration and purge sections (Harshe et al., 2005) and twin column system with alternate switching between columns for adsorption-regeneration operations (Djaeni et al., 2009a). Rotary wheels have better dynamic operability properties than switchable twin-column systems as switching transients are avoided unlike switched columns which are not purely continuous. This work adopts a continuous adsorption-regeneration system realized by a rotary wheel where the zeolite mass flowrate is manipulated by the wheel thickness and angular speed. The developed model is also applicable to twin column systems if the flowrate is expressed in terms of zeolite mass hold-up in the column and switching time.

### 2.3. Model formulation

The model is formulated on the following assumptions:

- Each system component is approximated by a lumped parameter model
- Thermodynamic properties of the solid and fluid phases are constant
- Heat losses are neglected
- Heat of sorption of the zeolite system is constant
- Thin layer drying is assumed so the drying process is governed by first-order kinetics
- At steady-state, the temperatures of the solid (product and zeolite) and air phases are equal.



## 2.3.1 Mathematical model

The drying, adsorption and regeneration processes are similar. In drying, the product loses moisture which is picked up by the drying air. In adsorption, the air is dried and the adsorbent picks up the moisture while in regeneration, the adsorbent is dried. It is thus convenient to represent common state, inlet variables and constants in 3-dimensional vectors (bold face terms) in the form [Dryer Adsorber Regenerator] so

$$\begin{bmatrix} \mathbf{X}_s \\ \mathbf{Y}_a \\ \mathbf{T}_a \\ \mathbf{T}_s \end{bmatrix} = \begin{bmatrix} X_p & X_{zA} & X_{zR} \\ Y_{aD} & Y_{aA} & Y_{aR} \\ T_{aD} & T_{aA} & T_{aR} \\ T_p & T_{zA} & T_{zR} \end{bmatrix} \quad (2.3)$$

$$\begin{bmatrix} \mathbf{X}_{sin} \\ \mathbf{Y}_{ain} \\ \mathbf{T}_{ain} \\ \mathbf{T}_{sin} \\ \mathbf{F}_a \\ \mathbf{F}_s \end{bmatrix} = \begin{bmatrix} X_{pin} & X_{zAin} & X_{zRin} \\ Y_{aDin} & Y_{aAin} & Y_{aRin} \\ T_{aDin} & T_{aAin} & T_{aRin} \\ T_{pin} & T_{zAin} & T_{zRin} \\ F_{aD} & F_{aA} & F_{aR} \\ F_p & F_z & F_z \end{bmatrix} \quad (2.4)$$

$$\begin{bmatrix} \mathbf{C}_{ps} \\ \boldsymbol{\rho}_s \\ \mathbf{V}_s \\ \mathbf{V}_a \end{bmatrix} = \begin{bmatrix} C_{pp} & C_{pz} & C_{pz} \\ \rho_p & \rho_z & \rho_z \\ V_p & V_{zA} & V_{zR} \\ V_{aD} & V_{aA} & V_{aR} \end{bmatrix} \quad (2.5)$$

$$\begin{bmatrix} \mathbf{k} \\ \mathbf{X}_e \\ \mathbf{h} \end{bmatrix} = \begin{bmatrix} k_D & k_{zA} & k_{zR} \\ X_{pe} & X_{zeA} & X_{zeR} \\ h_D & h_{zA} & h_{zR} \end{bmatrix} \quad (2.6)$$

The unified mass and energy balances governing the dynamic behavior of the dryer, adsorber and regenerator subsystems (where all divisions and products are element-wise) are thus given by

$$\frac{d\mathbf{Y}_a}{dt} = \frac{\mathbf{F}_a}{\rho_a \mathbf{V}_a} (\mathbf{Y}_{ain} - \mathbf{Y}_a) + \frac{\mathbf{k} \boldsymbol{\rho}_s \mathbf{V}_s}{\rho_a \mathbf{V}_a} (\mathbf{X}_s - \mathbf{X}_e) \quad (2.7)$$

$$\frac{d\mathbf{X}_s}{dt} = \frac{\mathbf{F}_s}{\rho_s \mathbf{V}_s} (\mathbf{X}_{sin} - \mathbf{X}_s) - \mathbf{k} (\mathbf{X}_s - \mathbf{X}_e) \quad (2.8)$$

$$\frac{d\mathbf{T}_a}{dt} = \frac{\mathbf{F}_a}{\rho_a \mathbf{V}_a (C_{pa} + \mathbf{Y}_a C_{pv})} \left[ \begin{array}{l} (C_{pa} + \mathbf{Y}_{ain} C_{pv}) \mathbf{T}_{ain} - (C_{pa} + \mathbf{Y}_a C_{pv}) \mathbf{T}_a \\ + (\mathbf{Y}_{ain} - \mathbf{Y}_a) (\Delta H_v + \boldsymbol{\alpha} H_{ads}) \\ - \mathbf{h} \mathbf{V}_s (\mathbf{T}_a - \mathbf{T}_s) - \rho_a \mathbf{V}_a (C_{pa} + C_{pv} \mathbf{T}_a) d\mathbf{Y}_a / dt \end{array} \right] \quad (2.9)$$

$$\frac{dT_s}{dt} = \frac{F_s}{\rho_s V_s (C_{ps} + X_s C_{pw})} \left[ \begin{array}{l} (C_{ps} + X_{sin} C_{pw}) T_{sin} - (C_{ps} + X_s C_{pw}) T_s \\ + \beta H_{ads} (X_s - X_{sin}) \\ + h V_s (T_a - T_s) - \rho_s V_s (C_{ps} + C_{pw} T_s) dX_s / dt \end{array} \right] \quad (2.10)$$

Vectors  $\alpha$  and  $\beta$  in (2.9) and (2.10) are “selection” vectors that qualify adsorption heat release/absorption. Here,  $\alpha$  qualifies adsorption heat release/absorption in the air phase, and  $\beta$  qualifies adsorption heat release/absorption in the solid phase. In the adsorber, the adsorption heat is released directly in the adsorbent alone making  $\beta$  unity only in the adsorber. The heat is then convectively transferred to the air phase. In the regenerator, the air directly loses the adsorption heat (endothermic reaction) thus making  $\alpha$  unity only in the regenerator. At the same time, the air loses heat by convection to the zeolite. Adsorption heat release and absorption are insignificant in the dryer and so,  $\alpha$  and  $\beta$  are zero in the dryer. In the light of the foregoing,  $\alpha$  and  $\beta$  are expressed as

$$\alpha = [0 \quad 0 \quad 1] \quad (2.11)$$

$$\beta = [0 \quad 1 \quad 0] \quad (2.12)$$

### 2.3.2. Constitutive Relations

For the zeolite system, a set of 2-dimensional vectors is defined

$$\begin{bmatrix} T_{az} \\ Y_{az} \end{bmatrix} = \begin{bmatrix} T_{aA} & T_{aR} \\ Y_{aA} & Y_{aR} \end{bmatrix} \quad (2.13)$$

The kinetic and equilibrium relations (van Boxtel et al., 2012) are determined as

$$k_z = [k_{zA} \quad k_{zR}] = k_0 \exp(-E_0/RT_{az}) \quad (2.14)$$

$$X_{ze} = [X_{zeA} \quad X_{zeR}] = \frac{X_{zmax} b P_v}{1 + b P_v} \quad (2.15)$$

$$b = [b_A \quad b_R] = b_0 \exp\left(\frac{-E_1}{RT_{az}}\right) \quad (2.16)$$

where the vapour pressure of the air is

$$P_v = \frac{Y_{az} P_{atm}}{0.62198 + Y_{az}} \quad (2.17)$$

The drying behavior of pumpkin (Krokida et al., 2003) is used in evaluating the performance of the proposed system. The equilibrium moisture content and drying rate constant are respectively given by

$$X_{ze} = 5 \times 10^{-7} \exp(3796.777/T_a) (a_w / (1 - a_w))^{1.2848} \quad (2.18)$$

$$k = 1.77 d_p^{4.9} T_{aD}^{-0.21} v^{0.45} RH^0 \quad (2.19)$$

### 2.3.3 Coupling Equations

Based on the configuration of Fig. 2.1, the following are the process coupling equations

$$[T_{aDin} \ Y_{aDin}] = [T_{aA} \ Y_{aA}] \quad (2.20)$$

$$\begin{bmatrix} T_{aAin} & Y_{aAin} & X_{zAin} \\ T_{zRin} & Y_{aRin} & X_{zRin} \end{bmatrix} = \begin{bmatrix} T_{amb} & Y_{amb} & X_{zR} \\ T_{zA} & Y_{amb} & X_{zA} \end{bmatrix} \quad (2.21)$$

### 2.3.4 Forcing Signals and State Space Representation

The external variables that affect the system follow from Fig. 2.1 and can be categorized in external inputs  $\mathbf{d}$  and control inputs  $\mathbf{u}$  defined as

$$\mathbf{d} = [T_{amb} \ Y_{amb} \ X_{pin} \ T_{pin} \ F_p]^T \quad (2.22)$$

$$\mathbf{u} = [F_{aA} \ F_{aR} \ F_z \ T_{aRin} \ T_{zAin}]^T \quad (2.23)$$

The system states (from (2.7) to (2.10)) are

$$\mathbf{x} = [X_p \ X_{zA} \ X_{zR} \ Y_{aD} \ Y_{aA} \ Y_{aR} \ T_{aD} \ T_{aA} \ T_{aR} \ T_p \ T_{zA} \ T_{zR}]^T \quad (2.24)$$

With these definitions, the system can be represented concisely in state space form as

$$\frac{d\mathbf{x}}{dt} = \mathbf{f}(\mathbf{x}, \mathbf{u}, \mathbf{d}, p) \quad (2.25)$$

where  $\mathbf{f}$  is a vector valued function that follows from (2.3) – (2.24), and  $p$  is a set of parameters as defined in Table A1, Appendix A.

### 2.3.5 Steady State Model Solution

By setting the time derivatives to zero, the steady-states are derived as

$$X_s = X_e + \frac{1}{1 + k\rho_s V_s / F_s} (X_{sin} - X_e) \quad (2.26)$$

$$Y_a = \frac{F_s}{F_{aA}} (X_s - X_e) + Y_{ain} \quad (2.27)$$

$$T_a = \frac{F_{aA} [(C_{pa} + Y_{ain} C_{pv}) T_{ain} + (\Delta H_v + (\alpha + \beta) H_{ads})(Y_{ain} - Y_a)] + F_s [(C_{ps} + X_{sin} C_{pw}) T_{sin}]}{F_{aA} (C_{pa} + Y_a C_{pv}) + F_s (C_{ps} + X_s C_{pw})} \quad (2.28)$$

$$T_s = T_a \quad (2.29)$$

## 2.4. Model validity

Simulations using the model and results presented in Section 2.7 indicate that mass and energy balances are satisfied and efficiencies obtained for optimized conventional dryers are in the typical range of 20-60% as obtained in practice (Mujumdar, 2007a). All constitutive equations are based on experimentally validated mathematical models (Krokida et al., 2003; van Boxtel et al., 2012). The dryer model for instance is made up of equipment heat and mass balances in conjunction with well-established psychrometric relations and experimentally validated product drying kinetic and equilibria models (Krokida et al., 2003). To further demonstrate the validity of the adsorber-regenerator system model, the model was simulated using experimental data for a twin column system (Djaeni et al., 2009a). In this system, the approximate steady-state operating conditions include: drying air flowrate  $F_{aA}=102\text{kg/h}$  and regeneration air flowrate  $F_{aR}=102\text{kg/h}$ . For a twin column system with hold-up mass  $2.5\text{kg per column}$  (i.e.  $5\text{kg total}$ ) and switching time of 60 minutes, the equivalent zeolite flowrate is  $F_z=5\text{kg/h}$ . The corresponding inlet conditions are adsorber air humidity  $0.009\text{kg/kg}$ , adsorber air temperature,  $28^\circ\text{C}$  and regeneration air inlet humidity,  $130^\circ\text{C}$  (Djaeni et al., 2009a). Table 2.1 compares the experimental and model results for the output variables. All deviations are found to be within 5% which shows good agreement.

Table 2.1. Comparison of model results with published experimental data

<i>Output</i>	<i>Experimental</i>	<i>Model</i>
Adsorber outlet air moisture content $\text{kg/kg}$	0.002	0.0021
Adsorber outlet air temperature $^\circ\text{C}$	54	52.1
Regenerator outlet air temperature $^\circ\text{C}$	108	106

## 2.5. Optimization problem formulation

The instantaneous energy rate associated with the removed water is given by

$$Q_{evap} = F_p (X_{pin} - X_p) \Delta H_v \quad (2.30)$$

Energy is only used for regeneration (assuming sorption heat is sufficient to take the drying air to desired low temperature). Hence, the instantaneous input energy rate is

$$Q_{in} = F_{aR} (C_{pa} + Y_{aRin} C_{pv}) (T_{aRin} - T_{amb}) \quad (2.31)$$

For steady-state optimization (see Fig. 2.1), it is assumed that of the 10 free inputs,  $F_p$ ,  $T_{amb}$ ,  $Y_{amb}$ ,  $T_{pin}$ ,  $X_{pin}$  are fixed. Of the remaining 5,  $T_{zain}$  is chosen to be equal to ambient temperature for which the cooler is appropriately rated. The remaining variables  $F_{aA}$ ,  $F_z$ ,  $F_{aR}$ ,  $T_{aRin}$  can be chosen as optimization variables. For a given product flow, an optimal drying air flowrate is required. Conversely, for a given drying air flow, an optimal flow of zeolite is required, and for this, an optimal flow of regeneration air is needed. Hence, operational design variables  $r_0$ ,  $r_1$ ,  $r_2$  are defined as:

$$F_{aA} = r_0 F_p \quad (2.32)$$

$$F_z = r_1 F_{aA} \quad (2.33)$$

$$F_{aR} = r_2 F_z \quad (2.34)$$

The ratios  $r_0$ ,  $r_1$  and  $r_2$  are chosen as optimization variables in addition to  $T_{aRin}$ . Hence, the optimization problem is formulated as

Maximize

$$\eta_U = \frac{Q_{evap}}{Q_{in}} = \frac{F_p (X_{pin} - X_p) \Delta H_v}{F_{aR} (C_{pa} + Y_{aRin} C_{pv}) (T_{aRin} - T_{amb})} \quad (2.35)$$

where

$$U = [r_0 \quad r_1 \quad r_2 \quad T_{aRin}] \quad (2.36)$$

subject to (2.3 – 2.34), and the constraints

$$\text{Product final moisture content } X_p = 0.05 \quad (2.37)$$

$$\text{Product maximum temperature } T_p \leq 50 \quad (2.38)$$

$$\text{Regeneration temperature constraint } T_{aRin_{min}} \leq T_{aRin} \leq 400 \quad (2.39)$$

The optimization problem is implemented in TOMLAB® Optimization software with MATLAB interface using the “KNITRO” solver-based interior-point method (Holmström et al., 2009). The method uses an iterative conjugate gradient approach to compute each optimization step.

## 2.6. Energy recovery

To fully exploit the energy saving possibilities of the adsorption drying system, heat recovery is essential after efficiency optimization. Pinch analysis is a targeting procedure that indicates the maximum energy recoverable from a given process. The studied drying system has two main “hot streams”, the regenerator outlet air (H1) and zeolite (H2) and one “cold stream”, the ambient air to the regenerator (C1) (see Fig. 2.1). Kemp (2005) shows a tabular method of determining the pinch in which the cold stream temperatures are shifted upwards by one-half the minimum exchanger temperature difference  $\Delta T_{min}$  while those of the hot streams are reduced by the same value (Table 2.2). Sensible heat exchange  $Q_{sens}$  on each shifted temperature interval  $\Delta i$  is then calculated by equation (2.40) where  $FC_{ph}$  and  $FC_{pc}$  are respectively the total heat capacity rates of the hot and cold streams. The same approach is used in this work but the feasibility of latent heat recovery is now included. Latent heat recovery (2.41) in each interval is proportional to the amount of water condensed in cases where the hot regeneration air cools below its dew-point  $T_{dptR}$ .

$$Q_{sens}(\Delta i) = \left( \sum FC_{pH}(\Delta i) - \sum FC_{pC}(\Delta i) \right) (S(i) - S(1+i)) \quad (2.40)$$

$$Q_{lat}(\Delta i) = F_{aR} \Delta H_v (Y_{aR}(T_{dptR}) - Y_{aR}(T_{H1out})) \quad (2.41)$$

## 2.7. Results and discussion

### 2.7.1. Process optimization results and discussion

The drying process optimization (without heat recovery) was performed at different starting points and bounds on the decision variables. The results are found to be independent of the starting points, suggesting there are no local minima. Of all the decision variable bounds, the maximum energy efficiency corresponds only to the upper bound on regeneration air inlet temperature. This upper bound is set at 400°C which is the maximum allowable beyond which the zeolite deforms (van Boxtel et al., 2012), so kinetic and equilibria relations presented no longer hold. Fig. 2.2(a), (b), (c) & (d) show the variation of the optimization decision variables with the upper bound on regeneration air inlet temperature. It is seen in Fig. 2.3, that contrary to intuition, maximum efficiency is always achieved at this upper bound. This is attributable to the fact that at higher regeneration temperatures, the adsorber inlet zeolite has a higher adsorption capacity (after cooling) and thus, should enhance reduction in the humidity of the drying air, and hence increase drying capacity. However, since the drying

Table 2.2. Determination of shifted stream temperatures &amp; associated heat capacity rates

Stream type	Supply temperature $T_s$	Target temperature $T_t$
H1	$T_{aR}$	$T_{amb}$
H2	$T_{zR}$	$T_{zAin} = T_{amb}$
C1	$T_{amb}$	$T_{aRin}$
Stream type	Shifted supply Temperature $S_s$	Shifted target temperature $S_t$
H1	$T_{aR} - 0.5\Delta T_{min}$	$T_{amb} - 0.5\Delta T_{min}$
H2	$T_{zR} - 0.5\Delta T_{min}$	$T_{amb} - 0.5\Delta T_{min}$
C2	$T_{amb} + 0.5\Delta T_{min}$	$T_{aRin} - 0.5\Delta T_{min}$

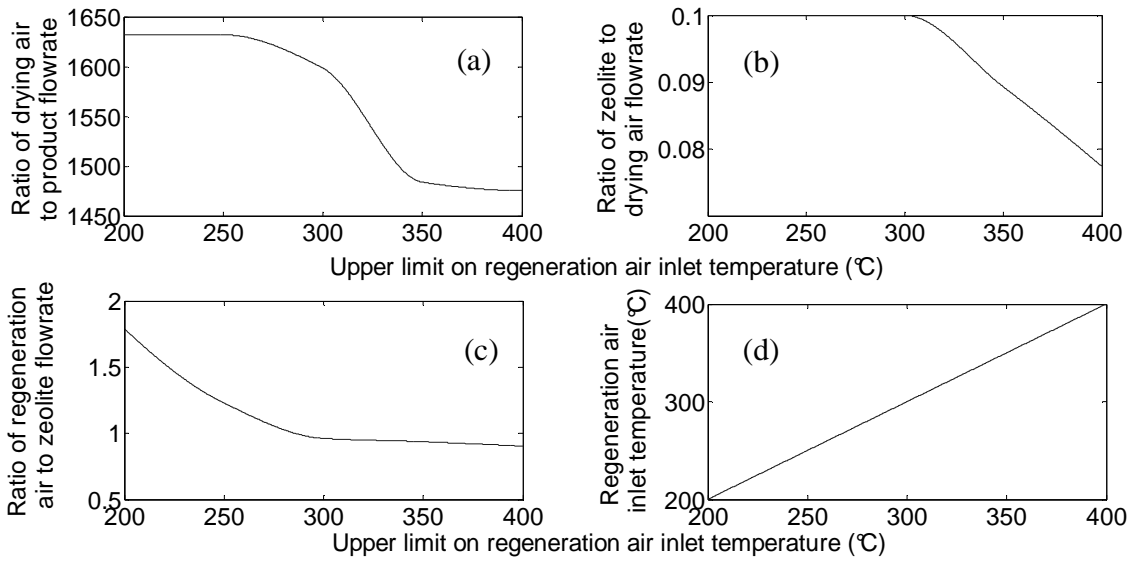


Fig. 2.2. Variation of optimal decision variables with regeneration air inlet temperature

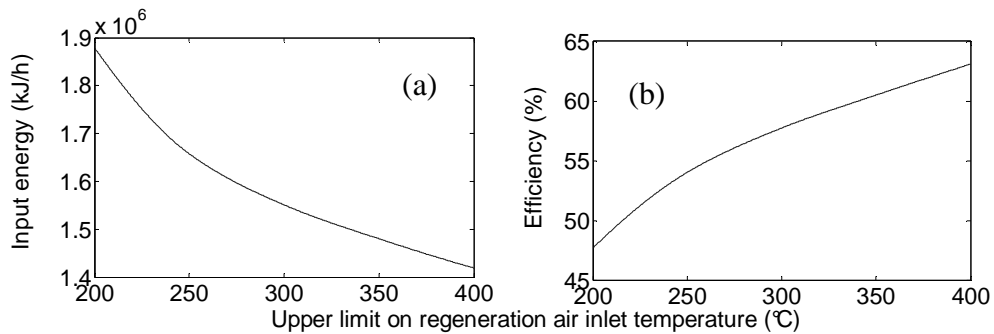


Fig. 2.3. Input energy and thermal efficiency variation with regeneration air inlet temperature

capacity of the dryer is constrained to be constant (see (2.35) and (2.37)), two scenarios present themselves. First, for constant zeolite flow as occurs between regeneration temperatures 200 to about 300°C (see Fig. 2.2b), the regeneration air

flow needed for optimal regeneration reduces (Fig. 2.2c). Conversely, the zeolite flow required for this drying capacity is reduced when the regeneration air inlet temperature is between 300 and 400°C (Fig. 2.2b). The result of these system interactions is that the product  $F_{aR}T_{aRin}$  in the cost function reduces progressively.

### 2.7.2. Energy efficiency analysis (without heat recovery)

For drying of pumpkin from a water content of 10kg/kg to 0.05kg/kg, representing an evaporative energy load  $Q_{evap}=8.995 \times 10^5$  kJ/h, the energy consumption reduces from  $1.88 \times 10^6$  kJ/h for  $U=[1632 \ 0.1 \ 1.793 \ 200]$  to  $1.4 \times 10^6$  kJ/h for  $U=[1476 \ 0.0775 \ 0.9024 \ 400]$ . This represents an efficiency rise from 48% to 64% (Fig. 2.3b) – a significant improvement over previous results (Djaeni et al., 2007a) where an equivalent one-stage adsorption dryer without heat recovery recorded an efficiency of 48.6%. System operating conditions at regeneration air inlet temperature  $T_{aRin}=400^\circ\text{C}$  are shown in Table 2.3 with stream numberings as designated in Fig. 2.4. The system performance indicators as returned by the optimization and design variables are as shown in Table 2.4. Regenerating the zeolite at the maximum possible temperature is seen to be desirable but on the condition that the regeneration air flowrate is sufficiently low. This way, high temperature energy is concentrated in low volumes of air, thus reducing the energy spent on regeneration while by no means reducing the regeneration effectiveness and hence, drying capacity of the dehumidified air. Another important issue is that the high temperature heat contents of the zeolite and air from the regenerator creates opportunities for heat recovery which could further increase energy efficiency.

Table 2.3. Optimized adsorption drying process stream variables

Stream	Flow kg/h	Humidity kg/kg	Temperature °C	Stream	Flow kg/h	Humidity Kg/h	Temperature °C
1	$5.3 \times 10^4$	0.01	25	6	$4.1152 \times 10^3$	0.0868	25
2	$5.3 \times 10^4$	0.0038	49	7	$4.1152 \times 10^3$	0.1664	49
3	$5.3 \times 10^4$	0.0106	32	8	$3.7134 \times 10^3$	0.01	25
4	36	10	25	9	$3.7134 \times 10^3$	0.01	400
5	36	0.05	49	10	$3.7134 \times 10^3$	0.0982	170
6'	$4.1152 \times 10^3$	0.0868	170				

Table 2.4. Process design and performance variables

Mass Hold up (product)	1000kg
Fresh product rate	400kg/h
Evaporative load (dryer)	358kg/h
Evaporative energy equivalent	$0.8995 \times 10^6$ kJ/h
Dehumidification/Regeneration rate	383kg/h
Latent heat equivalent	$0.8205 \times 10^6$ kJ/h
Sensible heat equivalent (due to sorption heat)	$1.05 \times 10^6$ kJ/h
Regeneration energy load	$1.42 \times 10^6$ kJ/h
Sorption wheel	1m <sup>2</sup> face area, 0.2m thickness (Harshe et al., 2005), 25rev/h, area ratio 4:1
Dryer size	Volume=5m <sup>3</sup> , length=5m, width =1m, height = 1m



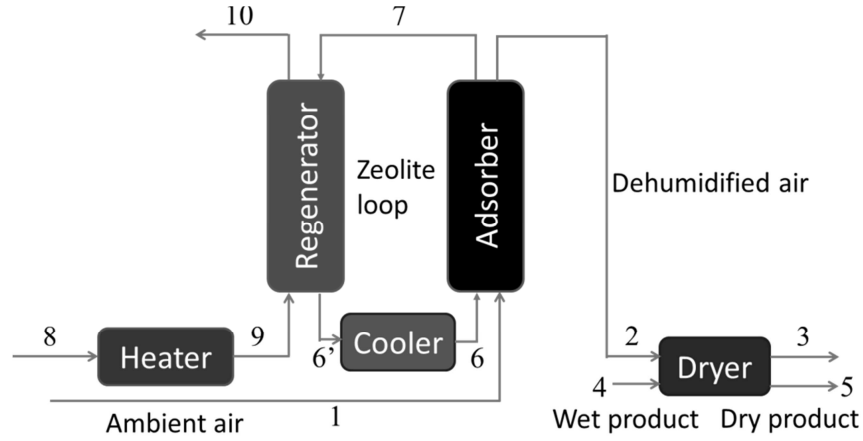


Fig. 2.4. Adsorption drying system with process stream numbering

### 2.7.3 Process and heat recovery interactions

Pinch analysis results (Fig. 2.5) show two options to recover heat while keeping the dried product at low temperature. The regenerator inlet air is pre-heated using either the regenerator exhaust air or the hot zeolite both of which are at the same temperature level. Consider a heat recovery system with one heat exchanger, two scenarios are possible

1. Where the hot stream is the heat transfer limiting stream, the cold stream heats up to  $\Delta T_{min}$  less than the hot stream inlet temperature. The temperature of the cold stream outlet becomes  $T_{cout} = T_{hin} - \Delta T_{min}$
2. Where the cold stream is the heat transfer limiting stream, the hot stream cools down to  $\Delta T_{min}$  more than the cold stream inlet temperature. The temperature of the hot stream outlet becomes  $T_{hout} = T_{cin} + \Delta T_{min}$

In both cases, for  $F_h = F_c$ , the heat recovered becomes

$$Q_{rec} = F_c(T_{cout} - T_{cin}) = F_h(T_{hin} - T_{hout}) = F_h(T_{hin} - T_{cin} - \Delta T_{min}) \quad (2.42)$$

For ambient air pre-heated by regeneration exhaust air the heat recovered is

$$Q_{rec} = F_{aR}(T_{aR} - T_{amb} - \Delta T_{min}) \quad (2.43)$$

$T_{aR}$  is directly proportional to  $T_{aRin}$  and so, comparing with results of Section 2.7.1, we see that while an increase in  $F_{aR}T_{aRin}$  reduces the efficiency of the process itself, it also increases the magnitude of heat recovered and hence, overall efficiency (see Fig. 2.6(a) & (b)). These conflicting forces explain the existence of extrema in overall input energy (Fig. 2.6(c) & hence, energy efficiency (d)). However, there is no significant difference between overall efficiency at different regeneration temperatures. With heat recovery, the overall efficiency is about 95% which corresponds to an energy consumption of about  $9.04 \times 10^5 \text{ kJ/h}$ . The results of Fig. 2.6

are determined for  $\Delta T_{min}=10^{\circ}\text{C}$ . Maximum temperature regeneration is best in the absence of heat recovery but this comes at a price of more expensive and robust heaters. However, gas and oil-fired heaters operating up to  $400^{\circ}\text{C}$  are commercially available. Moreover, with high temperatures and low flows, equipment size is reduced. When heat recovery is incorporated, there is no need to regenerate at the highest temperatures as the overall energy efficiency is not significantly different. Overall economics should be the guiding principle in actual implementation. Heat recovery economics is based on trade-offs between increased capital costs which are proportional to heat exchange area and running costs, the reduction of which is proportional to the amount of heat recovered. By manipulating  $\Delta T_{min}$  at values of 5, 8, 10, 15 and  $20^{\circ}\text{C}$ , different possibilities arise as shown in Fig. 2.7 (for an overall heat

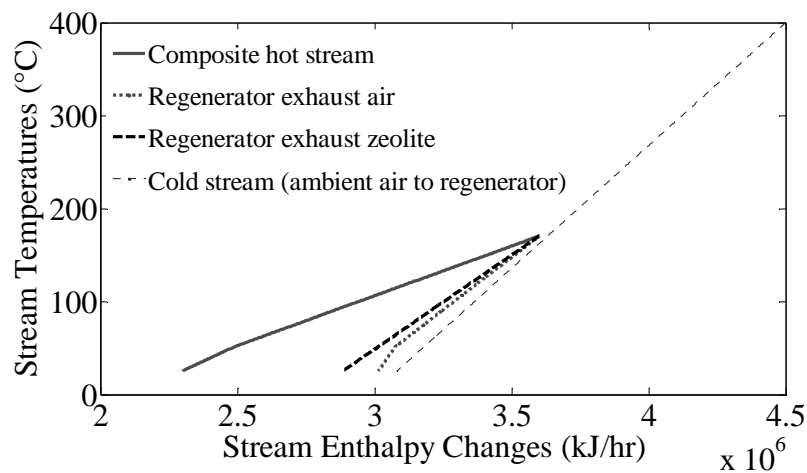


Fig. 2.5. Pinch analysis results showing composite hot and cold streams as well as different match options

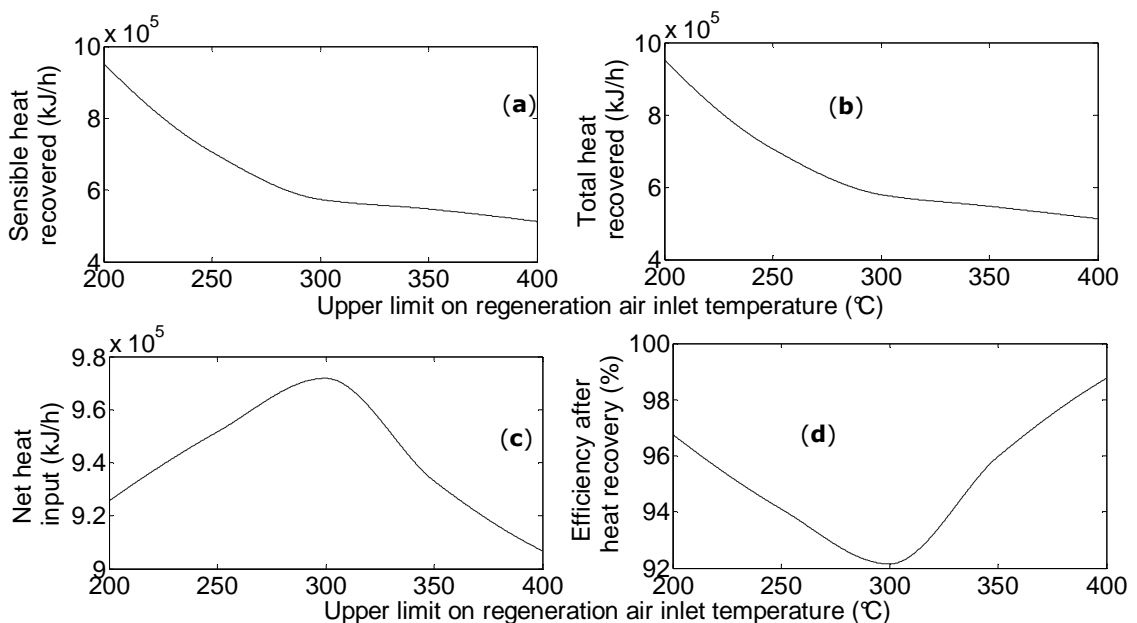


Fig. 2.6. Heat recoveries and overall energy efficiency at different regeneration air inlet temperatures  $\Delta T_{min}=10^{\circ}\text{C}$

transfer coefficient of  $200\text{W/m}^2\text{K}$ , Langrish, 1998). At lower values of  $\Delta T_{min}$ , more heat is recovered (Fig. 2.7(a)), largely due to latent heat recovery since the hot stream outlet temperatures in some cases become less than dew-point as seen in Fig. 2.7(b). This improvement however comes at the expense of more exchange area (Fig. 2.7(c)). Although less heat is recovered as regeneration air inlet temperature increases, the temperature level to which the cold stream rises becomes higher due to reduced regeneration air flowrate (Fig. 2.7(d)). For  $\Delta T_{min}=5, 8 \text{ \& } 10^\circ\text{C}$  throughout the studied temperature range of the regeneration air inlet temperature, the pinch occurs at the hot stream inlet (regenerator outlet air) as indicated by the parallelism between the hot stream inlet and the cold stream outlet (constant  $\Delta T_{min}$  in this region, see Fig. 2.7(d)).

At higher regeneration temperatures (corresponding to lower regeneration air flows) for  $\Delta T_{min}=15 \text{ \& } 20^\circ\text{C}$ , the situation is the same. However, at the lower end of the regeneration temperature range (corresponding to higher regeneration air flows), the cold stream inlet (ambient air to the regenerator) becomes the heat exchange limiting stream as the hot stream outlets from the heat exchanger tend to become parallel to the cold stream inlet as seen in Fig. 2.7(b). The entire situation suggests there is considerable interaction between the adsorption drying process and the heat recovery system. Fig. 2.8 shows the overall process flowsheet including heat recovery. The properties of streams 1 – 10 are identical to those of the original system (Fig. 2.4) as shown in Table 2.3. Stream 11 is the cold stream outlet at  $160^\circ\text{C}$  while stream 12 is the hot stream outlet at  $54^\circ\text{C}$ . The cold stream inlet as seen in Fig. 2.7(b). The entire situation suggests there is considerable interaction between the adsorption drying process and the heat recovery system. Fig. 2.9 shows the overall process flowsheet including heat recovery. The properties of streams 1 – 10 are identical to those of the original system (Fig. 2.4) as shown in Table 2.3. Stream 11 is the cold stream outlet at  $160^\circ\text{C}$  while stream 12 is the hot stream outlet at  $54^\circ\text{C}$  (all for  $\Delta T_{min}=10^\circ\text{C}$ ).

#### 2.7.4. Performance comparison with conventional systems

For a conventional convective dryer (Fig. 2.9) operating at the same temperature but without dehumidification, the potential for water uptake by the air is less than that of the dehumidified air from the adsorber of the adsorption dryer. Thus, to meet the same drying duty (evaporative load), the conventional dryer requires more air for the same product flow (as can be seen by comparing flowrates of stream 1 in Tables 2.3 & 2.5). More energy is therefore needed to heat this air to the required temperature. Also, the benefit of adsorption heat release does not accrue to this process. The overall effect is that the conventional dryer for the same evaporative load consumes  $1.73 \times 10^6 \text{kJ/h}$  as against the  $1.4 \times 10^6 \text{kJ/h}$  for the optimal adsorption dryer. The operating conditions as presented in Table 2.5 also show an exhaust airstream (no. 3) at a low temperature of  $36^\circ\text{C}$ . This low temperature level makes it impossible to recover the sensible heat because, for a minimum exchanger approach  $\Delta T_{min}=10^\circ\text{C}$ , the ambient air can only be heated to a maximum of  $26^\circ\text{C}$  ( $1^\circ\text{C}$  temperature increase) which is insignificant. Moreover, at a dew-point of  $20^\circ\text{C}$  which is lower than ambient temperature, latent

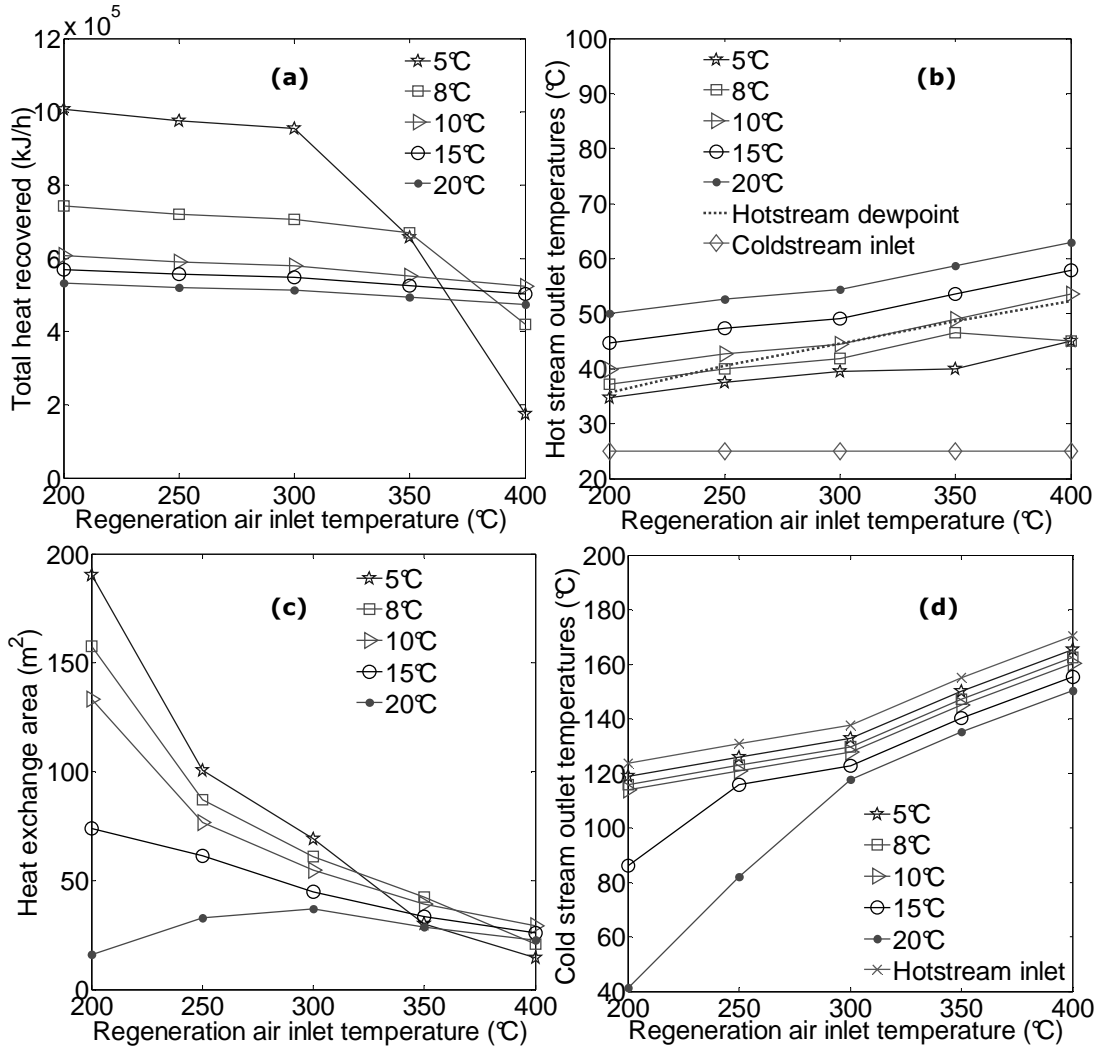


Fig. 2.7. Conditions at different regeneration air inlet temperatures and  $\Delta T_{\min}$  values (a). Total heat recovery (b). Hot stream outlet temperatures compared with dew-point and cold stream inlet temperature (c). Heat exchange areas (d). Cold stream outlet temperatures compared with hot stream inlet temperature

heat cannot be recovered without heat pumps which use expensive electrical energy. The optimal adsorption dryer however consumes  $1.4 \times 10^6$  kJ/h without heat recovery and  $0.9 \times 10^6$  kJ/h after heat recovery representing respectively, about 20% and 45% reduction in energy consumption for the same drying load.

Comparing mathematically, for an adsorption dryer (Fig. 2. 1), the drying capacity  $F_{aA}(Y_{aD}-Y_{aA})=F_{aA}(Y_{amb}-Y_{aA})+F_{aA}(Y_{aD}-Y_{amb})$ , where the first term on the RHS of the equation is the moisture removal capacity of the adsorber and the second term, the drying capacity of the stand-alone dryer. Thus, as the moisture removal capacity of the adsorber increases (smaller value of  $Y_{aA}$ ), so does the numerator of the energy efficiency equation (2.35). But then, more energy would have to be spent on regeneration. Moreover, increased dehumidification leads to higher adsorption heat release which should be constrained to preserve quality parameters. The constrained optimization problem presented in this work helps in solving these problems.

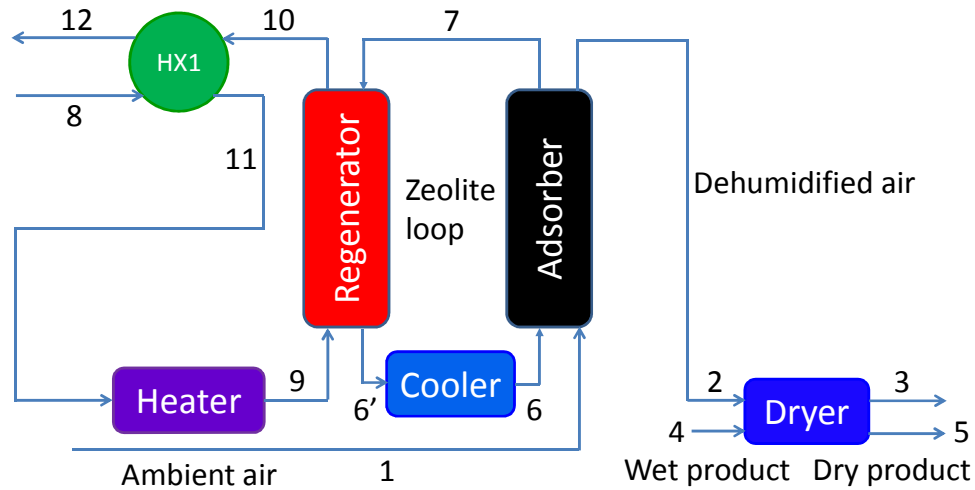


Fig. 2.8. Process flowsheet showing heat recovery by a heat exchanger

Table 2.5. Stream properties for conventional dryer

Stream	Flowrate kg/h	Humidity kg/kg	Temperature °C
1	$7.08 \times 10^4$	0.010	25
2	$7.08 \times 10^4$	0.010	49
3	$7.08 \times 10^4$	0.0151	36
4	36	10	25
5	36	0.05	36

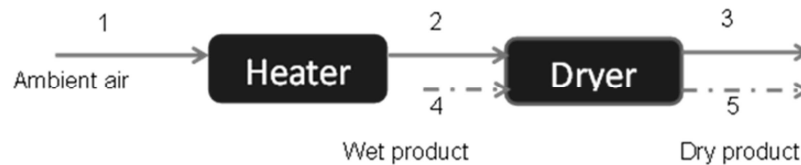


Fig. 2.9. Conventional dryer operating at the same temperature as optimized adsorption dryer

## 2.8. Conclusions

Previous studies showed the potential of adsorption dryers to increase the energy efficiency in low temperature drying based on general knowledge of the system without specific adsorbent, product characteristics and system optimization. In this work a generalized model of an adsorption dryer has been developed with the adsorption, regeneration and drying sub-processes shown to be governed by similar equations. The system has been optimized for energy efficiency subject to quality represented as constraints on product temperature and moisture. In the studied case of pumpkin drying at about 50°C, the optimal adsorption dryer without heat recovery reduces energy consumption by about 20% compared to a conventional dryer. The optimization results show that regenerating at the maximum possible temperature is desirable but on the condition that the regeneration air flowrate is sufficiently low.

This way, high temperature energy is concentrated in low volumes of air, thus reducing the regeneration energy while by no means reducing the regeneration effectiveness and hence, drying capacity of the dehumidified air. The high mass transfer effects of high temperatures are utilized in the regenerator while isolating the heat-sensitive dried product from the quality degrading effect. By preheating the regenerator inlet air using the exhausts, energy consumption is reduced by up to 45% compared to the conventional dryer. For minimum exchanger temperature differences less than 10°C, latent heat is recoverable leading to increased efficiencies but required exchanger area gets very high. Strong interactions between process conditions and heat recovery system are observed from the analysis of Section 2.7.3. This suggests further improvement might be possible by simultaneous optimization of the process and the heat recovery system. This is a subject for future work.

In general, the optimization results show that for a given dryer size, the dehumidification capacity of the adsorber must be high enough to meet the drying requirements of the product without violating temperature constraints in spite of adsorption heat release. The dehumidification must also be low enough to limit regeneration energy expenditure. Low regeneration energies can be realized with high temperatures and low flows. Sensible and latent heat recovery improve efficiency but the extent to which this is implemented must be based on trade-offs between increased capital costs which are proportional to heat exchange area and running costs, the reduction of which is proportional to the amount of heat recovered.

### Improving adsorption dryer energy efficiency by simultaneous optimization and heat integration

Published as Atuonwu, J.C., Straten, G. van., Deventer, H.C. van., Boxtel, A.J.B. van (2011). Improving adsorption dryer energy efficiency by simultaneous optimization and heat integration, *Drying Technology* 29(12), 1459-1471.

#### Abstract

Conventionally, energy saving techniques in drying technology are sequential in nature. First, the dryer is optimized without heat recovery, and then, based on obtained process conditions, heat recovery possibilities are explored. This work presents a methodology for energy efficient adsorption dryer design that considers sensible and latent heat recovery as an integral part of drying system design. A one-step pinch-based optimization problem is formulated to determine the operating conditions for optimal energy performance of such an integrated system subject to product quality. Since the inlet and target stream properties of the heat recovery network are determined by the adsorption drying conditions, they are unknown *a priori* and thus, determined simultaneously within the overall optimization using the pinch location method. Energy balances are written above and below the various pinch point possibilities and the optimal pinch point is that which minimizes the amount of external heating utility required while satisfying drying and thermodynamic constraints. Results on a single-stage zeolite adsorption drying process with simultaneous heat recovery optimization show a 15% improvement in efficiency (13% reduction in energy consumption) compared to a sequentially optimized system. The improvement is traceable to alterations in enthalpy related variables like temperatures and flowrates. The discrepancy in optimal operating conditions between the sequential and simultaneous cases underscores the need to change system operating conditions when retrofitting for heat recovery as previous optimal conditions are sub-optimal when heat recovery is introduced. Also, compared to a conventional dryer (without an adsorption process) operating under similar conditions, energy consumption is reduced by about 55%.

*Keywords:* adsorption drying, energy efficiency, heat recovery, simultaneous optimization, pinch location

#### 3.1. Introduction

Drying accounts for as much as 15% of industrial energy consumption (Kemp, 2005) and so, contributes significantly to industrial operating costs and environmental

impact. Conventional convective dryers have low energy efficiencies particularly at low drying temperatures suitable for heat sensitive products like foods and pharmaceuticals. Consequently, the development of energy efficient drying systems particularly at low drying temperatures becomes important. Thermal efficiency  $\eta$ , the most important index of dryer energy performance, is defined (Kudra, 2004) as the ratio of the latent heat of evaporation  $Q_{evap}$  of the water removed from the product to the total energy input of the dryer  $Q_{in}$ :

$$\eta = \frac{Q_{evap}}{Q_{in}} \quad (3.1)$$

To increase the capacity of the air to evaporate water from the product at low drying temperatures and hence  $Q_{evap}$ , zeolite adsorption drying has been proposed. (Djaeni et al., 2007a; Atuonwu et al., 2010a; Hauer, 2011; Djaeni et al., 2007b; Djaeni et al., 2008) The main energy input is in adsorbent regeneration which typically takes place at high temperatures. This in itself presents opportunities for beneficial heat integration as the regenerator exhaust has high energy content with minimal dusts. Recently, Atuonwu et al. (2010a) showed by mathematical programming that under optimized conditions of regeneration temperature, drying air, regeneration air and zeolite flows, a one-stage adsorption dryer without heat recovery consumes 20% less energy than a conventional dryer for the same moisture evaporation. By recovering the energies of the exhaust streams of the optimized process using pinch analysis, energy consumption is reduced by 45%.

Heat recovery has long been identified (Strumillo et al., 1995; Krokida and Bisharat, 2004; Laurijssen et al., 2010; Moraitis and Akiritidis, 1997; Atkins et al., 2010) as a means of improving the energy efficiency of dryers. As most of the heat used in conventional convective drying appears in the dryer exhaust air stream (Moraitis and Akiritidis, 1997), heat recovery for conventional dryers typically entails preheating the dryer inlet air by the exhaust air using heat exchangers (Strumillo et al., 1995; Krokida and Bisharat, 2004; Laurijssen et al., 2010; Moraitis and Akiritidis, 1997). Substantial energy savings have been shown by heat recovery from dryer exhaust air streams. For instance, Krokida and Bisharat (2004) report that 25% of the exhaust air energy is recovered using heat exchangers in a drying application. The percentage increases to about 40% using a heat pump, heat exchanger combination. Using a heat exchanger system complemented by intelligent optimal control, up to 30% of the exhaust air heat could be recovered in a drying system (Moraitis and Akiritidis, 1997). Similarly, Atkins et al. (2010) report energy savings in the order of 21% in heat recovery for a spray drying plant. Nevertheless, industrial dryers usually operate without any provision for heat recovery (Moraitis and Akiritidis, 1997). One reason for this is the presence of dust in the dryer exhaust air as a result of which, heat exchanger fouling is a major problem (Kaiser et al., 2002).



For zeolite adsorption dryers however, energy is recovered from the regenerator which is less prone to dust. Furthermore, for low temperature conventional dryers, the exhaust air temperature is too low (close to ambient), thus rendering heat recovery thermodynamically and economically infeasible (Atuonwu et al., 2010a). This limitation is overcome in adsorption dryers since the regenerator exhaust contains high temperature energy. In general, heat recovery is only considered after energy auditing on the existing drying process. The common reasoning is that the heat flows of the dryer streams must first be optimized for energy performance before the determination of a heat recovery scheme (Kemp, 2005). Dryer heat recovery cases in literature e.g. (Strumillo et al., 1995; Krokida and Bisharat, 2004; Laurijssen et al., 2010; Moraitis and Akiritidis, 1997; Tippayawong et al., 2008; Sivill and Ahtilla, 2009; Gong et al., 2011) have thus, always concentrated on already designed dryers. Hence, current energy saving techniques in drying technology can be said to be largely sequential in nature. From an optimization standpoint, this entails first minimizing the energy input ( $Q_{in}$ ) for a given evaporative energy load ( $Q_{evap}$ ) and then, maximizing the heat recovered ( $Q_{rec}$ ) based on the values of the process variables returned by the dryer optimization. Although this approach has the advantage of distributing the computational load over two simpler optimization problems, it does not give globally optimal solutions since interactions among the variables  $Q_{in}$ ,  $Q_{evap}$  and  $Q_{rec}$  are not considered. It is known for instance that for conventional dryers, energy efficiency is increased when for a given inlet air temperature, the exhaust temperature is made as low as possible (Kudra, 2004). What this also means is that the scope of heat recovery is reduced. Similarly, Atuonwu et al. (2010a) showed that for an adsorption dryer, the magnitude of the product  $F_{aR}T_{aRin}$  of the regeneration air flow  $F_{aR}$  and inlet temperature  $T_{aRin}$  is critical to energy savings. While an increase in  $F_{aR}T_{aRin}$  reduces energy efficiency, it at the same time, increases the heat recovery possibilities. The converse is also true. These results suggest the possibility of a better optimum when the dryer and heat recovery are simultaneously optimized for overall energy efficiency. In conventional dryers operating at low temperatures however, the improvement potential of simultaneous optimization is limited by thermodynamic constraints, because the only available energy source (the dryer exhaust air) is at low temperature. In “assisted” systems, e.g., zeolite adsorption dryers where there are more independent heat sources and sinks, simultaneous optimization is expected to yield significant improvements in energy performance, especially as high temperature heat sources are available via the regenerator. The improvement potential is expected to increase with system complexity (number of sources and sinks) – e.g. for multistage systems.

Applications of simultaneous optimization (usually based on complex mixed integer nonlinear programming (MINLP) models) to various processes like water allocation, bio-ethanol process and thermo-chemical hybrid biomass plants, thermally coupled distillation and reactor/separator systems are available in literature (Dong et al., 2008; Francesconi et al., 2011; Baliban et al., 2011; Yiqing et al., 2010; Papalexandri and Pistikopoulos, 1998) but not in drying. In view of the significant contribution of

drying to global energy consumption, it becomes important to explore this option for improved energy efficiency. The aim of this study is to exploit the possibilities of simultaneous process and heat recovery optimization in an adsorption drying process to improve the overall energy efficiency while satisfying constraints on product temperature and moisture content.

In this work, sensible and latent heat recovery are considered an integral part of the adsorption drying process design, while ensuring that product quality, represented by temperature constraints is not compromised. The simultaneous optimization is based on the pinch point location method Duran and Grossmann (1986), modified in this work to include latent heat recovery possibilities. Selected process inlet and outlet streams of unknown temperatures and flowrates are inputs to the heat exchanger network. Since these properties are unknown *a priori*, they are calculated within the overall optimization. After determining the continuous variables for which the overall system is maximally efficient, the ultimate configuration can be implemented in more than one way as will be shown later. This final design is achieved heuristically.

### 3.2. General problem statement

Conventional pinch analysis depends on the availability of knowledge on the process enthalpy variables, namely the flowrates, supply and target temperatures. In a sequentially optimized system e.g. as in Atuonwu et al. (2010a) the process flowrates and temperatures as returned by the dryer optimization are then used as inputs for pinch analysis and optimal heat recovery. In systems not previously optimized (Djaeni et al., 2007a; Strumillo et al., 1995; Krokida and Bisharat, 2004; Laurijssen, et al., 2010; Moraitis and Akiritidis, 1997; Tippayawong et al., 2008; Sivill and Ahtilla, 2009), the design of heat recovery systems is also based on the given process operating conditions. In a simultaneously optimized system however, neither the target temperatures for which the heat recovery system should be designed, nor the supply temperatures as determined by the drying process is known. Also, process stream flowrates which determine the stream heat capacities are unknown *a priori*. These variables must be included as optimization decision variables unlike in conventional pinch analysis where the aim is to determine which stream matches would yield the highest heat recovery, given already known flows and temperatures.

The problem addressed in this work is formulated as:

Given:

- An adsorption drying process of a given structure (see Fig. 3.1) with dried product, adsorbent and air kinetic and equilibrium relations.
- A set of possible hot and cold streams from the process, determined on the basis of prior process knowledge

To:

- Determine the operating conditions that will maximize overall energy efficiency, taking into consideration, the heat recovery from the outlet streams of the adsorption drying process.
- Ensure that product quality represented by constraints on product temperature is not compromised.
- Design, using heuristic rules, the overall system based on optimization results

### 3.3. Process description

The basic adsorption drying process as shown in Fig. 3.1 consists of the dryer, heat sources and a zeolite adsorption/regeneration system. Ambient air is passed through a zeolite adsorber bed where it is dehumidified (a process accompanied by sorption heat release) and then used for drying the wet product. The spent zeolite is regenerated using hot air obtained by passing ambient air through a heater. The zeolite circulates alternately between the adsorber and the regenerator. To regain adsorption capacity after regeneration, the hot zeolite is cooled. For practical implementation, the adsorption-regeneration system is usually fitted as an add-on to the dryer. For continuous operation, available configurations include rotary wheels with adsorption, regeneration and purge sections (Harshe et al., 2005) and twin column system with alternate switching between columns for adsorption-regeneration operations (Djaeni et al., 2009a). Rotary wheels have better operability properties than twin-column systems as switching transients are avoided. For the former, the zeolite mass flowrate is determined by wheel diameter, thickness and angular speed while for the latter; it is determined by the zeolite height in the column and switching time. Due to the high regeneration temperatures usually employed, the regenerator outlet air and zeolite have high energies available for exchange with potential cold streams. The cold streams include the ambient air to the adsorber and the ambient air to the regenerator (both of which could be preheated before passing through a Heater).

Atuonwu et al. (2010a) developed a mathematical model describing the continuous operation of the adsorption drying system based on mass and energy balances around the individual units. Complete details of the model including the modeling assumptions, constitutive and coupling equations are available in Atuonwu et al. (2010a) and presented concisely in Appendix B. The product considered in this work was pumpkin, to be dried at a maximum temperature of 50°C. From a degree of freedom analysis (Atuonwu et al. 2010a), key decision variables to maximize adsorption dryer energy efficiency (see Fig. 3.1) are regeneration air inlet temperature,  $T_{aRin}$ , ratio  $r_0 = F_{aA}/F_p$  of drying air to product flowrates, ratio  $r_1 = F_z/F_{aA}$  of zeolite to drying air flowrates, and ratio  $r_2 = F_{aR}/F_z$  of regeneration air to zeolite flowrates. These variables also determine the heat capacity rates and temperatures of the process streams. They thus determine the energy properties of the hot streams as well as the energy requirements of the cold streams.

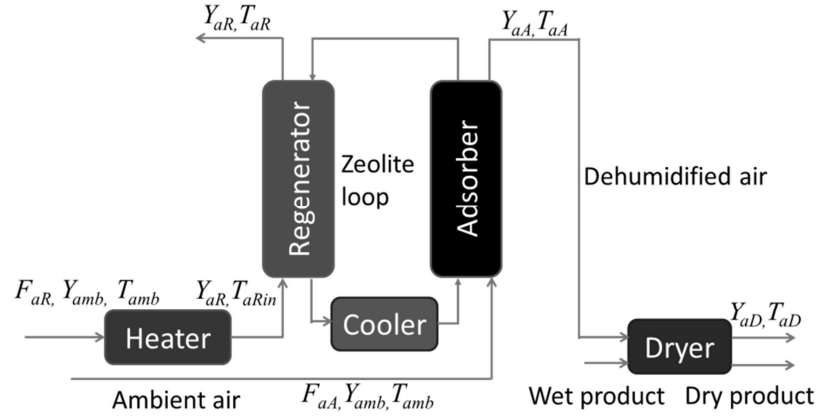


Fig. 3.1. Drying system process configuration with adsorber-regenerator subsystem

### 3.4. Methodology

#### 3.4.1. Simultaneous Heat Integration

The following outputs that are important from the perspective of energy efficiency are defined. The instantaneous energy rate associated with the removed water is given by

$$Q_{evap} = F_p (X_{pin} - X_p) \Delta H_v \quad (3.2)$$

The outlet air temperature of the adsorber after sorption heat release is high enough for low temperature drying hence, the instantaneous total input energy rate for the process is that required for regeneration

$$Q_{in} = F_{aR} (C_{pa} + Y_{aRin} C_{pv}) (T_{aRin} - T_{amb}) \quad (3.3)$$

If part of this energy  $Q_{rec}$  is recovered using a heat exchanger network (HEN), then, the effective heating utility required is

$$q_h = Q_{in} - Q_{rec} \quad (3.4)$$

Effective energy efficiency is thus defined as

$$\eta_{eff} = \frac{Q_{evap}}{q_h} = \frac{Q_{evap}}{Q_{in} - Q_{rec}} \quad (3.5)$$

Heat recovery is achieved by heat exchange between hot and cold streams. Based on prior knowledge of the process behavior, the hot streams are:

- Exhaust air from the regenerator, H1
- Outlet zeolite from the regenerator, H2

The cold streams are:

- Ambient air to the regenerator, C1
- Ambient air to the adsorber, C2

Fig. 3.2 shows the heat recovery streams as designated in Table 3.1. H1 (stream 11) enters the HEN and after cooling, exits as stream 12. H2 enters the HEN from the regenerator as stream 6' and after cooling (by heat exchange and possibly, utility cooling), returns to the adsorber as stream 6. Similarly, ambient air, C1 enters the HEN for preheating as stream 8 and exits as stream 9, before heating (in the Heater) to the desired temperature as determined by the optimizer, while C2 is ambient air (stream 0) preheated in the HEN before feeding the adsorber as stream 1.

### 3.4.2. Pinch Point Optimization

Although the hot and cold streams are known, the exact values of their energy properties, i.e., flowrates, heat capacity rates and temperatures are unknown *a priori*. Consider the hypothetical temperature-enthalpy diagram (Fig. 3.3). In a sequentially

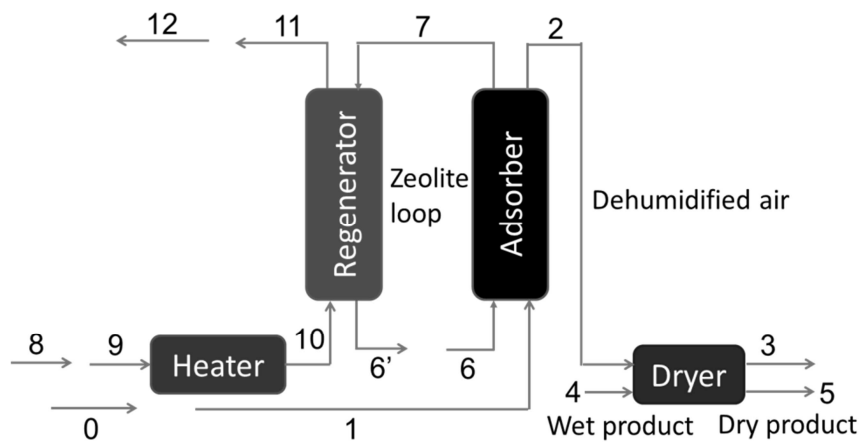


Fig. 3.2. Drying system process configuration showing heat recovery streams (numbered)

Table 3.1. Designation of streams as shown in Fig. 3.2

Stream type	Designation	Stream number
Hot	H1 to HEN	11
Hot	H1 from HEN	12
Hot	H2 to HEN	6'
Hot	H2 from HEN	6
Cold	C1 to HEN	8
Cold	C1 from HEN	9
Cold	C2 to HEN	0
Cold	C2 from HEN	1

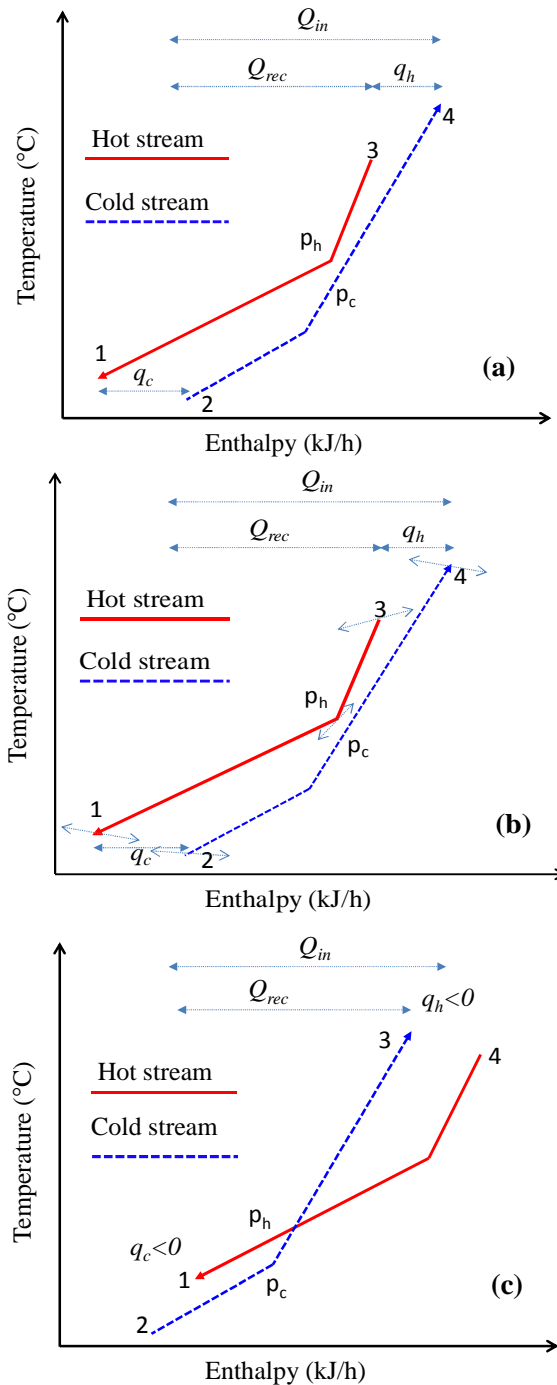


Fig. 3.3. Hypothetical temperature-enthalpy diagram (a). Sequentially optimized system with fixed pinch point (b). Simultaneously optimized system with variable edges (see arrows at 1, 2, 3,4) and pinch point (c). Infeasible option rejected in simultaneous optimization;  $q_h$  and  $q_c$  are minimum heating and cooling requirements respectively

optimized system, the stream temperatures (co-ordinates of points 1, 2, 3, 4 on the temperature axis) and the heat capacity rates (which determine the slopes of each portion of the graph) are determined in the first optimization step (drying process optimization). There thus exists a unique pinch point [ $p_h$   $p_c$ ] (see Fig. 3.3(a)) for a given  $dT_{min}$  which can be determined by a straight-forward application of pinch

analysis for optimal heat recovery. In simultaneous optimization however, some temperatures (e.g. co-ordinates of points 3 and 4) are free to move (as shown by the arrows at points 1, 2, 3, 4 and the pinch point in Fig. 3.3(b)). In addition, the heat capacity rates which determine the slope/shape of each region are unknown. There is therefore no unique pinch point, but a set of pinch point candidates. The optimal pinch point must be determined through optimization, implicitly by varying the slopes of the different portions of the graph and the temperature co-ordinates (1, 2, 3 & 4) as seen in Fig. 3.3(b). Meanwhile, the co-ordinates and shapes of the temperature-enthalpy diagram interact with the drying process and must be such that the drying requirements e.g. desired drying capacity  $Q_{evap}$  are met. In the same vein, the drying process must create stream properties such that the thermodynamic constraints on heat exchange (e.g.  $dT_{min}$ ) are satisfied.

Pinch point candidates for which  $dT_{min}$  is negative in some region of the temperature-enthalpy diagram or for which at least either the heating or cooling requirements are unrealistic (e.g. as seen in Fig. 3.3(c)) are infeasible and hence, rejected by the optimizer. To reduce the search space of possible pinch points, it is assumed that the pinch point occurs at one of the inlet sides of the possible heat exchangers. The philosophy behind this assumption is that a cold stream can only heat up until it is limited by the inlet temperature of the hot stream which is on the other side (for a counter-current heat exchanger). The converse is also true.

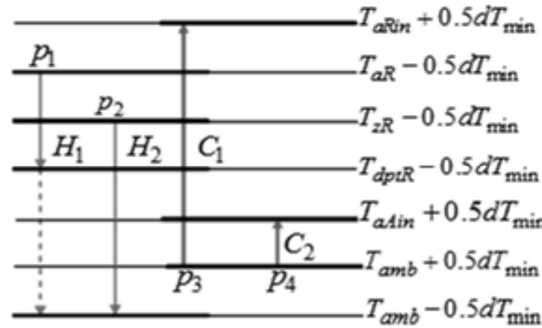


Fig. 3.4. Heat recovery grid where  $p_1$ ,  $p_2$ ,  $p_3$  &  $p_4$  are pinch point candidates;  $H_1$  &  $H_2$  hot streams;  $C_1$  &  $C_2$ , cold streams;  $T_{aRin}$ , Regeneration air inlet temperature,  $T_{aR}$ , Regeneration air outlet temperature,  $T_{zR}$ , regenerator zeolite outlet temperature,  $T_{dptR}$ , regenerator outlet air dewpoint,  $T_{aAin}$ , adsorber air inlet temperature and  $T_{amb}$ , ambient air temperature

Table 3.2. Stream properties of adsorption drying process

Stream	Supply Temp.	Target Temp.	Flowrate	Heat Capacity
H1	$T_{aR}$	$T_{amb}$	$F_{h1} = F_{aR}$	$C_{ph1} = C_{pa} + Y_{aR}C_{pv}$
H2	$T_{zR}$	$T_{amb}$	$F_{h2} = F_z$	$C_{ph2} = C_{pz} + X_{zR}C_{pv}$
C1	$T_{amb}$	$T_{aRin}$	$F_{c1} = F_{aR}$	$C_{pc1} = C_{pa} + Y_{aRin}C_{pv}$
C2	$T_{amb}$	$T_{aAin}$	$F_{c2} = F_{aA}$	$C_{pc2} = C_{pa} + Y_{amb}C_{pv}$

The heat recovery network possibilities are represented by the grid diagram of Fig. 3.4 with stream properties as shown in Table 3.2. The hot streams have their supply and target temperatures shifted downwards by one-half the minimum approach temperature  $dT_{min}$  while those of the cold streams are shifted upwards by the same value. The dotted line represents the possible condensation of the moist air stream (by cooling below its dew point  $T_{dptR}$ ) during heat recovery. In this region, potential heat exchange is determined as equal to the mass of moisture condensed in the cooling process multiplied by the latent heat of evaporation. p1, p2, p3 and p4 denote possible pinch points. p1 and p2 are hot stream (H1 and H2) pinch points respectively with the corresponding cold stream pinch points located at least  $dT_{min}$  below them on the temperature axis. p3 and p4 are cold stream (C1 and C2) pinch points respectively with corresponding hot stream pinch points located at least  $dT_{min}$  above them on the temperature axis. Above a pinch point, a heat deficit exists between the hot and cold process streams. Below the pinch, a heat surplus exists. By writing heat balances above and below each pinch candidate, the minimum external heating and cooling utilities to meet the deficit and surplus respectively can be established.

Denoting the minimum heating and cooling utility needs by the subscript  $hu$  and  $cu$ , respectively, and the hot and cold streams by subscripts  $h$  and  $c$ , respectively, the heat balances above and below the various pinch possibilities are:

Above p1,

$$q_{hu1} = F_{c1}C_{pc1}(T_{aRin} - dT_{min} - T_{aR}) \quad (3.6)$$

Below p1,

$$q_{cu1} = F_{h1}C_{ph1}(T_{aR} - T_{dptR}) + F_{h2}C_{ph2}(T_{zR} - T_{amb}) - F_{c1}C_{pc1}(T_{aR} - T_{amb} - dT_{min}) - F_{c2}C_{pc2}(T_{aAin} - T_{amb}) + F_{h1}\Delta H_v(Y_{aR}(T_{aR}) - Y_{aR}(T_{amb} - 0.5dT_{min})) \quad (3.7)$$

Above p2,

$$q_{hu2} = F_{c1}C_{pc1}(T_{aRin} + dT_{min} - T_{zR}) - F_{h1}C_{ph1}(T_{aR} - T_{zR}) \quad (3.8)$$

Below p2,

$$q_{cu2} = F_{h1}C_{ph1}(T_{zR} - T_{dptR}) + F_{h2}C_{ph2}(T_{zR} - T_{amb}) - F_{c1}C_{pc1}(T_{zR} - T_{amb} - dT_{min}) - F_{c2}C_{pc2}(T_{aAin} - T_{amb}) + F_{h1}\Delta H_v(Y_{aR}(T_{aR}) - Y_{aR}(T_{amb} + 0.5dT_{min})) \quad (3.9)$$

Above p3,

$$q_{hu3} = F_{c1}C_{pc1}(T_{aRin} - T_{amb}) + F_{c2}C_{pc2}(T_{aAin} - T_{amb}) - F_{h1}C_{ph1}(T_{aR} - T_{dptR}) - F_{h2}C_{ph2}(T_{zR} - T_{amb} - dT_{min}) - F_{h1}\Delta H_v(Y_{aR}(T_{aR}) - Y_{aR}(T_{amb} + 0.5dT_{min})) \quad (3.10)$$



Below p3,

$$q_{cu3} = F_{h1}\Delta H_v(Y_{aR}(T_{aR}) - Y_{aR}(T_{amb} + 0.5dT_{min})) + F_{h2}C_{ph2}dT_{min} \quad (3.11)$$

Above p4,

$$q_{hu4} = q_{hu3} \quad (3.12)$$

Below p4,

$$q_{cu4} = q_{cu3} \quad (3.13)$$

If  $q_{hu} = \{q_{hu1}, q_{hu2}, q_{hu3}, q_{hu4}\}$  and  $q_{cu} = \{q_{cu1}, q_{cu2}, q_{cu3}, q_{cu4}\}$ , the true pinch point candidate that assures minimum external energy usage under feasible heat exchange is that which features the maximum of both  $q_{hu}$  and  $q_{cu}$  (Duran and Grossmann, 1986). The maximum values of these minimum utilities arise because for any other pinch point candidate apart from the true pinch point, there is infeasible heat exchange. As a result, somewhere in the temperature-enthalpy diagram (e.g. as shown in Fig. 3.3(c)), thermodynamic constraints are violated so that negative, zero or less than realistic heating and cooling utilities are obtained for all except the true pinch point.

Hence, the optimal pinch point simultaneously satisfies the conditions:

$$q_h = \max(q_{hu1}, q_{hu2}, q_{hu3}, q_{hu4}) \quad (3.14)$$

$$q_c = \max(q_{cu1}, q_{cu2}, q_{cu3}, q_{cu4}) \quad (3.15)$$

$q_h$  and  $q_c$  are minimum heating and cooling duties respectively at actual pinch point.

### 3.4.3. Optimization Problem Formulation

The optimization problem is formulated as,

$$\text{Maximize } \eta_{eff} = \frac{Q_{evap}}{q_h} = \frac{F_p(X_{pin} - X_p)\Delta H_v}{q_h} \quad (3.16)$$

subject to process equations, minimum utility as well as the following product moisture, temperature and zeolite regeneration temperature constraints

$$\text{Final product moisture content: } X_p = 0.05 \quad (3.17)$$

$$\text{Product temperature } T_p \leq 50 \quad (3.18)$$

$$\text{Zeolite regeneration temperature limits: } T_{aRin_{min}} \leq T_{aRin} \leq 400 \quad (3.19)$$

In equation 3.16, it is assumed that no costs are involved with the cooling utility. The optimization problem is implemented in TOMLAB® Optimization software (Tomlab Optimization Inc., Seattle, WA) with MATLAB interface using the “KNITRO” solver–based interior-point method. The method uses an iterative conjugate gradient approach to compute each optimization step.

For comparison, a conventional convective dryer (Fig. 3.5) operating at the same temperature but without dehumidification is also simultaneously optimized for heat recovery. In this approach, the only hot stream is the outlet air which is used to pre-heat the cold inlet ambient air stream. The simultaneous optimization is also based on the pinch location method with the heat recovery grid as shown in Fig. 3.6. The heat balances written above and below potential pinch points  $p_{D1}$  and  $p_{D2}$  are as follows:

Above  $p_{D1}$ ,

$$q_{hu1(D)} = F_{aD}(C_{pa} + Y_{amb}C_{pv})(T_{aDin} - T_{aD} + dT_{min}) \quad (3.20)$$

Below  $p_{D1}$ ,

$$q_{cu1(D)} = F_{aD}(C_{pa} + Y_{aD}C_{pv})(T_{aD} - T_{dptD}) + F_{aD}\Delta H_v(Y_{aD} - Y_{aD}(T_{amb} - 0.5dT_{min})) - F_{aD}(C_{pa} + Y_{amb}C_{pv})(T_{aDin} - T_{amb}) \quad (3.21)$$

Above  $p_{D2}$ ,

$$q_{hu2(D)} = F_{aD}(C_{pa} + Y_{amb}C_{pv})(T_{aDin} - T_{amb}) - F_{aD}(C_{pa} + Y_{aD}C_{pv})(T_{aD} - T_{amb} - dT_{min}) \quad (3.22)$$

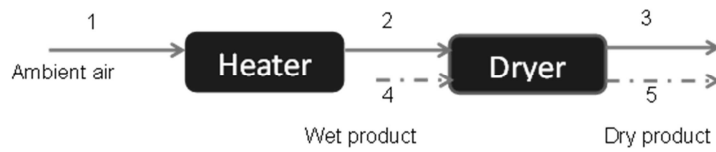


Fig. 3.5. Conventional dryer operating at the same temperature as optimized adsorption dryer

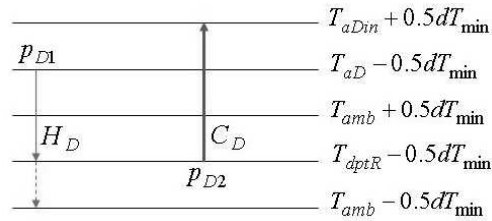


Fig. 3.6. Simultaneous heat recovery grid for conventional dryer where  $p_{D1}$  and  $p_{D2}$  are pinch point candidates,  $T_{aDin}$  dryer inlet air temperature,  $T_{aD}$ , dryer outlet air temperature,  $T_{dptR}$  dryer outlet air dew point,  $T_{amb}$ , ambient air temperature

Below  $p_{D2}$ ,

$$q_{cu2(D)} = F_{aD} (C_{pa} + Y_{aD} C_{pv}) (T_{amb} - T_{dptD} + dT_{min}) \quad (3.23)$$

The optimization problem (3.16) is then solved under conditions (3.14) and (3.15).

### 3.5. Results and discussion

#### 3.5.1. System Optimization

The minimum hot and cold utility demands returned by the optimizer at each potential pinch point  $p$  indicate that the optimal pinch point which satisfies equations (3.14) and (3.15) is located on  $p1$  (the hot stream H1 inlet). The pinch temperature is  $188^{\circ}\text{C}$  on the hot stream side. The minimum heating utility demand at this point is  $q_h = q_{hu1} = 7.95 \times 10^5 \text{ kJ/h}$  while the minimum cooling utility is  $q_c = q_{cu1} = 2.3 \times 10^5 \text{ kJ/h}$ . These correspond to the minimum hot and cold utility targets featured in the optimization constraints. For the sequentially optimized system, the pinch occurs at  $170^{\circ}\text{C}$  on the hot stream side with the corresponding minimum hot and cold utility targets as  $9.04 \times 10^5 \text{ kJ/h}$  and  $6.4 \times 10^5 \text{ kJ/h}$  respectively. The process variables determined by the optimizer for the simultaneously optimized system are shown in Table 3.3, compared with corresponding values for the sequentially optimized system. The stream numbering is as specified in Fig. 3.2. A striking observation is the 15% improvement in energy efficiency for the simultaneously optimized system. This improvement is traceable to the differences in the decision variables, and hence, other process variables. For a complex system like the one under study, an explanation for the differences is non-trivial. A possible explanation for the differences in the decision variables and how efficiency is affected is as follows. In the case of simultaneous optimization, the ambient air to the adsorber (stream 0, see Table 3.3) is now preheated from  $25$  to  $29^{\circ}\text{C}$  (stream 1). This results in a slight increase in adsorber outlet air temperature (stream 2). The adsorber outlet air humidity is lowered thus, for the same product flowrate; less air flow is needed to achieve the same evaporation.

The results of the simultaneous optimization also show better zeolite utilization as the difference between the adsorber and regenerator zeolite moisture contents (streams 6 and 7) is higher here. This allows a lower flowrate of zeolite to achieve more dehumidification. For this lower zeolite flowrate, a lower flowrate of regeneration air would be expected at first thought especially as this would reduce the energy spent heating it up to the required regeneration temperature. However, a higher regeneration air flowrate favours heat recovery. Atuonwu et al. (2010a) showed that although efficiency without heat recovery reduces with regeneration air flowrate, the quantity of heat recovered increases with it.

Table 3.3. Optimal process variables for simultaneous and sequential cases compared

Stream	<i>Simultaneous: Efficiency, 113%</i>			<i>Sequential: Efficiency 98% with heat recovery</i>		
	Flowrate (kg/h)	Humidity (kg/kg) db	Temperature (°C)	Flowrate (kg/h)	Humidity (kg/kg) db	Temperature (°C)
0	$5.07 \times 10^4$	0.01	25	$5.3 \times 10^4$	0.01	25
1	$5.07 \times 10^4$	0.01	28	$5.3 \times 10^4$	0.01	25
2	$5.07 \times 10^4$	0.0031	49.5	$5.3 \times 10^4$	0.0038	49
3	$5.07 \times 10^4$	0.0101	31.3	$5.3 \times 10^4$	0.0106	31.8
4	36	10	25	36	10	25
5	36	0.05	31	36	0.05	31
6	$2.9 \times 10^3$	0.0403	185	$4.1152 \times 10^3$	0.0868	35
6	$2.9 \times 10^3$	0.0403	35	$4.1152 \times 10^3$	0.0868	35
7	$2.9 \times 10^3$	0.1611	49	$4.1152 \times 10^3$	0.1664	49
8	$8.96 \times 10^3$	0.01	25	$3.7134 \times 10^3$	0.01	25
9	$8.96 \times 10^3$	0.01	265	$3.7134 \times 10^3$	0.01	400
10	$8.96 \times 10^3$	0.0492	188	$3.7134 \times 10^3$	0.0982	170
Energy consumption= $7.95 \times 10^5$ kJ/h Specific energy consumption =2219 kJ/kg water evaporated			Energy consumption= $9.04 \times 10^5$ kJ/h Specific energy consumption =2524 kJ/kg water evaporated			

In simultaneous optimization both factors are taken into consideration in one step. The optimizer looks beyond the process alone and finds the operating conditions for which both the process and heat recovery are simultaneously optimized so that overall efficiency is optimal. Also, with a higher regeneration air flowrate, the heat capacity rate is increased which leads to an increased “reluctance” to temperature drop (note: by definition, the higher the heat capacity rate, the higher the energy that must be lost to achieve a temperature reduction of 1°C). This explains why the temperature drop across the regenerator (265 to 188°C) is much less than the one for the sequential case (streams 10 and 11). A higher regeneration air outlet temperature (188°C as against 170°C for the sequential case, stream 11) means more sensible heat is available for recovery. Finally, a higher regeneration air flow is justified because for the simultaneously optimized system, there is more dehumidification (ambient air is dehumidified to 0.0031kg/kg as against 0.0038kg/kg in the sequential system). More regeneration energy is thus needed, but since the regeneration air inlet temperature is reduced, the regeneration flowrate is increased. The result is that more energy is spent on regeneration in the simultaneously optimized system but with a much higher heat recovery so that overall, less energy is spent. From the foregoing, simultaneous process optimization and heat integration is seen to entail the manipulation of process stream temperatures, heat capacities, and in the particular case of drying, condensation properties like dew point so that overall system energy performance is optimized within constraints.

3.5.2. Possible Implementation

Fig. 3.7 shows a possible design implementation of the heat recovery within the simultaneously optimized adsorption drying system. Conditions of streams 1 to 12 are the same as presented in Table 3.3. Ambient air (stream 0) is preheated by the zeolite exiting the regenerator from 25 to 29°C. The hot zeolite (stream 6' at 185°C) is cooled in the process to 114.5°C (stream 6''). At the same time, the regenerator exhaust air (stream 11 at 188°C) preheats the ambient air (stream 8 at 25°C) to a temperature of 178°C (stream 9). Stream 11 thus cools down from 188 to 46 °C (stream 12). Extra heat is then supplied to stream 9 by the heater to achieve the required temperature of 265°C (stream 10). Here, latent heat is not recovered. Another possible implementation of the optimal heat recovery is shown in Fig. 3.8. Here, instead of recovering the sensible heat of the regenerator outlet zeolite, the outlet air from the first heat exchanger HX1 (stream 12) at 46°C (and a dew point of 40.5°C) is cooled down to 38°C (stream 13) using heat exchanger HX2. In so doing, part of its latent heat is recovered and used in pre-heating the ambient air to the adsorber. Any of these methods can be implemented as there is no distinct energy advantage in giving priority to either high grade sensible heat recovery (from the zeolite) or latent heat

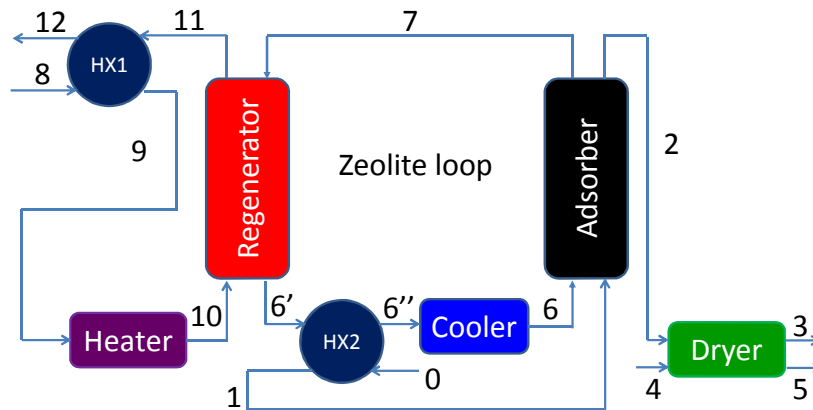


Fig. 3.7. Adsorption drying system showing sensible heat recovery through heat exchangers HX1 and HX2

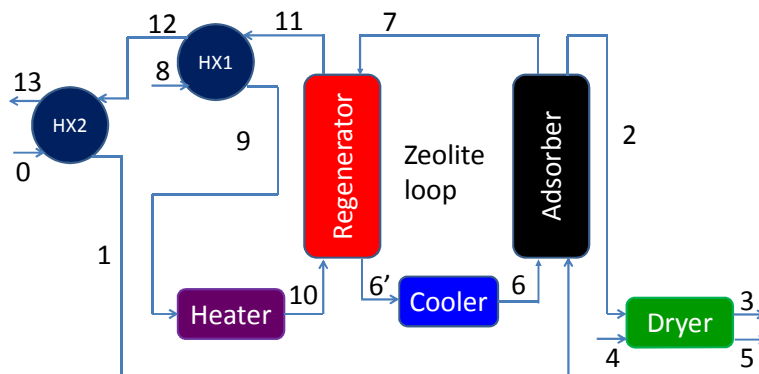


Fig. 3.8. Adsorption drying system showing heat exchangers with latent heat recovery through HX2

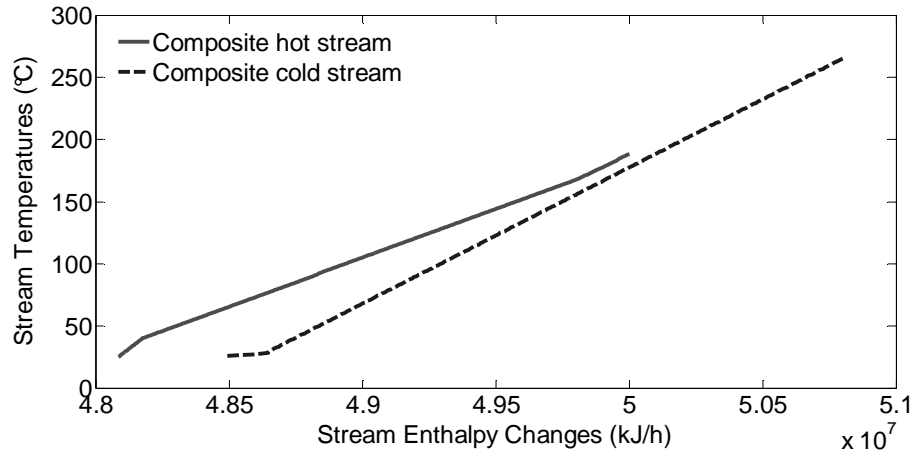


Fig. 3.9. Composite curve of simultaneously optimized system

recovery (from the previously cooled regenerator exhaust air). Decisions on the eventually applied method would be based primarily on an appraisal on which option is more technically and economically feasible. Fig. 3.9 shows a composite curve of the system, and in general, part of the sensible and latent heat cannot be recovered from the adsorption drying process (as shown in the cooling requirement). This opens opportunities for energy integration with surrounding low temperature processes when considered in relation to other unit operations in a process plant.

### 3.5.3. Performance Comparisons with Conventional Systems

To further compare the simultaneously and sequentially optimized systems (under similar conditions), the drying system without heat recovery (Fig. 3.1) is simulated with the optimal operating conditions returned by simultaneous optimization. An interesting observation is that without heat recovery an energy efficiency of 41% is obtained. This is much less than the optimal value of 63% obtained for the sequentially optimized system (Atuonwu et al., 2010a). Whereas, when heat is optimally recovered (by simultaneous optimization) from this relatively inefficient system, the overall efficiency becomes 15% higher than that of the initially optimal system even with heat later recovered. This clearly demonstrates that when retrofitting systems for heat recovery, the system has to be “re-tuned” for optimal performance since initially optimal operating conditions may become sub-optimal with the introduction of heat recovery. Thus, simultaneous optimization is useful in revamping existing dryers operating sub-optimally without heat recovery. It provides a means of determining new optimal conditions when heat recovery is eventually considered as against merely recovering heat based on existing operating conditions (which is sub-optimal). Slight design modifications (e.g. in pipe-work) may or may not be required to cater for the new flows and temperatures returned by the simultaneous optimizer.

For a simultaneously optimized conventional dryer, the results as presented in Table 3.4 show an energy consumption of  $1.64 \times 10^6$  kJ/h for the same evaporative load

Table 3.4. Optimal stream properties and energy use for conventional dryer

<i>Stream</i>	<i>Flowrate (kg/h)</i>	<i>Humidity (kg/kg) db</i>	<i>Temperature (°C)</i>
1	7.0835x10 <sup>4</sup>	0.01	26.25
2	7.0835x10 <sup>4</sup>	0.01	49.5
3	7.0835x10 <sup>4</sup>	0.0151	36.25
4	36	10	25
5	36	0.05	36
Energy consumption = 1.64x10 <sup>6</sup> kJ/h			
Specific energy consumption = 4578 kJ/kg water evaporated			

$Q_{evap}=8.995 \times 10^5$ kJ/h. The same result is obtained when the system is sequentially optimized. It can therefore be concluded that simultaneous optimization does not yield any benefit for a conventional dryer operating at low temperatures. If however higher operating temperatures are used (e.g. for materials less sensitive to heat), simultaneous optimization will exploit the high energy potential of the dryer exhaust just like for the regenerator exhaust of the adsorption drying system. The conventional dryer requires more air flow for the same product moisture evaporation (compare flowrates of stream 1 in Tables 3.3 & 3.4). Hence, more energy is spent to heat this air to the required temperature. The benefit of adsorption heat release does not accrue to this process. Moreover, since there is no dehumidification, drying capacity is reduced. Also, the severe thermodynamic limits on the only heat recovery source (the dryer exhaust air at 36°C) means that very little heat can be economically recovered. For instance, for a heat exchanger temperature difference of 10°C, the ambient air of 25°C is only heated by 1°C. Comparing the results of Tables 3.3 and 3.4, the simultaneously optimized adsorption dryer is seen to reduce energy consumption by about 55% compared to the conventional dryer for the same evaporative load and drying temperature.

### 3.5.4. Sensitivity Analysis Results

Ambient conditions are not constant in practice and hence, it is important to know how sensitive the optimization results are to ambient condition variations. Figs. 3.10 (a) – (d) show the variation of system energy efficiency with ambient conditions for the conventional dryer, sequentially optimized adsorption dryer (before and after heat recovery) and the simultaneously optimized adsorption dryer.

The temperature-humidity combinations chosen are as obtainable in the Netherlands. As ambient temperature increases, ambient absolute humidity also tends to increase, so that of all patterns shown in Fig. 3.10 the ones along the diagonal are the most likely to occur. For the conventional low temperature dryer (Fig. 3.10 (a)), the efficiency drops substantially with decreasing ambient temperature since the heat required to raise the drying air to the required drying temperature rises as ambient temperature falls. Also, as air humidity falls, efficiency tends to rise since the drying capacity of the air increases. However, the higher efficiency values in the top right

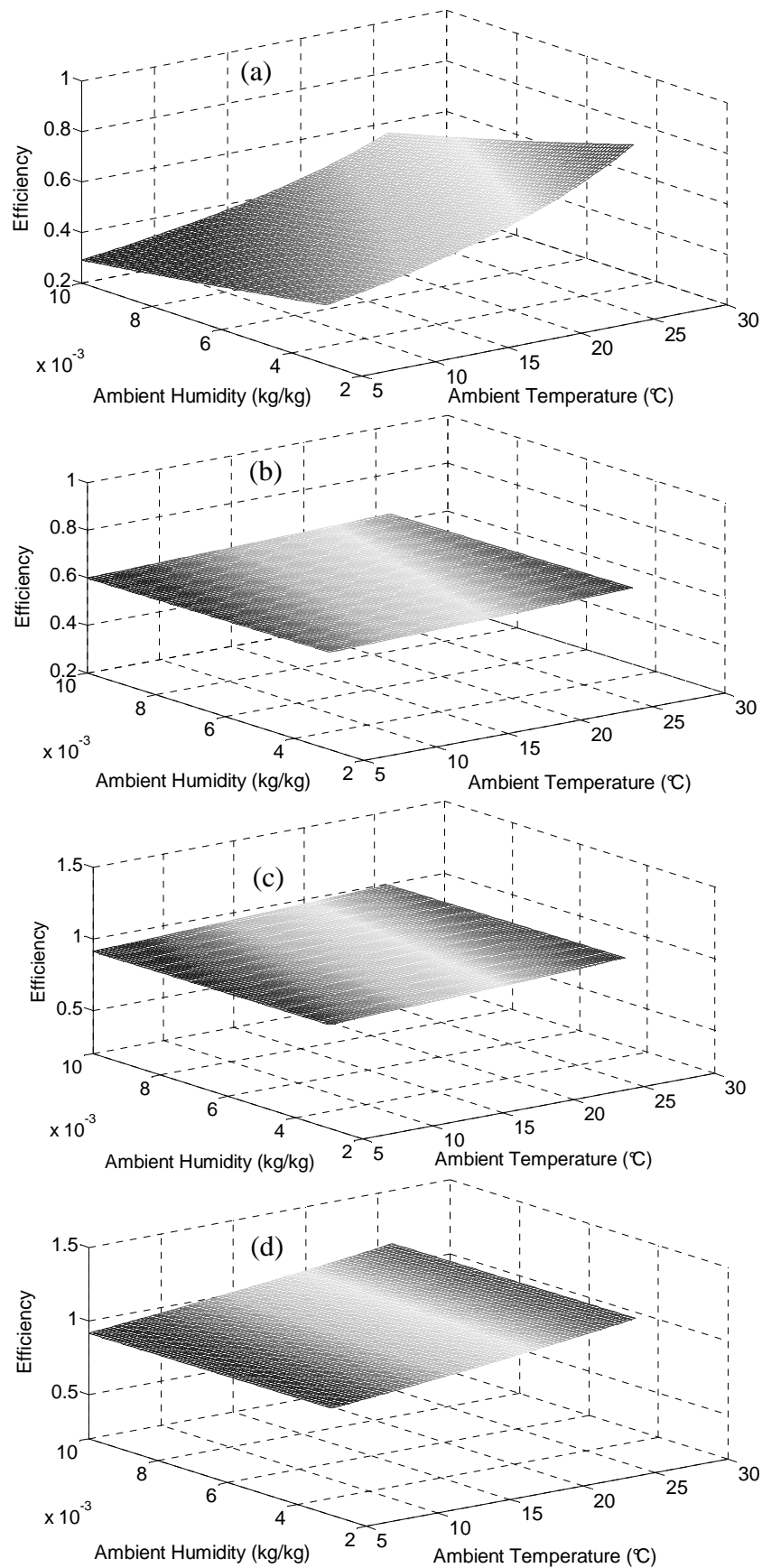


Fig. 3.10. Variation of system energy efficiency with ambient conditions for (a). a conventional dryer (b). a sequentially optimized adsorption dryer before heat recovery (c). a sequentially optimized adsorption dryer after heat recovery (d). a simultaneously optimized adsorption dryer



corner in the graph are not feasible as such ambient temperature-humidity combinations are very unlikely in practice.

For the adsorption dryers (Figs. 3.10 (b) – (d)) however, the adsorption dehumidification system proves to regulate ambient temperature changes since as temperatures fall, adsorption capacity rises (due to the normal adsorption characteristics of the zeolite). The result is that the driving force for dehumidification rises, thus increasing the capacity of the air to dry. This increased dehumidification is also accompanied by the release of more adsorption heat, further increasing the air drying capacity. Also, there is humidity regulation since a higher ambient air humidity leads to increased driving forces for adsorption and hence, dehumidification. In addition, regenerating at high temperatures means the energy input of the regenerator is less sensitive to ambient temperature variations unlike for conventional dryers where the drying temperature is in the same order of magnitude as the ambient. The resultant effect of the afore-mentioned phenomena is that the energy efficiencies of the adsorption dryers are less sensitive to ambient variations when compared with conventional dryers.

### 3.6. Conclusion

Conventionally, heat recovery is only considered after energy auditing on existing drying process conditions. In this work, heat integration is considered an integral part of adsorption dryer design and the system simultaneously optimized for energy efficiency within drying constraints. Compared to the results of a sequentially optimized system where operating conditions are determined in advance of heat recovery, a 15% improvement in energy efficiency (13% reduction in energy consumption) has been observed. Energy consumption is reduced by about 55% compared to a simultaneously optimized conventional convective dryer operating under similar conditions. Depending on local economic conditions, this significant drop in energy consumption should justify the extra investment costs. The performance improvement is traceable to alterations in enthalpy related variables like temperatures and flowrates. The discrepancy in optimal operating conditions between the sequential and simultaneous cases underscores the need to change system operating conditions when retrofitting for heat recovery as previous optimal conditions become sub-optimal when heat recovery is introduced. Thus, simultaneous optimization is useful in revamping existing dryers operating sub-optimally without heat recovery. It provides a means of determining new optimal conditions when heat recovery is eventually considered as against merely recovering heat based on existing operating conditions (which is sub-optimal).

Simultaneous optimization is seen to entail the manipulation of process stream temperatures, heat capacity rates, condensation-based properties like dew point to optimize the energy performance of the system consisting of the main process, and its

associated heat exchanger network. The manner in which the optimizer achieves this is process-specific. For an adsorption dryer, the optimizer basically manipulates the adsorber and regenerator inlet and outlet adsorbent and air temperatures as well their flowrates in such a way that energy efficiency is maximized. In spite of the heat recovery, a significant part of the hot stream energies cannot be recovered. When drying is considered in the context of the overall process plant, the adsorption drying process can serve as a source of energy to surrounding low temperature processes. Moreover, adopting the simultaneous optimization approach to the overall plant at the process design phase will reduce overall energy consumption.

### **A mixed integer formulation for energy efficient multistage adsorption dryer design**

Published as Atuonwu, J.C., Straten, G. van., Deventer, H.C. van., Boxtel, A.J.B. van (2012). A mixed integer formulation for energy efficient multistage adsorption dryer design. *Drying Technology* 30(8), 873-883.

#### **Abstract**

This work presents a mixed integer nonlinear programming (MINLP) formulation for the design of energy efficient multistage adsorption dryers within constraints on product temperature and moisture content. Apart from optimizing temperatures and flows, the aim is to select the most efficient adsorbent per stage and product to air flow configuration. Superstructure models consisting of commonly used adsorbents: zeolite, alumina and silica-gel are developed and optimized for a two-stage low temperature adsorption drying system. Results show that the optimal configuration is a hybrid system with zeolite as the first-stage adsorbent and silica-gel as the second-stage adsorbent in counter-current flow between drying air and product. A specific energy consumption of 2,275kJ/kg is achieved which reduces to 1,730kJ/kg with heat recovery by a heat exchanger. Compared to a conventional two-stage dryer at the same drying temperature, this represents a 59% reduction in energy consumption. The optimal system ensures the exhaust air temperature of the first-stage regenerator is high enough to regenerate the second-stage adsorbent so no utility energy is spent in the second stage. A higher second-stage adsorbent wheel speed favours energy performance as it becomes optimized for energy recovery while the first is optimized for dehumidification. Although this work considers three candidate adsorbents in a two-stage system, the same reasoning can be applied to systems with more stages and adsorbents. The developed superstructure optimization methodology can by extension be applied to optimize multistage hybrid drying systems in general for any objective.

*Keywords:* Dryer energy optimization, mixed integer nonlinear programming, multistage dryers, adsorption drying, hybrid dryers, product quality

#### **4.1. Introduction**

Drying is an important unit operation applied in a wide range of process industries. It is an energy intensive process that accounts for as much as 15% of industrial energy consumption (Kemp, 2005) and thus, a major contributor to greenhouse gas emissions and the associated negative environmental impacts (Baker, 2005). For convective

dryers which constitute over 85% of all industrial dryers (Mujumdar, 2007a), the energy-related operating costs amount to about five times the capital costs (Baker, 2005). In addition, the heat treatment associated with drying tends to degrade quality and hence, market value of products. In heat-sensitive products specifically, drying is characterized by a wide variety of irreversible physiochemical and biological degradation reactions as well as physical and structural modifications. Minimizing energy consumption within the limits of product quality is thus an important drying system design problem. This work focuses on minimizing the energy consumption of low temperature multistage adsorption drying systems using stage-wise adsorbent choices, product and air flow relative directions (integer variables), process flows and temperatures (continuous variables) as decision variables. This leads to a mixed integer nonlinear programming (MINLP) optimization problem.

Although MINLP based design procedures have been successfully deployed in a wide variety of process systems like pump networks, reactor networks, distillation sequencing, heat exchanger networks, cooling towers etc., applications to drying processes have been relatively rare. A possible reason for this is the difficulty in determining which of the many dryer design variations are technically and economically feasible to form a superstructure of alternatives from which the final optimal system can be derived. There are few reported applications of MINLP based design of drying systems to date. Kiranoudis et al. (1995) employed an MINLP model to determine the production policy and equipment configuration that optimize total annual profit of a multiproduct dehydration plant. In the same vein, Kiranoudis, et al. (1997) obtained the optimal number of trucks and dryers as well as the drying air humidity that minimizes the total annual cost of running a semi-batch system of parallel industrial truck and tray dryers. The same reasoning was applied in Kiranoudis (1998) to the batch drying of grapes. Phongpipatpong and Douglas (2003) formulated a superstructure flowsheet comprising serial structures of drying, cooling and tempering (internal moisture content equilibration for reduced crack formation) units in a rice processing plant. An MINLP optimization was performed using various performance objective functions including energy consumption. The results showed a 22% reduction in energy consumption compared with what is obtained under typical design and operating conditions. More recently, Younes et al. (2010) used a Generalized Disjunctive Programming-based MINLP model to determine the optimal sequencing of drying, tempering and cooling unit operations in rice processing using the quantity of head (un-fissured) rice yield and energy consumption as objective functions. In that work, energy consumption in particular was identified as the dominant factor in total capital and operating costs.

Multistage drying has been proposed as a means of reducing dryer energy consumption for low temperature drying (Spets and Ahtila, 2004). In conventional multistage drying systems, the exhaust air from the earlier drying stages is reheated (to regain drying capacity lost due to moisture uptake) and reused in subsequent

stages. The inlet air temperature per stage required to achieve the same moisture removal from a product is reduced as compared to a single stage dryer. However, the reheating in each stage is not suitable for heat sensitive products as product heating increases rapidly in the falling rate periods usually encountered in latter stages. Moreover, reheating means energy expenditure. One method for solving this problem is the use of multistage hybrid drying systems. In this approach, the system is made to consist of different dryer types such that the characteristics of each dryer and the product drying behaviors under the operating conditions in each stage are matched to yield favourable outcomes in terms of efficiency and quality. In these systems, optimal sequencing could be a design problem. Menshutina et al. (2004) proposed a two-stage dryer consisting of a plug-flow fluid bed dryer in series with a belt conveyor dryer for enhanced energy savings. The first dryer was found by experiments to be more efficient in removing bulk water encountered during the constant-rate drying period while the second was better for residual water removed during the falling-rate period. Dryer sequencing was thus based on the results of experiments which could sometimes be costly and time consuming, particularly for large-scale systems. Moreover, the choice of the dryer types used in this study was based on heuristics without a systematic search method. The same approach was employed by Namsanguan et al. (2004) who used a two-stage dryer consisting of a superheated steam dryer in the first stage and a heat pump dryer in the second stage to obtain improved quality for dried shrimp. Selecting the optimal dryer type and sequence for a multistage hybrid system would involve many experiments on the various alternatives; comparing the performances of each, to get the best. A well-formulated mathematical model-based methodology would help in circumventing this by lumping the highly combinatorial problem into a superstructure (search space of alternatives) and solving the resulting MINLP problem in one step. In this work, this is done by formulating adsorbent choice in the superstructure of a multistage adsorption drying system.

When the exhaust air from a dryer is passed through an adsorbent, dehumidification occurs accompanied by the release of adsorption heat. With the reduced moisture content and the increased temperature of the air, drying capacity is regained so the air can be used for drying in subsequent stages without reheating to high temperatures. This is multistage adsorption drying. Multistage adsorption drying using zeolites has been shown to improve energy performance for low temperature drying (Djaeni et al., 2007a). The main energy consumption is for zeolite regeneration which typically takes place at high temperatures. The high regeneration temperatures on the other hand provide increased opportunities for sensible and latent heat recovery (Atuonwu et al., 2011b, c). Djaeni et al. (2007a) reported a specific energy consumption of 4,237kJ/kg for a two-stage counter current adsorption dryer without heat recovery. With heat recovery using conventional heat exchangers, the specific energy consumption is reduced to 3,125kJ/kg and further to 2,083kJ/kg (for a three-stage system) if the exhaust regeneration air is compressed to recover latent energy. In these studies, zeolite was used as adsorbent in all the stages. However, since the

psychrometric properties of the air and the product drying behavior at each drying stage are different, there is no guarantee that a particular adsorbent performs best in all the stages. Different adsorbents perform differently in terms of dehumidification under different air conditions with correspondingly varying magnitudes of adsorption heat release. Required regeneration temperatures are also different and air and adsorbent flowrates significantly impact on energy consumption. The selection of adsorbents most suitable in each stage, together with the optimal operating conditions with respect to efficiency and quality thus becomes an important design problem.

The usefulness of adsorption drying technology in product quality retention has been stressed in various works (Hodali and Bougard, 2001; Witinantakit et al., 2006; Madhiyanon et al., 2007). Similarly, energy efficiency in drying has been shown to be improved using adsorbents. Energy efficient drying at low temperatures (for quality retention) has been demonstrated. (Djaeni et al., 2007a; Atuonwu et al., 2011b; van Boxtel et al., 2012). However, in these studies, there has not been any firm theoretical framework for the choice of adsorbents, both in single and multistage systems. The purpose of this work is to simultaneously determine using MINLP methods, the process conditions, product-air flow configuration and choice of adsorbents in each stage of a multistage adsorption dryer that minimize energy consumption within the limits of product quality requirements.

## 4.2. Process description

As shown in Fig. 4.1, a continuously rotating adsorbent-coated wheel successively passing through adsorption and regeneration sections is an add-on to the basic conventional dryer, like the ones currently in use in various process industries. Ambient air flowing through adsorber A1 is dehumidified. The process is accompanied by the release of adsorption heat. It is then used in the first stage dryer, Dryer1 for drying the wet product. The dryer exhaust air is passed through a second-stage adsorber A2 and reused for drying in the second-stage dryer Dryer2. The product flow direction could be co- or counter-current to the airflow direction and the number of stages can be greater than two. Meanwhile, the spent adsorbent in each stage is regenerated in regeneration sections R1 and R2 by streams of hot air (ambient air heated in Heater1 and Heater2) also flowing continuously. For low temperature drying, note that the drying air in each stage is not heated by an external heater, but only dehumidified with sorption heat released. For an  $M$ -stage system where  $M > 2$ , the same process is repeated for all the stages. Continuous rotation of the adsorbent wheels ensures the adsorbent system is continuous, while continuous flow of the drying and regeneration air as well as the product (e.g. in belt dryers) ensures continuous operation of the air and product systems.

In this work, two choices of system configuration are considered: the co-current system where the flow path of the drying air is the same as that of the product and the

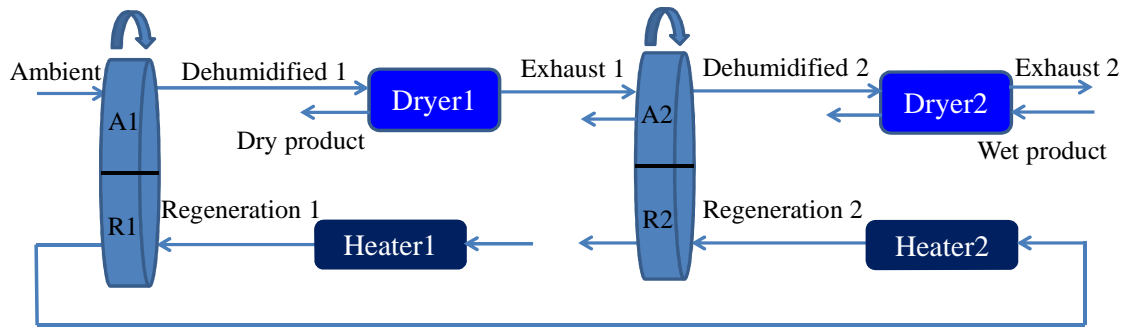


Fig. 4.1. Multistage adsorption drying system

counter-current operation where the directions are opposite. Zeolite, silica gel and alumina are considered possible adsorbents per-stage. The objective is to find the adsorbent choice structure, flow configuration and process conditions that minimize system energy consumption subject to the satisfaction of drying requirements.

### 4.3. System superstructure and superstructure modeling

To structurally optimize a process system, a so-called superstructure or search space of alternatives from which the optimal choices would be made must first be postulated. Superstructure representations are generally classified in two major types (Yeomans and Grossmann, 1999): the state-task-network (STN) and the state-equipment-network (SEN). In an STN representation, the states (stream properties) and the tasks (state transformation processes) are known while the equipment (state transformation devices) to which these tasks should be optimally assigned are unknown and form part of the optimization problem. In the SEN, the states and equipment are known, but the optimal task structure is unknown.

Fig. 4.2 shows an STN superstructure representation of the adsorption drying system under study with the states, tasks and possible equipment as shown in Table 4.1. Ambient air is dehumidified by passing through an adsorbent system consisting of a number of different adsorbent material-based adsorption subsystems, each, constituting a unique piece of equipment. The dehumidified air is then used in drying the product in the first-stage dryer. The dryer exhaust air is dehumidified resulting in state transformation before being used in a subsequent product drying operation in the second-stage dryer. In addition to the ambient and exhaust air dehumidification tasks which take place in the adsorbents, the spent adsorbent in each stage is regenerated in the regenerators by streams of hot air. Thus for each adsorbent in each stage, a regeneration task exists which from a technical point of view is mutually inclusive with respect to the corresponding dehumidification task. S1, S2, S3 and S4 are splitting/ logic selection nodes of which S1 and S2 are equivalent; S3 and S4 are also equivalent. This means, if an adsorbent is chosen in any stage for adsorption, the same adsorbent is regenerated. In the same vein, the inlet and outlet air of the optimal solution flow through the selected adsorbents.

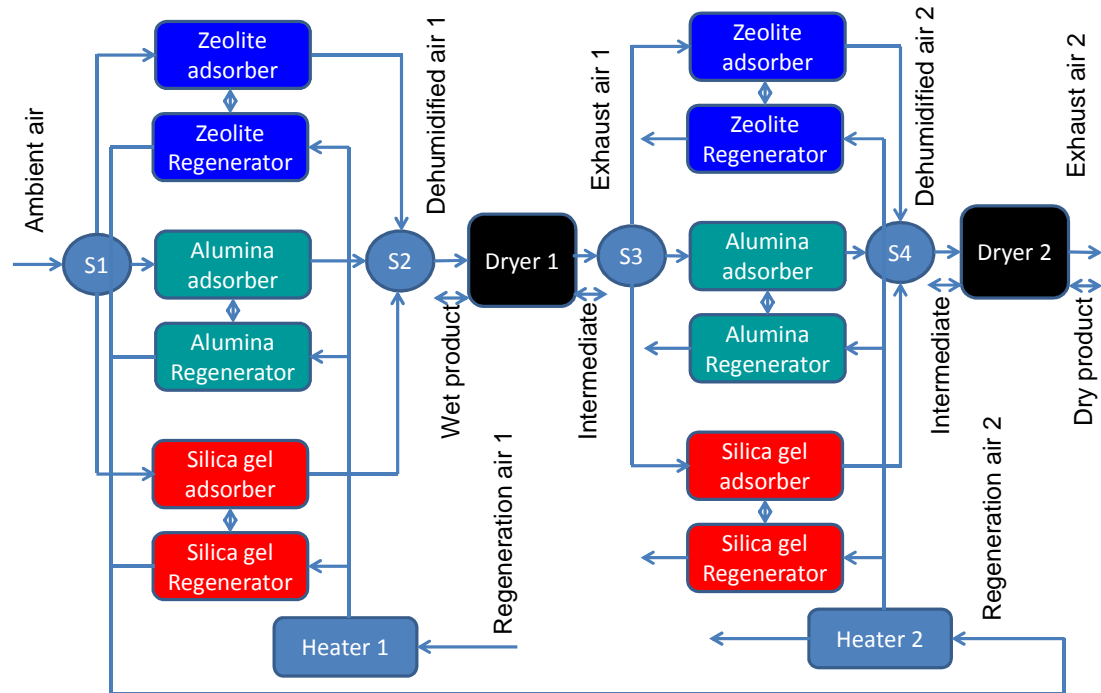


Fig. 4.2. State-task-network representation of system superstructure showing different adsorbent possibilities per stage

Table 4.1. State-task-network superstructure description

<i>State</i>	<i>Task description</i>	<i>Possible equipment</i>
Ambient air	Ambient air dehumidification	Zeolite, alumina or silica gel adsorber
Wet product	First stage drying	Dryer: determinate
Exhaust air	Exhaust air dehumidification	Zeolite, alumina or silica gel adsorber
Intermediately dry product	Second stage drying	Dryer: determinate
Wet adsorbent (stage 1)	First stage regeneration	Zeolite, alumina or silica gel regenerator
Wet adsorbent (stage 2)	First stage regeneration	Zeolite, alumina or silica gel regenerator

While adsorption favours drying efficiency, the more the amount of water adsorbed, the more the regeneration energy required. The interplay of these “conflicting” subprocesses determines the energy efficiency of the overall process and an optimal balance must be found. The optimization problem addressed in this work entails assigning the stated tasks to specific equipment and simultaneously determining the best operating conditions on the basis of energy efficiency optimality, while assuring product quality requirements, represented by temperature and moisture constraints are satisfied. The continuous decision variables adopted in the work are as determined in (Atuonwu et al., 2011b). They are the regeneration air inlet temperature, ratio of adsorbent to drying air flowrate and the ratio of regeneration air to adsorbent flowrate in each stage in addition to the drying air flowrate. Based on their well-established dehumidification capabilities, the adsorbent materials considered in this study are zeolite, alumina and silica gel.

Let the set of adsorbent materials be defined as



$$I = \{i : i = 1, \dots, M\} \quad (4.1)$$

And the stages of the drying system be

$$J = \{j : j = 1, \dots, N\} \quad (4.2)$$

The continuous decision variable vector defining the operating conditions for each adsorbent in each stage in a two-stage system is given by

$$x_{ij} = [T_{aRinij} \quad r_{ij} \quad s_{ij}] \quad i \in I, j \in J \quad (4.3)$$

where  $T_{aRinij}$  denotes the regeneration inlet air temperature for adsorbent  $i$  and stage  $j$ ,  $r_{ij} = F_{zij}/F_{aA}$  is the ratio of adsorbent to drying air flowrate, while  $s_{ij} = F_{aRij}/F_{zij}$  denotes the ratio of regeneration air to adsorbent flowrate in each case.

The mass balance governing the behavior of each adsorption-regeneration subsystem per stage is derived from (Atuonwu et al., 2011b) as follows: For the adsorber and regenerator respectively, the humidity of the outlet air is

$$Y_{aAij} = Y_{aAinij} - \frac{F_{zij}}{F_a} (X_{zAij} - X_{zAinij}) \quad (4.4)$$

$$Y_{aRij} = Y_{aRinij} + \frac{F_{zij}}{F_{aR}} (X_{zRinij} - X_{zRij}) \quad (4.5)$$

The energy balances state that the aggregate sensible and latent heat of the outlet air is equal to the algebraic sum of the sensible heat, latent heat of the inlet air and the released (or absorbed) heat of sorption. This gives the following corresponding outlet temperatures:

$$T_{aAij} = \frac{F_{aA}((C_{pa} + Y_{aAinij}C_{pv})T_{aAinij} + (\Delta H_v + H_{adsi})(Y_{aAinij} - Y_{aAij})) + F_{zij}((C_{pzij} + X_{zAinij}C_{pw})T_{zAin})}{F_{aA}(C_{pa} + Y_{aAij}C_{pv}) + F_{zij}(C_{pzij} + X_{zAij}C_{pw})} \quad (4.6)$$

$$T_{aRij} = \frac{F_{aRij}((C_{pa} + Y_{aRinij}C_{pv})T_{aRinij} + (\Delta H_v + H_{adsi})(Y_{aRinij} - Y_{aRij})) + F_{zij}((C_{pzij} + X_{zRinij}C_{pw})T_{zRin})}{F_{aRij}(C_{pa} + Y_{aRij}C_{pv}) + F_{zij}(C_{pzij} + X_{zRij}C_{pw})} \quad (4.7)$$

The following coupling equations apply

Adsorber-regenerator coupling

$$X_{zRinij} = X_{zAij} \quad (4.8)$$

$$T_{zRinij} = T_{zAij} \quad (4.9)$$

Regenerator – adsorber recycle looped coupling

$$X_{zAinij} = X_{zRij} \quad (4.10)$$

The state variables of the dehumidified air in each stage are a binary-weighted sum of those of the outlet air from each adsorber subsystem.

$$Y_{aAj} = \sum_{i=1}^{i=M} y_{ij} Y_{aAij} \quad j \in J \quad (4.11)$$

$$T_{aAj} = \sum_{i=1}^{i=M} y_{ij} T_{aAij} \quad j \in J \quad (4.12)$$

where the discrete variable defining the assignment of dehumidification-regeneration tasks to each subsystem is

$$y_{ij} \in \{0,1\} \quad i \in I \quad j \in J \quad (4.13)$$

Only one adsorbent is usable in each stage, hence,

$$\sum_{i=1}^{i=M} y_{ij} = 1 \quad j \in J \quad (4.14)$$

The dryer in each stage is fed by the dehumidified air from the adsorbent system preceding it, hence, the following mass and energy balance equations for the air through each dryer apply

$$Y_{aDj} = Y_{aAj} + \frac{F_p}{F_{aA}} (X_{pinj} - X_{pj}) \quad j \in J \quad (4.15)$$

$$T_{aDj} = \frac{F_{aA}((C_{pa} + Y_{aAj}C_{pv})T_{aAj} + \Delta H_v(Y_{aAj} - Y_{aDj})) + F_p((C_{pp} + X_{pinj}C_{pw})T_{pinj})}{F_{aA}(C_{pa} + Y_{aAj}C_{pv}) + F_p(C_{pp} + X_{pj}C_{pw})} \quad j \in J \quad (4.16)$$

The adsorber in each stage is fed with air from the exhaust of the dryer preceding it, hence,

$$Y_{aAinj} = Y_{aDj-1} \quad j \in J \quad (4.17)$$

$$T_{aAinj} = T_{aDj-1} \quad j \in J \quad (4.18)$$

An imaginary “zeroth stage dryer”, the ambient, supplies air to the first stage adsorber system,

$$Y_{aD0} = Y_{amb} \quad j \in J \quad (4.19)$$

$$T_{aD0} = T_{amb} \quad j \in J$$

The mass balance for the product phase in each stage assuming thin layer drying is given by

$$X_{pj} = X_{pinj} + k_{Dj}(X_{pej} - X_{pj})(\rho_{pj}V_p/F_p) \quad j \in J \quad (4.20)$$

For co- and counter-current operations the following product coupling constraints must respectively be satisfied

$$PC_1 = \{X_{pinj} = X_{pj-1}; T_{pinj} = T_{pj-1}; X_{p0} = X_{pin}; T_{p0} = T_{pin}; X_{pN} = X_{pfinal}; T_{pj} \leq T_{pmax}\} \quad (4.21)$$

$$PC_2 = \{X_{pinj} = X_{pj+1}; T_{pinj} = T_{pj+1}; X_{pM} = X_{pin}; T_{pM} = T_{pin}; X_{p1} = X_{pfinal}; T_{pj} \leq T_{pmax}\} \quad (4.22)$$

If  $v_1$  and  $v_2$  be integer variables representing the existence of co-current and counter-current product-air flows respectively, the effective coupling constraint is

$$PC = v_1 PC_1 + v_2 PC_2 \quad (4.23)$$

where

$$v_1, v_2 \in \{0,1\}, v_1 + v_2 = 1 \quad (4.24)$$

The adsorbents considered are zeolite ( $i=1$ ), alumina ( $i=2$ ) and silica gel ( $i=3$ ) in a 2 stage system, hence,  $M=3$  and  $N=2$ . The regeneration air inlet temperatures are constrained to satisfy the maximum usually allowed for each adsorbent to prevent deformation (Atuonwu et al., 2011b; van Boxtel et al., 2012)

$$T_{aRinj} \leq [400 \quad 200 \quad 200]_j \quad j \in J \quad (4.25)$$

Detailed mathematical relations describing the specific behaviors of the different adsorbents in terms of their sorption isotherms and capacities, heats of adsorption and kinetics (Djaeni et al., 2007a; Atuonwu et al., 2011b; Moore and Serbezov, 2005; Nastaj and Ambrozek, 2009; Kodama et al., 2001; Tahat et al., 1995) are presented in Appendix B. To evaluate the performance of the proposed methodology, the drying behavior of pumpkin is used to simulate drying. The equilibrium moisture content (Krokida et al., 2003) and drying constant (Doymaz, 2007) are within the temperature range of concern and so, are used in this work. These parameters are also presented in Appendix B. The product at a dry basis flowrate of 72 kg/h is dried from a moisture content of 10 kg/kg to 0.05 kg/kg dry basis. Thus, the total drying capacity or evaporative load is 716.4 kg/h.

## 4.4. Optimization and system analysis

### 4.4.1. Optimization problem formulation

The objective of the optimization procedure is to minimize the system energy consumption subject to the drying requirements. The main energy consumption is in regeneration and hence, the total energy consumption rate is

$$Q_{in}(x_{ij}, y_{ij}) = \sum_{i=1}^{i=M} \sum_{j=1}^{j=N} y_{ij} F_{aRj} (C_{pa} + Y_{aRinj} C_{pv}) (T_{aRinj} - T_{arinj}) \quad i \in I, j \in J, T_{arin1} = T_{amb} \quad (4.26)$$

The MINLP optimization problem is therefore formulated as minimize energy consumption (4.26) subject to constraints (4.1) to (4.25) as well as (B1) to (B8), Appendix B. The use of energy consumption as an optimization criterion is based on the fact that energy costs constitute the main operating costs of a dryer. Moreover, for reasons of environmental conservation and sustainability, energy consumption is paramount and should be minimized. The purchase costs corresponding to the different adsorbent choices are highly variable and depend on prevailing local economic conditions. In addition, as the adsorbents are reused, their costs are infinitesimal compared to energy costs which are continually incurred over the entire lifetime of the drying system.

The system under consideration is a 3-adsorbent, 2-stage system and hence, has  $2^6=64$  discrete adsorbent choice possibilities of which 55 are rendered infeasible by constraint (4.14) which stipulates that only one adsorbent can be used per stage. 2 product-air flow configurations for each feasible case imply 18 discrete choices. There are 3 continuous decision variables per adsorbent per stage. Hence, ordinarily, there are 18 continuous decision variables overall as shown in equation (4.3). The system is however characterized by the presence of algebraic loops that make explicit analytical solutions impossible. At the equipment level, the regenerator outlet adsorbent must be recycled to the adsorber, thus creating an algebraic loop. In addition, at the state level, there are algebraic loops in the system equations. For instance, the steady-state values of the air, product and sorbent temperatures depend on the values of their moisture contents (Atuonwu et al., 2011b). These in turn depend on the sorption properties which are again, functions of the temperatures. An iterative solution algorithm was proposed in (Atuonwu et al., 2011b) to solve the problem but this would be computationally cumbersome when implemented within the framework of MINLP optimization. In this work, the problem is solved by taking the temperatures and moisture contents as additional decision variables and then, specifying constraints for which the algebraic loops (e.g. as found in equation (4.8) to (4.10)) are satisfied. The solution algorithm is implemented in TOMLAB® Optimization software using the “KNITRO” solver (Holmström, et al., 2009). The solver uses the branch and bound technique by which the integer constraints are first

relaxed and the NLP relaxation solved to obtain the lower bound on the integer variable. For each integer variable with non-integer solutions, new bound constraints are added to form two new NLP problems. The NLP relaxation is solved with interior point methods. To ensure the solution is as close as possible to the global optimum, the solver employs a multi-start procedure which generates multiple new start points by randomly selecting values of continuous variables that satisfy the variable bounds.

#### *4.4.2. Heat recovery from the optimal system*

Here, the possibilities of recovering sensible and latent heat from the regenerator and drying air exhausts of the optimal system are explored. These exhausts constitute hot (energy surplus) streams. The ambient air to the regenerator and dryer constitute cold streams (energy deficit). For high temperature heat recovery, an option is to pre-heat the ambient air to the regenerator using the regenerator exhaust. Latent heat is also available if the hot streams could be cooled below dew point. Preheating the dryer inlet ambient air using the second-stage dryer exhaust is also an option if the dryer exhaust air temperature level is high enough. Pinch analysis (with latent heat recovery possibilities) is employed in exploring these options using the procedure proposed in (Atuonwu et al., 2011b, also in Chapter 2 of this thesis).

#### *4.4.3. Comparison with existing alternative systems*

To give an indication of the extent of improvement obtained by the proposed optimal system, the results are compared with the following cases of conventional dryers (without adsorption subsystems):

1. Exhaust air from each stage, partially recycled; fresh air introduced per stage (Kiranoudis et al., 1995) with 70% recycle assumed.
2. Product and air flow in the same direction; exhaust air from stage 1 reheated and used in stage 2 (Spets and Ahtila, 2004).

The dryer inlet air temperature per-stage is set equal to that of the optimal sorption system for equivalence. Also, the results are compared with those for two-stage adsorption drying systems with the same adsorbent in each stage: zeolite-zeolite; alumina-alumina and silica-silica. For each of the cases, an optimization problem that minimizes energy consumption subject to the same drying requirement is solved.

## 4. 5. Results and discussion

### 4.5.1. Optimization results and discussion

Fig. 4.3 shows the optimal choices of adsorbents (zeolite – first stage and silica gel – second stage) and flow-configuration (countercurrent). The values of the corresponding continuous variables are shown in Table 4.2 with stream numberings as designated in Fig. 4.3. The regeneration energies consumed per-stage for the optimal system is compared with those for same adsorbent systems in Fig. 4.4(a). The results show that for the optimal system, the regenerator exhaust air temperature for the first stage is equal to that of the inlet of the second regenerator. Hence, no utility energy is required for the second stage and Heater 2 (in Fig. 4.3) becomes redundant.

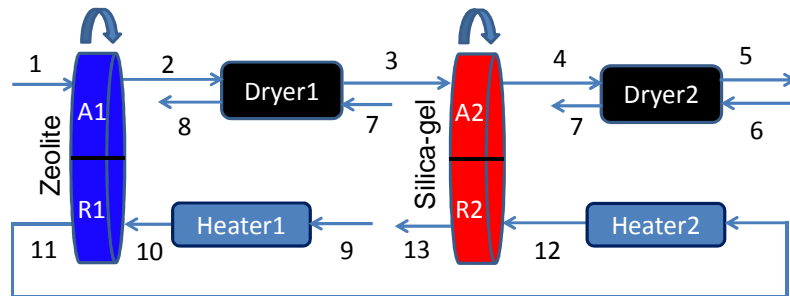


Fig. 4.3. Optimal drying process showing adsorbents in each stage (zeolite first stage and silica-gel second stage).

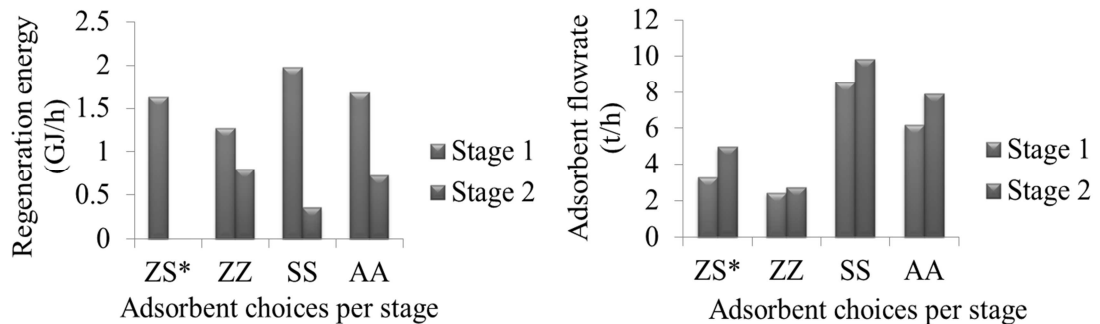


Fig. 4.4. Charts of (a). Regeneration energy per-stage (b). Adsorbent flowrate per-stage for different options (ZS\*- optimal, ZZ-zeolite-zeolite, SS-silica gel-silica gel, AA-alumina-alumina)

Table 4.2. Operating conditions for optimal system

No.	Flow(kg/h)	Temp.(°C)	Humidity(kg/kg)	No.	Flow(kg/h)	Temp.(°C)	Humidity(kg/kg)
1	54,000	25	0.0100	8	72	46	0.0500
2	54,000	46	0.0030	9	4,269	25	0.0100
3	54,000	24	0.0114	10	4,269	400	0.0100
4	54,000	36	0.0061	11	4,269	200	0.0990
5	54,000	24	0.0109	12	4,269	200	0.0990
6	72	24	10.0000	13	4,269	120	0.1663
7	72	36	6.3674				

The result is that minimum regeneration energy is spent for this system. Also, from known adsorbent isotherm characteristics, zeolites have high dehumidification capacity at low vapour pressures while silica-gels dehumidify better for high vapour-pressure air. The choice of zeolite for ambient air dehumidification and silica-gel for the moister dryer exhaust air dehumidification thus ensures that the dehumidification characteristics of both adsorbents are well-matched to the drying air properties for each stage. From Fig. 4.4(b), it is seen that in all instances, the optimal adsorbent flowrate (proportional to wheel speed) is higher in the second stage than the first. The second-stage therefore behaves like an enthalpy wheel usually applied in HVAC systems (Zhang and Niu, 2002) which because of its higher rotary speed, is optimized for heat recovery while the first stage (at lower speed) is optimized for air dehumidification. The results of Table 4.2 also show that for the optimal system, the regeneration air inlet temperature equals the upper constraint, in agreement with previous results (Atuonwu et al., 2011b). In summary, the operating conditions are such that both dehumidification and heat recovery (from drying and regeneration air exhausts) are optimized (by wheel speed behavior). The drying air properties (vapour pressures) and adsorbent isotherm characteristics are matched. System heat requirements are matched by appropriate regeneration temperatures per-stage. The adsorbents are chosen to satisfy these requirements. An adsorbent requiring high regeneration temperature (zeolite) is used in the first stage so it provides enough driving force to regenerate the second-stage adsorbent (silica). From the foregoing, the system component choices and operating conditions are matched with process and energy demands per-stage to optimize the specified objective which is energy consumption. In principle therefore, the developed superstructure optimization methodology can by extension, be applied to optimize multistage hybrid drying systems in general for any objective.

For drying the selected product at a dry basis flowrate of 72 kg/h from an initial moisture content of 10 kg/kg to a final value of 0.05 kg/kg (an evaporative load of 716.4 kg/h), the optimal system consumes  $1.6316 \times 10^6$  kJ/h of energy. This amounts to a specific energy consumption of 2,275 kJ/kg water evaporated. Given a specific latent heat of vaporization of water of 2,500 kJ/kg, the energy efficiency is 110%. For the two-stage zeolite, silica and alumina systems, the specific energy consumption calculated are 2,850, 3,260 and 3,368 kJ/kg water respectively.

#### 4.5.2. Heat recovery from optimal system by heat exchanger

The results computed in the preceding section assume that the exhaust air from the second-stage regenerator (stream 13) and dryer (stream 5) are discharged (See Fig. 4.3). However, these constitute heat sources for the inlet ambient air to the regenerator (stream 9) and the dryer (stream 1). Fig. 4.5(a) and (b) show the system pinch analysis results. The composite hot stream plots show the heat surplus of the system exhausts while the cold stream plots show the heat demands of the inlet streams. Two cases are

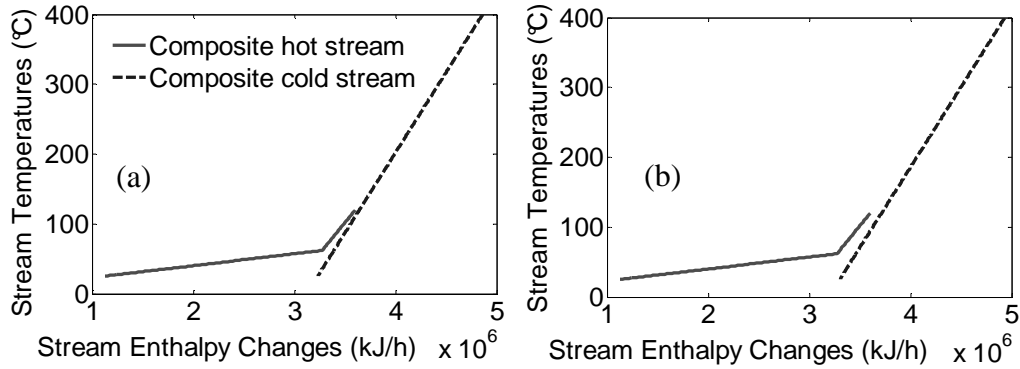


Fig. 4.5. Pinch analysis results on the system (a).  $\Delta T_{min}=5^{\circ}\text{C}$  (b).  $\Delta T_{min}=20^{\circ}\text{C}$

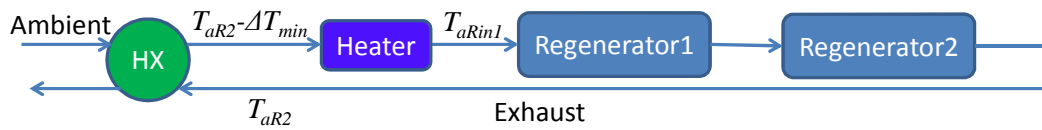


Fig. 4.6. Regenerator heat recovery ambient air pre-heating by 2<sup>nd</sup>-stage exhaust

presented: (a). Minimum exchanger temperature difference  $\Delta T_{min}=5^{\circ}\text{C}$  (b).  $\Delta T_{min}=20^{\circ}\text{C}$ . In the case with  $\Delta T_{min}=5^{\circ}\text{C}$ , the second-stage regeneration outlet air cools below dew-point of  $62^{\circ}\text{C}$  (indicated by the point where the hot stream curve bends) since the overlap between the two streams extends below this temperature. The cold stream (the ambient air to the regenerator) heats up to  $115^{\circ}\text{C}$  ( $5^{\circ}\text{C}$  less than the regenerator exhaust) as a result of which,  $3.9163 \times 10^5$  kJ/h of heat is recovered. Note that heat recovered is the enthalpy change corresponding to the overlap between the hot and cold composite curves. Fig. 4.6 shows an implementation of the heat recovery system. The only energy spent therefore is used in heating the air from  $115$  to  $400^{\circ}\text{C}$ . Under this arrangement, the net energy spent is  $1.2401 \times 10^6$  kJ/h corresponding to a specific energy consumption of  $1,730$  kJ/kg (or an efficiency of  $144\%$ ). For a heat exchanger heat transfer coefficient of  $0.2$  kW/m<sup>2</sup>K (Langrish, 1998), this translates to a total exchanger area of  $26.5$  m<sup>2</sup>. For the case  $\Delta T_{min}=20^{\circ}\text{C}$ , latent heat is not recovered as the hot air cools to about  $63^{\circ}\text{C}$ . The ambient air heats up to  $100^{\circ}\text{C}$  with  $3.2635 \times 10^5$  kJ/h of heat recovered. The net energy spent is  $1.3054 \times 10^6$  kJ/h corresponding to a specific energy consumption of  $1,822$  kJ/kg (or an efficiency of  $137\%$ ).  $15.6$  m<sup>2</sup> of heat exchange area is required.

#### 4.5.3. Comparison with conventional systems

Fig. 4.7(a) shows the flowsheet for the conventional convective dryer with  $70\%$  recycle of exhaust air in each stage and  $30\%$  fresh make-up air. Fig. 4.7(b) shows the flowsheet when the exhaust air in each stage is reheated and reused in the next stage. The corresponding energy consumption minimization conditions are shown in Tables



4.3(a) & (b). In general, net energy consumption reduces as percentage recycle increases. However, particularly at high percentage recycles, the flowrate of air required to achieve the same water evaporation from the product increases. For the studied case, above 70% recycle, the required air flowrate rises sharply; hence, the choice of 70% recycle. The results of Table 4.3(a) show that much air is required for evaporation due to the low capacity of the moist inlet air (streams 2, 3, 5 & 6). Much energy is required to reheat this air and the low temperature levels of the air means little energy benefits due to recycle. The total energy consumption is  $3.0147 \times 10^6$  kJ/h corresponding to a specific energy consumption of 4,208 kJ/kg (or 60% energy efficiency). For the case in Fig. 4.7(b), less air is needed compared to Fig. 4.7(a) but the low temperature energy in the exhaust air of the first stage (stream 3) being not much different from the ambient does not provide much extra benefit. Moreover, the outlet air of the second stage (stream 5) is at such a low temperature that precludes its economic use in preheating the inlet ambient air (stream 1) by heat exchangers.

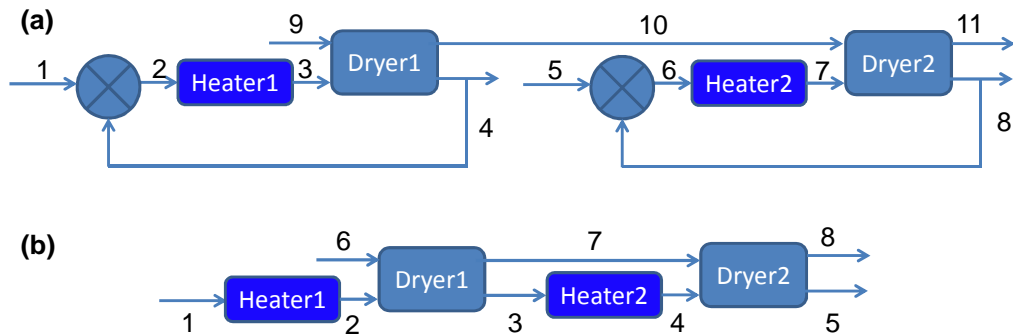


Fig. 4.7. Conventional two-stage dryer configurations: (a). With recycle: drying air streams 1-8; product streams 9-11 (b). Exhaust air reheated and reused: drying air streams 1-5; product streams 6-8

Table 4.3(a). Operating conditions for conventional two-stage dryer, case (a). 70% exhaust air recycle per stage

Stream	Flowrate (kg/h)	Temperature (°C)	Humidity (kg/kg)	Stream	Flowrate (kg/h)	Temperature (°C)	Humidity (kg/kg)
1	56,850	25	0.0100	7	189,490	36	0.0148
2	189,490	37	0.0131	8	132,640	31	0.0169
3	189,490	46	0.0131	9	72	25	10.0000
4	132,640	43	0.0144	10	72	43	6.5000
5	56,850	25	0.0100	11	72	31	0.0500
6	189,490	29	0.0148				

Table 4.3(b). Operating conditions for conventional two-stage dryer, case (b). Exhaust air reheated and reused

Stream	Flowrate (kg/h)	Temperature (°C)	Humidity (kg/kg)	Stream	Flowrate (kg/h)	Temperature (°C)	Humidity (kg/kg)
1	71,067	10	0.0100	5	71,067	28	0.0141
2	71,067	46	0.0100	6	72	10	10.0000
3	71,067	29	0.0108	7	72	29	3.2894
4	71,067	36	0.0108	8	72	28	0.0500

Table 4.4. Energy performance comparison among dryers

Drying system	Specific energy (kJ/kg)	Energy Efficiency (%)
Optimal adsorption dryer	1,730	144
Conventional dryer with 70% exhaust air recycle	4,208	60
Conventional dryer: exhaust air reheated, reused	4,332	58

The resulting effect of these conditions is an energy consumption of  $3.1035 \times 10^6$  kJ/h corresponding to a specific energy consumption of 4,332 kJ/kg (or 58% energy efficiency). Table 4.4 shows in concise form, the energy performances of the conventional dryers compared with the optimal adsorption drying system. The optimal adsorption drying system reduces energy consumption by about 59% compared to the conventional systems. Since the corresponding energy efficiency values are 144% and 60% respectively, this represents a rise in energy efficiency of 84%. In addition to these, the adsorption system provides higher drying capacity which permits the use of much lower flowrates of drying air; hence, a smaller dryer. The two-stage adsorption dryer with zeolite in the first stage and silica-gel in the second stage thus provides a significant step ahead in reducing drying energy consumption and improving process sustainability.

#### 4.5.4. Economic Considerations

The preceding sections have shown how energy consumption can be reduced by combinatorial optimization of a multistage adsorption drying system. Actual implementation depends largely on economic considerations. However, many aspects of cost, like sorption wheel costs, extra labor, installation and maintenance are highly dynamic both in time and in terms of plant location. In this study, we analyze the economic feasibility of the process by evaluating the costs associated with savings in energy and CO<sub>2</sub> emission penalties. From this, payback periods can be estimated based on local cost data. Table 4.5 shows an economic analysis of the proposed system based on energy costs and costs associated with CO<sub>2</sub> emissions in the European Union EU in 2011 with the Netherlands as a case study.

Table 4.5. Economic analysis of proposed system

<i>Economic variables</i>	<i>Values</i>
I=Operational time (h/year)	5,000
II=Energy costs (€/GJ) <sup>(Europe's Energy Portal, 2012)</sup>	16.9
III=CO <sub>2</sub> emissions per energy consumption (kg/GJ) <sup>(Vreuls and Zijlema, 2009)</sup>	56.7
IV=Costs per ton of CO <sub>2</sub> emissions (€/ton) <sup>(Clements et al., 2012)</sup>	15
<i>Calculated variables</i>	<i>Values</i>
V=Drying performance (kg water/h)	720
VI=Specific energy savings (kJ/kg water)	2,478
VII=Total energy savings (kJ/year)=I*V*VI	$8.9208 \times 10^9$
VIII=Cost value of energy savings (€/year)=II*VII*10 <sup>-6</sup>	150,760
IX=Cost value of reduced CO <sub>2</sub> emissions (€/year)=III*IV*VII*10 <sup>9</sup>	7,590
X=Total cost savings per year (€/year)=VIII+IX	158,350

It concerns small/medium-scale dryers of air flowrate about 60,000 kg/h and an annual operational time of 5,000 hours is assumed (Entry I). Entries II – IV show given values obtained from literature with natural gas as fuel (Europe’s Energy Portal, 2012; Vreuls and Zijlema, 2009; Clements et al., 2012), while entries V – X are calculated values based on results of the current study. Since the specific energy consumption is reduced from 4,208 to 1,730 kJ/kg, the specific energy savings is 2,478kJ/kg. Hence, calculations on the costs of these energy savings and associated CO<sub>2</sub> emissions show that the total annual cost savings is in the region of € 158,350. Assuming all the extra costs associated with the sorption system amount to € 150,000, the payback period is within one year. If we consider the rising energy costs and increasing pressure globally to reduce CO<sub>2</sub> emissions, the payback period could reduce further in future. Moreover, the optimal sorption system improves drying capacity (which permits the use of lower air flowrates). Thus, for the same dryer size, a higher quantity of products can be processed per unit time by the sorption dryer even though extra space would be needed for wheel installation. In any case, the value of the processed product when factored in would increase the profitability of using the proposed system.

#### 4.6. Conclusion

Reducing energy consumption in drying processes remains an important issue in view of the significant contribution of drying to industrial energy consumption, operating costs and environmental impact. In this work, a combinatorial optimization scheme based on mixed integer nonlinear programming (MINLP) has been developed for a two-stage adsorption drying system for the purpose of reducing energy consumption while satisfying drying requirements. Discrete variables like product-air flow configuration and adsorbent choice per-stage form a superstructure of alternatives while regeneration air inlet temperature and flow, as well as adsorbent flow speed constitute continuous decision variables. The developed superstructure optimization methodology is shown useful for optimizing multistage hybrid drying systems in general for any objective function. Unlike previous heuristic multistage hybrid dryer design techniques, the developed systematic search method lumps the highly combinatorial problem into a superstructure of alternatives, solving the resulting MINLP problem in one step and thus, providing a cost-effective solution. The existence of many advanced process optimization tools in the market today brings such optimizations closer to practice.

Results of the work show that a hybrid adsorbent structure with zeolite in the first stage and silica-gel in the second in counter-current flow between drying air and product yields the optimal solution. The results show heat requirement matching between the first and second stages. Zeolite which requires higher temperature regeneration is chosen in the first stage and silica-gel (requiring lower temperatures) in the second stage as a result of which zero utility energy is spent on regenerating the second-stage adsorbent. Also, there is vapour pressure and adsorption characteristics

matching as zeolite with a higher dehumidification capacity at lower humidity is chosen for ambient air dehumidification while silica-gel which is more effective at higher vapour pressures takes priority for exhaust air dehumidification. Furthermore, the wheel speed pattern show that the first stage adsorbent system is optimized for dehumidification and hence, drying capacity while the second stage by virtue of its higher speed behaves like an enthalpy wheel optimized for heat recovery.

For the optimal system, specific energy consumption amounts to 2,275 kJ/kg without using heat exchangers. By recovering the second-stage regenerator exhaust air heat using heat exchangers, specific energy consumption is further reduced to 1,730 kJ/kg. Compared to conventional two-stage dryers under similar operating conditions which consume about 4,208 kJ/kg of energy, a 59% reduction in specific energy consumption is achieved. This translates to an 84% increase in energy efficiency. The significant energy savings imply huge cost saving potentials in view of the rising energy costs and increased pressure with associated penalties on CO<sub>2</sub> emissions. Moreover, the optimal sorption system improves drying capacity (which permits the use of lower air flowrates). Thus, for the same dryer size, a higher quantity of products can be processed per unit time by the sorption dryer although extra space would be needed for wheel installation. Thus, the value of the processed product when factored in, would increase the profitability of using the proposed system.

# Simultaneous superstructure optimization and heat integration of multi-stage adsorption dryers

### Abstract

In Chapter 4 of this thesis (as appears in Atuonwu et al., 2012a), a mixed integer nonlinear programming (MINLP)-based superstructure model was used in realizing an energy-efficient two-stage drying system. Zeolite was chosen as the optimal adsorbent in the first stage and silica gel in the second stage. Heat integration was not considered simultaneously but was included as a second optimization step (sequential optimization). This work explores the possibility of improving system performance by formulating the drying system design, including adsorbent choice per-stage and heat integration problem in a single optimization step (simultaneous optimization). A 15% reduction in energy consumption is achieved compared to the sequential case with the same adsorbent choices but different operating conditions.

*Keywords:* Drying energy, superstructure optimization, simultaneous heat recovery

### 5.1. Introduction

Simultaneous optimization of unit operations together with heat integration has been identified as being useful in improving performance (Duran and Grossmann, 1986; Francesconi et al., 2011). In drying processes specifically, a recent study applying the pinch location simultaneous heat integration optimization approach to a single-stage zeolite dryer led to a 13% reduction in energy consumption compared to a two-step optimized system (Atuonwu et al., 2011). For multi-stage drying systems therefore, there exists the potential to explore simultaneous heat integration optimization techniques for energy performance improvement possibilities. However, previous work on such systems (for instance Atuonwu et al., 2012a) has focused on the sequential approach where heat recovery is only considered based on the stream conditions determined from a previous drying process optimization step. In this work, we explore energy efficiency improvement possibilities by formulating the multistage adsorption drying design problem for optimal adsorbent choice and operating conditions simultaneously with heat integration routing. As in Chapter 4, zeolite, silica gel and alumina are considered possible adsorbents.

### 5.2. Methodology: Superstructure development

In drying processes, there are essentially two ways of reusing process heat: heat exchange between energy-surplus and energy-deficit process streams and recycle of

energy-surplus streams. Fig. 5.1 shows the process superstructure for a two-stage dryer with air dehumidification incorporating both aspects for simultaneous heat integration. Here, hot and cold streams from the process are identified where hot streams are defined as streams with excess reusable heat (usually process exhausts) and cold streams, those requiring heat input (process inlets). The heat-exchange/heat-recovery options are incorporated as follows. First, each hot stream (represented by bold continuous lines) has the possibility of exchanging heat with each cold stream (shown by the dashed lines) via heat exchangers denoted by small circles that link both stream categories via dotted lines. Second, there is the recycle option where each regenerator hot stream can be recycled to the inlet heater of its circuit or the other regenerator. Blocks r1 and r2 show the recycle paths in the superstructure. Within the recycle option, there is the possibility to insert make-up ambient air to avoid saturation. The hot streams are: the exhaust air from regenerators 1 and 2 and the exhaust air from dryer 2. The cold streams are: the outlet air from adsorbers 1 and 2 (feeding dryers 1 and 2) and the inlet air to regenerators 1 and 2. In addition to the adsorbent choice and air-product flow configurations which are integer variables in Chapter 4, new integer variables are defined.  $W_{k,\ell}$  representing the existence of a heat exchanger between cold stream  $k$  and hot stream  $\ell$  and  $Z_j$  representing the recycling of a hot regenerator air stream. Also,  $y_{i,j}$  represents adsorbent choice per-stage. For each recycle, a fraction  $f$  of the hot-stream is assumed recycled with  $(1-f)$  the proportion of make-up ambient air. This fraction  $f$  is a continuous decision variable with value between 0 and 1. Let  $K = \{k: k=1 \dots N_K\}$  be the set of cold streams with temperatures defined as  $T_{c,k} = [T_{aA1}, T_{aA2}, T_{amb}, T_{amb}]$  where the first two temperatures refer to those of the adsorber outlet air in each stage (subset  $K_d$ ) and the last two, ambient air to the regenerator inlet heaters (subset  $K_r$ ). Also, let  $L = \{\ell: \ell = 1 \dots N_L\}$  be the set of hot streams with temperatures defined as  $T_{h,\ell} = [T_{aRout2}, T_{aRout1}, T_{aout2}]$ . The per-stage inlet temperature to the dryer heaters (between adsorber outlet and dryer inlet, not shown in the superstructure) after possible heat exchange is

$$T_{din,j} = T_{aAj} + Q_{dj} / (F_a (C_{pa} + Y_{aAj} C_{pv})) \quad (5.1)$$

where  $Q_{dj}$  is the heat recovered by the adsorber outlet air per-stage from the optimal hot stream combination. The heat recovered  $Q_{dj}$  is obtained by a short-cut procedure which assumes that the hot stream is the heat exchange-limiting stream in any heat exchange. Hence, for a minimum heat exchanger temperature difference  $\Delta T_{min}$ ,

$$Q_{dj} = F_a (C_{pa} + Y_{aAj} C_{pv}) \sum_{\ell=1}^{\ell=N_L} W_{k,\ell} (T_{h,\ell} - \Delta T_{min}) \quad \ell \in L, k \in K_d \quad (5.2)$$

The assumption is valid provided the hot stream does not cool below the corresponding cold stream temperature plus  $\Delta T_{min}$

$$T_{h,\ell,out} \geq T_{aA} + \Delta T_{min} \quad (5.3)$$

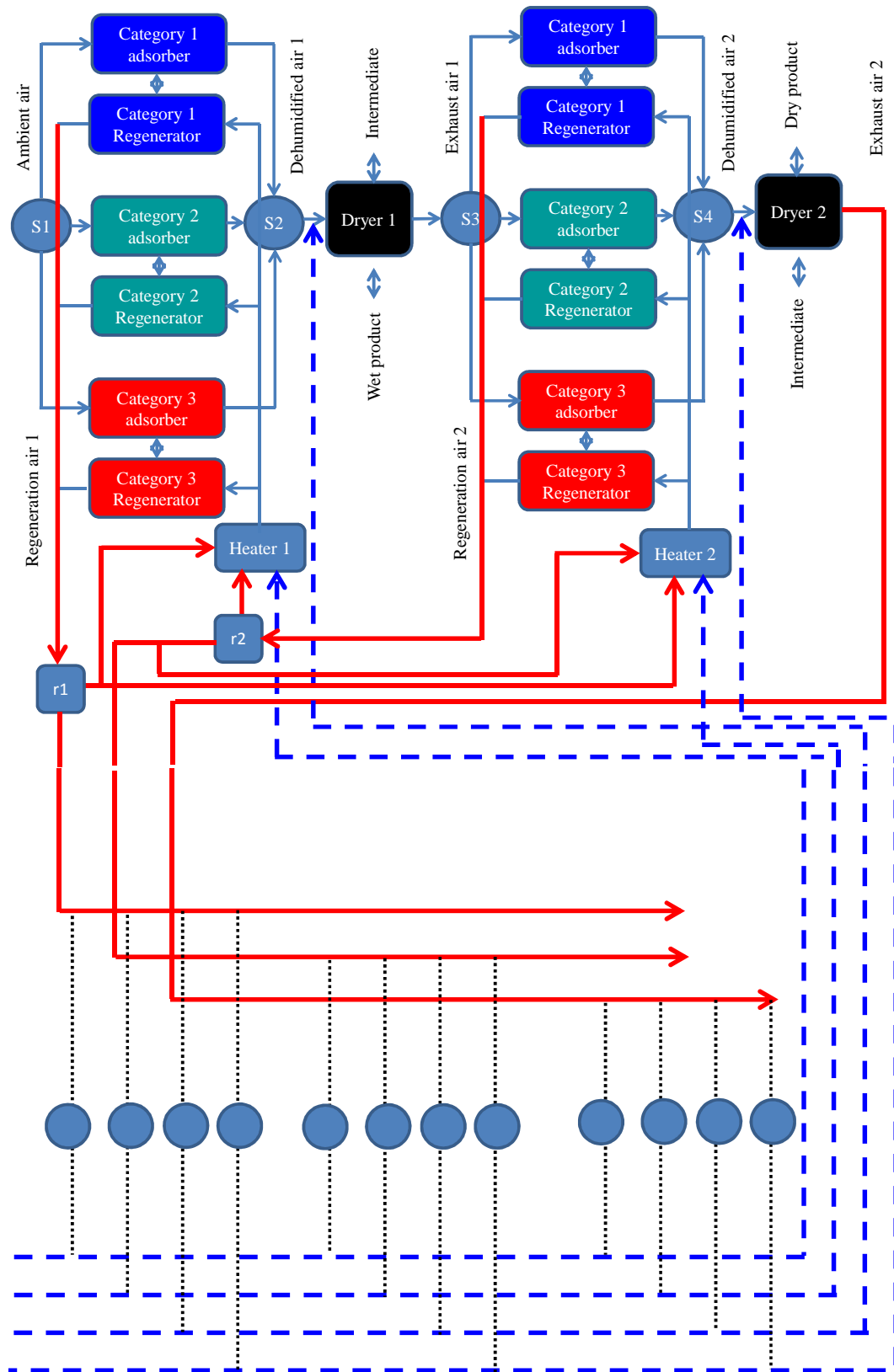


Fig. 5.1. Process superstructure with simultaneous heat integration: hot streams (continuous lines from process exhausts) either combine with cold streams (dashed lines) via heat exchangers (circles that link both streams through dotted lines) or are recycled to another part of the process; r1 and r2 are decision blocks

Equation (5.2) assumes that each cold stream combines with only one hot stream

$$\sum_{\ell=1}^{\ell=N_L} W_{k,\ell} \leq 1 \quad (5.4)$$

The temperature of the inlet air to the regenerator heater per stage  $j$  is determined as

$$T_{rin,j} = (1 - Z_j)(T_{amb} + Q_{rj}/(F_{aRj}(C_{pa} + Y_{amb}C_{pv}))) + Z_j T_{rrj} \quad (5.5)$$

where the first term represents the possible temperature after ambient air combines with some hot stream in which case the corresponding hot stream will not be recycled (hence the  $1 - Z_j$  term). By a process similar to that used in deriving (5.2), the heat  $Q_{rj}$  recovered by the ambient air to the regenerator through heat exchange with a hot stream is given by

$$Q_{rj} = F_{aRj}(C_{pa} + Y_{amb}C_{pv}) \sum_{\ell=1}^{\ell=N_L} W_{k,\ell} (T_{h,\ell} - \Delta T_{\min}) \quad j \in J, k \in K_r, \ell \in L \quad (5.6)$$

The second term (of 5.5) is the temperature of the recycled hot stream which becomes the regeneration heater inlet temperature for recycle integer variable  $Z_j=1$ .  $T_{rr}$  takes into account the mixing of fraction  $f$  of a recycled hot stream with fraction  $1-f$  ambient make-up air. From the method of mixtures, this is given by

$$T_{rrj} = \frac{(F_{aRj}(1-f)(C_{pa} + Y_{amb}C_{pv})T_{amb}) + (F_{aRj}f(C_{pa} + Y_{arinj}C_{pv})T_{h,\ell})}{F_{aRj}(1-f)(C_{pa} + Y_{amb}C_{pv}) + F_{aRj}f(C_{pa} + Y_{arinj}C_{pv})} \quad j \in J \quad \ell \in L \quad (5.7)$$

If  $T_{aDinj}$  and  $T_{aRinj}$  are the required dryer and regenerator inlet air temperatures per-stage, the utility heaters only supply the deficits after the respective inlet streams have optimally exchanged heat (or been recycled). These heater inlet temperatures  $T_{dinj}$  and  $T_{rinj}$  attained by the streams after heat exchange (or recycle) are given by (5.1) and (5.5) respectively. The heat required per stage for the drying air and regeneration air are therefore given respectively by

$$Q_{Dj} = F_a(C_{pa} + Y_{aAj}C_{pv})(T_{aDinj} - T_{dinj}) \quad (5.8)$$

$$Q_{Rj} = \sum_{i=1}^{i=M} y_{i,j} F_{aRj}(C_{pa} + Y_{arinj}C_{pv})(T_{aRinj} - T_{rinj}) \quad j \in J \quad (5.9)$$

The total heat input with simultaneous heat integration optimization is therefore

$$Q_{in,SHR} = \sum_{j=1}^{j=N} Q_{Dj} + Q_{Rj} \quad (5.10)$$



The optimization problem is thus posed as “minimize (5.10) subject to constraints (4.1) to (4.25) which also apply to the system without simultaneous heat integration as detailed in Chapter 4 and the additional constraints (5.1) to (5.7)”. The product is dried from an initial moisture content of 10kg/kg to a final value of 0.05kg/kg while constraining the drying temperature to within 50°C.

### 5.3. Results and discussion

Fig. 5.2 shows the optimal configuration with simultaneous heat integration. Process conditions of each stream are as shown in Table 5.1 compared with the case where the process is optimized first before heat recovery is considered (sequentially optimized system) as well as the conventional dryer. For the simultaneously optimized system, zeolite is chosen for the first stage just like the sequentially optimized system but regenerated at an inlet temperature of 320°C as against the 400°C required for the latter. This implies lower energy consumption. The exhaust at 200°C is used to directly regenerate the silica gel without extra heat addition via Heater 2. The exhaust of the second stage regenerator at temperature 150°C supplies energy to the ambient air (stream 15) which heats up to 130°C. The extra heat required to raise the temperature to 320°C is supplied by Heater 1, and represents the only energy spent in the system. The exhaust of the heat exchanger HX (stream 14) at 64°C and high humidity contains energy which when further exchanged with stream 4 (the outlet of the second adsorber) raises the temperature to 45°C, providing more drying power. The energy efficiency of this system is 170% as shown in Table 5.2. This corresponds to a specific energy consumption of 1470kJ/kg. Specific energy consumption is thus reduced by about 65% compared to an equivalent conventional dryer for which the process conditions are in Table 5.1 (right) and efficiencies in Table 5.2. (see also Chapter 4, Section 4.5). Note that for the conventional dryer conditions in Table 5.1., the adsorber sections (A1 and A2) of Fig. 5.2 are replaced by utility heaters and regenerator sections (R1 and R2) omitted. Compared to the sequentially optimized system, the energy consumption is reduced by 15% with simultaneous optimization. The adsorber-side process conditions for both the sequential and simultaneous cases are similar due to the imposition of the same drying capacity constraints. The main differences observed in process conditions are in the required first-stage regeneration air conditions. The inlet temperature is lower with simultaneous optimization. Also,

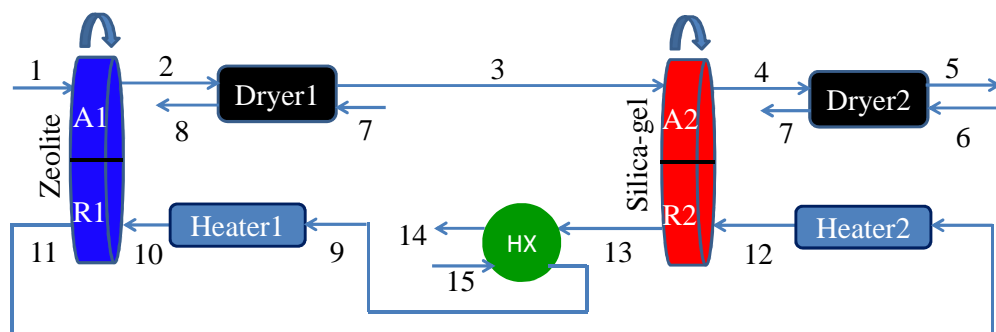


Fig. 5.2. Optimal drying system with simultaneous heat integration

Table 5.1. Operating conditions of optimal drying system with simultaneous heat integration optimization (first from left), sequential optimization (middle) and conventional dryer without adsorption system (right).  $F$  is for flowrate,  $T$  for temperature,  $Y,X$  for humidity or moisture content

No.	$F$ (kg/h)	$T$ (°C)	$Y,X$ (kg/kg)	$F$ (kg/h)	$T$ (°C)	$Y,X$ (kg/kg)	$F$ (kg/h)	$T$ (°C)	$Y,X$ (kg/kg)
1	54000	25	0.01	54000	25	0.01	71067	10	0.0100
2	54000	45	0.0031	54000	46	0.0030	71067	46	0.0100
3	54000	24	0.0114	54000	24	0.0114	71067	29	0.0108
4	54000	37	0.0065	54000	36	0.0061	71067	36	0.0108
5	54000	24	0.0115	54000	24	0.0109	71,067	28	0.0141
6	72	25	10	72	25	10	72	10	10.0000
7	72	37	6.2689	72	37	6.3674	72	29	3.2894
8	72	45	0.05	72	45	0.05	72	28	0.0500
9	5517	130	0.01	4269	115	0.01			
10	5517	320	0.01	4269	400	0.01			
11	5517	200	0.0777	4269	200	0.0990			
12	5517	200	0.0777	4269	200	0.0990			
13	5517	150	0.1255	4269	120	0.1663			
14	5517	64	0.1255	4269	62	0.1663			
15	5517	25	0.01	4269	25	0.01			

Table 5.2. Energy performance comparison among dryers

Drying system	Specific energy (kJ/kg)	Energy Efficiency (%)
Simultaneously optimized system	1470	170
Sequentially optimized system	1730	144
Conventional dryer without sorption system	4332	58

the required regeneration air flowrate is higher – a situation which favours heat recovery as reported in Atuonwu et al. (2011b). In that study where a one-stage zeolite drying system was simultaneously optimized with heat recovery, simultaneous optimization by pinch location was shown to reduce energy consumption by 13% compared to a sequentially optimized system. Simultaneous optimization therefore serves as a good method of debottlenecking both single-stage and multistage hybrid drying processes for better energy performance.

#### 5.4. Conclusion

This work demonstrates that simultaneous heat recovery optimization of a multistage adsorption drying system by appropriately modifying objective functions and adding new constraints, improves energy performance. For the studied case, zeolite retained its position as the optimal adsorbent in the first stage and silica gel in the second stage. The specific energy consumption is reduced by about 65% compared to an equivalent conventional dryer and 15% compared to a sequentially optimized system. The latter is achieved by changing the operating conditions to encourage more heat recovery while reducing the required regeneration temperatures drastically to ensure less strain on the primary energy source.

### **Synergistic process design: reducing drying energy consumption by optimal adsorbent selection**

Submitted as Atuonwu, J.C., Straten, G. van., Deventer, H.C. van., Boxtel, A.J.B. van (2012). Synergistic process design: reducing drying energy consumption by optimal adsorbent selection

#### **Abstract**

This work analyzes the synergy between two complementary unit operations – adsorbent dehumidification and drying and presents a mixed integer nonlinear programming approach to optimize energy performance in a two-stage system. Combined with active constraint analysis, the adsorbent properties that promote energy performance are derived to include high sorption capacities, surface heterogeneities and regeneration to adsorption rate constant ratios. Microporous adsorbents with higher sorption capacities at low vapor pressures and requiring higher regeneration temperatures are preferred for ambient air dehumidification in the first stage. For exhaust air dehumidification, mesoporous adsorbents with lower regeneration temperatures are preferred such that the exhaust air from the first regeneration stage can sufficiently regenerate them. For low temperature drying below 50°C, energy consumption reductions of about 70% are achieved depending on adsorbent properties, demonstrating the usefulness of superstructure optimization in matching the drying process with the capabilities of the adsorbents to enhance process synergy for improved energy efficiency.

*Keywords:* Multistage drying, dryer energy efficiency, desiccant dehumidification, process synergy, process integration, hybrid drying

#### **6.1. Introduction**

The significant contribution of drying to global industrial energy consumption necessitates the development of innovative drying process design techniques. Among these techniques is the so-called hybrid or “assisted” drying which involves combining more than one unit operation or dryer type in a single or multistage arrangement. Over the last decade, considerable research effort has been made in developing energy-efficient hybrid drying systems with most of them involving the combination of different dryer types. Examples of such efforts are found in (Kudra and Mujumdar, 2000; Ogura and Mujumdar, 2000; Chou and Chua, 2001; Raghavan et al., 2005; Witinantakit, et al., 2006; Salagnac et al., 2008; Djaeni et al., 2009;

Younes et al., 2010; Wang et al., 2011; Atuonwu et al., 2012a). In combining unit operations, it is important the unit operations be as complementary as possible for process synergy. During drying, the drying air in extracting water from the wet product undergoes a state transition from a relatively dry and hot state to a moister, cooler state. A process whose state transition is in the opposite direction would have the advantage of enhancing the drying potentials of the air hence making the system more energy-efficient. Air dehumidification by adsorbents offers this opportunity as water is extracted from the drying air with a simultaneous sensible heat gain due to the release of the adsorption heat that enhances the drying potential. To ensure continuous usability of the adsorbents, they must be regenerated by a process requiring energy expenditure of which part of the energy can be recovered. The energy efficiency of the overall process depends not only on the operating conditions but also on the adsorbent properties, selection and sequencing per-stage. The adsorbent properties in particular, place limits on achievable performance for any given process structure and operating condition. Including these properties as decision variables in process design extends the efficiency of the drying system.

The traditional approach to process design in general is first to find the structure (arrangement of unit operations) and then operating conditions that optimize a given performance criterion like energy consumption. The physical properties of the system components are usually already fixed with the choice of the unit operations even though they still have profound effects on system performance. This represents a missed opportunity to enhance system performance by improving interactions among components and enhancing synergy. This work presents a methodology based on constrained mixed integer nonlinear programming (MINLP) to define physical properties of the adsorbent in combination with sequencing per-stage as well as process conditions that promote energy efficiency in multistage drying. With this methodology, synergy is reached at two levels: combining unit operations which can be described as complementary, and deriving the physical properties, operating conditions and sequencing of system components that enhance performance while satisfying drying requirements.

Although this work considers only multistage adsorption drying systems for low temperature drying (around 50°C), the same principle can be applied to any hybrid dryer combinations for any search space of alternative system components chosen by the designer. The method can also be applied for adsorbent selection in energy-related applications like drying which has become necessary with the current development of many new pure and composite adsorbents (Thoruwa et al., 2000; La et al., 2010). The approach is also useful in other areas of Process Systems Engineering to derive material properties of feed options or unit operation devices that optimize any desired process performance criterion.

## 6.2. Process synergy analysis: a case for combinatorial optimization

For any process system, the goal is to transform a set of raw materials to value-added products using appropriate equipment operating in such conditions as would optimize given objective(s) while satisfying given requirements. Let  $J$  be the objective function to optimize. Then, the objective function depends on input variables whose values are bounded on the process constraints. The constraints can be classified into equality constraints like mass balances  $M$ , energy balances  $E$ , constitutive equations  $C$  and other constraints  $P$  (e.g. quality-oriented constraints like desired outlet product moisture content or temperature) which could also be inequality-based.

$$J = J(M, E, C, P) \quad (6.1)$$

Performance improvement for a given equipment lies in the ability to shift the constraints to a more-favorable point. When the processing system consists of a number of subsystems as in hybrid drying processes, synergy among subsystems is important for optimal performance. Assume that in a hybrid system we designate a main subsystem and the assisting subsystem. For instance, in an adsorption dryer, the dryer is the main subsystem while desiccant adsorption is an add-on. Let the performance objective we want to minimize for the hybrid system be  $J$ , and let  $J_m = J(M_m, E_m, C_m, P_m)$  be that of the main subsystem. Then there is synergy between the subsystems if

$$J < J_m \quad (6.2)$$

The synergy is obtained by the optimal choice of system properties (including physical properties) and operating conditions.

The aim of a drying process in particular is to reduce the moisture content of a product from an initial value  $X_{pin}$  to a final value  $X_p$  at a rate  $F_p$  in an energy efficient manner while meeting quality requirements. The operational objective function to be minimized is:

$$\text{Specific Energy Consumption} = \frac{\text{Total energy input}}{\text{Mass of evaporated water}} = \frac{Q_{in}}{F_p(X_{pin} - X_p)} \quad (6.3)$$

Consider the two-stage adsorption dryer shown in Fig. 6.1 with flows, temperatures and humidities as designated in Table 6.1. A continuously rotating adsorbent wheel successively passing through adsorption and regeneration sections is an add-on to the basic conventional dryer. Ambient air flowing through adsorber A1 is dehumidified in a process accompanied by adsorption heat release. It is then used in the first stage dryer, Dryer1 for drying the wet product. The dryer exhaust air is passed through a second-stage adsorber A2 and reused for drying in the second-stage dryer Dryer2.

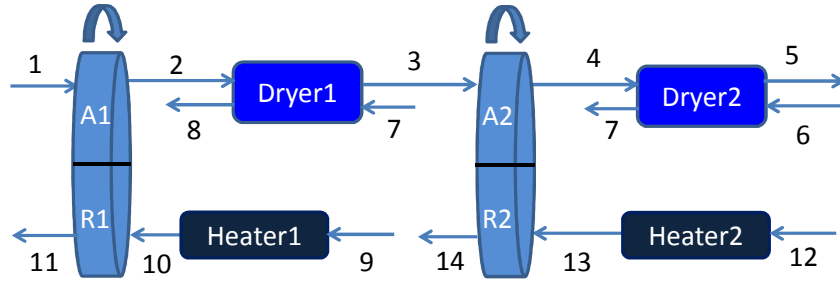


Fig. 6.1. Two-stage adsorption drying process: streams 1-7, drying air, 8-10, dried product, 11-15 regeneration air. See Table 6.1 for information on the flows.

Table 6.1. Flows, temperatures and humidities of air streams in Fig. 6.1

No.	Flow, Temp., Humidity	No.	Flow, Temp., Humidity	No.	Flow, Temp., Humidity
1	$F_a, T_{amb}, Y_{amb}$	6	$F_p, T_{pin}, X_{pin}$	11	$F_{aR1}, T_{aRout1}, Y_{aRout1}$
2	$F_a, T_{aA1}, Y_{aA1}$	7	$F_p, T_{pm}, X_{pm}$	12	$F_{aR2}, T_{arin2}, Y_{arin2}$
3	$F_a, T_{aDout1}, Y_{aout1}$	8	$F_p, T_{pout}, X_{pout}$	13	$F_{aR2}, T_{aRin2}, Y_{aRin2}$
4	$F_a, T_{aA2}, Y_{aA2}$	9	$F_{aR1}, T_{arin1}, Y_{arin1}$	14	$F_{aR2}, T_{aRout2}, Y_{aRout2}$
5	$F_a, T_{aDout2}, Y_{aout2}$	10	$F_{aR1}, T_{aRin1}, Y_{aRin1}$		

The product flow direction could be co- or counter-current to the airflow direction and the number of stages can be greater than two. Meanwhile, the spent adsorbent in each stage is regenerated in regeneration sections R1 and R2 by streams of hot air (heated via Heaters 1 and 2) also flowing continuously. The total energy consumption is

$$Q_{Reg} = \sum_{j=1}^{j=N} F_{aRj} (C_{pa} + Y_{aRin_j} C_{pv}) (T_{aRin_j} - T_{arin_j}) \quad (6.4)$$

Assuming a one-stage system, the mass balance with respect to product drying is

$$F_p (X_{pin} - X_p) = F_a (Y_{aout} - Y_{aA}) = F_a [(Y_{amb} - Y_{aA}) + (Y_{aout} - Y_{amb})] \quad (6.5)$$

The first two terms in (6.5) are the mass balance for the dried product and air respectively. The last term is a reformulation of the mass balance of air. The first part of the reformulation represents the dehumidification capacity of the adsorbent while the second term represents the drying capacity of the stand-alone dryer. Here we see synergy as the desiccant adsorption process shifts the drying capacity  $F_p(X_{pin}-X_p)$  upwards by a value equaling the dehumidification capacity of the adsorbent.

For a two-stage system, a similar result is obtained:

$$F_a [(Y_{aout} - Y_{aA1}) + (Y_{aout2} - Y_{aA2})] = F_a [(Y_{amb} - Y_{aA1}) + (Y_{aout1} - Y_{aA2}) + (Y_{aout1} - Y_{amb}) + (Y_{aout2} - Y_{aout1})] \quad (6.6)$$

The total drying capacity is the sum of the capacities of each adsorbent system and stand-alone dryer. Hence, the drying capacity is additive with the number of stages. In coupling to a dryer, synergy is thus achieved (based on condition (6.2)) with respect to product water removal (denominator of (6.3)). Barring the effects of other process constraints, energy efficiency is improved if more stages are added. There are however other constraints that limit this. For instance, the achieved dehumidification capacity which determines the adsorbent system mass balance depends on the operating conditions and the adsorbent material properties, specifically, water-vapor sorption properties:

$$F_a[(Y_{amb} - Y_{aA1}) + (Y_{aout1} - Y_{aA2})] = \text{Overall sorption capacity} \\ = f_1(\text{adsorbent properties}) \quad (6.7)$$

The regenerator system must take up this water to satisfy the mass balance and so the required regeneration air flow increases with the amount of water adsorbed. The adsorbent regeneration energy term  $Q_{Reg}$  in turn increases with the regeneration air flowrate by the expression

$$Q_{Reg} = F_{aR1}(C_{pa} + Y_{aRin1}C_{pv})(T_{aRin1} - T_{arin1}) + F_{aR2}(C_{pa} + Y_{aRin2}C_{pv})(T_{aRin2} - T_{arin2}) \quad (6.8)$$

The required regeneration temperatures are functions of the adsorbent properties

$$[T_{aRin1}, T_{aRin2}] = f_2(\text{adsorbent properties}) \quad (6.9)$$

The inclusion of the adsorbent system contributes positively to overall system performance due to the release of adsorption heat in the adsorbers which enhances drying potentials. Unlike conventional dryers which would require utility heaters to achieve higher drying temperatures, the dryer inlet temperatures in adsorption dryers are increased by sorption heat contributions which also depend on material properties

$$[T_{aA1}, T_{aA2}] = f_3(\text{adsorbent properties}) \quad (6.10)$$

The foregoing discussion highlights the potentials of the following for performance improvement:

1. Adding to the dryer, a unit with opposite state transition (6.5 and 6.6)
2. Consideration of other factors such as adsorption characteristics (6.7)
3. Consideration of ease of regeneration and corresponding energy requirements (6.8) and (6.9)
4. Consideration of sorption heat effects (6.10)

We need a method that incorporates all these issues. Section 6.3 provides this method. Since the key variables that determine performance are functions of adsorbent

properties as shown in (6.5) - (6.10), adsorbent properties are part of the optimization decision variables. Rather than advancing the synergy in an ad-hoc manner (e.g. by fixing the properties of the system components) like in most previous hybrid dryer design cases, a superstructure model of adsorbent types is postulated and the optimal system derived by solving the resulting MINLP problem.

### 6.3. Superstructure development: description, mathematical modeling and optimization

To find the adsorption drying process that maximally exploits synergy among system components to extend energy performance, it is important to explore as many as possible adsorbent options. However, the problem becomes highly combinatorial and so achieving a solution would involve several, probably, infinite number of existing adsorbent options. This problem is circumvented by formulating a superstructure model of alternatives, which lumps all possible adsorbent behaviors, into a general isotherm structure. These isotherms, regardless of the particular adsorbent involved have been classified into types 1 to 5 (Brunauer et al., 1940). The type 1 isotherm is largely described by the Langmuir equation (Lowell and Shields, 1991); the types 2 and 3 isotherms have been shown to be well-fitted by the BET equation (Thibodeaux, 1996) while types 4 and 5 isotherms are reasonably described by the Dubinin-Astakhov equations (Stoeckli, 1998). Hence, in this work, all isotherms are categorized in three as shown in the process superstructure model of Fig. 6.2. Category 1 corresponds to the type 1 behavior, which is applicable to microporous adsorbents described by monolayer adsorption. Category 2 corresponds to types 2 and 3 applicable to macroporous adsorbents described by multilayer adsorption with the type 2 having the stronger adsorbate-adsorbent affinity. Category 3 corresponds to systems with types 4 and 5 water-vapor sorption behavior applicable to mesoporous adsorbents whose description includes capillary condensation. The Dubinin-Astakhov model is modified (Moore and Serbezov, 2005) as a dual-mechanism adsorption potential equation. The isotherm model equations for the three categories of adsorbents are described respectively by

$$X_{ADSe1} = X_{01}bP/1+bP \quad (6.11)$$

$$X_{ADSe2} = X_{02}Vw/[(1-w)(1+(V-1)w)] \quad (6.12)$$

$$X_{ADSe3} = X_{03} \exp(-A/G)^m + X_{04} \exp(-A/H)^m \quad (6.13)$$

where

$$b = b_{0ij} \exp(-E_{ij}/RT_{ij}) \quad (6.14)$$

$$w = P/P_{sat} \quad (6.15)$$

$$A = RT \ln(P_{sat}/P) \quad (6.16)$$



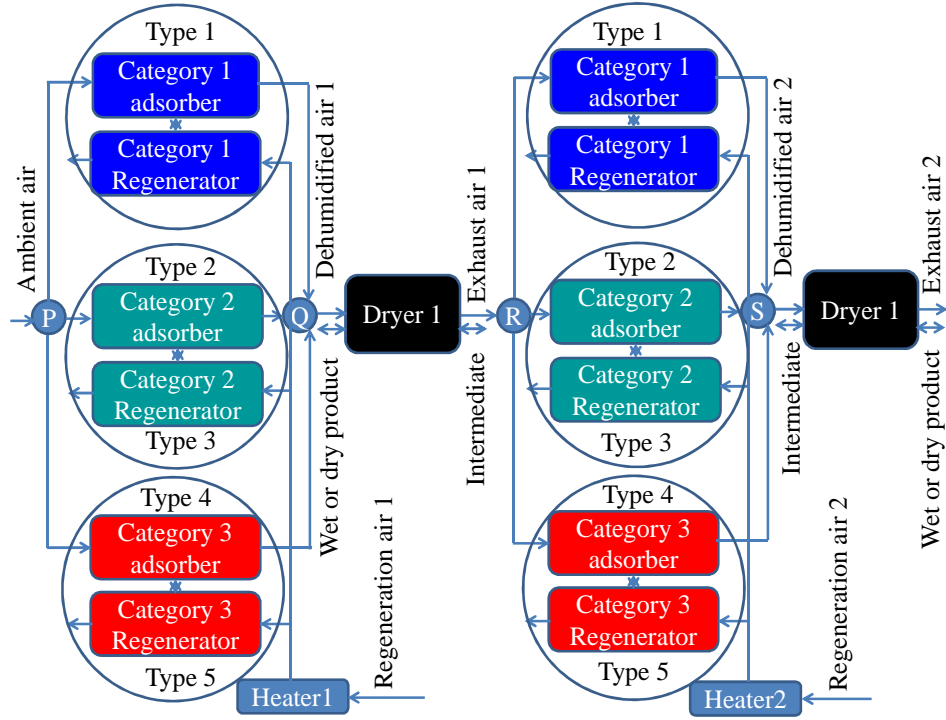


Fig. 6.2. Superstructure model of a two-stage adsorption drying process

Let  $I = \{i: i=1 \dots M\}$  and  $J = \{j: j=1 \dots N\}$  be the category of adsorbents  $i$  in stage  $j$  of the system. The first ten continuous variables in  $x_{ij}$

$$x_{ij} = [X_{01} \ X_{02} \ X_{03} \ X_{04} \ b_0 \ E \ V \ G \ H \ m \ T_{aRin} \ F_a \ F_z \ F_{aR}] \quad i \in I \ j \in J \quad (6.17)$$

consist of parameters of the isotherm models (6.11) – (6.13) describing each adsorbent isotherm type in the superstructure. These include sorption capacities, sorption heat and other thermodynamic parameters that appear in the lumped superstructure isotherm model as shown in Table 6.2. The parameters are constrained to be within ranges that are realistic relative to reported cases for existing adsorbents (see Table 6.2 for parameter values, literature sources and constraints used in the optimization). Operating conditions like adsorbent flow speed, regeneration air flowrate and inlet temperature are also included as continuous decision variables. The discrete variable consists in choosing which adsorbent isotherm type is most favorable for energy efficient drying per stage and which product-air flow configuration is best (co- or counter-current).

The mass balance for each adsorbent and regenerator where subscript  $z$  represents the adsorbent is given by

$$Y_{outij} = Y_{inij} - \frac{F_{zij}}{F_a} (X_{zoutij} - X_{zinij}) \quad (6.18)$$

Table 6.2. Adsorbent behavioral parameters and values from literature

Parameter	Description	Value <sup>(source)</sup>	Constraints
$X_{01}$ kgkg <sup>-1</sup>	Sorption capacity	0.1896 <sup>(Atuonwu et al., 2011a)</sup> , 0.1939 <sup>(Simo et al., 2009)</sup>	$0.15 \leq X_{01} \leq 0.3$
$X_{02}$ kgkg <sup>-1</sup>	Sorption capacity	0.0059, 0.058 <sup>(Likos and Lu, 2002)</sup> , 0.092 <sup>(Ferreira et al., 2011)</sup>	$0.005 \leq X_{02} \leq 0.25$
$X_{03}$ kgkg <sup>-1</sup>	Sorption capacity due to chemi- & physi-sorption	0.27530 <sup>(Park and Knaebel, 1992)</sup> , 0.1736 <sup>(Moore and Serbezov, 2005)</sup> , 0.33 <sup>(Chakraborty et al., 2003)</sup>	$0.15 \leq X_{03} \leq 0.3$
$X_{04}$ kgkg <sup>-1</sup>	Sorption capacity due to capillary condensation	0.07302 <sup>(Park and Knaebel, 1992)</sup> , 0.325 <sup>(Moore and Serbezov, 2005)</sup>	$0.05 \leq X_{04} \leq 0.4$
$b_0$ Pa <sup>-1</sup>	adsorption to desorption rate constant	$5.62 \times 10^{-11}$ <sup>(Atuonwu et al., 2011a)</sup> , 3.067 <sup>(Simo et al., 2009)</sup>	$2 \times 10^{11} \leq b_0 \leq 7 \times 10^{11}$
$E$ kJ/mol	Adsorption heat	-51.24 <sup>(Atuonwu et al., 2011a)</sup> , -57.95 <sup>(Simo et al., 2009)</sup>	$-6 \times 10^4 \leq E \leq -5 \times 10^4$
$V$ -	Energy constant	14.639 <sup>(Ferreira et al., 2011)</sup> , 1.359 <sup>(Ferreira et al., 2011)</sup>	$1 \leq V \leq 15$
$G$ kJ/mol	Adsorption heat	3.4434 <sup>(Park and Knaebel, 1992)</sup> , 7.606 <sup>(Moore and Serbezov, 2005)</sup> , 3.72 <sup>(Ferreira et al., 2011)</sup>	$1 \times 10^2 \leq G \leq 8 \times 10^3$
$H$ kJ/mol	Adsorption heat	10.931 <sup>(Park and Knaebel, 1992)</sup> , 0.862 <sup>(Moore and Serbezov, 2005)</sup>	$8 \times 10^2 \leq H \leq 1.1 \times 10^4$
$m$ -	Heterogeneity parameter	2 <sup>(Park and Knaebel, 1992)</sup> , 1 <sup>(Moore and Serbezov, 2005)</sup> , 0.9 <sup>(Ferreira et al., 2011)</sup>	$0.8 \leq m \leq 3.5$

where  $Y_{out}$  represents the outlet air humidities and  $Y_{in}$  the inlet values,  $X_{zin}$  and  $X_{zout}$  the solid inlet and outlet moisture contents respectively.

The energy balances of the sorption system state that the aggregate sensible and latent heat of the outlet air equals the algebraic sum of the inlet air sensible and latent heat and the released (or absorbed) sorption heat

$$T_{outij} = \frac{F_{aij}((C_{pa} + Y_{anij}C_{pv})T_{ainij} + (\Delta H_v + H_{ads})(Y_{ainij} - Y_{aoutij})) + F_{zij}((C_{pzij} + X_{zinij}C_{pw})T_{zinij})}{F_{aij}(C_{pa} + Y_{aoutij}C_{pv}) + F_{zij}(C_{pzij} + X_{zoutij}C_{pw})} \quad (6.19)$$

The same energy balance is used for the dryer except that the sorption heat term  $H_{ads}$  is negligible (Atuonwu et al., 2011a) and subscript  $z$  is replaced by  $p$ . Moreover,  $T_{out} = T_{aDout}$  for the dryer,  $T_{aRout}$  for the regenerator and  $T_{aA}$  for the adsorber. The adsorption heat  $H_{ads}$  is given by the Clausius-Clapeyron relation

$$H_{ADS} = -RT^2 \left( \frac{\partial \ln P}{\partial T} \right)_{X_{ze}} \quad (6.20)$$

The integer variable defining adsorbent category choice per stage is

$$y_{ij} \in \{0,1\} \quad i \in I \quad j \in J \quad (6.21)$$

Logical constraints are defined as follows: since the use of only one adsorbent is permissible per stage,

$$\sum_{i=1}^{i=M} y_{ij} = 1 \quad j \in J \quad (6.22)$$

If  $L_j$  represents any output variable (e.g. air humidity  $Y$ , temperature  $T$ , adsorbent moisture content ratio  $X$ ) from each adsorbent stage, then, if  $L_{ij}$  is the value for each adsorbent category,

$$L_j = \sum_{i=1}^{i=M} y_{ij} L_{ij} \quad j \in J \quad (6.23)$$

The two stage system can be operated in either co- or counter-current, which results in the following product coupling constraints:

For co-current operation,

$$PC_1 = \{X_{pinj} = X_{pj-1}; T_{pinj} = T_{pj-1}; X_{p0} = X_{pin}; T_{p0} = T_{pin}; X_{pN} = X_{pfinal}; T_{pj} \leq T_{pmax}\} \quad (6.24)$$

For counter-current operation,

$$PC_2 = \{X_{pinj} = X_{pj+1}; T_{pinj} = T_{pj+1}; X_{pM} = X_{pin}; T_{pM} = T_{pin}; X_{p1} = X_{pfinal}; T_{pj} \leq T_{pmax}\} \quad (6.25)$$

If  $v_1$  and  $v_2$  be integer variables representing the existence of co-current and counter-current product-air flows respectively, the effective coupling constraint is

$$PC = v_1 PC_1 + v_2 PC_2 \quad (6.26)$$

The dryer mass balances for co-current and countercurrent operations are respectively

$$F_p (X_{pout_{j-1}} - X_{pout_j}) = F_a (Y_{aout_j} - Y_{ain_j}) \quad X_{pout_0} = X_{pin} \quad (6.27)$$

$$F_p (X_{pout_{j-1}} - X_{pout_j}) = F_a (Y_{aout_{N+1-j}} - Y_{ain_{N+1-j}}) \quad (6.28)$$

The overall dryer mass balance is

$$F_p (X_{pin} - X_p) = F_a [v_1 (Y_{aout_j} - Y_{ain_j}) + v_2 (Y_{aout_{N+1-j}} - Y_{ain_{N+1-j}})] \quad (6.29)$$

where

$$v_1 + v_2 = 1, v_1, v_2 \in \{0,1\} \quad (6.30)$$

The goal of the study is to design the adsorbent system properties, operational sequences and conditions that minimize the total energy consumed when drying a

given product to specified moisture content. Here, the product at 72kg/h dry mass flowrate is dried from a moisture content of 10 to 0.05 kg water/kg dry product, the drying air temperature is constrained to 50°C (drying behavior described in Atuonwu et al. (2011a)). The total energy consumed is the sum of the regeneration inputs over the entire search space:

$$Q_{in}(x_{ij}, y_{ij}, v, T_{arin2}) = \sum_{i=1}^{i=M} \sum_{j=1}^{j=N} y_{ij} F_{aRij} (C_{pa} + Y_{aRin_j} C_{pv}) (T_{aRin_j} - T_{arin_j}) \quad i \in I, j \in J, T_{arin1} = T_{amb} \quad (6.31)$$

The MINLP optimization problem is therefore formulated as minimize process energy consumption (6.31) subject to constraints (6.11) to (6.30).

The corresponding energy efficiency  $\eta$  is defined as the ratio of the latent heat of water evaporated to the energy consumption:

$$\eta = \frac{F_p (X_{pin} - X_p) \Delta H_v}{Q_{in}} \quad (6.32)$$

where  $\Delta H_v$  is the specific latent heat of vaporization of water

The problem is implemented in TOMLAB® Optimization software (TOMLAB Optimization Inc. Seattle WA) using the “KNITRO” solver which uses the branch and bound method by which integer constraints are first relaxed and the NLP relaxation solved to obtain the lower bound on the integer variable. For each integer variable with non-integer solutions, new bound constraints are added to form two new NLP problems. The NLP relaxation is solved with interior point methods. To ensure the solution is as close as possible to the global optimum, the solver employs a multi-start procedure, which generates multiple new start points by randomly selecting values of continuous variables that satisfy the variable bounds. In a second step, heat recovery from the regenerator outlet is considered to further improve energy performance.

## 6.4. Results and Discussion

### 6.4.1. Adsorbent property optimization and energy efficiency analysis

Fig. 6.3 shows the adsorbent-water vapor isotherm behavior (for a range of temperatures) of the derived optimal adsorbent per-stage for the process with property constraint behavior shown in Table 6.3. From the results, the adsorbents with type 1 (Langmuir) water vapor sorption behavior are optimal for the first stage of the drying system while in the second stage; adsorbents with type 4 or 5 behavior take priority. Ambient air dehumidification which occurs in the first stage requires a type 1 adsorbent (example, zeolite) while exhaust air dehumidification in the second uses a type 4 or 5 isotherm-based adsorbent (example, silica-gel). Sorption capacity-vapour

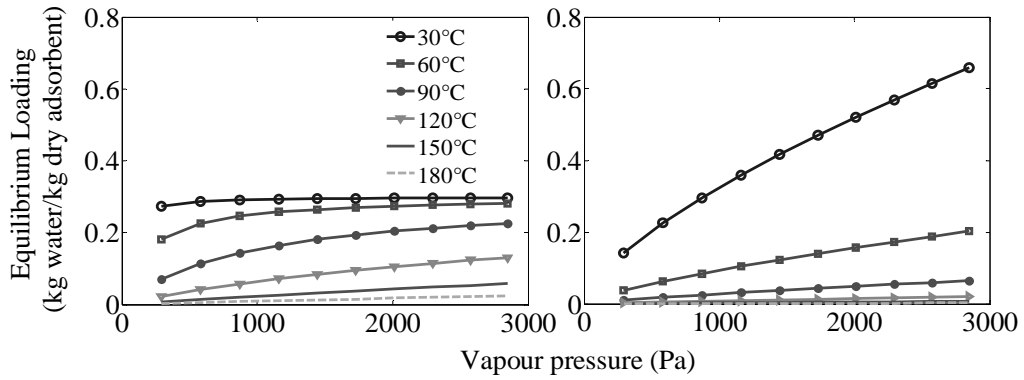


Fig. 6.3. Adsorbent-water vapour sorption isotherms for a range of temperatures for optimal adsorbent choices per stage showing type 1 in first stage (left) and type 4 (or 5) in second stage (right)

Table 6.3. Adsorbent parameters and their constraint behaviors in optimization (DNF means “Does not feature” in the solution)

Parameter	Description	Constraints	Behavior
$X_{01}$ kgkg <sup>-1</sup>	Sorption capacity	$0.15 \leq X_{01} \leq 0.3$	Active: upper limit
$X_{02}$ kgkg <sup>-1</sup>	Sorption capacity	$0.005 \leq X_{02} \leq 0.25$	Inactive (DNF)
$X_{03}$ kgkg <sup>-1</sup>	Sorption capacity due to chemi & physi-sorption	$0.15 \leq X_{03} \leq 0.3$	Active: upper limit
$X_{04}$ kgkg <sup>-1</sup>	Sorption capacity due to capillary condensation	$0.05 \leq X_{04} \leq 0.4$	Active: upper limit
$b_0$ Pa <sup>-1</sup>	adsorption to desorption rate constant	$2 \times 10^{11} \leq b_0 \leq 7 \times 10^{11}$	Active: lower limit
$E$ kJ/mol	Adsorption heat	$-6 \times 10^4 \leq E \leq -5 \times 10^4$	Inactive
$V$ -	Energy constant	$1 \leq V \leq 15$	Inactive (DNF)
$G$ kJ/mol	Adsorption heat	$1 \times 10^2 \leq G \leq 8 \times 10^3$	Inactive
$H$ kJ/mol	Adsorption heat	$8 \times 10^2 \leq H \leq 1.1 \times 10^4$	Inactive
$m$ -	Heterogeneity parameter	$0.8 \leq m \leq 3.5$	Active: lower limit

pressure matching is observed. The adsorbent chosen for ambient air dehumidification has a higher sorption capacity at lower drying air vapour pressures while for the moister higher vapour pressure 1<sup>st</sup> stage dryer exhaust air, another adsorbent of higher sorption capacity in that operating region is chosen. Fig. 6.4 shows a state transition diagram of the process air on a psychrometric chart for the optimal adsorption dryer and an equivalent conventional dryer with numberings 1 to 5 representing streams in the flowsheet of Fig. 6.5. The processes corresponding to the transitions in Fig. 6.4 are explained in Table 6.4. The total drying capacity for the adsorption dryer (measured by summing the values of humidity changes associated with the transitions 2 – 3'' and 3''' – 5, Fig. 6.4) is about 0.015kg water per kg dry air. For the conventional dryer (1' – 2c and 1c – 4c), it is 0.0085kg water per kg dry air. Hence, the conventional dryer requires 76% more air for the same water evaporation. In addition, it does not benefit from sorption heat release so the energy required to heat this large air flow to the desired temperature is sourced from utilities. Moreover, due to the low temperature of the exhaust at 3c (close to ambient) the exhaust heat cannot be economically used to preheat the inlet ambient air.

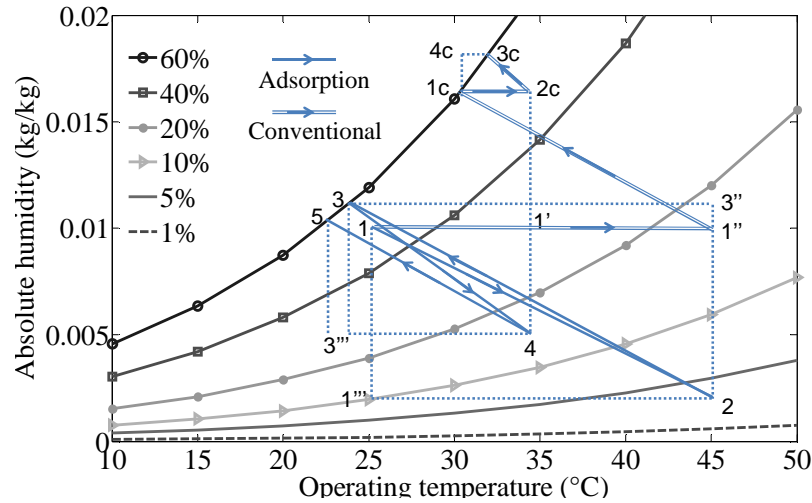


Fig. 6.4. Psychrometric chart showing the state transitions of the process air at each point on the optimal adsorption and equivalent conventional dryers. The routes of the adsorption dryer and the conventional dryer through the chart are given in Table 6.4. Product air equilibrium is assumed at 60% relative humidity.

Table 6.4. Description of state transition processes on Fig. 6.4

State transition	Process (Adsorption dryer)	State transition	Process (Conventional dryer)
1 – 2	First-stage adsorbent dehumidification	1 – 1''	First-stage air heating
1''' – 2	Corresponding sorption heat release	1'' – 1c	First-stage product drying
1 – 1'''	Corresponding dehumidification capacity.	1' – 2c	First-stage product drying capacity
2 – 3	First stage product drying	1c – 2c	Second-stage air heating
2 – 3''	First-stage product drying capacity	2c – 3c	Second-stage product drying
3 – 4	Second-stage adsorbent dehumidification	1c – 4c	Second-stage product drying capacity
3''' – 4	Corresponding sorption heat release		
3 – 3'''	Corresponding dehumidification capacity		
4 – 5	Second stage product drying		
3''' – 5	Second stage drying capacity		

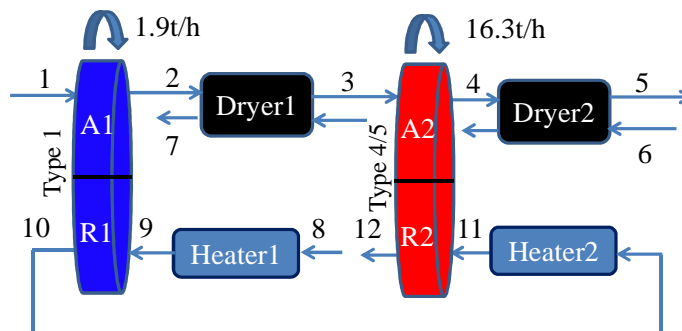


Fig. 6.5. Optimal drying system: Drying air flow  $54 \times 10^3 \text{ kg/h}$ , Regeneration air flow  $3.31 \times 10^3 \text{ kg/h}$ , Specific Energy Consumption= $1785 \text{ kJ/kg}$  without heat recovery,  $1345 \text{ kJ/kg}$  with heat recovery

Fig. 6.6 shows the regeneration air conditions of the optimal adsorption dryer with numberings also represented on Fig. 6.5. Heat requirement matching is observed. The optimal operating conditions shows the required regeneration air inlet temperature for the second stage adsorbent equals the first stage regenerator exhaust air temperature (streams 10 & 11 are coincident, see Fig. 6.6). Thus, Heater2, Fig. 6.5 is redundant. Also, the flowrate (speed) of the second-stage adsorbent is 16.3 t/h which is much higher than that of the first stage which is returned as 1.9 t/h (Fig. 6.5). This implies the second-stage wheel behavior is optimized for exhaust heat recovery while the first stage is optimized for air dehumidification. Overall, these effects in addition to the enhanced drying capacity ensure a highly energy-efficient system that improves further with heat recovery. The specific energy consumption is 1785kJ/kg of water evaporated which corresponds to about 57% reduction compared to the conventional dryer (4167 kJ/kg) for which there is no beneficial heat integration. The corresponding energy efficiencies are 140% and 60% respectively.

When the second-stage regenerator exhausts (stream 12 at 140°C) is used to pre-heat the ambient air to the first (stream 8 at 25°C), the ambient air heats up to 120°C, recovering part of the heat. Specific energy consumption reduces to 1345 kJ/kg (about 70% reduction compared to the conventional system) under the stated adsorbent property constraints. It should however be noted that the optimal solution hits some adsorbent property constraints. The type 1 sorption capacity  $X_{01}$  constraint is active at the upper limit 50% higher than that reported for a zeolite type (Simo et al., 2009), while the type 4(or 5) sorption capacities  $X_{03}$  and  $X_{04}$  are respectively active at limits 45% and 23% above that for silica gel (Park and Knaebel, 1992). The lower limit constraints hit are the ratio  $b_0$  of adsorption to regeneration rate constants (33% lower than that for zeolite (Simo et al., 2009)) surface heterogeneity parameter  $m$  (60% lower than that for silica gel (Park and Knaebel, 1992)). The constraint behaviors also presented in Table 3 show that high sorption capacities, surface heterogeneities and ratios of regeneration rate to adsorption rate constants are desirable properties in energy-efficient drying applications. In choosing adsorbents for drying applications it is therefore important to look out for adsorbents having high values of these properties. The sensitivity analysis results that follow show how variations in the constraints on these active parameters affect system performance.

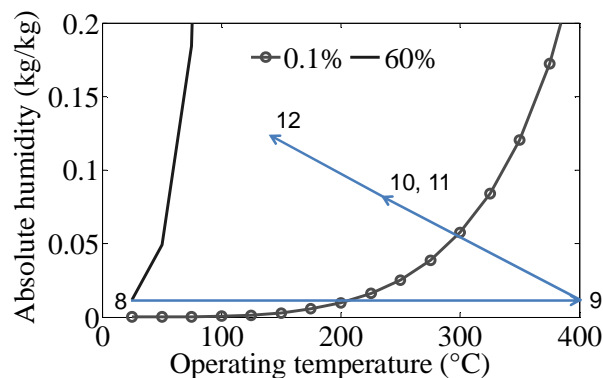


Fig. 6.6. Psychrometric chart showing regeneration air conditions for optimal system

## 6.4.2. Sensitivity analysis

Fig. 6.7(a), (b) and (c) show respectively, the sensitivities of the first stage adsorbent flowrate, regeneration air flowrate and the corresponding system energy efficiency to the category 1 active parameter variations (adsorption to desorption rate constant ratio and monolayer sorption capacity). A reduction in sorption capacity means the adsorbent wheel has to rotate faster in compensation to meet the same drying capacity

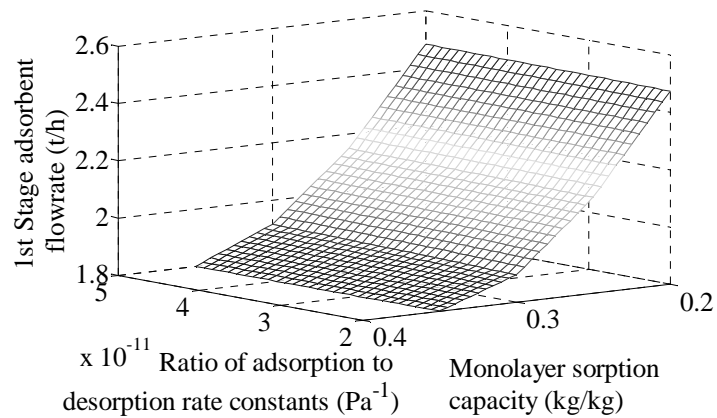


Fig. 6.7a. Sensitivity of 1<sup>st</sup> stage adsorbent flowrate to parameters  $X_{01}$  and  $b_0$

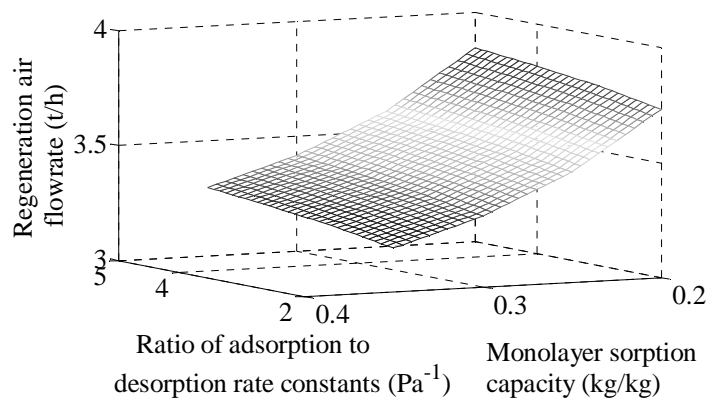


Fig. 6.7b. Sensitivity of regeneration air flowrate to parameters  $X_{01}$  and  $b_0$

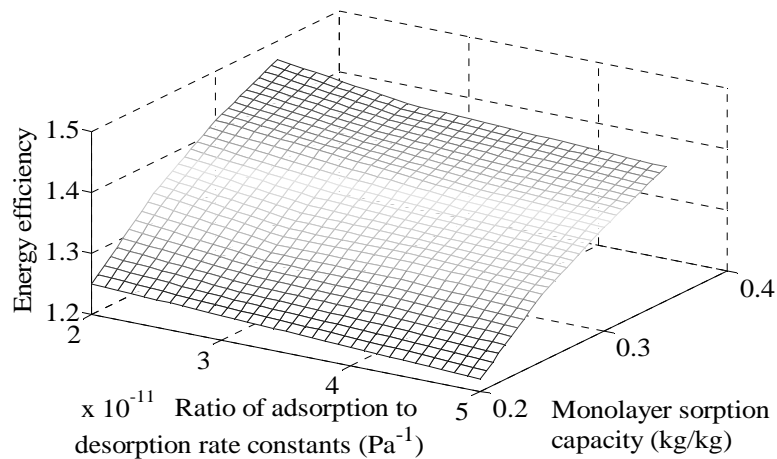


Fig. 6.7c. Sensitivity of system energy efficiency to parameters  $X_{01}$  and  $b_0$



requirements. This places higher regeneration air flow/temperature requirements and more energy consumption. Energy efficiency therefore reduces. The second wheel does not follow the trend but behaves in such a way as to satisfy overall mass balances. For Fig. 6.8(a), (b) and (c) which consider the sensitivities of the first stage adsorbent flowrate, regeneration air flowrate and the corresponding system energy efficiency with respect to the second-stage adsorbent parameter variations, similar results are obtained. High sorption capacities favor energy performance. A high surface heterogeneity which corresponds to a low value of heterogeneity parameter  $m$

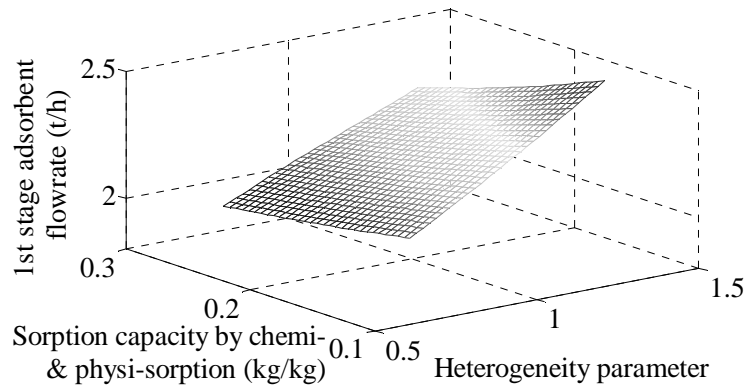


Fig. 6.8a. Sensitivity of 1<sup>st</sup> stage adsorbent flowrate to parameters  $X_{03}$  and  $m$

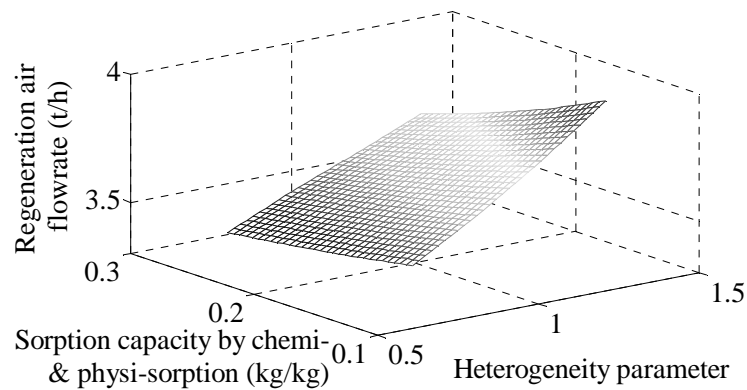


Fig. 6.8b. Sensitivity of regeneration air flowrate to parameters  $X_{03}$  and  $m$

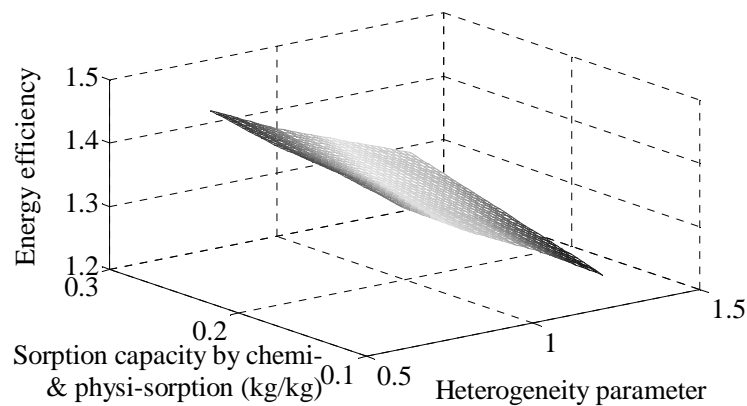


Fig. 6.8c. Sensitivity of system energy efficiency to parameters  $X_{03}$  and  $m$

(Dobruskin, 1998) also favors energy efficiency. In choosing adsorbents for drying applications therefore, these properties should be considered. Another important parameter, “adsorption heat” is inactive during the optimization. A reason is the fact that although high sorption heat promotes adsorption and hence drying capacity, it is also synonymous with high regeneration temperature requirements. A high or low adsorption heat therefore does not necessarily favor energy performance. The parameters corresponding to the category 2 adsorbents do not feature in the optimal solution and so do not form part of the active constraints. From the results it can be inferred that high sorption capacities, surface heterogeneities and regeneration to adsorption rate constant ratios are desirable properties for any adsorbent to be used in energy-efficient drying applications. To maintain the same dehumidification and hence product drying capacity for lower values of these property variables, adsorbent circulation rate and regeneration air flow/temperature would be increased, implying higher energy consumption.

### **6.5. Conclusion**

In this work, the synergy between two complementary unit operations – adsorbent dehumidification and drying has been analyzed and a mixed integer nonlinear programming approach developed to optimize energy performance in a two-stage system. Combined with active constraint analysis, the adsorbent properties that promote energy performance have been derived. For ambient air dehumidification as occurs in the first stage, microporous adsorbents with higher sorption capacities at low vapor pressures and requiring higher regeneration temperatures are preferred. For exhaust air dehumidification, mesoporous adsorbents with lower regeneration temperatures are preferred such that the exhaust air from the first regeneration stage can sufficiently regenerate them without the need for extra utility energy supply. For any operating condition per-stage, high sorption capacities, surface heterogeneities and regeneration to adsorption rate constant ratios are shown to be favorable. Sensitivity analysis of system behavior reveals that to maintain the same dehumidification for lower values of these property variables, adsorbent circulation rate and regeneration air flow/temperature would be increased, implying higher energy consumption. Under the studied constraints on adsorbent properties, energy consumed is about 1345 kJ/kg of water evaporated with heat integration as against the 4167 kJ/kg consumed in equivalent conventional dryers. This represents a 70% reduction. Using adsorbents with such properties or better, such low energy consumption can be achieved or surpassed. It is thus recommended to explore the application to drying processes of novel adsorbents developed for various other uses. The results demonstrate the superstructure optimization method as being useful not only for determining optimal operating conditions and structure of process systems but determining the optimal properties of unit operation components. For the studied case, it is found useful in choosing adsorbents for drying applications while at the same time matching the drying process with the capabilities of the adsorbents to enhance process synergy for improved energy efficiency.

### **On the controllability and energy sensitivity of heat-integrated desiccant adsorption dryers**

Published as Atuonwu, J.C., Straten, G. van., Deventer, H.C. van., Boxtel, A.J.B. van (2012). On the controllability and energy sensitivity of heat-integrated desiccant adsorption dryers. *Chemical Engineering Science* 80, 134-147.

#### **Abstract**

This work studies the controllability of heat-integrated zeolite adsorption dryers. Mean product moisture content, temperature and vitamin C concentration (representative of product quality) are considered as controlled variables. Set-point tracking and disturbance rejection controllability metrics are considered in addition to energy performance sensitivity. In adsorption dryers, the adsorption system introduces extra degrees of freedom of which some input-output pairs are promising. For corresponding inputs, adsorption dryers are shown to have higher steady-state gains than equivalent conventional dryers due to correlation between dehumidification, adsorption heat and the controlled variables. They also show improved resilience to ambient air disturbances due to adsorbent subsystem-induced self-regulation properties. The encouraging mechanisms of the self-regulation are adsorption heat, kinetic and equilibrium properties of the adsorbent. Due to the high correlation between product moisture content and temperature, improved controllability is observed when vitamin C concentration is used as an output variable instead of product temperature. It is thus proposed that on the availability of reliable soft sensors or state estimators, instead of product temperature, vitamin C or some other temperature-dependent quality measure should be controlled in addition to product moisture in decentralized drying system control. Under perfect rejection of unfavourable disturbances like ambient temperature drop and humidity rise, the energy performance of adsorption dryers is not significantly degraded, whereas, it is for conventional systems.

*Keywords:* Drying, Desiccant adsorption, Process control, Controllability analysis, Energy, Food processing

#### **7.1. Introduction**

Drying is an energy intensive unit operation. Assuming a 100% energy efficient dryer, the theoretical amount of heat required to evaporate 1kg of free water from a product is in the order of 2.5MJ. Yet, limitations imposed by product heating, presence of bound water and hence, falling rate period of drying, heat losses, among other things

mean that conventional dryers are far less than 100% efficient. Energy efficiencies of conventional convective dryers are usually in the range of 20 – 60% (Mujumdar, 2007b). With about 60000 products dried in application domains spanning virtually all industrial process systems, it comes as no surprise that drying consumes about 10 – 25% of the national industrial energy of the developed world (Mujumdar, 2004b). In all drying applications, it is required that the dried product be of acceptable quality. This requirement becomes more necessary when drying heat-sensitive products like food and pharmaceuticals which incidentally greatly impact daily life. In addition to traditional issues like drying to optimal storage conditions and weight reduction for easier transportation, many new quality indicators emerge. For instance, nutrient retention, flavor, microbial safety in food systems and stability of active ingredients in pharmaceutical systems must be assured thus necessitating precise control of drying conditions. A review (Dufour, 2006) of research efforts on control applications in drying technology corroborates this as applications in food and pharmaceutical processes together account for about 73% of all published articles on dryer control up till 2005. Over the years, many new technologies have been developed towards improving energy efficiency and product quality. However, without good control, these improvements could be lost (Robinson, 1992) as disturbances, propagating through the dryer may result in off-spec products, inefficient operation, and even safety problems. It therefore becomes necessary to ensure these innovative drying systems also have good controllability properties.

Adsorption drying has been identified as a means of improving energy efficiency in low temperature drying suitable for heat sensitive products like food (Atuonwu et al., 2011a, b). In this method, ambient air is dehumidified by passing through an adsorbent system (e.g. zeolite) before contacting the wet product so the driving force for drying at low temperatures is increased. Adsorption heat is released in the process. Although energy is spent on regenerating the adsorbent, it has been shown (Atuonwu et al., 2011a) that optimizing the drying air, regeneration air and zeolite flowrates as well as regeneration air inlet temperature introduces net energy advantages. The energy spent on regeneration under optimal conditions is less than the energy gain associated with the increased moisture carrying capacity of the air due to dehumidification and adsorption heat release. Thus, overall energy efficiency is improved while drying temperature is constrained for good product quality. This improvement in efficiency becomes more significant when part of the energy of the regenerator exhausts is recovered using heat exchangers. The introduction of the adsorption-regeneration subsystem with its recycle loops and the heat recovery however increase the complexity of the system so that controllability becomes an important issue for consideration. This work focuses on the ease with which decentralized control can be satisfactorily applied to an adsorption drying system for set-point tracking, disturbance rejection and optimal energy and quality performance using well-established controllability indicators. Although the last decade has witnessed a proliferation of advanced multivariable control techniques like Model

Predictive Control, multi-loop decentralized feedback control based on Proportional-Integral-Derivative (PID) controllers still remains the “workhorse” of industrial process control. It constitutes over 90% of all industrial control loops (Åström and Hägglund, 2006) and is still the main control tool in drying processes (Dufour, 2006) due to the simplicity, relatively low cost, ease of implementation, proven nature and general industrial acceptance. Controllability analysis using multi-loop controllability indices is thus still very important for emerging processes.

Not much work has been done on the controllability of dryers. One major treatment of the subject is Langrish (1998) who examined the controllability of high temperature conventional dryers operating at 400°C and used in timber veneer drying from a moisture content of 1.35 to 0.15kg/kg. Controllability indices used in that study are the relative gain array *RGA*, process condition number *PCN*, Morari integral controllability *MIC* and Niederlinski stability criterion *NI*. The drying system studied was a square plant characterized by two inputs, the air flowrate and the fuel gas flowrate and two outputs, the solids moisture content and temperature. *RGA* results indicated the preferred pairings as (solids outlet temperature-inlet air flowrate) and (solids outlet moisture content-fuel gas flowrate). When up to 30% of the exhaust air is recycled, the preferred pairings are changed and the system becomes less controllable. It can therefore be concluded from that study that recycling reduces controllability which is consistent with the results of several researchers (Kumar and Daoutidis, 2002; Horvarth and Mizsey, 2009). The interaction of energy performance and controllability was not investigated. Berghel and Renström (2004) investigated the controllability of a spouted bed dryer used in drying non-screened sawdust with air and superheated steam as drying media. Only one input, feed-rate and one output, product moisture content, were considered. Ogura et al. (2005) studied the controllability of hot air production in chemical heat pump assisted dryers and concluded that the hot air temperature can be controlled by adjusting the reactor temperature, pressure or thermal power input. More recently, Ortega et al. (2007) used pole-zero analysis, singular value decomposition and *RGA* analysis to analyze the controllability of a rotary dryer. *CN*, *MIC* and *NI* all do not completely consider the disturbance rejection properties of the system. Disturbance rejection is, however, the main objective of process control (Skogestad and Morari, 1987; Chang and Yu, 1992) in general and for drying systems in particular where disturbances have high effects on product quality (Dufour, 2006). In the cited studies, neither disturbance rejection nor energy sensitivity and product quality was investigated.

The objective of this work is to assess the controllability of a heat-integrated adsorption dryer in comparison with equivalent conventional dryers while evaluating the sensitivity of energy performance to disturbances which also relates with controllability. In addition to traditional outputs like product moisture content and temperature, vitamin C concentration, a main quality indicator, is taken as an output. Vitamin C, while itself is important in many dried food products, stands here mainly as a model for any thermo-degradable quality attribute.

## 7.2. Process description

The adsorption drying process consists of the dryer, heat sources, a zeolite adsorption/regeneration system usually realized by a continuously rotating zeolite-coated wheel successively passing through adsorption and regeneration sections and a heat exchanger for heat recovery. As shown in Fig. 7.1, ambient air is dehumidified in a zeolite adsorber and heated (in Heater2) before being used for drying the wet product in the dryer. The dehumidification is accompanied by the release of adsorption heat the magnitude of which is proportional to the amount of water adsorbed. Meanwhile, the spent zeolite is regenerated using hot air obtained by passing ambient air through Heater1. To regain adsorption capacity after regeneration, the hot zeolite is cooled between the regenerator and adsorber. The exhaust air from the regenerator is hot and is used to preheat ambient air through heat exchanger HX1 before being fed to Heater1.

The system is represented in state space form (Atuonwu et al., 2011a) as

$$\frac{dx}{dt} = f(x, u, d) \quad (7.1)$$

Where  $f$  is a nonlinear vector-valued function. The state, input and disturbance vectors in this work are respectively

$$\mathbf{x} = [X_p \ T_p \ X_{zA} \ T_{zA} \ X_{zR} \ T_{zR} \ Y_{aD} \ T_{aD} \ Y_{aA} \ T_{aA} \ Y_{aR} \ T_{aR} \ N_p \ T_x \ T_y]^T \quad (7.2)$$

$$\mathbf{u} = [Q_{h1} \ Q_{h2} \ F_{aA} \ F_z \ F_{aR}]^T \quad (7.3)$$

$$\mathbf{d} = [F_p \ X_{pin} \ T_{amb} \ Y_{amb}]^T \quad (7.4)$$

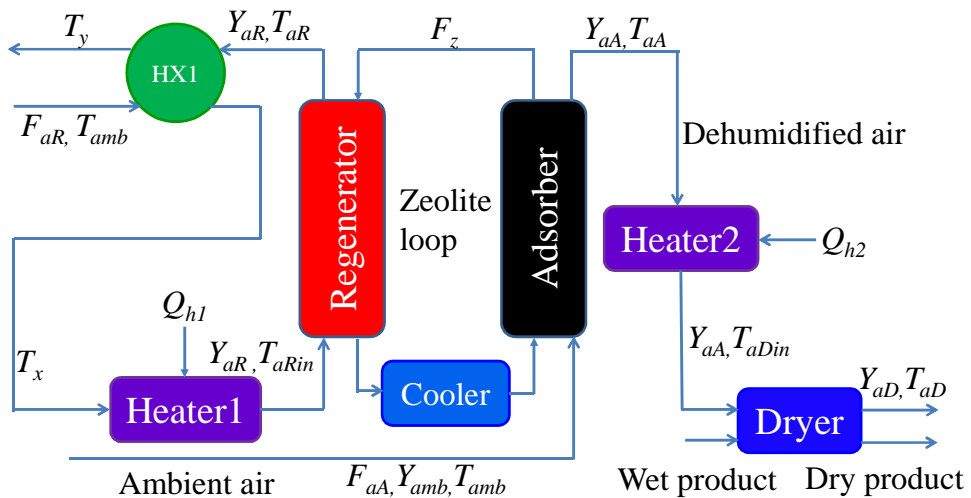


Fig. 7.1. Heat-integrated adsorption dryer

The overall output vector is

$$\mathbf{y} = [X_p \quad T_p \quad N_p]^T \quad (7.5)$$

where  $X_p$ ,  $X_{zA}$  and  $X_{zR}$  are the outlet moisture contents (kg/kg dry solid) of the product, adsorber and regenerator zeolite respectively while  $T_p$ ,  $T_{zA}$  and  $T_{zR}$  are the corresponding temperatures (°C).  $Y_{aD}$ ,  $Y_{aA}$  and  $Y_{aR}$  are the absolute humidities (kg/kg dry air) of the air from the dryer, adsorber and regenerator respectively while  $T_{aD}$ ,  $T_{aA}$  and  $T_{aR}$  are the corresponding temperatures.  $T_x$  and  $T_y$  are the heat exchanger outlet temperatures on the cold and hot stream sides respectively.

To indicate product quality which is very important in food drying applications, vitamin C concentration  $N_p$  (normalized as a percentage of the initial or maximum value) is included as a state variable. Of the inputs (which are derived from degree of freedom analysis),  $Q_{h1}$  is the heat input (Heater1) to the regeneration air, while  $Q_{h2}$  is the heat input (Heater2) to the drying air. Both can be manipulated by changing variables like fuel flowrates in fuel-fired systems or heating current in electrical heating systems.  $F_{aA}$ ,  $F_z$  and  $F_{aR}$  are the flowrates of the drying air, zeolite and regeneration air respectively. The disturbance variables are feed flowrate,  $F_p$ , moisture content  $X_{pin}$ , ambient air humidity  $Y_{amb}$  and temperature  $T_{amb}$ . Detailed information on the model is available in Chapter 2 of the thesis and elsewhere (Atuonwu et al., 2011a, c) with the vitamin C model derived from Mishkin et al. (1983), see Appendix C. The steady-state operating conditions are as shown in Table 7.1. These steady-state operating conditions are based on energy efficiency optimization of the system (Atuonwu et al., 2011a).

Traditionally, product moisture content and temperature are output variables in drying systems (Langrish, 1998; Langrish and Harvey, 2000; Abdel-Jabbar, et al., 2005; Luz et al., 2010). Product moisture content can be regarded as the main output variable since the objective of drying is to reduce the moisture content to an optimal value. Also, good moisture content control has been shown to improve energy efficiency (Wang et al., 2009). Product temperature is usually included to gauge some other quality measure. It is generally observed that if vitamin C is well retained in foods, other nutrients are also well retained so vitamin C can be taken as an index of nutrient quality of foods (Marfil et al., 2008). Thus, in this work, the output variables are product moisture content, temperature and vitamin C concentration.

For the manipulated inputs  $\mathbf{u}$ , there is the possibility of replacing the heat inputs, by the corresponding temperatures, i.e.  $Q_{h1}$  is replaced by  $T_{aRin}$  and  $Q_{h2}$  by  $T_{aDin}$ . Here it is assumed the temperatures are controlled by pre-existing control loops and can be manipulated directly either automatically (e.g. as a set-point in cascade control systems) or manually. This approach is common in food drying applications where precise temperature control is important.

Table 7.1. Steady-state values of input and state variables

<i>Input</i>	<i>Description</i>	<i>Value</i>	<i>States</i>	<i>Description</i>	<i>Value</i>
$Q_{h1}$	Heat input to regenerator air (kJ/h)	$9.04 \times 10^5$	$X_p$	Dried product outlet moisture content (kg/kg)	0.05
$Q_{h2}$	Heat input to drying air (kJ/h)	$3.6 \times 10^4$	$T_p$	Dried product outlet temperature (°C)	50
$F_{aA}$	Drying air flowrate (kg/h)	$5.3 \times 10^4$	$X_{zA}$	Adsorber zeolite outlet moisture content (kg/kg)	0.1664
$F_z$	Zeolite flowrate (kg/h)	$4.12 \times 10^3$	$T_{zA}$	Adsorber zeolite outlet temperature (°C)	50
$F_{aR}$	Regenerator air flowrate (kg/h)	$3.71 \times 10^3$	$X_{zR}$	Regenerator zeolite outlet moisture (kg/kg)	0.0868
			$T_{zR}$	Regenerator zeolite outlet temperature (°C)	170
			$Y_{Ad}$	Drying air outlet absolute humidity (kg/kg)	0.0106
			$T_{aout}$	Drying air outlet temperature (°C)	32
			$Y_{aA}$	Adsorber air outlet absolute humidity (kg/kg)	0.0038
			$T_{aA}$	Adsorber air outlet temperature (°C)	50
			$Y_{aR}$	Regenerator air outlet absolute humidity (kg/kg)	0.0982
			$T_{aR}$	Regenerator air outlet temperature (°C)	170
			$N_p$	Normalized vitamin C concentration (%)	76
			$T_x$	Heat exchanger outlet air temperature (°C)	160

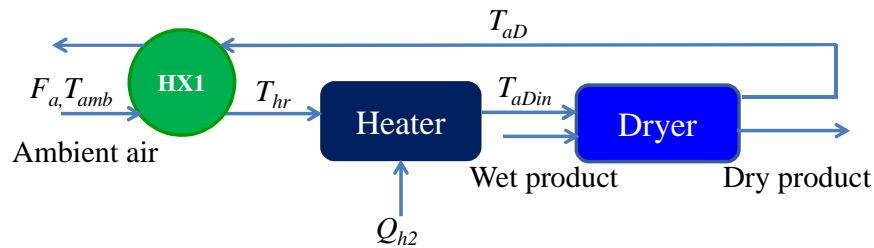


Fig. 7.2. Heat-integrated conventional dryer

Based on the foregoing, the following cases are considered in this study:

1. Control of product moisture content  $X_p$  and vitamin C concentration  $N_p$  with possible inputs as  $[Q_{h1}, Q_{h2}, F_a, F_z, F_{aR}]$
2. Control of  $X_p$  and  $N_p$  with the following inputs  $[T_{aRin}, T_{aDin}, F_{aA}, F_z, F_{aR}]$
3. Control of  $X_p$  and product temperature  $T_p$  with the following possible inputs  $[Q_{h1}, Q_{h2}, F_{aA}, F_z, F_{aR}]$
4. Control of  $X_p$  and  $T_p$  with the following inputs  $[T_{aRin}, T_{aDin}, F_{aA}, F_z, F_{aR}]$



In all these cases, comparisons are made with an equivalent heat-integrated conventional dryer without an adsorbent system and with heat recovered through the dryer exhaust air (see Fig. 7.2).

### 7.3. Controllability analysis

The basis for the current study is the input-output controllability (Skogestad, 1996) defined as the ability to keep the outputs of a system within specified bounds in spite of unknown variations in the plant (e.g. disturbances and model perturbations) using available inputs and measurements. Input-output controllability follows from the properties of the process and is independent of specific controller design. The main purpose of this work is to evaluate the controllability and energy performance sensitivity of the heat-integrated adsorption dryer independent of specific controller design. Different input-output pairing possibilities are investigated and comparisons made with conventional dryers. Specific transient behaviors in closed-loop depend on actual controller design and tuning which is not part of the current study. Various controllability indices have appeared in literature over the years, each with its significance, advantages and limitations. Examples are the Relative Gain Array *RGA* (Bristol, 1966), the Niederlinski index *NI* (Niederlinski, 1971), the Single Input Effectiveness, *SIE* (Cao and Rossiter, 1997), amongst others. The afore-mentioned controllability indices are primarily concerned with set-point tracking using available inputs. Controllability measures that indicate the capacity of the system to reject disturbances include Disturbance Condition Number *DCN* (Skogestad and Morari, 1987), Closed-loop Disturbance Gain *CLDG* (Hovd and Skogestad, 1992), amongst others. Comprehensive reviews of controllability indices, their definitions and applications are available elsewhere (Ricardez-Sandoval et al., 2009; Yuan et al., 2011). Table 7.2 shows a summary of the definition, significance and interpretation of each of the indices used in this work.

Dufour (2006) classified drying problems in two categories: regulation (set-point tracking and disturbance rejection) and optimization problems. Since 1998, publications relating to optimal control have increased by a factor of 10 while those relating to regulation increased by a factor of 3 (Dufour, 2006). This is not unconnected with the increasing need to optimize dryer performance, e.g. in terms of energy efficiency and product quality as against the traditional control of some states like product moisture content and temperature. Van Straten and Van Boxtel (1996) emphasized the need for goal oriented control of dryers and indeed other process systems as against mere temperature regulation for instance. It is thus, useful to determine the sensitivities of performance measures (e.g. energy efficiencies) to disturbances if the outputs are held constant. The discussions that follow evaluate the controllability of heat-integrated adsorption dryers with respect to set-point tracking and disturbance rejection. Thereafter, for one of the promising control structures, the sensitivity of energy performance to disturbances is evaluated. In each case, comparisons are made with equivalent conventional dryers.

Table 7.2. Definition, significance and interpretation of the various indices used in this work

<i>Index</i>	<i>Definition and significance</i>	<i>Interpretation</i>
RGA	It is a normalized form of the system gain matrix in which each element denotes the ratio of the open loop gain to the corresponding closed loop gain. The open loop gain is the ratio of a specific output to a specific input when all other inputs are inactive (i.e. at nominal values) while the closed loop gain is the ratio when all other inputs act so, all outputs are kept constant. In a square RGA, rows and columns each add up to 1.	For each RGA element: if 1, the corresponding input-output pairing is perfect – no interaction with other loops. If 0, the specific input has no control effect on the output. If greater than 0 but less than 1, closed loop interaction increases gain. Interaction most severe for RGA=0.5. If greater than 1, interaction reduces gain, leading to a plant that is more difficult to control.. Interaction more severe as number increases. If negative, closed loop gain is in opposite direction to open loop gain and the corresponding pairing should be avoided.
NI	Ratio of the determinant of the process gain matrix to the product of the diagonal elements. Useful to determine if the system can be controlled by multi-loop single-input single-output SISO controllers with integral action for offset-free control and if the system will remain stable when a subset of loops is taken out of service.	If negative, the closed loop system is unstable under PI control with positive loop gain and integral action.
PCN	The ratio of the maximum to the minimum singular value of the process gain matrix. A measure of uncertainty in process gain matrix inversion and hence, sensitivity of control input computation to model errors	The lower the value, the less sensitive the system is to uncertainties and so, the more controllable the system is. The minimum value of the condition number of a MIMO system is 1 which corresponds to a SISO system. Thus condition number is a measure of loop interactions
SIE	A vector of which each element (corresponding to each input) is the square root of the sum of each row (corresponding to each output) of the non-square RGA	The value ranges from 0 to 1. The higher the value of an element, the higher the effect of the input on the corresponding output and the better the controllability.
CLDG	Quantifies the effect of disturbances on decentralized control when interactions are considered	The lower the magnitude of an element, the better the rejection of the corresponding disturbance by the corresponding output
DCN	Same as process condition number except that in this case, the process gain matrix is replaced by disturbance sensitivity matrix	Same as process condition number with the process gain matrix replaced by disturbance matrix (i.e. manipulated inputs replaced by disturbance inputs)

### 7.3.1 Set point tracking measures

These are determined based on the properties of the drying system gain matrix which determine the ability of the system to track set outputs using the inputs. For the adsorption drying system, the overall process gain matrix whose elements constitute ratios of system output amplitudes to input amplitudes and which in general is frequency dependent is given by

$$\mathbf{G} = \begin{pmatrix} \frac{\partial X_p}{\partial Q_{h1}} & \frac{\partial X_p}{\partial Q_{h2}} & \frac{\partial X_p}{\partial F_a} & \frac{\partial X_p}{\partial F_z} & \frac{\partial X_p}{\partial F_{aR}} \\ \frac{\partial T_p}{\partial Q_{h1}} & \frac{\partial T_p}{\partial Q_{h2}} & \frac{\partial T_p}{\partial F_a} & \frac{\partial T_p}{\partial F_z} & \frac{\partial T_p}{\partial F_{aR}} \\ \frac{\partial Q_{h1}}{\partial N_p} & \frac{\partial Q_{h2}}{\partial N_p} & \frac{\partial F_a}{\partial N_p} & \frac{\partial F_z}{\partial N_p} & \frac{\partial F_{aR}}{\partial N_p} \\ \frac{\partial Q_{h1}}{\partial Q_{h1}} & \frac{\partial Q_{h2}}{\partial Q_{h2}} & \frac{\partial F_a}{\partial F_a} & \frac{\partial F_z}{\partial F_z} & \frac{\partial F_{aR}}{\partial F_{aR}} \end{pmatrix} \quad (7.6)$$

where the full dynamic equations defining the behavior of each output are given in Atuonwu et al. (2011a). For the controllability cases considered (as stated earlier),  $X_p$  and  $N_p$  are taken as outputs in cases 1 and 2 while  $X_p$  and  $T_p$  are outputs in cases 3 and 4. In cases 2 and 4, heat inputs  $Q_{h1}$  and  $Q_{h2}$  as appear in the matrix of equation 7.6 are replaced by temperatures  $T_{aDin}$  and  $T_{aRin}$ . The steady-state gain matrix  $\mathbf{G}_{ss}$ , a special case of  $\mathbf{G}$  gives important information on the system closed-loop properties and steady-state controllability since it is important to maintain the process at steady-state. In each input-output case  $\mathbf{G}_{ss}$  is readily obtained by finding the ratio of output deviations to step input changes within narrow regions of the operating point. The frequency-dependent extensions  $\mathbf{G}(\omega)$ , are determined by finding the amplitude ratios at different frequencies for sinusoidal input changes within regions of the operating point for which the process is linear.

$\mathbf{G}$  is squared down in each case by taking any two columns in turns to obtain a total of 40 square subsystems. For each of these 2x2 subsystems, the RGA  $\mathbf{A}$ , the condition number  $\sigma$ , and the Niederlinski indices  $NI$  are calculated from

$$\mathbf{A} = \mathbf{G} \otimes (\mathbf{G}^{-1})^T \quad (7.7)$$

$$\sigma = \|\mathbf{G}\| \|\mathbf{G}^{-1}\| \quad (7.8)$$

$$NI = \det(\mathbf{G}) / \prod_{i=1}^{i=2} g_{ii} \quad (7.9)$$

where  $\otimes$  stands for element-by-element multiplication.

The  $NI$  depends on the arrangement of the matrix columns. If the positions of the two columns are interchanged, the result is different and so, the values of these indices depend on the specific input that is used to control each specific output.

The single input effectiveness *SIE* (Cao and Rossiter, 1997) for an  $n$ -input,  $m$ -output system where  $i$  represents the rows (from 1 to  $m$ ) and  $j$  represents the columns from 1 to  $n$  is such that each element of the vector is

$$SIE_j = \sqrt{\sum_{i=1}^{i=m} A_{Nij}} \quad (7.10)$$

where  $A_{Nij}$  is the  $ij$ th element of the non-square RGA  $A_N$  of matrix  $\mathbf{G}$ .

Of these, the process condition number is both input and output scaling dependent. The minimum attainable condition number is scaling independent and is determined (Engell et al., 2004) by solving the optimization problem

$$\sigma_{\min} = \min_{L,R}(\sigma(\mathbf{LGR})) \quad (7.11)$$

where  $\mathbf{L}$  and  $\mathbf{R}$  are non-singular diagonal scaling matrices.

### 7.3.2 Disturbance rejection measures

Perfect control depends on the ability to track set points irrespective of the presence of disturbances  $\mathbf{d}$ . This depends on the open-loop disturbance sensitivity matrix  $\mathbf{G}_d$  of the system which is given by

$$\mathbf{G}_d = \begin{pmatrix} \frac{\partial X_p}{\partial F_p} & \frac{\partial X_p}{\partial X_{pin}} & \frac{\partial X_p}{\partial T_{amb}} & \frac{\partial X_p}{\partial Y_{amb}} \\ \frac{\partial F_p}{\partial N_p} & \frac{\partial X_{pin}}{\partial N_p} & \frac{\partial T_{amb}}{\partial N_p} & \frac{\partial Y_{amb}}{\partial N_p} \\ \frac{\partial F_p}{\partial F_p} & \frac{\partial X_{pin}}{\partial X_{pin}} & \frac{\partial T_{amb}}{\partial T_{amb}} & \frac{\partial Y_{amb}}{\partial Y_{amb}} \end{pmatrix} \quad (7.12)$$

Note: where appropriate for the studied cases,  $N_p$  is replaced with  $T_p$ .

The closed-loop disturbance gain *CLDG* is

$$CLDG = \tilde{\mathbf{G}} \mathbf{G}^{-1} \mathbf{G}_d \quad (7.13)$$

where  $\tilde{\mathbf{G}}$  is a matrix with diagonal elements equal to the diagonals of  $\mathbf{G}$  and other elements, zero.

The disturbance condition number (Skogestad and Morari, 1987) is

$$\sigma_d = \frac{\|G^{-1}G_d\|_2 \text{SVD}_{\max}(G)}{\|G_d\|_2} \quad (7.14)$$

The disturbance sensitivities  $G_d$  (both steady-state and dynamic) are in each case determined like the process gain  $G$  except that disturbance inputs are used instead of manipulated inputs. Like the process condition number, the disturbance condition number is scaling-dependent. This can be remedied by replacing in equation 7.14 the term  $\text{SVD}_{\max}(G)$  by  $\text{SVD}_{\max}(LGR)$ , using equation 7.11, where diagonal matrices  $L$  and  $R$  are scaling matrices corresponding to minimum process condition number.

### 7.3.3 Energy performance sensitivity

When disturbances are rejected using available manipulated variables, energy performance is affected. For any drying process, the energy performance is judged by the energy efficiency defined as the ratio of the thermal energy output (the latent heat of vaporization of the water removed from the product) to the total thermal energy input. The thermal energy output is:

$$Q_{out} = F_p (X_{pin} - X_p) \Delta H_v \quad (7.15)$$

For the heat-integrated adsorption dryer (Fig. 7.1), the thermal energy input is the sum of the energy  $Q_{h1}$  used in heating the regeneration air after heat exchange and that  $Q_{h2}$  used in heating the adsorber outlet air to the dryer.

$$Q_{in} = F_{aR} (C_{pa} + Y_{amb} C_{pv}) (T_{aRin} - T_x) + F_{aA} (C_{pa} + Y_{aA} C_{pv}) (T_{aDin} - T_{aA}) \quad (7.16)$$

Hence, the energy efficiency is given by

$$\eta = \frac{Q_{out}}{Q_{in}} = \frac{F_p (X_{pin} - X_p) \Delta H_v}{F_{aR} (C_{pa} + Y_{amb} C_{pv}) (T_{aRin} - T_x) + F_{aA} (C_{pa} + Y_{aA} C_{pv}) (T_{aDin} - T_{aA})} \quad (7.17)$$

For the heat-integrated conventional dryer (Fig. 7.2),  $Q_{h1}=0$ , while  $T_{aA}$  and  $Y_{aA}$  in the expression for  $Q_{h2}$  are replaced by  $T_{hr}$  and  $Y_{amb}$  respectively where  $T_{hr}$  is the temperature of the ambient air after heat recovery from the dryer exhaust air. From the foregoing, the energy efficiency can be expressed as  $\eta=\eta(\mathbf{u},\mathbf{d},\mathbf{y})$  so, the following sensitivity holds:

$$\left. \frac{d\eta}{dd} \right|_{\mathbf{y}=\mathbf{y}^{ss}} = \left. \frac{\partial \eta}{\partial d} \right|_{\mathbf{y}=\mathbf{y}^{ss}} + \left. \frac{\partial \eta}{\partial \mathbf{u}} \cdot \frac{\partial \mathbf{u}}{\partial d} \right|_{\mathbf{y}=\mathbf{y}^{ss}} + \left. \frac{\partial \eta}{\partial \mathbf{y}} \cdot \frac{\partial \mathbf{y}}{\partial d} \right|_{\mathbf{y}=\mathbf{y}^{ss}} \quad (7.18)$$

Apart from  $Q_{h1}$  and  $Q_{h2}$ , the other main energy spent in the system is that used for driving the zeolite continuously in a rotary wheel. The drive power required for the wheel is given by

$$Q_{wheel} = 2\pi n T_Q / 60 \quad (7.19)$$

where  $n$  is the rotary speed in rpm and  $T_Q$ , the load torque. The rotary speeds for desiccant wheels are low (less than 100 revolutions per hour). Hence, the energy for the wheel is negligible. For instance, for a wheel mass  $m=50\text{kg}$  and radius  $r=0.2\text{m}$ , the load torque  $T_Q=mgr\mu$  is about  $100\text{Nm}$  where acceleration due to gravity  $g=10\text{m/s}^2$  and coefficient of dynamic friction  $\mu$  is assumed equal to unity. The energy consumption rate calculated from (7.19) is about  $0.00047 \times 10^5 \text{kJ/h}$  which is infinitesimal compared to the  $8.955 \times 10^5 \text{kJ/h}$  corresponding to the evaporated moisture (Atuonwu et al., 2011a). Ideal insulation is assumed so heat losses due to leakages are neglected.

To evaluate and compare the sensitivities of the adsorption and conventional dryers when disturbances are rejected, we consider the case where promising pairings (determined based on Sections 7.3.1 and 7.3.2) are used in rejecting simulated disturbances. In this work, only steady-state effects are considered. Disturbances used are the changes in ambient temperatures and humidity. The ambient is simulated to have a temperature range of  $5\text{-}25^\circ\text{C}$  and a humidity range of  $0.003$  to  $0.01\text{kg water/kg dry air}$ . The lower humidities correspond to the lower temperatures while the higher humidities correspond to the higher temperatures as obtains in practice. Values of the chosen input variables for which there are minimal deviations of the outputs from steady-states are determined from the nonlinear process model using zero-finding techniques. If successful, the last term on the right hand side of (7.18) becomes zero.

## 7.4. Results and discussion

### 7.4.1 System behavior and set point tracking

Fig. 7.3 shows the time responses of the product moisture and temperature to input step changes of  $\pm 20\%$  from steady-state for the heat-integrated adsorption dryer. The nonlinear nature of the process is clearly demonstrated by the discrepancies in the responses to positive and negative input deviations from steady-state. For sufficiently small input deviations, the system approximates linearity and the steady-state process gain matrices  $G_{ss}$  in each studied case are shown in Table 7.3(a) compared with an equivalent conventional dryer. The corresponding  $NIs$  and  $PCNs$  for both drying systems are shown in Tables 7.3(c) & (d) respectively.

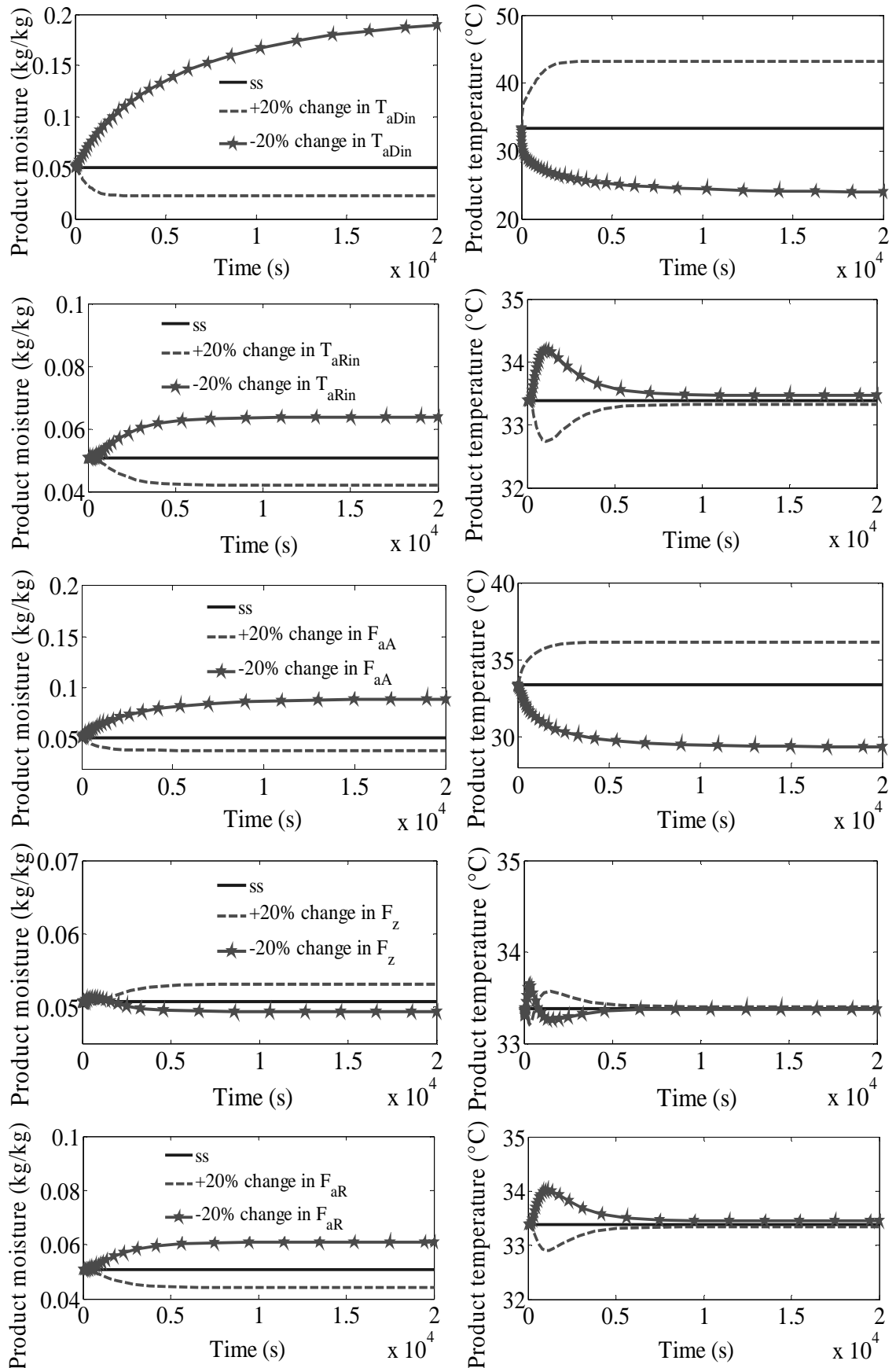


Fig. 7.3. Time responses of output variables of heat-integrated adsorption dryer to ±20% changes in inputs from steady-state

Table 7.3 (a). Process gain matrices ( $\times 10^{-4}$ ) for the heat-integrated adsorption dryer (left) and heat-integrated conventional dryer (right); input variables on each column and output variables on each row

	$Q_{h1}$	$Q_{h2}$	$F_{aA}$	$F_z$	$F_{Ar}$		$Q_{h2}$	$F_{aA}$
$X_p$	-0.2598	-1.4264	24.4008	-89.5594	19.7243		-1.4	19.0
$N_p$	-0.3746	-3.7902	103.2156	-206.6601	28.4401		-3.2	67.9
$T_p$	54.1391	515.4821	-13170	28815	-4110.3		476.8	-9464
	$T_{aRin}$	$T_{aDin}$	$F_{aA}$	$F_z$	$F_{aR}$		$T_{aDin}$	$F_{aA}$
$X_p$	-0.065698	-23.2608	-17.7981	-9.5054	-15.9174		-27.3	-14.7
$N_p$	0.0857	-61.8100	-8.9585	12.3990	20.7776		-63.2	-10.0
$T_p$	-5.7714	8406.3	2085.4	-835.0	-1399.25		9389.3	2120.4

To understand the effect of the adsorption subsystem on the drying process behavior, it is important to compare corresponding elements of the steady-state gain matrices of the adsorption and conventional dryer using the input variables common to both systems  $Q_{h2}$  (or  $T_{aDin}$ ) and  $F_{aA}$  (see Table 7.3(a)). For these inputs, the magnitudes of the steady state gains of  $X_p$ ,  $N_p$  and  $T_p$  are higher for the adsorption dryer than the conventional dryer. Dehumidification leads to adsorption heat release and thus, temperature rise. The drying air temperature rise and humidity drop both reduce  $X_p$  thus creating a higher process gain with respect to  $X_p$  than would occur in a conventional dryer without desiccant dehumidification. The adsorption heat release increases the process gain with respect to product temperature and hence, vitamin C concentration. Exceptions occur when  $T_{aDin}$  is used instead of  $Q_{h2}$  in which case, the adsorption heat effects are regulated out by control of  $T_{aDin}$ .

Presented in Table 7.3(b) are the diagonal elements of the *RGA* corresponding to  $G_{ss}$  for each studied case. As the sum of elements in each row and each column of an *RGA* add up to 1, it suffices for a 2x2 matrix to report the diagonal element only. The promising pairings from the results are shown colored in the map (Fig. 7.4). Of the forty possible input-output pairings in this study, fourteen are favorable. These are those for which the diagonal elements are positive and as close to unity as possible.

Table 7.3(b). Diagonal elements of the *RGA* matrix in which input variables on each row control product moisture content  $X_p$  while those on each column control vitamin C concentration  $N_p$  (or temperature  $T_p$ ): Adsorption (left) Conventional (right)

	$Q_{h2}$	$F_{aA}$	$F_z$	$F_{aR}$	$Q_{h2}$	$F_{aA}$	$F_z$	$F_{aR}$	$F_{aA}$	$F_{aA}$
$Q_{h1}$	2.12	1.52	2.67	$4.9 \times 10^5$	2.36	1.63	2.84	$1.2 \times 10^7$		
$Q_{h2}$		2.69	-6.6	-1.19		3.03	-8.12	-1.36	2.84	3.23
$F_{aA}$			-1.2	-0.52			-1.48	-0.63		
$F_z$				-1.67				-1.84		
	$T_{aDin}$	$F_{aA}$	$F_z$	$F_{aR}$	$T_{aDin}$	$F_{aA}$	$F_z$	$F_{aR}$	$F_{aA}$	$F_{aA}$
$T_{aRin}$	0.67	0.28	$5.4 \times 10^5$	$-3.3 \times 10^6$	0.8	0.37	$1.6 \times 10^6$	$-7.8 \times 10^5$		
$T_{aDin}$		-0.23	0.33	0.33		-0.47	0.2	0.2	-0.4	-0.7
$F_{aA}$			0.72	0.72			0.63	0.63		
$F_z$				$-4.6 \times 10^5$				$-5.3 \times 10^5$		



## Heat flows as inputs

		$N_p$ or $T_p$ Control				
		$Q_{h1}$	$Q_{h2}$	$F_{aA}$	$F_z$	$F_{aR}$
$X_p$ control	$Q_{h1}$					
	$Q_{h2}$					
	$F_{aA}$					
	$F_z$					
	$F_{aR}$					

## Temperatures as inputs

		$N_p$ or $T_p$ Control				
		$T_{aRin}$	$T_{aDin}$	$F_{aA}$	$F_z$	$F_{aR}$
$X_p$ control	$T_{aRin}$					
	$T_{aDin}$					
	$F_{aA}$					
	$F_z$					
	$F_{aR}$					

Fig. 7.4. Maps showing promising input-output pairings (colored) unfavourable pairings (blank) based on RGA results (Table 7.3(b)). Diagonal blocks indicate one input controlling two outputs and are thus, not considered

For the pairings whose diagonal *RGA* elements are negative, the alternate pairing has a positive diagonal *RGA* which makes the alternate pairing more favorable. For instance, from Table 7.3(b), the pairing  $\{[Q_{h2}-X_p]; [F_{aR}-N_p]\}$  has a diagonal *RGA* equal to  $-1.19$ ; hence, the alternate pairing  $\{[Q_{h2}-N_p]; [F_{aR}-X_p]\}$  has a diagonal *RGA* of  $2.19$ , which makes it the preferred pairing.

The Niederlinski indices of Table 7.3(c) also favour the above pairings as the *NI* elements are positive in each case. The minimized process condition numbers *PCN* (Table 7.3(d)) are also reasonably low in each of the cases. All other pairing possibilities are unfavourable due to the corresponding *RGA* elements being negative, less than 0.5 or extremely large. A notable unfavourable pairing with large *RGA* values is when the inputs  $Q_{h1}$  (or  $T_{aRin}$ ) and  $F_{aR}$  are used together, irrespective of the specific input-output pairing. A possible explanation for this is the fact that each input produces similar effects on each output through many intermediate state variables. A change in either of these inputs is first reflected in the regeneration temperature  $T_{aR}$  which then affects the zeolite moisture content  $X_{zR}$  at the regenerator outlet or adsorber inlet. Consequently, the adsorber outlet zeolite moisture content  $X_{zA}$ , air humidity  $Y_{aA}$  and temperature  $T_{aA}$  are affected thus impacting simultaneously on product moisture content and temperature (and hence vitamin C concentration). At each propagation level, there are interactions so that the overall interaction is high.

Table 7.3(c). Niederlinski indices; inputs on each row control  $X_p$  while those on each column control  $N_p$  (or  $T_p$ ); adsorption dryer (left) and conventional dryer (right)

$X_p$ & $N_p$					$X_p$ & $T_p$					$X_p$ & $N_p$		$X_p$ & $T_p$	
$Q_{h1}$	$Q_{h2}$	$F_{aA}$	$F_z$	$F_{aR}$	$Q_{h1}$	$Q_{h2}$	$F_{aA}$	$F_z$	$F_{aR}$	$F_{aA}$	$F_{aA}$	$F_{aA}$	$F_{aA}$
$Q_{h1}$	0.45	0.66	0.38	0.00		0.42	0.61	0.35	0.00				
$Q_{h2}$	-0.8		0.37	-0.2	-0.8	-0.7		0.33	-0.1	-0.7	0.35	0.3	
$F_{aA}$	-1.9	-0.6		-0.8	-1.9	-1.6	-0.5		-0.7	-1.6			
$F_z$	-0.6	0.13	0.45		-0.6	-0.5	0.11	0.40		-0.5			
$F_{aR}$	0.00	0.46	0.66	0.38		0.00	0.42	0.61	0.35				
$T_{aRin}$ $T_{aDin}$ $F_{aA}$ $F_z$ $F_{aR}$					$T_{aRin}$ $T_{aDin}$ $F_{aA}$ $F_z$ $F_{aR}$					$F_{aA}$ $F_{aA}$			
$T_{aRin}$		1.49	3.59	0.00	0.00		1.24	1.75	0.00	0.00			
$T_{aDin}$	3.0		-4.3	3.0	3.0	5.1		-2.1	5.1	5.1	-2.4	-1	
$F_{aA}$	1.39	0.81		1.39	1.39	2.33	0.68		2.33	2.33			
$F_z$	0.00	1.49	3.59		0.00	0.00	1.24	1.75		0.00			
$F_{aR}$	0.00	1.49	3.59	0.00		0.00	1.24	1.75	0.00				

Table 7.3(d). Minimized Process condition numbers of the adsorption dryer (left) and conventional dryer (right)

	$Q_{h2}$	$F_{aA}$	$F_z$	$F_{aR}$	$Q_{h2}$	$F_{aA}$	$F_z$	$F_{aR}$	$F_{aA}$	$F_{aA}$
$Q_{h1}$	6.59	3.80	8.55	$1.9 \times 10^6$	7.31	4.28	9.25	$5.8 \times 10^{10}$		
$Q_{h2}$		8.64	28.36	6.59		10.00	34.43	7.31	9.26	10.89
$F_{aA}$			6.65	3.81			7.78	4.28		
$F_z$				8.55				9.25		
	$T_{aDin}$	$F_{aA}$	$F_z$	$F_{aR}$	$T_{aDin}$	$F_{aA}$	$F_z$	$F_{aR}$	$F_{aA}$	$F_{aA}$
$T_{aRin}$	1.00	1.00	$2 \times 10^6$	$1.3 \times 10^7$	1.0	1.0	$2.0 \times 10^{10}$	$3.16 \times 10^6$		
$T_{aDin}$		2.54	1.00	1.00		3.64	1.00	1.00	3.39	4.68
$F_{aA}$			1.00	1.00			1.00	1.00		
$F_z$				$1.84 \times 10^6$				$2.1 \times 10^6$		

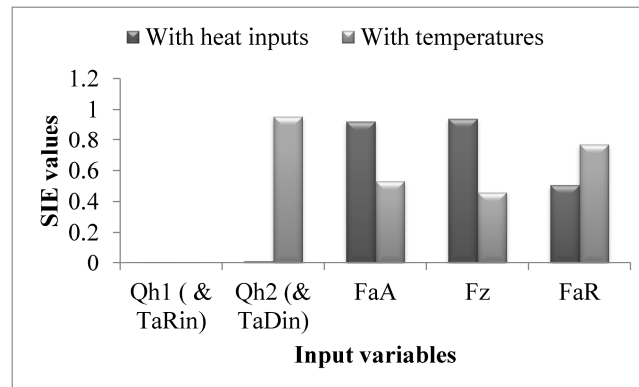


Fig. 7.5. Single Input Effectiveness (SIE) showing effects of each input variable on the outputs

All results true for vitamin C concentration  $N_p$  control are also found true for product temperature  $T_p$ . This is possibly due to the correlation between  $T_p$  and  $N_p$  which can be seen in the vitamin C degradation kinetics (Mishkin et al., 1983), also in Appendix C. This correlation is confirmed by the fact that the *SIE* values of each input remain unchanged when  $T_p$  is controlled instead of  $N_p$ .

The *SIE* values show that when  $Q_{h1}$ ,  $Q_{h2}$ ,  $F_{aA}$ ,  $F_z$  and  $F_{aR}$  are considered as inputs, the input effectiveness in descending order is  $F_z$ ,  $F_{aA}$ ,  $F_{aR}$ ,  $Q_{h2}$  and  $Q_{h1}$ . When  $T_{aRin}$ ,  $T_{aDin}$ ,  $F_{aA}$ ,  $F_z$  and  $F_{aR}$  are considered as inputs, the input effectiveness in descending order is  $T_{aDin}$ ,  $F_{aR}$ ,  $F_{aA}$ ,  $F_z$  and  $T_{aRin}$ . The effects of  $Q_{h1}$  and  $T_{aRin}$  are in the order of  $10^{-3}$  and so not clearly visible in the chart (Fig. 7.5). They are thus relatively ineffective.

The correlation between product moisture content and temperature is known to be high, since temperature is the driving force for drying. This is confirmed by the results of Table 7.3(d) which show that for most cases; the minimized process condition number when  $X_p$  and  $T_p$  are controlled is higher than when  $X_p$  and  $N_p$  are controlled. The difference is significant. It is therefore preferable to control  $X_p$  and  $N_p$  in a 2x2 decentralized control system instead of controlling  $X_p$  and  $T_p$ . This is an advantage as the product quality is controlled directly instead of using a correlate – temperature. The feasibility however depends on the availability of reliable sensors or state estimators for vitamin C concentration.

The use of temperatures ( $T_{aRin}$  or  $T_{aDin}$ ) as manipulated variables implies the temperatures are already controlled by pre-existing control loops and then either used to control the adsorption dryer manually or sent as a set-point for automatic control. This changes the system from what it used to be when provisions are only made for direct control by heat inputs ( $Q_{h1}$  &  $Q_{h2}$ ). Hence, corresponding open loop gains of the two systems differ even when analyzing loops that contain other input variables (say  $F_{aA}$  &  $F_z$ ). The pre-existing temperature control is seen to improve controllability in most cases. For instance, the minimized process condition numbers of Table 7.3(d) are low, in most cases, unity, which is the lowest attainable. Exceptions occur where two regenerator-based inputs e.g. [ $F_z$ ,  $F_{aR}$ ] or [ $F_{aR}$ ,  $T_{aRin}$ ] are used possibly due to loss of a degree of freedom. When heat inputs are used for control (top side of Table 7.3(d)), this is compensated for since  $T_{aRin}$  can be controlled by adjusting either  $Q_{h1}$  or  $F_{aR}$ . However, when temperatures are used instead of heat inputs (bottom side of Table 7.3(d)),  $F_{aR}$  loses its control power over  $T_{aRin}$ . The regenerator subsystem becomes stiffer and the negative effect of the degree of freedom loss on controllability is fully manifested when any two of ( $T_{aRin}$ ,  $F_{aR}$  and  $F_z$ ) is used in control. As seen in Table 7.3(d), the minimized process condition numbers are very large for the cases where any of these pairs is used for control.

#### 7.4.2. Disturbance rejection

For feed related disturbances ( $F_p$  &  $X_{pin}$ ), the sensitivities (open-loop disturbance gains) are the same for the conventional and adsorption dryers as shown in Table 7.4(a). This is expected as the adsorption system does not have any effect on the feed. However, for ambient air disturbances ( $T_{amb}$  &  $Y_{amb}$ ), the sensitivities of the product moisture and temperature of the adsorption dryer are less than those of the conventional dryer. Adsorption dryers are thus seen to have better disturbance resilience than conventional dryers. Thus, when disturbances that tend to reduce

energy efficiency (like ambient temperature drop or humidity rise) occur, the steady-state deviation of product moisture content and temperature is less for the adsorption dryer than the conventional dryer. The control effort required for disturbance rejection is therefore less. The lower magnitudes of corresponding closed-loop disturbance gain (*CLDG*) elements (Table 7.4(a)) for the adsorption dryer confirms improved closed-loop disturbance resilience. The improvement is traceable to self-regulation properties introduced by the zeolite adsorption/regeneration system. For instance, when ambient humidity rises, the driving force for adsorptive mass transfer is increased, thus, resulting in more dehumidification so that the original ambient air humidity rise is opposed. Also, when ambient temperature falls, the adsorption capacity rises as shown in the zeolite equilibrium characteristics (Fig. 7.6). Consequently, the adsorptive mass transfer is increased, leading to increased release of adsorption heat so that the original temperature drop is opposed. The converse is true in each of these cases. The zeolite adsorption/regeneration system is thus a negative feedback element preceding the dryer and implements feed-forward control by acting on disturbances before they reach the dryer so minor feedback compensation would give good control.

The adsorption capacity determines the control space for self-regulation and depends on adsorbent properties. The effective adsorption capacity can be manipulated by the regeneration temperature  $T_{aRin}$ . From Fig. 7.6, as regeneration temperature increases, the “space” between the adsorption and desorption isotherms increase.

Table 7.4(a). Open and Closed-loop disturbance gains for adsorption and conventional dryers (same control inputs:  $Q_{h2}$  &  $F_{aA}$ )

<i>Adsorption</i>	<i>Open-loop disturbance gains</i>				<i>Closed-loop disturbance gains</i>			
	<i>Conventional</i>		<i>Adsorption</i>		<i>Conventional</i>		<i>Adsorption</i>	
	$X_p$	$N_p$	$X_p$	$N_p$	$X_p$	$N_p$	$X_p$	$N_p$
$F_p$	5.23	23.6252	5.23	23.6252	-0.9693	26.1318	-3.9387	32.733
$X_{pin}$	0.0053	0.0067	0.0053	0.0067	0.0098	-0.020	0.0010	-0.020
$T_{amb}$	-0.0013	-0.0034	-0.0028	-0.0064	-0.0012	0	-0.003	0
$Y_{amb}$	1.4139	-2.2135	2.0182	-1.1367	5.1706	-15.9974	6.639	-16.489

Table 7.4(b). Minimized disturbance condition number for the adsorption dryer (left), conventional (right)

	$Q_{h2}$	$F_{aA}$	$F_z$	$F_{Ar}$	$Q_{h2}$	$F_{aA}$	$F_z$	$F_{aR}$	$F_{aA}$	$F_{aA}$
$Q_{h1}$	3.70	1.00	1.00	$1.06 \times 10^6$	4.08	1.01	1.00	$1.9 \times 10^{11}$		
$Q_{h2}$		2.12	15.52	3.70		2.12	28.96	6.17	5.3	8.67
$F_{aA}$			1.51	2.24			2.01	3.64		
$F_z$				1.00				2.52		
	$T_{aDin}$	$F_{aA}$	$F_z$	$F_{aR}$	$T_{aDin}$	$F_{aA}$	$F_z$	$F_{aR}$	$F_{aA}$	$F_{aA}$
$T_{aRin}$	1.00	1.00	$1.8 \times 10^6$	$1.1 \times 10^7$	1.00	1.00	$4.3 \times 10^9$	$2.66 \times 10^6$		
$T_{aDin}$		1.62	1.00	1.00		3.11	1.00	1.00	2.12	3.37
$F_{aA}$			1.00	1.00			1.00	1.00		
$F_z$				$1.55 \times 10^6$				$1.15 \times 10^6$		

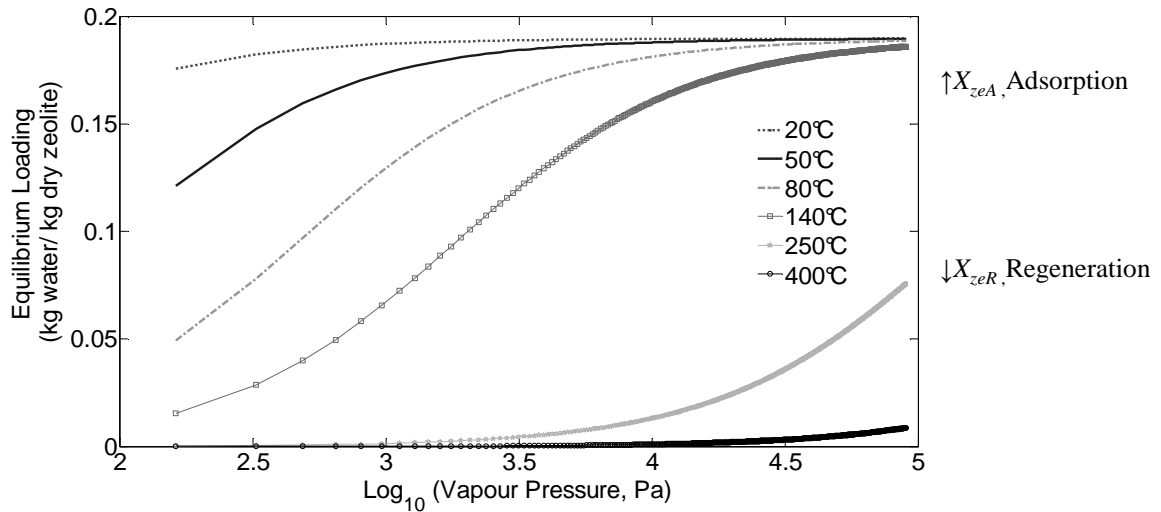


Fig. 7.6. Zeolite equilibrium loading at different vapour pressures and temperatures

Within limits, high regeneration temperatures thus, promote disturbance resilience all other factors remaining constant. The adsorption/regeneration system can thus be seen as a spring-like buffer tank of variable “height”  $X_{zeA}-X_{zeR}$  with the regeneration temperature  $T_{aRin}$  determining the height and hence, control space to damp out oscillations in ambient conditions. The control space would be different if another adsorbent is used as sorption isotherms differ. Also, adsorption capacity can be manipulated by zeolite flow. As zeolite flow increases, the zeolite is less wet on the adsorber side, which means more capacity to adsorb. However, the effect of regeneration is also less, thus reducing capacity. The drying and regeneration air flows also influence the capacity to adsorb, sorption heat release and hence, the overall self-regulation property. In summary, regulation behavior can be set by adsorption/regeneration system design and operating conditions.

From the results of Table 7.4(b), deductions applicable to the minimized process condition numbers  $PCN$  (Table 7.3(d)) are also applicable to the minimized disturbance condition numbers  $DCN$ . An interesting observation is that disturbance condition numbers of the conventional heat-integrated dryer can be higher or lower than those for the adsorption dryer depending on the specific control structure. This indicates that the superior disturbance rejection properties of the adsorption dryer can only be exploited if the right control structure is selected. For example, from Table 7.4(b), the pairings involving  $[F_{aA} F_z]$ ,  $[F_{aA} F_{aR}]$  and in the heat input manipulated case  $[F_z F_{aR}]$  have very low and so, good disturbance condition numbers. The results overall confirm the favorable pairings presented in Section 7.3.

To obtain more information on dynamic controllability, (for set-point tracking and disturbance rejection), the frequency-dependent minimized process and disturbance condition numbers ( $PCN$  and  $DCN$ ) are analyzed. For illustration, some of the combinations, both promising and non-promising, from Fig. 7.4 (top) are shown plotted in Fig. 7.7. The left-hand side contains results for the control of  $X_p$  and  $T_p$

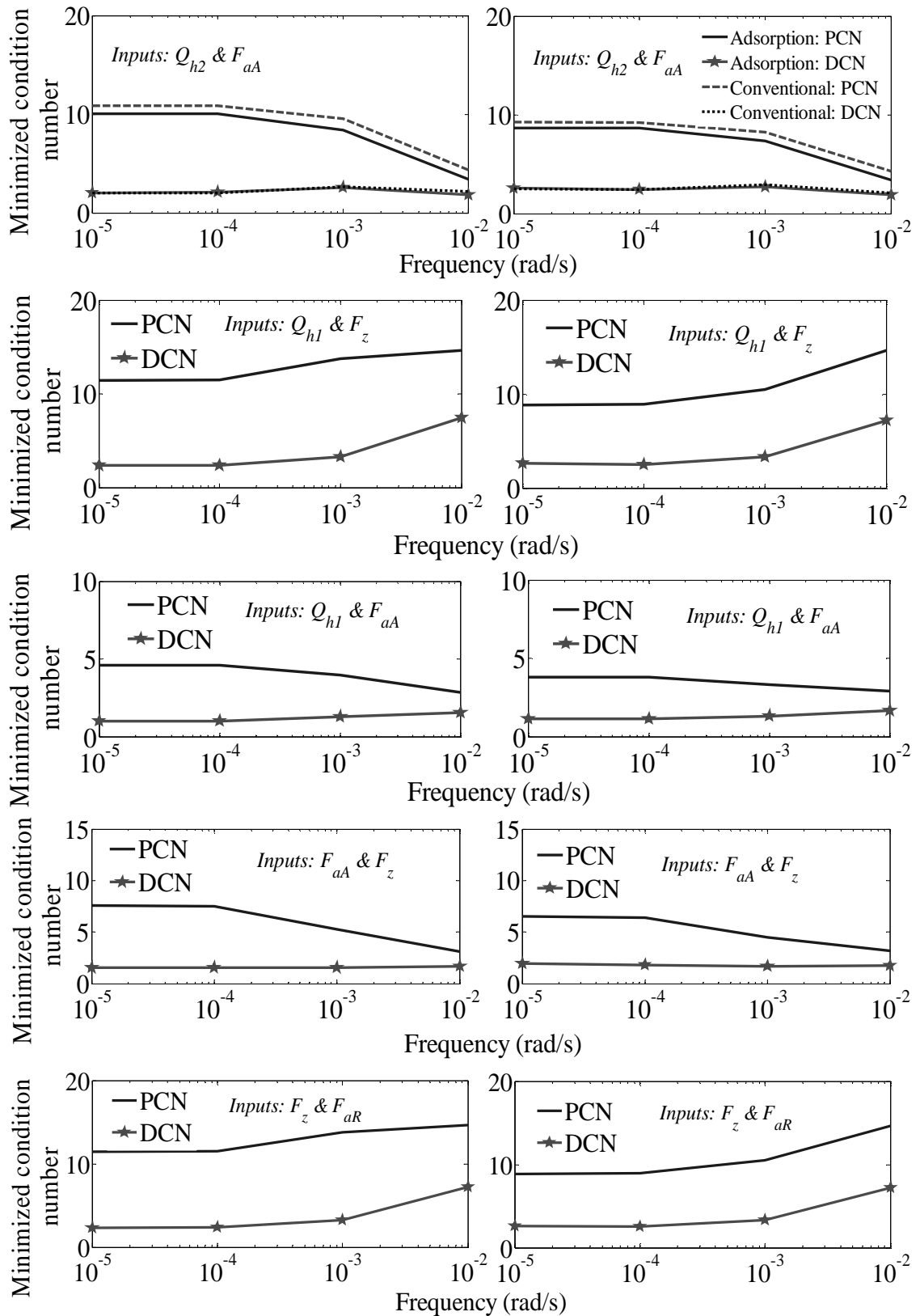


Fig. 7.7. Process and disturbance condition numbers as functions of frequency using different inputs to control  $X_p$  and  $T_p$  (left),  $X_p$  and  $N_p$  (right)

while the right hand side figures are for the control of  $X_p$  and  $N_p$  using the stated inputs. Throughout the entire frequency range, process and disturbance condition numbers are less for  $X_p$  and  $N_p$  control than for  $X_p$  and  $T_p$  control which agrees with deductions from steady-state controllability studies. Also, for the same inputs ( $Q_{h2}$  and  $F_{aA}$ ), the adsorption drying system shows improved controllability properties than the conventional dryer. Promising input choices like  $[Q_{h1}, F_{aA}]$  and  $[F_{aA}, F_z]$ , established from the preceding steady-state analyses are still characterized by relatively low process and disturbance condition numbers and so good controllability throughout the studied frequency range.

### 7.4.3 Energy performance disturbance sensitivity

Figs. 7.8 and 7.9 show the energy efficiency variations that occur with ambient changes for the conventional and adsorption dryers respectively when the shown input variables are used for disturbance rejection. The results show that over a wide disturbance range, the energy performance of the adsorption drying system is relatively stable compared to the conventional dryer. Comparing the adsorption dryer energy efficiency with that of the conventional dryer, the main energy input to the adsorption dryer depends on regeneration temperature  $T_{aRin}$  which is usually much higher than the ambient. For the conventional dryer, the input energy depends on dryer inlet temperature  $T_{aDin}$  which for low temperature drying is in the same order of magnitude as the ambient. Thus, if the ambient air temperature falls tremendously, the effect on regeneration energy input for is far less than the effect on conventional dryer heat input. This reduced energy input sensitivity coupled with the self-regulation properties discussed earlier make the energy performance of the adsorption drying system more resilient to disturbances as seen in Fig. 7.9(a) as against the conventional dryer in Fig. 7.8(a). The use of zeolite and drying air flowrates ( $F_z$  &  $F_{aA}$ ) as manipulated inputs for the adsorption dryer comes in handy since manipulating  $F_z$  changes the extent of dehumidification while at the same time, generating high adsorption heat. For a maximum difference of 0.2 kg water/kg dry zeolite between adsorption and desorption and an adsorption heat of 3200kJ/kg water adsorbed, the maximum sorption heat release corresponding to the maximum zeolite flowrate of about  $2 \times 10^4$  kg/h (the low ambient temperature region of Fig. 7.9(b)) is about  $12.8 \times 10^6$  kJ/h. This provides control power of the same order of magnitude as could be supplied by an external heater for a conventional dryer (Fig. 7.8(b)).

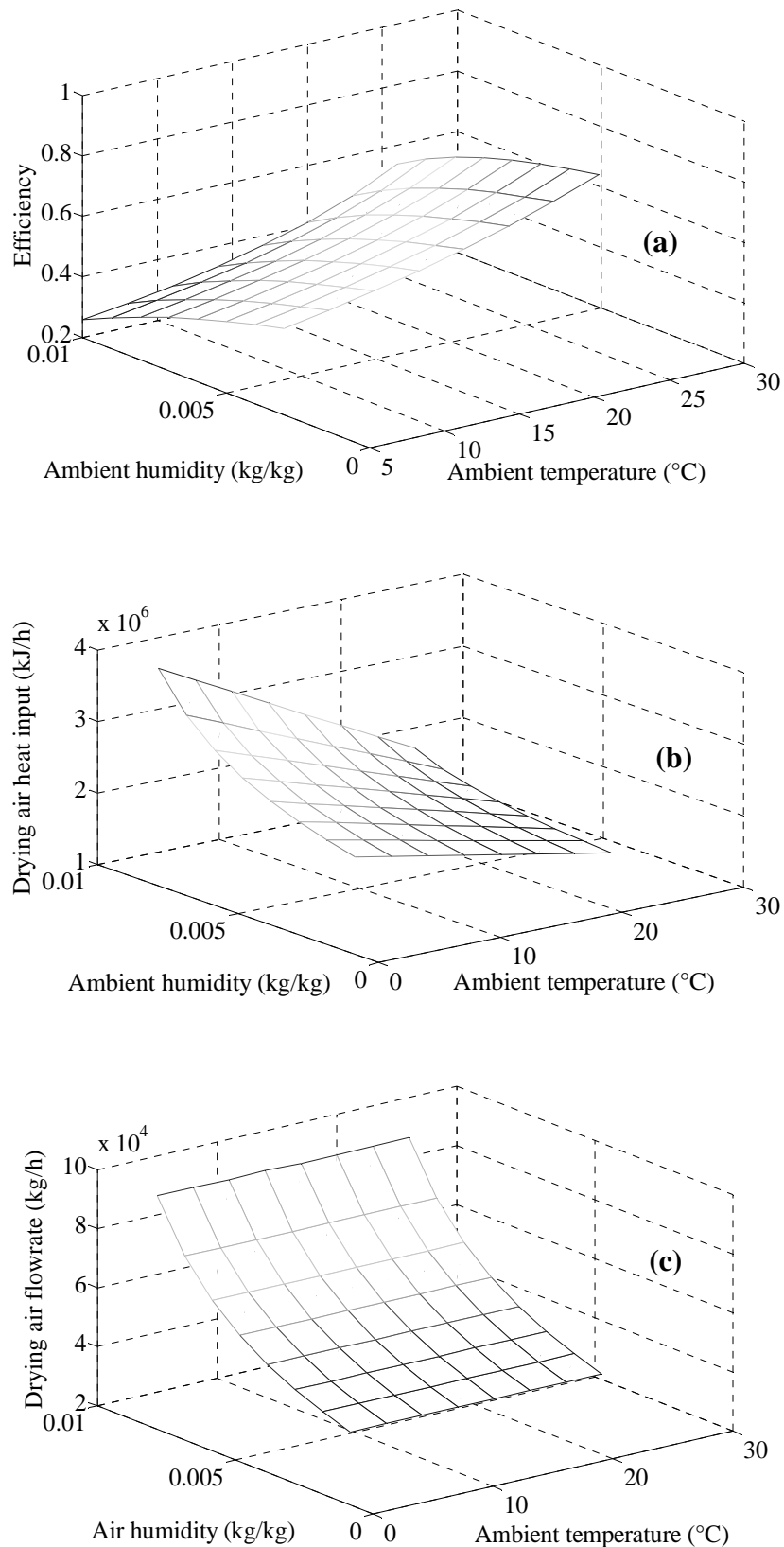


Fig. 7.8. (a). Energy efficiency variation with ambient air temperature and humidity for conventional heat-integrated dryer (b). Steady state input map of drying air heat input (c). Steady state input map of drying air flowrate



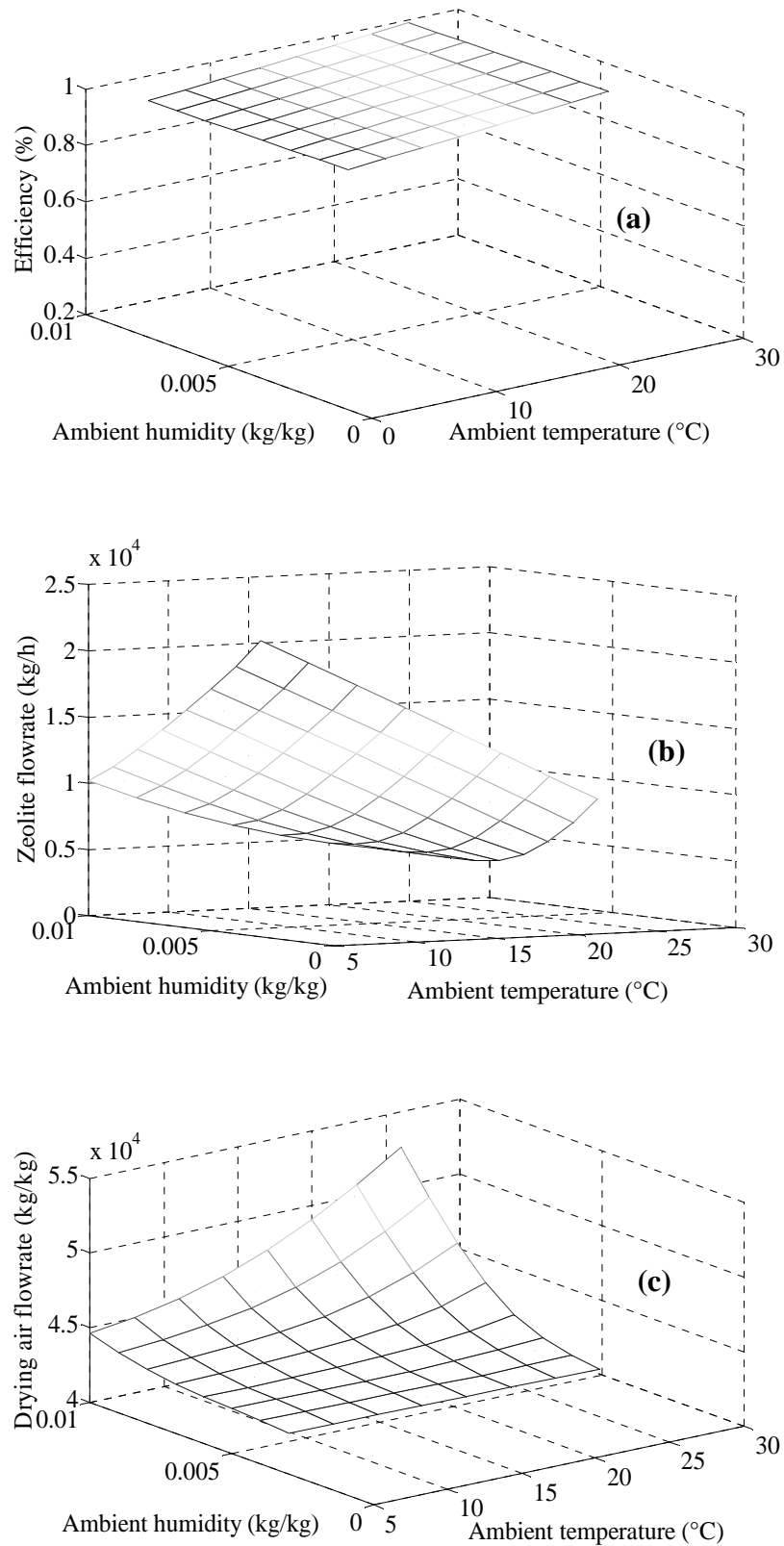


Fig. 7.9. (a). Energy efficiency variation with ambient air temperature and humidity for heat-integrated adsorption dryer (b). Steady state input map of drying air flowrate (c). Steady state input map of zeolite flowrate

## 7.5. Conclusions

In this work, the controllability of heat-integrated adsorption dryers has been examined using set-point-tracking and disturbance-rejection indices with product moisture content, temperature and vitamin C concentration (representative of quality) as output variables. Also, the sensitivities of energy performance to disturbances have been evaluated. The results show improved controllability properties over conventional dryers due to the extra control degrees of freedom introduced by the desiccant adsorption system. Forty input-output pairing possibilities have been identified of which twenty-six have been screened out. Adsorption dryers are shown to have improved resilience to ambient air disturbances than conventional dryers due to self-regulation properties introduced by the adsorbent subsystem which thus implements feed-forward control by acting on disturbances before they get to the dryer. Adsorption heat, kinetic and equilibrium properties of the adsorbent are shown to be the encouraging mechanisms for self-regulation which also depends on operating conditions like adsorbent, drying air flowrates and regeneration temperatures. Under perfect rejection of unfavourable disturbances such as ambient temperature drop and humidity rise, the energy performance of adsorption dryers is not significantly degraded as in conventional systems. Correlation between product moisture content and temperature is found to be higher than that between product moisture content and vitamin C concentration regardless of specific input-output pairings. It is thus, preferable to control product moisture content and vitamin C concentration in a 2x2 decentralized control system instead of product moisture content and temperature. This is an advantage as the product quality is controlled directly instead of the standard practice of using a correlate – temperature. The feasibility however depends on the availability of reliable sensors or state estimators for vitamin C concentration.

### **Improving dryer controllability and energy efficiency simultaneously by process modification**

Submitted as Atuonwu, J.C., Straten, G. van., Deventer, H.C. van., Boxtel, A.J.B. van. (2012). Improving dryer controllability and energy efficiency simultaneously by process modification

#### **Abstract**

This work establishes a relationship between dryer energy performance and controllability using energy balances and process resiliency analysis. It is shown that using the process gain matrix, the dryer energy efficiency can be reliably calculated with conditions for simultaneous controllability improvement established. By incorporating a drying rate modifying system such as a desiccant dehumidifier as an add-on, these conditions are shown to be achievable due to the extra dehumidification which can be manipulated using the additional degrees of freedom introduced by the sorption system. Due to the adsorbent regulation properties which are enhanced by high-temperature regeneration, the resilience of energy performance to disturbances is significantly improved compared to conventional dryers. Also, a desiccant system performance indicator, the “adsorber-regenerator net energy efficiency *ARNEE*” is introduced and it is shown that energy efficiency improvement is possible only if the *ARNEE* is greater than the energy efficiency of the stand-alone dryer.

*Keywords:* Dryer controllability, energy efficiency, desiccant dehumidification, desiccant performance indicators, design and control

#### **8.1. Introduction**

Drying consumes a significant proportion of total industrial energy and is a product quality-defining step in most industrial processes like in the food, pharmaceutical, chemical, pulp, paper industries and many more. The control of drying operations is important to achieve desired set-points with minimum product variability, reject disturbances to minimize off-spec products and optimize various aspects of process/product behavior such as energy efficiency and nutrient retention. Many innovative dryer designs have been developed over time to meet with the increasingly stringent demands on reducing energy consumption and improving product quality. With every such innovative step comes the question of controllability. Hence, the controllability of various categories of drying processes has been studied over the years. Examples include the controllability of conventional convective dryers (Langrish and Harvey, 2000); superheated steam spouted bed dryers (Berghel and

Renström, 2004); chemical heat pump dryers (Ogura et al., 2005) and more recently, heat-integrated adsorption dryers (Atuonwu et al., 2012b). Studies on the energy performance of drying processes also abound in the literature (Ogura et al., 2003; Kudra, 2004; Raghavan et al., 2005; Kemp, 2005; Atuonwu et al., 2012a; Kudra, 2012). However, the relationship between dryer controllability and energy performance is not yet well-investigated. Extensive knowledge of this relationship will help in developing design techniques that simultaneously improve steady-state economics and controllability. This would yield significant improvements over the conventional sequential approach to process design and control which in general has been identified as sub-optimal for process systems (Perkins and Walsh, 1996; Patel, et al., 2008; Yuan et al., 2012). This work shows from energy balances and resiliency analysis how dryer energy efficiency and controllability can be improved simultaneously. The dryer open-loop process gain matrix which has been used for controllability analysis by previous researchers is shown in this work to be related to the energy performance. From mass and energy balances, it is shown that by pre-conditioning the drying air using desiccant adsorption, the conditions necessary for simultaneous energy efficiency and controllability improvement over conventional dryers are achieved. Extra degrees of freedom are introduced which enhance process flexibility and improve the resilience of energy performance to disturbances. To guide decisions on choosing the appropriate desiccant dehumidifier for a dryer, an index of merit is introduced which considers the specifics of the drying process.

## 8.2. Dryer system gain matrix and energy efficiency

Fig. 8.1 shows a typical drying system where product moisture content  $X_p$  and outlet air temperature  $T_{aout}$  are output variables controlled by air flowrate  $F_a$  and inlet temperature  $T_{ain}$ . The steady-state mass balances governing the system states that the mass rate of water leaving the product equals the mass rate of water entering the drying air:

$$F_p(X_{pin} - X_p) = F_a(Y_{aout} - Y_{amb}) = r \quad (8.1)$$

where  $r$  is the overall drying rate from the dryer.

Taking energy balances assuming no heat losses across the dryer body, the sensible heat loss of the drying air across the dryer equals the latent heat gain

$$F_a(C_{pa} + Y_{ain}C_{pv})(T_{ain} - T_{aout}) = F_p(X_{pin} - X_p)\Delta H_v \quad (8.2)$$

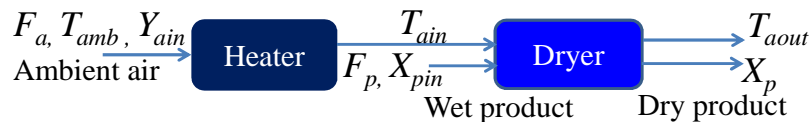


Fig. 8.1. Typical conventional dryer set-up

In (8.1) – (8.2),  $F_p$  and  $X_{pin}$  are product flow and inlet moisture respectively,  $Y_{amb}$  is inlet air humidity,  $Y_{aout}$  the outlet air humidity,  $C_{pa}$  and  $C_{pv}$  are specific heat capacities of air and water vapour respectively.  $\Delta H_v$  is the latent heat of vaporization of water.

The energy efficiency is defined as the ratio of the latent heat of water evaporated to the total dryer input energy. The latent heat of water evaporated is given by

$$Q_{outD} = F_a(Y_{aout} - Y_{amb})\Delta H_v \quad (8.3)$$

while the dryer input energy for ambient temperature  $T_{amb}$ , is

$$Q_{inD} = F_a(C_{pa} + Y_{amb}C_{pv})(T_{ain} - T_{amb}) \quad (8.4)$$

Hence, by combining (8.3) and (8.4), the energy efficiency  $\eta$  is

$$\eta = (F_a(Y_{aout} - Y_{amb})\Delta H_v) / (F_a(C_{pa} + Y_{amb}C_{pv})(T_{ain} - T_{amb})) \approx (T_{ain} - T_{aout}) / (T_{ain} - T_{amb}) \quad (8.5)$$

The process gain matrix consists of the sensitivities of each output to each input and is

$$G = \begin{pmatrix} \partial X_p / \partial F_a & \partial X_p / \partial T_{ain} \\ \partial T_{aout} / \partial F_a & \partial T_{aout} / \partial T_{ain} \end{pmatrix} \quad (8.6)$$

Now, differentiating the energy balances (8.2) with respect to air flowrate  $F_a$ ,

$$(F_a \partial T_{aout} / \partial F_a) - (1/K)(\partial X_p / \partial F_a) = T_{ain} - T_{aout} \quad (8.7)$$

and with respect to dryer inlet air temperature  $T_{ain}$ ,

$$(\partial T_{aout} / \partial T_{ain}) + (1/KF_a)(\partial X_p / \partial T_{ain}) = 1 \quad (8.8)$$

where the constant  $K = (C_{pa} + Y_{ain}C_{pv}) / (F_p \Delta H_v)$

From (8.5) – (8.7), a relationship (based on temperature drop  $T_{ain} - T_{aout}$ ) is established between the system energy efficiency and some elements of the process gain matrix on which the controllability properties depend. For a dryer with constant inlet air temperature, a change in air flowrate always produces a change of the same sign on the outlet air temperature and a change of the opposite sign on the outlet product moisture content (Langrish and Harvey, 2000). Thus, from (8.7), it is seen that by increasing the magnitudes of the sensitivities  $\partial X_p / \partial F_a$  and  $\partial T_{aout} / \partial F_a$  (elements of the first column of the gain matrix), energy efficiency (8.5) increases. Also, by reducing the inlet air humidity  $Y_{ain}$ , the constant  $K$  reduces so drying capacity increases. For constant air flowrate, a change in inlet air temperature produces a change of the same

sign on the outlet air temperature and an opposite sign change on the outlet product moisture content. Hence, to satisfy the unity constraint (8.8), an increase in the magnitude of  $\partial T_{aout}/\partial T_{ain}$  leads to an increase in that of  $\partial X_p/\partial T_{ain}$ .

### 8.3. Relating dryer controllability and energy efficiency

Various controllability measures have been proposed in the literature. Among them is the Morari Resiliency Index *MRI* (Morari et al., 1985) defined as the minimum singular value of the gain matrix. Mathematically,

$$MRI = \min(\text{svd}(G)) = 1/\|G^{-1}\| = |\det(G)|/\text{norm}(G) \quad (8.9)$$

The higher the *MRI* of a system, the easier the system tracks desired set-points and the more resilient it is to disturbances. It is related to the ease of inverting the matrix  $G$  and sets the limits of achievable control performance independent of specific controller design. The *MRI* is useful for evaluating square and non-square systems and applicable to steady-state and frequency domain analysis. Although scaling-dependent, it is useful for comparing design alternatives and testing the effect of process modifications where the same input and output variables are involved. Thus, the *MRI* is adopted as a measure of controllability in this work. From (8.9), one way to increase the *MRI* is reducing the norm of the gain matrix while the magnitude of the determinant is, at most, reduced less than proportionately. That would mean reducing the magnitudes of at least some elements of the gain matrix. Clearly, this reduces energy efficiency if the elements  $\partial X_p/\partial F_a$  and  $\partial T_{aout}/\partial F_a$  are affected.

Another option is to increase the magnitude of the determinant while the norm at most increases less than proportionately. From the relative gain array theory, increasing both elements in the first column of  $G$  may lead to increased loop interactions in multi-loop SISO control. In this case, the other matrix elements are modified so that while these gains are increased, the net *MRI* is also increased. Overall, the net value (8.5) increases thus simultaneously improving energy efficiency and controllability. In general therefore, energy efficiency and controllability improvements will occur if the gain matrix elements  $\partial X_p/\partial F_a$  and  $\partial T_{aout}/\partial F_a$  are increased with the *MRI* constrained to be non-decreasing taking into consideration the interactions with the other gain matrix elements  $\partial T_{aout}/\partial T_{ain}$  and  $\partial X_p/\partial T_{ain}$ . The discussion that follows shows from mass and energy balances, how the gain matrix elements can be modified.

### 8.4. Process Modification

From the steady-state mass balances (8.1), the overall drying rate  $r$  is given by

$$r = F_p(X_{pin} - X_p) \quad (8.10)$$

Hence, if due to a change  $\partial u$  in any of the input variables, the system transits from one steady-state 1, to another, 2, the change in product moisture  $\partial X_p$  is

$$\frac{\partial X_p}{\partial u} = \frac{X_{p2} - X_{p1}}{\partial u} = \frac{1}{F_p \partial u} (r_1 - r_2) = \frac{1}{F_p} \frac{\partial r}{\partial u} \quad (8.11)$$

From the energy balances, the change in outlet temperature in response to a change in input is

$$\frac{\partial T_{aout}}{\partial u} = \frac{\Delta H_v (r_1 - r_2)}{F_a (C_{pa} + Y_a C_{pv}) \partial u} = \frac{\Delta H_v}{F_a (C_{pa} + Y_a C_{pv})} \frac{\partial r}{\partial u} \quad (8.12)$$

The gain matrix can thus be modified by process or product modifications that change the sensitivity of drying rate to the input variable (i.e.,  $\partial r/\partial u$ ). Various methods have been proposed to modify the drying rates. These include, product pre-treatments like blanching, chilling and freezing (Dandamrongrak, et al., 2003) and drying air dehumidification strategies using desiccant adsorption and heat pumps (Atuonwu et al., 2011c). Fig. 8.2, showing the responses of drying rates of a conventional drying process and two hypothetical modified processes (Modified and Modified 2) illustrates this. Although the Modified 1 process alters the drying rate at the two operating points, the slope of the graph is the same as that of the original process because the modification-induced additive element is the same at both input variable values. Here, the additive element is defined as the “addition (positive or negative)” or the change in drying rate introduced by the modification. If however this additive element varies with the input variable as in the case of the Modified 2 process, the slope and hence process gain is modified. Thus in addition to modifying the drying rate and hence energy efficiency, the gain matrix properties are also modified giving rise to simultaneous energy efficiency and controllability modification.

The discussion that follows shows how the use of a desiccant adsorption system as a preconditioning element to the dryer inlet air ensures the satisfaction of the conditions required for process gain modification.

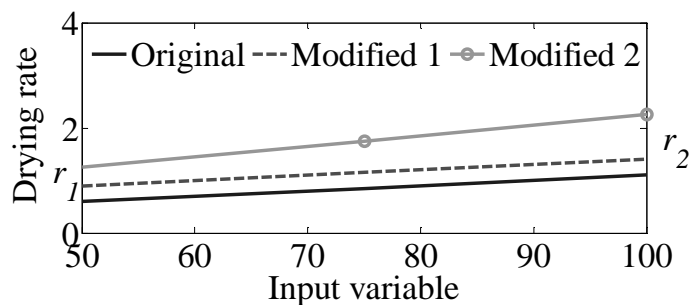


Fig. 8.2. Responses of drying rates to changes in input variables (like air flowrate) for original and two hypothetical modified drying processes

### 8.4.1. Desiccant adsorption drying for drying rate gain modification

In the adsorption drying process (Fig. 8.3), an adsorbent (zeolite)-coated rotary wheel with adsorption and regeneration sections (A and R respectively) is an add-on to the conventional dryer. Ambient air is dehumidified in the adsorber section, heated and used in the dryer for drying the wet product. The dehumidification is accompanied by the release of adsorption heat such that ambient air exits the adsorber at a lower humidity  $Y_{aA}$  and a higher temperature  $T_{aA}$ . Meanwhile, the spent adsorbent is regenerated using hot air. The system is described by the following mathematical model (details available in Atuonwu et al. (2011a) and presented in Chapter 2 of this thesis). The nominal operating conditions are listed in Table D1, Appendix D.

$$\frac{dx}{dt} = f(x, u) \quad (8.13)$$

$$\mathbf{x} = [X_p \quad X_{zA} \quad X_{zR} \quad Y_{aout} \quad Y_{ain} \quad Y_{aR} \quad T_{aout} \quad T_{aA} \quad T_{aR} \quad T_p \quad T_{zA} \quad T_{zR}]^T \quad (8.14)$$

$$\mathbf{u} = [F_{aA} \quad T_{ain} \quad F_z \quad F_{aR} \quad T_{aRin}]^T \quad (8.15)$$

Apart from the dryer state variables, other states are introduced.  $X_{zA}$  and  $X_{zR}$  are the outlet moisture contents of the adsorber and regenerator zeolite respectively;  $T_{zA}$  and  $T_{zR}$  are corresponding temperatures.  $Y_{aA}$  and  $Y_{aR}$  are absolute humidities of the air from the adsorber and regenerator respectively while  $T_{aA}$  and  $T_{aR}$  are corresponding temperatures. Extra degrees of freedom are zeolite flowrate  $F_z$  (proportional to wheel speed), regeneration air flowrate  $F_{aR}$  and temperature  $T_{aRin}$ .

From steady-state mass balances, the moisture evaporation rate from the product is

$$F_a(Y_{aout} - Y_{aA}) = F_a(Y_{aout} - Y_{amb}) + F_a(Y_{amb} - Y_{aA}) \quad (8.16)$$

The term on the left-hand side of (8.16) is the overall moisture evaporation rate of the dryer as a result of the adsorber dehumidification. The first term on the right-hand side represents the moisture evaporation rate assuming the dryer is alone without the adsorbent system, while the second represents the dehumidification rate of the adsorber alone. This dehumidification rate is the additive element that modifies the drying rate and as seen in (8.16), it is a function of the input variable (in this case, the air flowrate  $F_a$ ). The inclusion of the adsorbent system thus ensures system gain matrix modification as the system behaves like the Modified 2 process on Fig. 8.2.

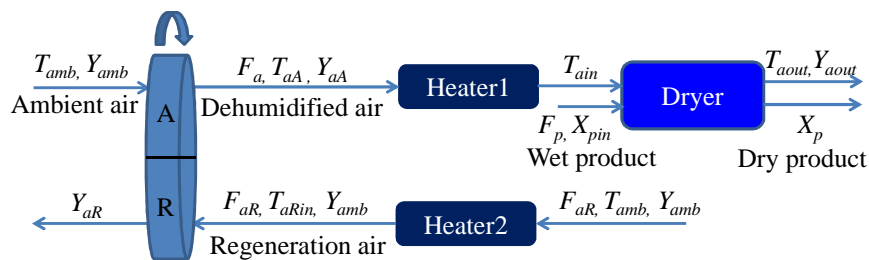


Fig. 8.3. Adsorption drying system



Fig. 8.4 shows the variation of dehumidification rate with drying air flowrate using experimental data for a wheel speed of 58rph and regeneration temperature 87.8°C and flowrate of 6120kg/h (Vineyard et al., 2000). In principle, the curves vary for changes in wheel speed, regeneration temperature and flowrate. Since the additive element (desiccant dehumidification rate) is positive, the process gain matrix elements with respect to  $F_a$  rise, thus increasing the numerator of energy efficiency defined by (8.7). The extra degrees of freedom provide opportunities for manipulating the dehumidification rate within constraints to desired values of the gain matrix elements so the  $MRI$  can be increased simultaneously as will be shown later.

#### 8.4.2. Desiccant adsorption drying: energy efficiency analysis

Although the adsorption system increases drying capacity and rate, the accompanying regeneration process requires energy. Hence, even though the numerator of the energy efficiency expression has the same form as that of the conventional dryer (8.5), the denominator or energy consumed is different. It is therefore important to derive how the temperature drop-based energy efficiency equation is affected. The total energy consumed for the adsorption drying system is the sum of the energies used in heating up the regeneration air from ambient value and that used in heating the drying air from the adsorber outlet temperature to the desired inlet temperature:

$$Q_{nSYS} = F_{aR}(C_{pa} + Y_{amb}C_{pv})(T_{aRin} - T_{amb}) + F_a(C_{pa} + Y_{aA}C_{pv})(T_{ain} - T_{aA}) \quad (8.17)$$

Hence, the energy efficiency is derived as

$$\eta_{SYS} = (F_a(Y_{aout} - Y_{aA})\Delta H_v) / Q_{nSYS} \approx (T_{ain} - T_{aout}) / (T_{ain} - T_{amb} - \Delta T_{ads} + (F_{aR}/F_a)(T_{aRin} - T_{amb})) \quad (8.18)$$

where  $\Delta T_{ads} = T_{aA} - T_{amb}$  is the temperature rise in the adsorber outlet air due mainly to sorption heat release. The numerator has the same form as that of the conventional dryer; however, the temperature drop is higher than that of the conventional dryer since it is due to the combined effect of the desiccant dehumidification rate and the drying rate of the dryer alone. This can also be interpreted from (8.7) as an increase in the process gain elements. In the denominator, the extra term  $\Delta T_{ads}$  accounts for adsorption heat release which reduces the required energy input to the drying air. The

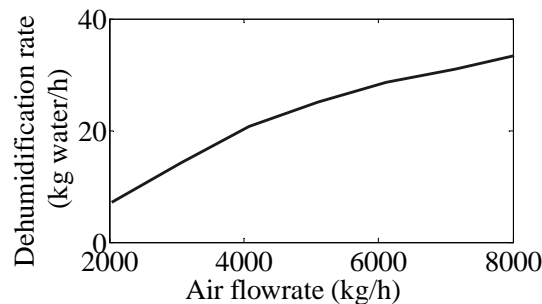


Fig. 8.4. Variation of water dehumidification rate with air flowrate

term in  $F_{aR}$  represents regeneration energy expenditure. Increasing energy efficiency lies in ensuring that the rise in temperature drop across the dryer, and the effect of adsorption heat release is not offset by regeneration energy expenditure.

#### 8.4.3. Desiccant adsorption drying: condition for energy efficiency improvement

Desiccant adsorption systems are defined by various performance indicators. The prominent indicators are moisture removal capacity (or dehumidification rate already described), specific dehumidification power, coefficient of performance, regeneration specific heat input and latent heat load defined as dehumidification rate multiplied by latent heat of vaporization  $\Delta H_v$  (ASHRAE, 1998). Zhai (2008) introduced unified performance indicators for comparing various designs and calculating the outlet air conditions based on the inlet air conditions. Among them is the regeneration efficiency defined as the ratio of the latent heat of the water removed from the regenerator to its input energy. This is synonymous with the energy efficiency equation applied to dryers as defined in (8.5). The other is the heat carry-over ratio defined as the ratio of energy added to the adsorber air (due to sorption heat release and other heat transfer) to the regeneration energy input. All the afore-mentioned indicators have been developed specifically for air conditioning applications.

For incorporation into the drying process, the required criterion is different. For instance, in air-conditioning applications, high sorption heat release or heat carry over is undesirable (Eicker et al., 2012) since it is counterproductive to the desired cooling requirement and as such represents energy wastage. In drying however, the sorption heat released can be positively exploited as it increases drying capacity.

Since in the adsorber-regeneration system, energy is consumed in the regenerator and released exothermically at the adsorber outlet, the “adsorber-regenerator net energy input”  $Q_{inAR}$  can be defined as the differential between the energies, that is,

$$Q_{inAR} = F_{aR}(C_{pa} + Y_{amb}C_{pv})(T_{aRin} - T_{amb}) - F_a(C_{pa} + Y_{amb}C_{pv})(T_{aA} - T_{amb}) \quad (8.19)$$

The system energy output or latent heat load is

$$Q_{outAR} = F_a(Y_{amb} - Y_{aA})\Delta H_v \quad (8.20)$$

Hence, a performance indicator for the desiccant dehumidifier alone, the adsorption-regeneration net energy efficiency ARNEE is defined as

$$ARNEE = \eta_{AR} = \frac{Q_{outAR}}{Q_{inAR}} = \frac{F_a(Y_{amb} - Y_{aA})\Delta H_v}{F_{aR}(C_{pa} + Y_{amb}C_{pv})(T_{aRin} - T_{amb}) - F_a(C_{pa} + Y_{amb}C_{pv})(T_{aA} - T_{amb})} \quad (8.21)$$

When a dryer is incorporated into the system as shown in Fig. 8.3, the evaporation energy is the total water removal rate (8.16) multiplied by latent heat of vaporization

$$Q_{outSYS} = F_a(Y_{aout} - Y_{aA})\Delta H_v \quad (8.22)$$

A close examination of equations (8.3), (8.4), (8.17), (8.19), (8.20) and (8.22) reveals that a superposition theory holds for the interactions between the dryer and the adsorber-regenerator system

$$Q_{outSYS} = Q_{outD} + Q_{outAR} \quad (8.23)$$

$$Q_{inSYS} = Q_{inD} + Q_{inAR} \quad (8.24)$$

Hence an alternative definition of the temperature drop equation (8.18) is,

$$\eta_{SYS} = \frac{Q_{outSYS}}{Q_{inSYS}} = \frac{Q_{outD} + Q_{outAR}}{Q_{inD} + Q_{inAR}} = \frac{\eta_D Q_{inD} + \eta_{AR} Q_{inAR}}{Q_{inD} + Q_{inAR}} \quad (8.25)$$

From which the following condition is derived,

$$\eta_{SYS} > \eta_D \quad \text{iff} \quad \eta_{AR} > \eta_D \quad (8.26)$$

This is stated as: “the incorporation of the desiccant system (without heat recovery) improves dryer energy efficiency only if the adsorber-regenerator net energy efficiency *ARNEE* is greater than the energy efficiency of the stand-alone dryer”. Thus in choosing a desiccant system suitable for improving the energy efficiency of an existing convective dryer it is important to specify the design and operating conditions appropriately. These conditions must be such that the latent heat capacity of the desiccant system, required regenerator heat input and corresponding sorption heat release will yield a ratio (8.21) greater than the energy efficiency of the stand-alone conventional dryer. Achieving an increase in dryer temperature drop due to the process gain modifications is a necessary condition for energy efficiency improvement while satisfying the above requirement is a sufficient condition. The existence of extra degrees of freedom helps in increasing possibilities of obtaining conditions for which both the energy efficiency and *MRI* are increased.

## 8.5. Process simulation and analyses

The process gain matrix  $\mathbf{G}$  is obtained for each dryer (conventional and adsorption) by linearizing about the respective operating points defined in Atuonwu et al. (2011b) and calculating the relevant slopes. For the conventional dryer, this gives rise to a 2x2  $\mathbf{G}$  matrix since there are two inputs (drying air flowrate and temperature) and two outputs (product moisture and temperature). For the adsorption dryer, the three

additional degrees of freedom (regeneration air flowrate, temperature and adsorbent flowrate) give rise to a  $2 \times 5$   $G$  matrix overall. Besides there are other output-input possibilities to which the overall  $G$  matrix can be decomposed, namely, 10  $2 \times 2$  possibilities, 10  $2 \times 3$  possibilities and 5  $2 \times 4$  possibilities. For each, the  $MRI$ s are computed using (8.9). The same is done for the conventional dryers. Energy efficiencies are computed at the nominal operating points using (8.5) for the conventional dryer and (8.18) for the adsorption dryer. Then, using the sensitivity-based temperature drop equation (8.7), energy efficiencies are recomputed to test the validity of the sensitivity-based equations.

To evaluate the effect of disturbance rejection control actions on the energy consumption of both systems, ambient disturbances are simulated and energy consumption  $Q$  calculated from the denominator of (8.5) for the conventional dryer and from (8.17) for the adsorption dryer constraining product moisture to remain constant. The percentage change in energy consumption is then computed as:

$$\% \Delta Q = \frac{Q - Q_{nom}}{Q_{nom}} \quad (8.27)$$

where  $Q_{nom}$  is energy consumption under nominal condition  $T_{amb}=25^\circ\text{C}$ ,  $Y_{amb}=0.01\text{kg/kg}$ .

To indicate how variations in degrees of freedom introduced by the adsorbent system influence the relationship between energy efficiency and controllability properties, the process is simulated at different regeneration air inlet temperatures  $T_{aRin}$ , but with a constraint that the drying requirement of product outlet moisture  $F_p(X_{pin}-X_p)=358\text{kg/h}$  is satisfied. This gives rise to different regeneration air flowrates that satisfy the constraint with all other process conditions remaining constant. Energy efficiency and  $MRI$  values are then calculated at these different conditions using (8.18) and (8.9). To verify condition (8.26), energy efficiencies of the desiccant drying system are calculated for different operating conditions together with  $ARNEE$  values of the desiccant dehumidifier. The  $ARNEE$  values are then compared with the energy efficiency of the conventional dryer.

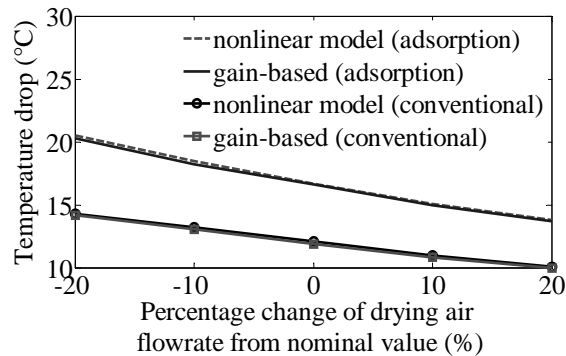


Fig. 8.5. Comparison of temperature drops: sensitivity-based and actual temperature-based

### 8.5.1. Gain-based approach: validation

Fig. 8.5 shows the relationship between the dryer temperature drops calculated from the gain-based approach (8.7) and that obtained using the full nonlinear model (Chapter 2 of this thesis) at different flows for both the adsorption and conventional dryers. Good agreement is observed in both cases, thus validating the gain-based model irrespective of the dryer type. As seen in the figure, the adsorption dryer temperature drop is greater than that of the conventional dryer at each flowrate. This is explainable by the dehumidification-induced drying rate increase and the consequent extraction of more water from the product per unit mass of drying air.

From these temperature drops, energy efficiencies for the conventional and adsorption dryers can be obtained (using (8.5) and (8.18)). The gain-based model thus provides another way of accurately calculating the energy efficiency of dryers using results obtainable from simple step tests around desired operating conditions. In addition to giving information on energy efficiency, system controllability properties can also be derived simultaneously when the sensitivities with respect to drying air flowrate (in the model) are combined with other input (e.g. inlet air temperature) sensitivities.

### 8.5.2. Performance analysis of design modification

Using the gain-based model for energy efficiency calculations, the results obtained as presented in Table 8.1 show that when  $F_a$  and  $T_{ain}$  are inputs for both dryers, a higher energy efficiency is attained for the adsorption dryer. Simultaneously, a higher  $MRI$  is achieved. One reason for this is the fact that the conditions stipulated in Section 8.3 are met. The elements  $\partial X_p / \partial F_a$  and  $\partial T_{aout} / \partial F_a$  are increased in magnitude relative to that of the conventional dryer while the changes in  $\partial T_{aout} / \partial T_{ain}$  and  $\partial X_p / \partial T_{ain}$  are such that the determinant magnitude to the norm ratio of  $\mathbf{G}$  slightly increases. A reason for the increased gain magnitudes is the fact that dehumidification leads to sorption heat release so the combined effect drives the output moisture and temperature further than would be possible without dehumidification. The greatest controllability advantage of an adsorption dryer is the introduction of extra control degrees of freedom. The  $MRI$ s of the 10 SISO control structure possibilities (Table 8.1) shows that some of them (e.g.  $F_a$  &  $F_{aR}$ ;  $T_{ain}$  &  $F_{aR}$  or  $T_{ain}$  &  $F_z$ ) are higher than that of the only option for the

Table 8.1. Gain matrices, MRIs & Efficiencies

		Adsorption dryer					Conventional dryer		
		$F_a$	$T_{ain}$	$F_z$	$F_{aR}$	$T_{aRin}$	$F_a$	$T_{ain}$	
$G$	$X_p$	-0.010	-0.0075	0.0080	-0.0441	$-1.3 \times 10^{-4}$	$X_p$	-0.0045	-0.0053
	$T_{aout}$	1.0937	0.9739	0.0481	-0.2642	$-7.7 \times 10^{-4}$	$T_{aout}$	0.6140	0.9827
$MRI$	<i>Full</i>	$F_a/T_{ain}$	$F_a/F_z$	$F_a/F_{aR}$	$F_a/T_{aRin}$	$T_{ain}/F_z$	$9.96 \times 10^{-4}$		
		$T_{ain}/F_{aR}$	$T_{ain}/T_{aRin}$	$F_z/F_{aR}$	$F_z/T_{aRin}$	$F_{aR}/T_{aRin}$			
		0.0445	$1.4 \times 10^{-4}$	$4e \times 10^{-16}$	$6.8 \times 10^{-18}$	$3.3 \times 10^{-19}$			
$\eta$		60%					51%		

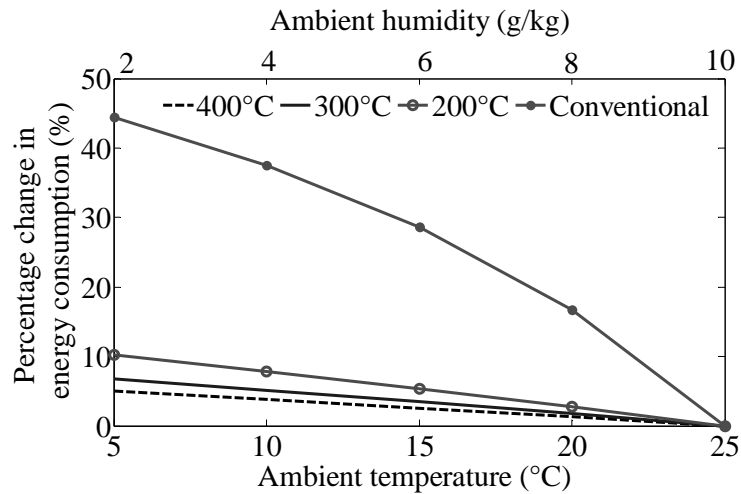


Fig. 8.6. Resilience of energy consumption to ambient air temperature variations at different regeneration temperatures (adsorption dryer) and at the drying temperature (Conventional dryer)

conventional dryer ( $F_a$  &  $T_{ain}$ ). Moreover, the full 5x2 system matrix has an  $MRI$  as high as 50 times that of the conventional dryer although the controller becomes more complex. Other intermediate control structures (not shown in the Table) like the use of 3 or 4 inputs to control the 2 outputs also exist (15 possibilities) with most of them having higher  $MRI$ s than the conventional dryer.

Fig. 8.6 shows the sensitivities of energy consumption to ambient air temperature/humidity changes for both the conventional dryer and the adsorption dryer at different regenerator inlet temperature/flowrate combinations required to keep the product moisture constant. By regenerating at high temperatures (which is a requirement for desiccant adsorption systems to ensure effective utilization), the system energy input of the regenerator is less sensitive to ambient temperature variations. For conventional low-temperature dryers however, the energy consumption rises substantially with decreasing ambient temperature as more energy is required to heat the drying air to the required temperature. In view of this, the energy efficiency of the adsorption dryer is less sensitive to ambient variations when compared with conventional dryers.

By varying the extra degrees of freedom introduced by the desiccant system, variations in the process gain matrix occur. Thus as shown in Fig. 8.7 (where different regenerator air inlet temperature/flowrate combinations required to keep the product moisture constant are applied), the energy efficiency and  $MRI$  vary. Higher regeneration temperatures promote energy efficiency with regeneration temperatures usually constrained by the need to keep the adsorbent in working conditions (van Boxtel et al., 2012). The efficiency improvement occurs due to the increase in the capacity of the adsorbent to take in more moisture from the drying air, increasing dehumidification rate (i.e. the additive element derived in (8.18) and illustrated in Fig. (8.2)). In the same vein, an increase in the  $MRI$  occurs for the full system matrix due

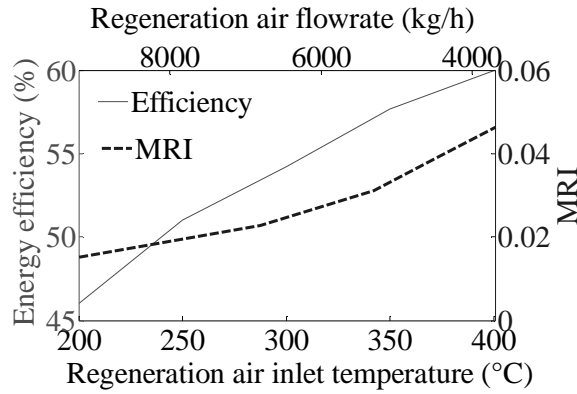


Fig. 8.7. Variation of energy efficiency and MRI with additional degrees of freedom

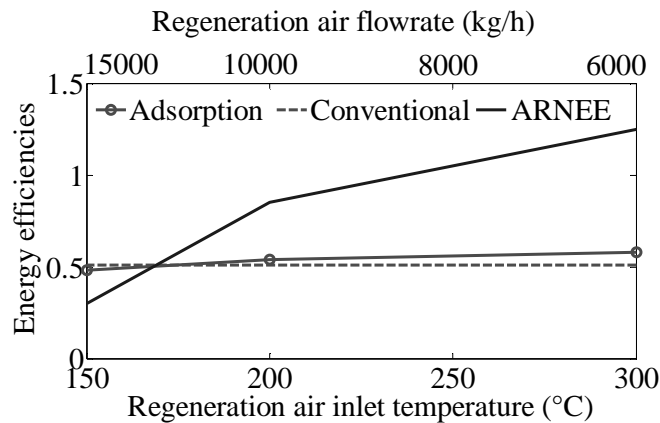


Fig. 8.8. Variation of adsorption drying system energy efficiency and ARNEE with conventional dryer energy efficiency showing the condition under which the adsorption dryer is more efficient

to the extra degrees of freedom. In summary, the existence of regeneration air flow, temperature and wheel speed as extra degrees of freedom creates opportunities to further manipulate energy performance and controllability than would be possible in conventional dryers.

### 8.5.3. Adsorber-regenerator net energy efficiency (ARNEE) analysis

Fig. 8.8 shows the adsorber-regenerator net energy efficiency *ARNEE* at different operating conditions necessary to maintain the same product outlet moisture content. As regenerator air inlet temperature reduces, the required flowrate increases more than proportionately. Similarly, dehumidification and sorption heat reduce. The result is that the denominator of *ARNEE* (8.21) reduces. As soon as the *ARNEE* falls below the energy efficiency of the conventional dryer, the system energy efficiency also goes below about simultaneously (as indicated by the intersections around the 170°C regeneration temperature). At this point, the regenerator energy input just more than offsets the gain associated with drying air dehumidification and the attendant sorption heat release. This establishes the *ARNEE* as a useful indicator for characterizing the suitability or otherwise of a given desiccant system for improving the energy efficiency of a dryer.

## 8.6. Conclusion

The relationship between process gain matrix with associated controllability properties and energy efficiency has been established for convective dryers together with conditions necessary for simultaneous improvement. It has been shown that using the process gain matrix, the dryer temperature drop and hence, energy efficiency can be reliably calculated. The gain matrix thus provides another way of calculating the energy efficiency of dryers using results obtainable from simple step tests around desired operating conditions. In addition to giving information on energy efficiency, system controllability properties can also be derived simultaneously.

From mass and energy balances it has been shown that by introducing a drying rate modifying system as an add-on to the basic convective dryer, simultaneous improvement of energy efficiency and controllability can be achieved. The use of a desiccant adsorption system as such an add-on is demonstrated as a strategy for ensuring this as it provides a drying rate additive element in form of dehumidification rate which can further be manipulated using the extra degrees of freedom also introduced by the system. By virtue of the adsorbent regulation properties which are enhanced by high-temperature regeneration, the resilience of energy performance to disturbances is significantly improved compared to conventional dryers.

Also, a desiccant wheel performance indicator, the adsorber-regenerator net energy efficiency *ARNEE* is introduced which though related to existing indicators is better-suited to the specifics of the use of desiccant dehumidifiers in drying operations. It is shown that the desiccant is effective in improving energy performance only if the *ARNEE* is greater than the energy efficiency of the stand-alone dryer. This result is valuable as the indicator provides a short-cut means of making decisions on the wheel specifications required to improve the performance of existing convective dryers.



### **On dryer controllability and energy performance: generalized modeling and experimental validation**

Submitted as Atuonwu, J.C., Asselt, C.J. van., Straten, G. van., Deventer, H.C. van., Boxtel, A.J.B. van (2012). On dryer controllability and energy performance: generalized modeling and experimental validation.

#### **Abstract**

Measured temperatures as commonly used in dryer energy efficiency calculations lead to severe over-estimations when heat losses are significant. In this work, an approach establishing the relationship between dryer process gains and energy efficiency is developed and generalized for continuous and batch dryers with significant heat losses. Using the process gains, the dryer temperature drop due to water evaporation is successfully decoupled from heat loss and product heating effects. The process gains in addition to providing controllability information thus also provide a viable alternative for reliable energy efficiency calculation even for non-adiabatic processes where the use of measured temperature drops is grossly inaccurate. The approach is tested and verified on two experimental case studies involving significant heat losses: the first, a continuous fluidized-bed dryer (from literature) and the second, a conventional and zeolite wheel-assisted batch dryer designed in the current study. Effects of the zeolite wheel on system performance are also investigated.

*Keywords:* Energy efficiency, dryer heat loss, process gain, controllability, desiccant wheel effects, batch and continuous dryers

#### **9.1. Introduction**

Drying is a high energy-consuming operation for which process control is important to achieve optimal energy performance and product quality regardless of disturbances. When hot air contacts the wet product during drying, the sensible heat of the air is converted to latent heat and the air temperature drops. The magnitude of this temperature drop is a measure of the amount of water evaporated for the given input energy. Consequently, the temperature drop across the dryer is often taken as a measure of the dryer energy performance. Examples of temperature drop-based energy performance measures include the specific energy consumption (Baker and McKenzie, 2005; Al Mansour et al., 2011) and energy efficiency (Raghavan et al., 2005; Kudra, 2004; Kudra, 2012). The temperature drop attainable for a given drying process has also been shown to be dependent on the air humidity which can be manipulated by dehumidifiers (Atuonwu et al., 2011c). Consider a typical drying system as in Fig. 9.1, where ambient air at temperature  $T_{amb}$  is heated to a desired

temperature  $T_{ain}$  and used for drying so the air exits the dryer at temperature  $T_{aout}$ . The energy efficiency is often computed (Raghavan et al., 2005; Kudra, 2012) as

$$\eta = (T_{ain} - T_{aout}) / (T_{ain} - T_{amb}) \quad (9.1)$$

The temperature drop across the dryer ( $T_{ain} - T_{aout}$ ) is thus an important variable and for a given inlet temperature, the degree of energy utilization depends on how low the outlet temperature is. It is also an established measure for product moisture control (Robinson, 1992). Recently, Atuonwu et al. (2012a) established a link between dryer energy efficiency and controllability in which it was found that the temperature drop is linearly related to process output sensitivities to flowrates. The study which was also extended to desiccant-assisted dryers did not consider heat losses and was limited to continuous dryers. Heat losses however have significant impacts not only on energy efficiency but also on controllability. Carrington et al. (2000) in a study of a batch dehumidifier dryer showed the difficulty, due to heat losses, in maintaining the drying temperature at the design point leading to higher drying times and energy consumption than necessary. Heat losses thus represent loss of control power as well.

The use of the temperature drop in energy efficiency calculation is reasonably accurate only if the outlet temperature is constant and representative of the drying process (Grabowski et al., 2002). For practical dryers however, this is usually not the case for a number of reasons. The dryer outlet temperature is not constant when the process goes through different drying regimes like the falling-rate period especially in batch dryers. Also, not all the heat energy supplied is used for water evaporation. Part of the energy constitutes heat loss from the dryer body to the environment and part used for product heating in the falling-rate drying period. As shown in Fig. 9.2, the dryer inlet temperature  $T_{ain}$  reduces as a result of evaporation effects to a quasi-outlet temperature  $T_{aout}^s$  and further to the measurable outlet temperature  $T_{aout}$  due to dryer heat loss and product heating effects. The measurable outlet temperature is therefore not only representative of the drying process but also of heat losses and product heating. If the effect of water evaporation is successfully decoupled from product heating and heat losses, the resulting energy efficiency calculation based on the difference  $T_{ain} - T_{aout}^s$  remains valid regardless of product heating and heat losses.

In this work, this decoupling is achieved using the elements of the dryer process gain matrix. The quasi-outlet temperature is truly representative of the drying process. Hence, reliable energy efficiency calculations are achieved even for non-adiabatic processes where using measured temperature drops is inaccurate. Experimental validation is provided by considering two case studies. The first involves a continuous

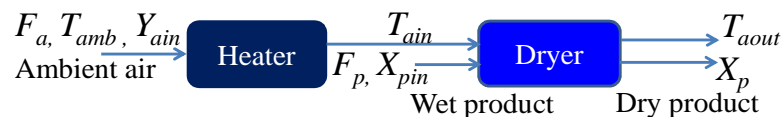


Fig. 9.1. Typical drying system set-up

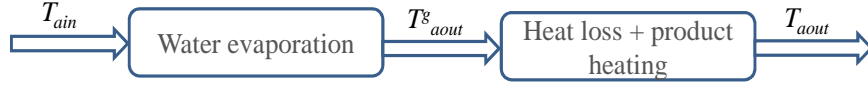


Fig. 9.2. Equivalent circuit of typical drying system set-up heat utilization

fluidized bed dryer taken from the literature at a dryer inlet temperature of 180°C. In the second, an experimental set-up involving a batch dryer with the possibility of incorporating a zeolite wheel is designed. Drying temperature is limited to 50°C. The link between energy efficiency and process gains established earlier is also shown to be valid for the batch dryers and continuous dryers with significant heat losses. The effect of zeolite wheel dehumidification on system performance is also evaluated.

## 9.2. Background and mathematical model

### 9.2.1. Continuous dryers

Consider the continuous drying system (Fig. 9.1). The dryer output variables product moisture content  $X_p$  and air temperature  $T_{aout}$  are controlled by input variables air flowrate  $F_a$  and inlet temperature  $T_{ain}$  to minimize the effect of disturbances. Taking energy balances around the system, the sensible heat loss of the drying air across the dryer equals the latent heat gain plus heat losses and product heating

$$F_a(C_{pa} + Y_{ain}C_{pv})(T_{ain} - T_{aout}) = F_p(X_{pin} - X_p)\Delta H_v + Q_{loss} + Q_{pheat} \quad (9.2)$$

The energy efficiency is defined as the ratio of the latent heat of water evaporated to the total dryer input energy. The latent heat of water evaporated is given by

$$Q_{outD} = F_p(X_{pin} - X_p)\Delta H_v = F_a(Y_{aout} - Y_{amb})\Delta H_v \quad (9.3)$$

while the dryer input energy for ambient temperature  $T_{amb}$  is

$$Q_{inD} = F_a(C_{pa} + Y_{amb}C_{pv})(T_{ain} - T_{amb}) \quad (9.4)$$

Hence, by combining (9.3) and (9.4), the actual energy efficiency  $\eta$  is

$$\eta = (F_a(Y_{aout} - Y_{amb})\Delta H_v) / (F_a(C_{pa} + Y_{amb}C_{pv})(T_{ain} - T_{amb})) \quad (9.5)$$

From (9.2), the rate of latent heat gain by the drying air is

$$F_a(Y_{aout} - Y_{amb})\Delta H_v = F_a(C_{pa} + Y_{amb}C_{pv})(T_{ain} - T_{aout}) - Q_{loss} - Q_{pheat} \quad (9.6)$$

Putting (9.6) in (9.5), the actual energy efficiency can be written as

$$\eta = [(T_{ain} - T_{aout}) / (T_{ain} - T_{amb})] - [(Q_{loss} + Q_{pheat}) / (F_a(C_{pa} + Y_{amb}C_{pv})(T_{ain} - T_{amb}))] \quad (9.7)$$

This clearly shows that when heat losses are significant, the common expression (9.1) grossly over-estimates energy efficiency.

Now, performing sensitivity analysis of the energy balance (9.2) with respect to the inputs, air flowrate  $F_a$  and temperature  $T_{ain}$  respectively,

$$T_{ain} - T_{aout} = (F_a \partial T_{aout} / \partial F_a) - (F_p / K) (\partial X_p / \partial F_a) + (1 / K \Delta H_v) (\partial (Q_{loss} + Q_{pheat}) / \partial F_a) \quad (9.8)$$

$$(\partial T_{aout} / \partial T_{ain}) + (F_p / K F_a) (\partial X_p / \partial T_{ain}) + (1 / K \Delta H_v) (\partial (Q_{loss} + Q_{pheat}) / \partial T_{ain}) = 1 \quad (9.9)$$

where  $K = (C_{pa} + Y_{ain} C_{pv}) / \Delta H_v$

The rate of heat loss  $Q_{loss}$  at any air flowrate  $F_a$  is given by

$$Q_{loss} = F_a (C_{pa} + Y_{ain} C_{pv}) (T_{ain} - T_{aout}^{NL}) \quad (9.10)$$

where  $T_{aout}^{NL}$  which is less than  $T_{ain}$  because of heat loss is defined as the no-load outlet air temperature (assuming no product is being dried in the dryer). Hence, using (9.10) to evaluate the last term of (9.9),

$$\partial Q_{loss} / \partial F_a = (C_{pa} + Y_{ain} C_{pv}) \left( -F_a \partial T_{aout}^{NL} / \partial F_a + (T_{ain} - T_{aout}^{NL}) \right) \quad (9.11)$$

Substituting into (9.9),

$$T_{ain} - T_{aout} = F_a \left( \partial T_{aout} / \partial F_a - \partial T_{aout}^{NL} / \partial F_a \right) - (F_p / K) (\partial X_p / \partial F_a) + (1 / K \Delta H_v) \left( \partial Q_{pheat} / \partial F_a + K \Delta H_v (T_{ain} - T_{aout}^{NL}) \right) \quad (9.12)$$

The last term of (9.12) is exclusively due to the effects of product heating and dryer heat loss while the first two terms are mainly due to water evaporation from the product. The system is therefore decoupled. Hence, a close approximation to the temperature drop due to water evaporation effects alone is

$$T_{ain} - T_{aout}^g = F_a \left( \partial T_{aout} / \partial F_a - \partial T_{aout}^{NL} / \partial F_a \right) - (F_p / K) (\partial X_p / \partial F_a) \quad (9.13)$$

The corresponding energy efficiency is

$$\eta_g = \frac{T_{ain} - T_{aout}^g}{T_{ain} - T_{amb}} \quad (9.14)$$

The gain matrix element-dependent temperature drop (9.13) is thus valid for energy efficiency computation regardless of heat losses. Industrial data from Reay (1984) for a continuous fluidized bed dryer with significant heat losses, described in Langrish and Harvey (2000) is used to demonstrate this result later.

### 9.2.2. Batch dryers

For a batch dryer, the product moisture and temperature cannot achieve steady-states. However, under certain product conditions for instance high surface area to volume ratio, constant drying rate regimes can be experienced where the drying rate is essentially constant for any given input conditions. In contrast to continuous systems, the control objective is to ensure the product moisture follows a given trajectory and terminates at given conditions (Trelea et al., 1997). Achieving this path means manipulating the drying rate, which in many cases boils down to remain steady during large portions of the process. Hence in translating the results (9.13) to batch systems, the sensitivities with respect to drying rate is used instead of product moisture. The following energy balance applies on the drying air under steady-state (drying rate):

$$r\Delta H_v = F_a ((C_{pa} + Y_{ain}C_{pv})T_{ain} - (C_{pa} + Y_{aout}C_{pv})T_{aout}) - Q_{loss} \quad (9.15)$$

Product heating is minimal for constant drying rate and so is neglected in (9.15). The actual energy efficiency is the ratio of evaporated water energy to total input energy

$$\eta_{batch} = \frac{r\Delta H_v}{F_a (C_{pa} + Y_{ain}C_{pv})(T_{ain} - T_{amb})} \quad (9.16)$$

Differentiating the energy balance (9.15) with respect to  $F_a$ , considering the expression for  $Q_{loss}$  sensitivity (9.11) as was done in the case of the continuous dryers,

$$T_{ain} - T_{aout}^s = F_a \left( \partial T_{aout} / \partial F_a - \partial T_{aout}^{NL} / \partial F_a \right) + (1/K) (\partial r / \partial F_a) \quad (9.17)$$

By (9.17), the temperature drop due to water evaporation is decoupled from heat loss effects. The gain-based energy efficiency calculation for the batch system is then calculated from (9.14) with the new  $T_{ain} - T_{aout}^s$  (9.17). Considering the equations (9.13) for continuous dryers and (9.17) for batch dryers, the difference lies in the second part where product moisture content and product flowrate are replaced by drying rate. The difference in signs is because drying rate  $r$  is an increasing function of air flowrate  $F_a$  while product moisture  $X_p$  decreases with  $F_a$ . The approach is thus generalized.

### 9.2.3. Adsorption dryers

If a continuously-rotating adsorbent wheel is coupled to the batch drying process as shown in Fig. 9.3, the temperature of the inlet to the drying air heater (Heater1) is increased from ambient value  $T_{amb}$  to a higher value  $T_{aA}$  due to adsorption heat release which accompanies the dehumidification. Also, extra energy is spent heating the regeneration air (via Heater2) from ambient temperature to regenerator inlet temperature  $T_{aRin}$ . For a regeneration air flowrate  $F_{aR}$ , the energy consumed becomes

$$Q_{inSYS} = F_{aR} (C_{pa} + Y_{amb}C_{pv})(T_{aRin} - T_{amb}) + F_a (C_{pa} + Y_{aA}C_{pv})(T_{ain} - T_{aA}) \quad (9.18)$$

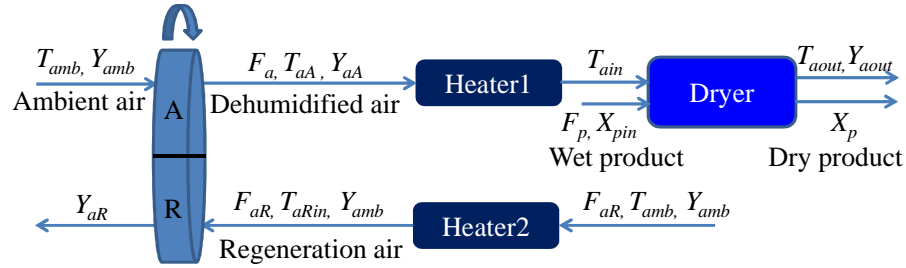


Fig. 9.3. Adsorbent wheel-assisted drying system

By the same method used in deriving (9.1), the temperature drop-based energy efficiency approximation is

$$\eta_{SYS} = r\Delta H_v / Q_{mSYS} \approx (T_{ain} - T_{aout}) / (T_{ain} - T_{aA} + (F_{aR} / F_a)(T_{aRin} - T_{amb})) \quad (9.19)$$

For the gain-based approximation we replace  $T_{ain} - T_{aout}$  in (9.19) by  $T_{ain} - T_{aout}^g$  (9.17).

### 9.3. Case studies

Two case studies are used to test the relationship between the process gains and energy efficiencies as derived in Section 9.2. First, industrial data taken from Reay (1984) and described in Langrish and Harvey (2000) for a continuous fluidized bed dryer with significant heat losses is used. The operating temperature is 180°C which is reasonably high and the product dried is calcium oxide. Second, an experimental set-up involving a batch tray dryer is designed with a detachable rotary wheel filled with zeolite acting as a dehumidifier. Part of the aims of the study is to determine the effect of the dehumidifier wheel on the sensitivities (process gains) and energy performance. Thus in a reference experiment, the wheel is detached, reducing the dryer to a conventional one. Since steady-state conditions cannot be achieved for product moisture content in a batch dryer, the product dried are in such experimental conditions that constant drying rates can be achieved at each input operating point. The drying rate is taken as the state variable instead of product moisture content.

#### 9.3.1. Case 1: Continuous fluidized bed dryer with significant heat losses

##### 9.3.1.1. Process description and method

Depending on the scale of a drying system and the operating conditions, heat losses can be highly significant as is the case in Fig. 9.4 which presents an experimental study (Reay, 1984), reproduced in Langrish and Harvey (2000). The measured process conditions (the operating inlet, outlet air and product conditions) and process gain matrix elements as obtained in Langrish and Harvey (2000) are shown in Table 9.1. Heat loss is reported to be of magnitude 76±18kW which for a calculated drying latent heat load  $F_p(X_{pin} - X_p)\Delta H_v$  of 80kW is highly significant. To test the effect of the heat losses on the proposed gain-based temperature drop model as opposed to using

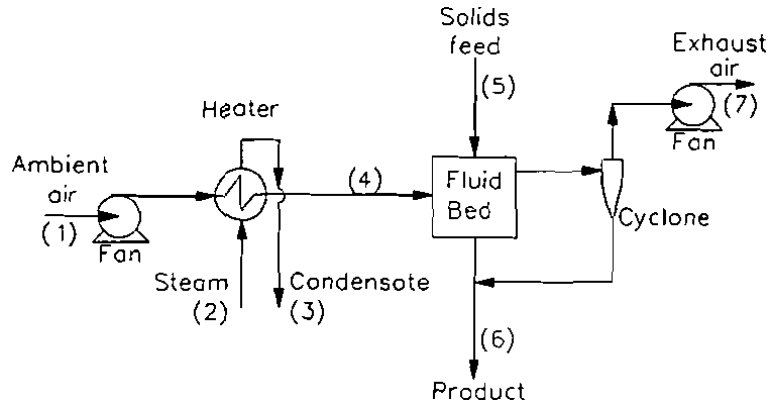


Fig. 9.4. Continuous fluidized bed drying system (Reay, 1984)

Table 9.1. Operating conditions of the fluidized bed dryer (Reay, 1984)

Measurement point	Measurement (Units)	Value	Calculated Gains
4	Process air mass flowrate (kgs <sup>-1</sup> )	1.55	$\partial X_p / \partial F_a = -0.0144$
	Process air temperature (°C)	180	$\partial T_{aout} / \partial F_a = 25.3871$
	Ambient air humidity (kgkg <sup>-1</sup> )	0.027	
5	Feed moisture content (kgkg <sup>-1</sup> )	0.15	
	Feed temperature (°C)	25	
6	Product mass flowrate (kgs <sup>-1</sup> )	0.3	
	Product moisture content (kgkg <sup>-1</sup> )	0.02	
	Product temperature (°C)	60	
7	Exhaust air temperature (°C)	60	
	Exhaust air humidity (kgkg <sup>-1</sup> )	0.052	
	Exhaust gas mass flowrate (kgs <sup>-1</sup> )	1.55	

measured temperature drops, energy efficiencies are computed using three equations:

- i. The equation (9.5) which computes the actual efficiency
- ii. The temperature drop approximation (9.1) using given measurements
- iii. The gain-based approach (9.13) and (9.14) proposed in this work

The ambient temperature is an important variable not given. Hence, calculations are done for an ambient temperature range 30-50°C for which the ambient air relative humidities are realistic considering the value of the ambient air humidity (0.027kg/kg). The no-load temperature sensitivity is neglected (being not given in Reay, 1984). This is a reasonable assumption for high-temperature low flow dryers with very high heat losses as in the current case where  $(T_{ain} - T_{aout}^{NL}) \gg F_a \partial T_{aout}^{NL} / \partial F_a$  so  $F_a \partial T_{aout}^{NL} / \partial F_a$  disappears from (9.13).

### 9.3.1.2. Results on continuous dryer case study

The results of lumped energy efficiencies calculated using the equations in (i), (ii) and (iii) are presented in Fig. 9.5. It is observed that for all ambient temperatures, the efficiencies calculated by the gain-based temperature drops closely approximates the actual energy efficiency while the normal temperature drop calculations derived from

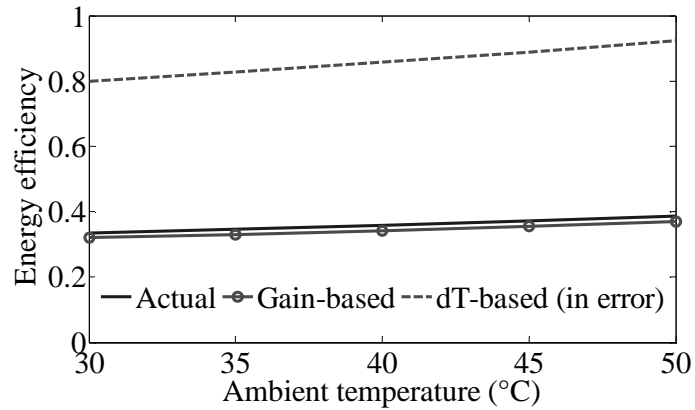


Fig. 9.5. Variation of energy efficiencies as computed by different equations with ambient temperatures

measurements severely overestimate the energy efficiency and as such are grossly inaccurate. This confirms the derivations in Section 9.2. The gain-based approach thus provides another reasonably accurate way of calculating energy efficiencies of dryers. The process gains can be obtained experimentally from the plant by step response tests around desired operating conditions. In addition to giving information on energy efficiency, system controllability properties can be derived simultaneously when the sensitivities with respect to drying air flowrate are combined with other input (e.g. inlet air temperature) sensitivities as was shown in Langrish and Harvey (2000).

### 9.3.2. Case 2: Batch dryer (Conventional and zeolite wheel-assisted)

#### 9.3.2.1. Experimental equipment: description and design

The experimental set-up is as shown in Fig. 9.6a. Air is drawn into the system from the environment via the fan (A), driven by an induction motor. The air is divided at junction B between the process and regeneration sides. The flowrates of the air through the process and regeneration sides are respectively controlled by means of control valves C and D. The regeneration air goes through the regenerator air heater E before passing through the upper side F of the chamber G containing the regeneration section of the motor-driven adsorbent-filled rotary wheel (Fig. 9.6b) of which the bottom through I is the adsorber side. The exhaust air from the regenerator from pipe H is vented to the atmosphere. The process air on the other hand flows through the adsorption section of the wheel, through I. It is heated by heater J, flows through the inlet K of the drying chamber L to contact the wet product and exits the drying chamber through pipe M. Heaters E and J are controlled by time-proportional heating elements. The flowrates are measured by hot wire anemometers while adsorber and regenerator inlet and outlet temperatures are measured by thermocouples. For the dryer, the inlet and outlet temperatures are measured by combination temperature and relative humidity sensors from which humidity ratios (kg water/kg air) are calculated. The mass of the product in the dryer is determined by continuous mass measurements from a weighing scale N to which the dryer tray suspended from loosely tied rods is attached so it directly bears the weight on the tray. To set up a reference experiment,



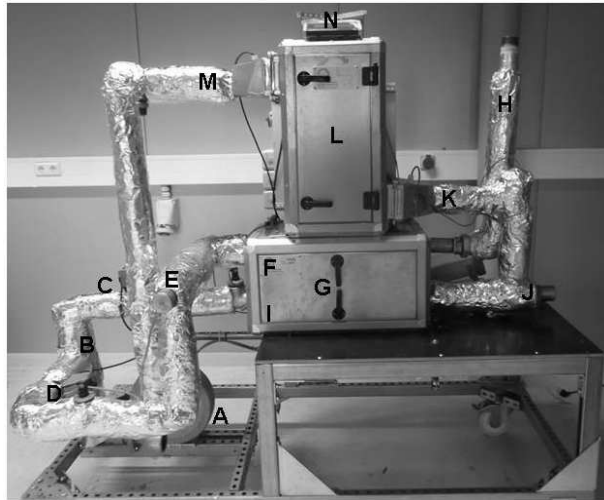


Fig. 9.6a. Experimental set-up of zeolite wheel-assisted tray dryer

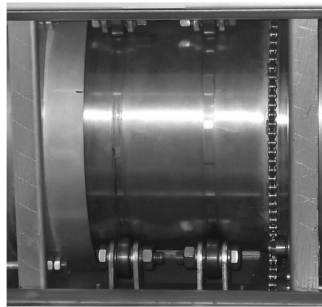


Fig. 9.6b. Rotary zeolite wheel within Chamber G of Fig. 9.6a (regenerator top, adsorber bottom).

the wheel is detached so the system reduces to a conventional dryer. Details of the experimental equipment and sensor specifications are in Table E1, Appendix E.

#### 9.3.2.2. *Experimental equipment: primary control system design and tuning*

The primary input variables of the system are the control valve positions for the adsorber and regenerator air flows and the “ON” time of the heating elements for corresponding temperatures. The system is thus a 4-input, 4-output system. The aim of the experiment is to investigate the step responses of the outputs to process inputs and on the basis of the obtained gains, compute the gain-based energy efficiencies. It is therefore important to have a means of delivering controlled flows and temperatures which can then be varied in steps as necessary. This is done by designing Proportional Integral (PI) control loops details of which are available in Fig. E1, Appendix E. The control system is implemented in LABVIEW® (National Instruments, Austin TX).

#### 9.3.2.3. *Experimental method*

The experiment essentially involves a series of step tests in which the input variable, air flowrate is varied in steps and system responses determined. From these, gain-based energy efficiencies are calculated. For a reference experiment, the wheel is detached and the regeneration airflow set to zero so the system reduces to a conventional dryer. The drying system is started up and the set-point for dryer air

flow set to a nominal value of 50kg/h. Then the sensitivity of no-load outlet temperature to air flowrate  $\partial T_{aout}^{NL}/\partial F_a$  is determined by running the dryer (without any product within) and changing the flowrate in steps at an inlet temperature of 50°C. The dryer is then loaded with the product.

Since the experiment requires constant drying rates under constant input conditions, the product dried is chosen to be in such structural conditions as would permit constant drying rate periods for appreciable periods of time within which each experiment would take place. Water-soaked sponges of length 9cm, width 6cm and thickness 3cm are used as drying materials. By virtue of their porous structure, they exhibit appreciable constant-rate drying periods. Also, the surface area to volume ratio is sufficiently large. For material preparation, the sponges are soaked in water, brought out, squeezed gently to take out excess water and then left to stand for about thirty minutes to drain off excess water before loading onto the dryer.

An important requirement is that the dried product remains in the constant-rate drying regime throughout the experiment since under falling-rate conditions; it is not straightforward to distinguish the change in drying rates due to input conditions from that due to product properties. A test is done to determine the time for which constant-rate drying is maintained under nominal flows and temperatures of 50 kg/h and 50°C respectively. The drying curves are shown in Fig. E2, Appendix E. Over a period of 2 hours the drying rate is practically constant, as illustrated by the detailed plot for the first two hours in Fig E2(b). Each experiment is thus designed to be concluded within 2 hours. Step-flowrate patterns are applied to the system and the drying rate and outlet temperature responses determined. The drying rates are determined by differentiating continuous mass measurements with respect to time (Kemp, et al., 2001).

The same procedure stated in the foregoing is repeated for the entire system with the zeolite-filled wheel attached. Throughout this experiment, the regeneration air flow is set to one-third of the drying air flow while regeneration temperature is set at 100°C, and wheel speed at 10rph. For fair comparison between the energy efficiencies of two dryers under different inlet (input) conditions, it is important to ensure the drying capacity of the exhaust air (determined by the relative humidity) is the same in both cases. That way, the difference in energy efficiencies is determined by the input conditions and not the outlet air conditions. This is the case with the conventional and zeolite-assisted dryers where the dehumidification in the latter reduces the inlet air humidity and hence increases drying capacity. This means lower drying air flowrate is required for the same wet product size to achieve the same outlet air relative humidity. But since the main aim of the experiment is to establish how drying air flowrate step responses can be used to calculate energy efficiencies, it is also necessary to excite both dryers with the same air flowrate magnitudes. Hence, a higher wet product loading (with more contact surface area) is used for the zeolite-assisted dryer to ensure that for the same air flow, the exit air has the same relative humidity as that of the conventional dryer.

9.3.3. Results on batch drying system

9.3.3.1. Conventional system

Fig. 9.7 shows the drying air flowrate step patterns used in exciting the dryer under no-load conditions and the corresponding outlet temperature variations. As air flow decreases, the specific heat loss increases since absolute heat loss remains essentially constant. The outlet temperature thus falls. And vice versa. The no-load dryer outlet temperature sensitivity  $\partial T_{aout}^{NL} / \partial F_a$  is calculated from here. On loading the conventional dryer (zeolite wheel detached) with product, the step pattern shown in Fig. 9.8 is applied and the corresponding responses of product mass, outlet air temperature and drying rate are also shown in Fig. 9.8. Based on the drying rate and input conditions, the actual energy efficiency is calculated by (9.16) and compared in Fig. 9.9 with efficiencies calculated by the conventional temperature drop-based equation (9.1) and the gain-based equation (9.14) and (9.17) proposed in this work.

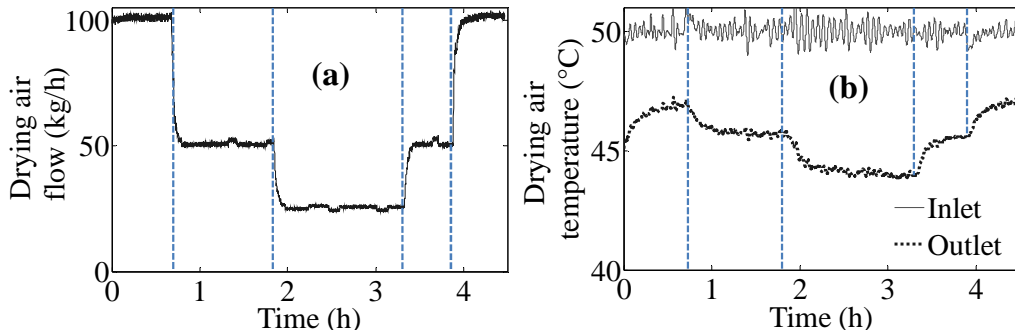


Fig. 9.7. (a) No-load steps in drying air flowrate (b) Corresponding dryer outlet temperature responses at an inlet temperature of 50°C: vertical dashed line show step times

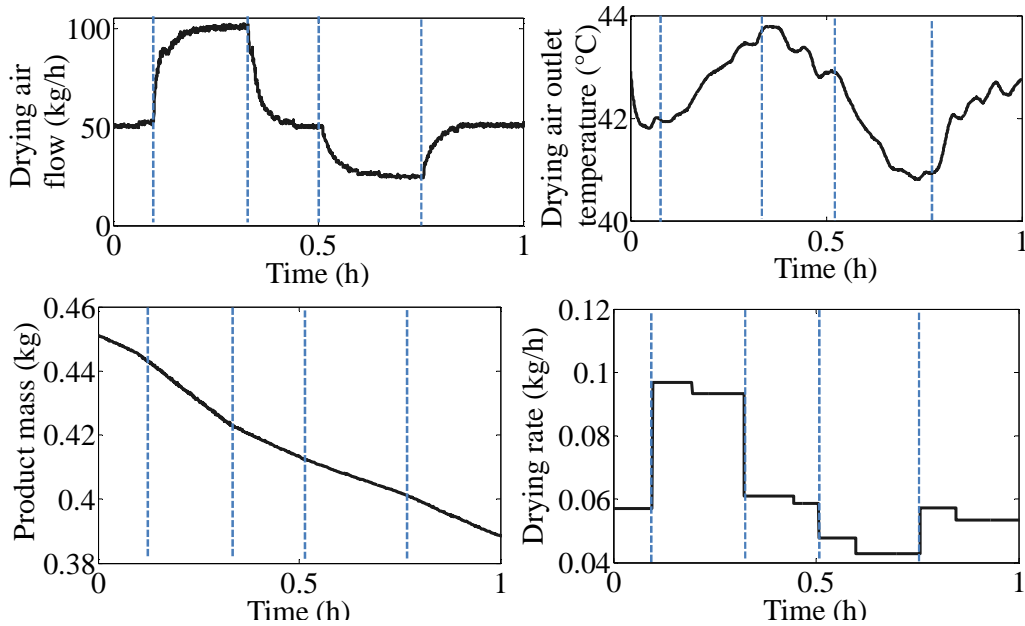


Fig. 9.8. Step air flowrate input and corresponding output responses showing step times (vertical dashed lines): conventional batch dryer

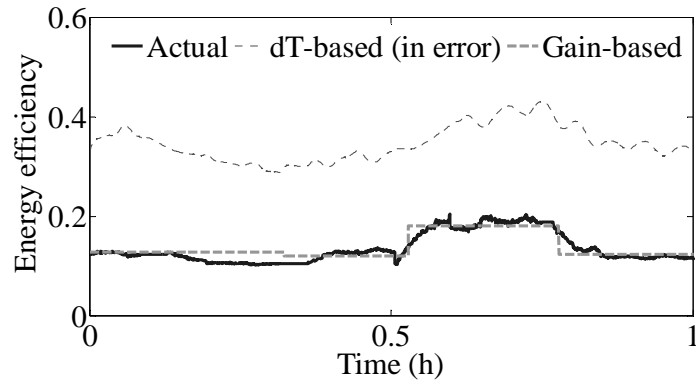


Fig. 9.9. Comparison of energy efficiencies calculated using various methods based on results for conventional batch dryer

For the gain-based approach, the instantaneous energy efficiency is approximated by a piecewise constant function at each step region. The results as presented in Fig. 9.9 shows that once again, the results of the gain-based temperature drop approach more closely approximates the actual dryer energy efficiency than the conventional temperature drop approach based on measurements.

### 9.3.3.2. Zeolite wheel-assisted batch dryer

With the zeolite wheel in place, the air is dehumidified. As shown in Fig. 9.10a, the dryer inlet air humidity is reduced relative to that of the conventional system from about 0.0082kg water/kg air to 0.005kg water/kg air. For a fair comparison with the conventional dryer (as already explained in section 9.3.2.3), the zeolite dryer is loaded with 0.660kg wet product as against the 0.450kg used for the conventional system. This ensures that the exhaust air relative humidities (as shown in Fig. 9.10b) are about the same (that of the zeolite-assisted system still remains slightly lower for most of the time and hence still has more unutilized capacity).

When the same dryer step magnitudes as for the conventional system are applied to the current system, the responses of product mass, outlet air temperature and drying rate are as shown in Fig. 9.11. Relative to the conventional system, similar trends in output variable behavior in response to the steps are observed. However, the magnitudes are different as will be discussed in the next section.

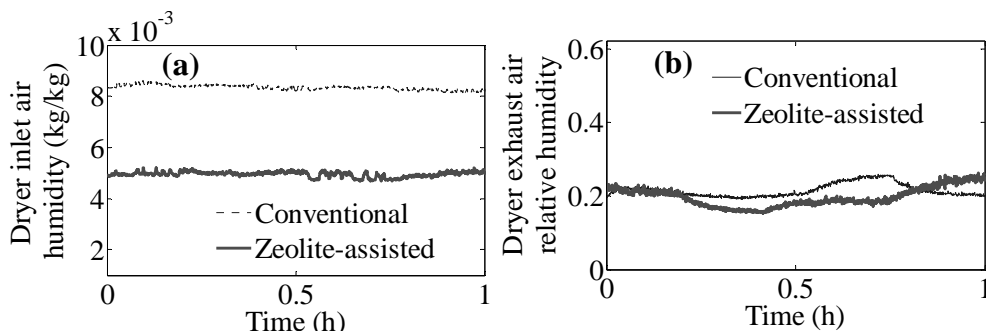


Fig. 9.10. Dryer inlet air absolute humidities (a) and outlet air relative humidities (b) of conventional and zeolite wheel-assisted dryers

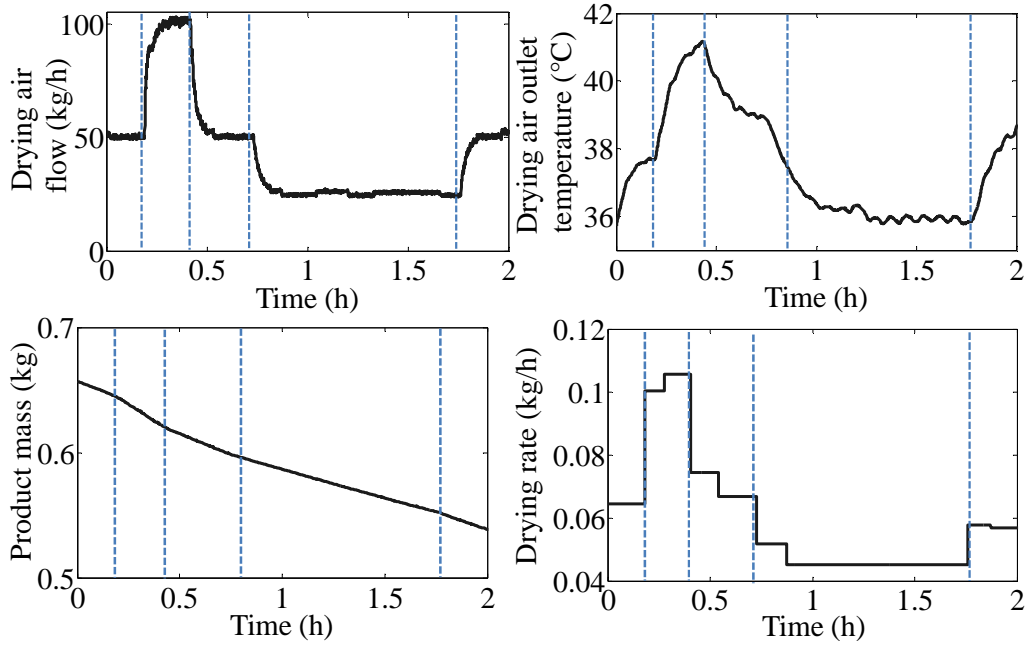


Fig. 9.11. Step air flowrate input and corresponding output responses showing step times (dashed lines): zeolite wheel-assisted batch dryer

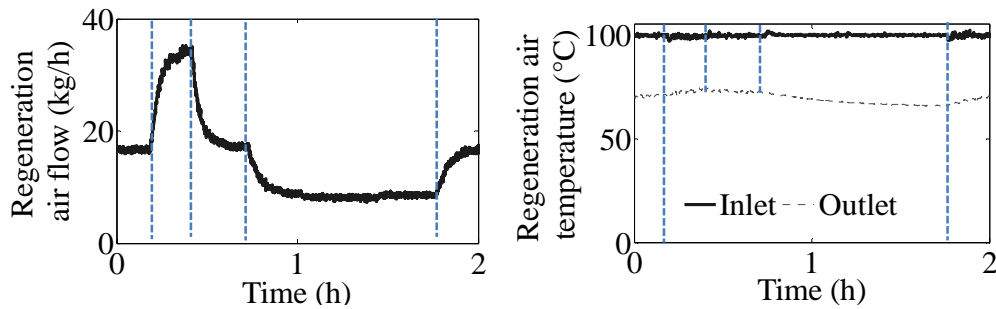


Fig. 9.12. Applied regeneration conditions

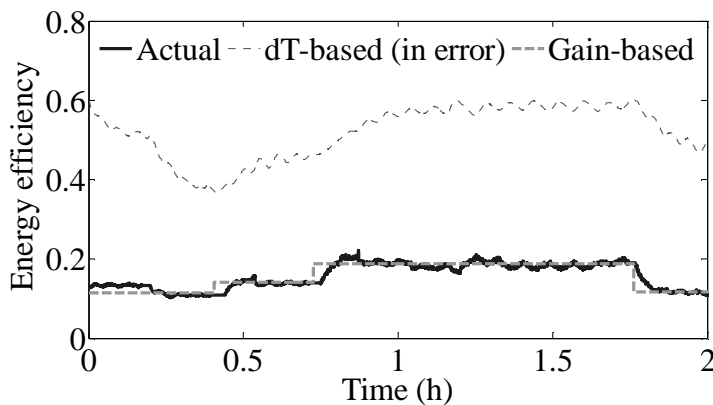


Fig. 9.13. Comparison of energy efficiencies calculated using various methods based on results for zeolite wheel-assisted batch dryer – without heat recovery via regenerator

The applied regeneration conditions are shown in Fig. 9.12. A comparison of the energy efficiency calculations as presented in Fig. 9.13 also show that the gain-based temperature drop approach is far more accurate than the conventional temperature drop approach. The gain-based approach is thus confirmed as a viable alternative for

energy efficiency calculations for both conventional and adsorbent dehumidifier-assisted systems even in cases of significant heat losses where conventional temperature measurements grossly over-estimate energy efficiency. Hence, using the gain-based approach, information on system energy efficiency can be obtained in addition to controllability properties, as has already been shown.

### 9.3.3.3. Effects of the zeolite wheel on overall system performance

By comparing the results of Figs. 9.8 and 9.9 (for the conventional system) and Figs. 9.11, 9.13 and 9.14 (for the zeolite system), the following observations stand out:

- Drying rate is increased for the zeolite system. For instance at nominal drying air flowrate of 50kg/h (first period in Figs. 9.8 and 9.11), drying rate increases by 14% from 0.057kg/h to 0.065kg/h. At the maximum flow (100kg/h), the increase is also about 14% from 0.093kg/h to 0.106kg/h.
- Drying capacity per unit mass of air is increased by about 34% using the zeolite system. Here, drying capacity per unit mass of air is defined as the grams of water evaporated from the product per kg of drying air in bringing the air to a certain exhaust relative humidity. For the conventional dryer, 63g of water (480-387) is evaporated in 1h with an air flowrate (averaged over time) of 58.4kg air h<sup>-1</sup>. The drying capacity is thus 1.08g water/kg air. For the zeolite-assisted dryer, the amount of water removed in 2h is 130g (660-130) or 65g water h<sup>-1</sup>. The air flowrate averaged over time is 44.875kg air h<sup>-1</sup>. The drying capacity is thus 1.45g water/kg air, representing a 34% increment.
- The sensitivities (process gains) of drying rate to product air flow increases due to the zeolite. For instance, in response to the same change of flowrate from 50 to 100kg/h, the drying rate changes from 0.065 to 0.106kg water/h for the zeolite-assisted system representing a gain of  $8.2 \times 10^{-4}$  kg water/kg of air. Whereas for the conventional system, the drying rate changes from 0.057kg/h to 0.093kg/h representing a gain of  $7.2 \times 10^{-4}$  kg water/kg of air. Similar results are obtained for other flowrate steps and for the dryer outlet temperatures. A reason for the increased gain magnitudes is the fact that dehumidification increases drying capacity which drives the drying rate and temperature further than would be possible without dehumidification. This agrees with the results of previous work (Atuonwu et al., 2012b) for continuous systems.
- In terms of energy efficiency (compare Figs. 9.9 and 9.13), the increase in the drying rate and capacity is offset by the extra regeneration energy requirement. This is because the operating conditions of the zeolite system are not optimized to higher regeneration temperatures and lower regeneration air flows (see Atuonwu et al., 2011b) due to heater power limitations of the experimental set-up. However, the zeolite system introduces opportunities for beneficial heat recovery by virtue of the relatively high regenerator exhaust temperature which does not exist for the conventional dryer.

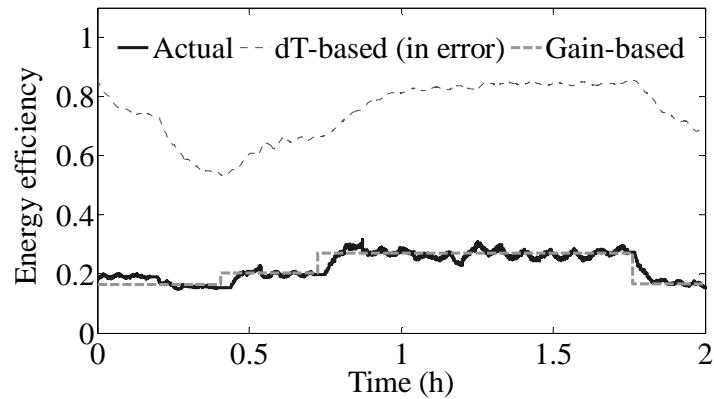


Fig. 9.14. Comparison of energy efficiencies calculated using various methods based on results for zeolite wheel-assisted batch dryer – with heat recovery via regenerator

To demonstrate the foregoing, a calculation is done where part of the regeneration outlet air energy is recovered and used in pre-heating the regeneration inlet air. For a mean regeneration exhaust air of  $70^{\circ}\text{C}$  as shown in Fig. 9.12 and assuming heat recovery is by a heat exchanger with minimum temperature difference of  $20^{\circ}\text{C}$ , the air to the regenerator heater is preheated from an ambient value of  $28^{\circ}\text{C}$  to  $50^{\circ}\text{C}$ . As shown in Fig. 9.14, energy efficiency is increased at each time by about 50% compared to the conventional system. This represents a 33% reduction in specific energy consumption. If higher regeneration temperatures are used, the possibilities of beneficial heat integration increases even further.

#### 9.3.4. Further discussion

The low energy efficiency magnitudes recorded in this experiment for the conventional and zeolite-assisted batch dryers is due to a number of factors. First, the small size of the dryer and low product loading results in a low degree of energy utilization as a result of which the dryer outlet air relative humidity is still too low, about 20% (Fig. 9.10b). Assuming the dryer is larger and well loaded or the air recycled until it exits at higher humidities, energy efficiency will be increased considerably. An alternative arrangement will be the use of low air flowrates but this has the disadvantage that the system will not be sufficiently excited to get good process gains necessary to prove the main concept of this work. Secondly, heat losses are significant. Under nominal drying air flow of  $50\text{kg/h}$ , heat loss is  $215\text{kJ/h}$  as shown in a heat loss estimation test (Fig. E3, Appendix E). This is higher than the latent heat of the water evaporated per hour (about  $160\text{kJ/h}$ ).

It should be noted that this analysis considers only constant-rate drying regimes. The results are also applicable to other drying materials e.g. food products provided the surface area to volume ratio is sufficiently high to facilitate appreciable constant rate drying regimes. This can be seen for instance in Jin et al. (2011) where there is an appreciable constant rate drying period for broccoli florets and stalks at low sample

thickness. During the falling rate periods, energy efficiency is expected to drop due to product drying kinetic limitations. To extend the gain-based energy efficiency calculation approach to this drying regime, an additional challenge would be to distinguish drying rate changes due to the air flow changes (at step tests) from those due to product behavior-dependent diffusion-controlled falling-rate mechanisms. This should represent an interesting research challenge.

#### 9.4. Conclusions

In this work, a generalized model relating drying process gains and energy efficiency has been formulated taking into consideration, heat loss effects for both continuous and batch operation. For batch operation, the product moisture content for which steady states do not exist was replaced by drying rate. The effect of incorporating a rotary zeolite wheel on the batch drying system performance was also investigated. The following are the major conclusions of the work:

- The energy efficiency computation by the gain-based temperature drop approach closely approximates the actual energy efficiency irrespective of heat losses. This is because the gain-based approach decouples dryer temperature drop due to water evaporation from heat loss effects. Conventional temperature drop approaches based on actual measurements however grossly over-estimate energy efficiency when heat losses are significant. The results are valid for both continuous and batch systems with or without adsorbent dehumidification and also for adsorbent-assisted systems with regenerator heat integration. The gain-based approach thus provides a reliable alternative to energy efficiency calculations. Hence using simple step tests, information on system energy efficiency can be obtained in addition to controllability properties.
- By incorporating a desiccant wheel to the basic drying system, drying rates and capacities are increased. In terms of energy efficiency, these advantages may be offset by the extra regeneration energy requirements. However, opportunities for beneficial heat integration are introduced by virtue of the high regenerator exhaust temperature, thus promising a considerable increase in energy efficiency.
- Using the desiccant wheel, process gains are increased, confirming experimentally, the results of previous studies (Atuonwu et al., 2011a; 2012b) which focused only on continuous systems without appreciable heat losses. The process gain increase is linked to the energy efficiency improvement.



### **Reducing drying energy consumption using adsorbents: reflections and outlook**

#### **10.1. Reducing drying energy consumption: a reflective look**

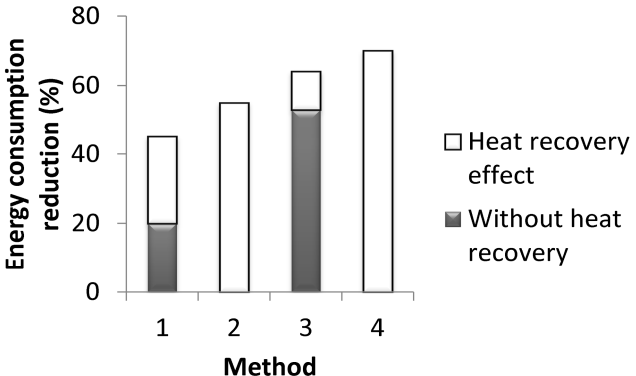
Reducing energy consumption in process systems remains an important research challenge in view of the continuous strain on the depleting energy resources and the associated cost and environmental implications. For any given energy source, a major way of reducing energy consumption in any process is to increase the degree of energy utilization or energy efficiency. For drying processes, removing 1kg of water from a product requires about 2500 kJ of energy assuming a 100% efficient system. Yet, for conventional dryers, energy efficiency is in the range of 20-60% which implies an energy requirement of about 4170 kJ corresponding to about 1.6 kg of steam to remove 1kg of water at the upper end of the range. Drying thus consumes a significant proportion of total industrial energy, and it remains a research challenge to improve the energy efficiency especially in drying heat-sensitive products at low temperatures for which energy efficiencies are characteristically low.

The use of desiccant dehumidification as an add-on to the convective dryer possesses the potential to improve energy efficiency of dryers as has been shown in recent studies. The objective of this thesis was to improve the energy efficiency of low-temperature convective dryers by more intelligent design and operation of the desiccant dehumidifier-assisted drying system. In so doing, the idea was to contribute to the advancement of Process Systems Engineering approaches in drying technology using advanced modeling, simultaneous heat integration, process sequence analysis for structural optimization, operational optimization, and controllability analysis.

The following questions formed the basis for the research:

1. How best should the adsorbent-based dehumidification dryer be operated energy-wise while drying at low temperatures?
2. What is the optimal energy recovery routing among process streams?
3. How can process and energy integration techniques be applied to optimize synergy among components in multi-pass or multi-stage systems?
4. What key adsorbent properties should guide selection in adsorbent dryers as far as energy efficiency is concerned?
5. How can such a system be controlled?
6. What are the disturbance rejection capabilities?
7. How can controllability be integrated within energy-efficient dryer design and how does the adsorbent system affect this?
8. Are there any practically-relevant theoretical insights from the developments?

Table 10.1. Summary of the major contributions of this thesis

<b>New application methods</b>	<ol style="list-style-type: none"> <li>Operational optimization of the desiccant adsorption drying process</li> <li>Simultaneous heat integration optimization by pinch location method</li> <li>MINLP superstructure optimization for multistage hybrid dryer design</li> <li>MINLP superstructure optimization with simultaneous heat integration</li> <li>Unified matrix modeling of drying, adsorption &amp; regeneration processes</li> </ol>															
<b>Improved insights</b>	<ol style="list-style-type: none"> <li>Deriving adsorbent physical properties that promote energy efficiency using superstructure optimization and active constraint analysis</li> <li>Deriving optimal adsorbent sequences in multistage adsorption dryers</li> <li>Establishing operating condition patterns that favour energy efficiency</li> <li>Identifying the need to change system operating conditions when retrofitting for heat recovery as previous optimal conditions become sub-optimal when heat recovery is introduced</li> <li>Establishing a link between dryer energy efficiency and controllability</li> <li>Reasonably accurate estimation of dryer energy efficiency from process gain-based temperature drops even when heat losses are significant unlike when temperature measurements are directly used</li> <li>Showing the feed-forward effects of the dehumidifier on air-side disturbances and the encouraging mechanisms for such effects</li> <li>Showing additional promising input-output pairings for adsorption dryers</li> <li>Increased dryer gain matrix due to desiccant system and explanation by the reinforcing effects of dehumidification and sorption heat release</li> <li>Establishing by condition number analyses that vitamin C or other thermo-degradable quality be controlled rather than temperature in addition to product moisture in SISO systems</li> <li>Deriving an index of merit for desiccant dehumidifiers that qualifies their suitability or otherwise in improving the energy efficiency of a dryer</li> </ol>															
<b>Reducing energy consumption</b>	<p>Base case: conventional convective dryer. Methods 1, 2, 3 and 4 on the bar chart are designated on the first row of this table</p>  <table border="1"> <caption>Data from Energy consumption reduction bar chart</caption> <thead> <tr> <th>Method</th> <th>Without heat recovery (%)</th> <th>With heat recovery (%)</th> </tr> </thead> <tbody> <tr> <td>1</td> <td>~20</td> <td>~45</td> </tr> <tr> <td>2</td> <td>0</td> <td>~55</td> </tr> <tr> <td>3</td> <td>~50</td> <td>~65</td> </tr> <tr> <td>4</td> <td>0</td> <td>~70</td> </tr> </tbody> </table>	Method	Without heat recovery (%)	With heat recovery (%)	1	~20	~45	2	0	~55	3	~50	~65	4	0	~70
Method	Without heat recovery (%)	With heat recovery (%)														
1	~20	~45														
2	0	~55														
3	~50	~65														
4	0	~70														
<b>System design and experiments</b>	<ol style="list-style-type: none"> <li>Design of a dehumidifier dryer with rechargeable desiccant wheel</li> <li>Design of PI control system for the zeolite wheel assisted dryer</li> <li>Design of experiment to prove gain-efficiency relations and adsorbent effects</li> </ol>															

In proffering solutions to the issues, the work presented in Chapters 2 – 9 was done and the major contributions are discussed next.

## **10.2. Major contributions of the present study**

The major contributions of this work are broadly categorized in four themes as shown in Table 10.1. The first is the extension of the application domains of some Process Systems Engineering approaches into drying technology to improve energy performance. The second deals with the generation of more insights on issues relating to dryer energy performance and controllability. The third, and perhaps most important contribution is the energy efficiency improvement recorded while the fourth is concerned with the development of a rechargeable desiccant wheel-assisted drying system with associated proportional-integral (PI) control schemes and subsequent design of experiments to prove some earlier-developed concepts.

The application domain of Process Systems Engineering approaches like simultaneous pinch location, mixed integer nonlinear programming (MINLP) among others, have been extended to drying technology, specifically, drying based on adsorbent dehumidification. New modeling and optimization schemes have been developed and applied in this regard leading to some practically-relevant theoretical developments that give insights on how operations can be improved.

In terms of insights gained, the physical properties of adsorbents that promote energy performance have been derived to include high sorption capacities, surface heterogeneity and desorption rate to adsorption rate constant ratios. In two-stage systems, the use of adsorbents with type 1 water vapour sorption isotherms in the first stage like zeolite and type 4 or 5 systems like silica gel in the second stage is most favourable energy-wise. Reasons for this include the matching of the capabilities of the adsorbents with the air-stream and operating conditions. The choices and operating conditions reveal heat requirement matching between the first and second stages. Adsorbents that require higher temperature regeneration are chosen in the first stage so the exhaust temperature is sufficient to regenerate the lower temperature requiring second-stage adsorbent. Thus, no utility energy is spent on regenerating the second-stage adsorbent. Also, there is vapour pressure and adsorption characteristics matching as adsorbents with a higher dehumidification capacity at lower humidity are chosen for ambient air dehumidification while those more effective at higher vapour pressures are chosen for exhaust air dehumidification. The adsorbent flowrate patterns show the first stage adsorbent system as being optimized for dehumidification while the second by virtue of its higher flow speed is optimized for heat recovery. It has also been shown by simultaneous optimization that changing system operating conditions is necessary when retrofitting drying systems for heat recovery as previously optimal conditions become sub-optimal when heat recovery is introduced.

Another insight provided by the work is the derivation of the existence of a relationship between the dryer process gain matrix on which controllability depends

and energy efficiency. From the gain matrix, the dryer temperature drop due to water vapour evaporation is decoupled from heat loss effects. As a result, energy efficiency can be estimated from process gains obtainable from step tests. Apart from providing information on controllability, the gain matrix thus provides another way of reliably calculating energy efficiency with and without significant heat losses. In contrast, the use of temperature drop measurements as is common in practice severely over-estimates energy efficiency. It has also been shown that for corresponding inputs, adsorption dryers have higher steady-state gains than equivalent conventional dryers due to the correlation between dehumidification, adsorption heat and the controlled variables. Dehumidification leads to sorption heat release so the combined effect drives the output moisture and temperature further than would be possible without it.

The adsorption dryer also shows improved resilience to ambient air disturbances due to adsorbent subsystem-induced self-regulation properties of which the encouraging mechanisms are adsorption heat, kinetic and equilibrium properties of the adsorbent. Due to the self-regulation, the sensitivity of energy performance to unfavourable disturbances is reduced compared to conventional dryers. Additional input possibilities for controlling the product moisture, temperature and vitamin C content are shown by controllability analysis. Apart from using air flowrate and temperatures as is the traditional way of controlling product moisture and temperature respectively in conventional dryers, other possibilities are shown promising as well. These include regeneration temperature-product moisture pairing and dryer inlet temperature-product outlet temperature pairing. Also, there is the use of air flowrate to control product moisture and wheel speed to control product temperature amongst other possibilities. By analyzing conventional and adsorption dryers using process condition numbers, a higher correlation between product moisture and temperature is observed than that between product moisture and vitamin C concentration. It has thus been proposed that on the availability of reliable soft sensors, instead of product temperature, vitamin C or some other temperature-dependent quality measure should be controlled in addition to product moisture in decentralized drying system control.

Another important insight from this work is the derivation of a new performance indicator for desiccant dehumidifiers. Known as the adsorber-regenerator net energy efficiency *ARNEE*, this indicator is better-suited to the specifics of the use of desiccant dehumidifiers in drying operations than pre-existing indicators which were mainly derived for HVAC systems. By mathematical analysis it has been shown that the desiccant is effective in improving energy performance only if the *ARNEE* is greater than the efficiency of the stand-alone dryer. The result is thus valuable in providing short-cut means of making decisions as to the wheel specifications required to improve the performance of existing convective dryers.

The most important contribution of this work is the energy efficiency improvements recorded as shown in the Figure inscribed in Table 10.1. Compared to the base case, a conventional single-stage convective dryer operating at the same drying temperature,

the operational optimization (method 1) of regeneration air inlet temperature and flowrate, drying air and adsorbent flow rates in a single-stage zeolite adsorption dryer reduces energy consumption by 20% without heat integration. After sensible and latent heat recovery from the regenerator exhausts, the energy consumption reduces overall by 45%. When heat integration is simultaneously considered an integral part of the system design (method 2), energy consumption reduces overall by 55%.

For a two-stage drying system without heat recovery designed by MINLP optimization (method 3), a system with zeolite in the first stage and silica gel in the second stage reduces energy consumption by 53% compared to the same base case. When heat recovery is introduced to the optimized system, the reduction becomes 64%. Compared to a two-stage conventional system at the same drying temperature, the reduction in energy consumption using this strategy is 59%. With simultaneous optimization of heat integration in a multistage system by modifying objective functions and adding extra constraints (method 4), the specific energy consumption reduces by 70% compared to the base case and 65% compared to an equivalent two-stage conventional dryer.

Finally, an experimental set-up incorporating an adsorbent (zeolite)-filled rotary wheel to a batch dryer has been designed with appropriate instrumentation and PI control scheme. The uniqueness of the system is two-fold. First is the relative ease with which the wheel can be detached to create a reference – the conventional dryer. In addition, the adsorbents can easily be changed for research purposes, in contrast to commercially available honeycomb rotor wheels. Using this system, some earlier developed concepts on the relationship between process gains and energy efficiency, effects of heat losses and impacts of adsorbent dehumidification on system performance have been experimentally validated.

### **10.3. General conclusions and challenges for future work**

The results of the work have demonstrated that the application of Process Systems Engineering approaches in drying technology leads to significant energy performance improvements. At the same time, other theoretical developments are achieved providing useful insights on how operations can be improved.

The following are recommendations for further investigation:

1. The extension of the methods presented here (like the MINLP-based superstructure optimization and pinch location-based simultaneous heat integration) to other drying objectives, for instance quality-related indices.
2. The application of the methods to classes of hybrid drying systems other than desiccant-assisted systems as hybrid drying is still an active research field.
3. The design and use of novel adsorbents such that the physical properties that promote energy performance are designed into the desiccant during the manufacturing process using appropriate chemical/biological pathways.

4. Exploration of multi-objective optimization as a tool for optimizing objectives like energy efficiency, controllability properties and product quality indicators.
5. Exergy analysis to explore further opportunities for process performance improvement.
6. The study of effects of ageing on system performance, and formulation of tools to guide decisions on when to replace adsorbents.
7. The dynamic optimization of intermittent drying operations using adsorbents.
8. The application of advanced control schemes such as Model Predictive Control MPC, fuzzy logic and neural networks in dehumidification drying processes. The use of MPC for instance would be advantageous from the point of view of fully exploiting the advantages of the extra degrees of freedom introduced by the adsorbent system since explicit input-output pairing is not required. Moreover, energy and quality-related aspects may be directly formulated in the objective functions and constraints.

With the prevailing trend of global population growth, occasioned by improved standards of living and knowledge availability, the demand for processed material and high quality consumer products is expected to rise. So also is the strain on the already depleting energy resources. Drying as an important operation in any processing system would still remain critical in the energy utilization chain. Although attention is gradually shifting from the use of fossil fuels to bio-based and other renewable sources, the demand for fossil fuels is also expected to rise. This situation no doubt has cost and environmental implications. Hence, energy efficiency research in general and for drying systems in particular will remain challenging. Novel designs particularly based on hybrid systems are expected to emerge.

Hand-in hand with these issues, developments in mathematical modeling, software engineering and computing power are expected going by the current trend. It is hoped that these developments will increasingly be applied in drying systems. This way, the symbiotic relationship that exists between the two-some as demonstrated in this thesis will be preserved and strengthened. The growth in mainstream Chemical Engineering through the incorporation of systems approaches to form what is now known as “Process Systems Engineering” is a testament to this fact. The process and energy performance improvements achievable by the incorporation of Process Systems approaches in drying technology would no doubt contribute positively to higher living standards and by extension, a better society.

## References

- Abdel-Jabbar, N.M., Jumah, R.Y., Ali, M.Q.A. (2005). State estimation and state feedback control for continuous fluidized bed dryers. *Journal of Food Engineering*, 70, 197-203.
- Alikhani, Z., Raghavan, G.S.V., Mujumdar, A.S. (1992). Adsorption drying of corn in zeolite granules using a rotary drum. *Drying Technology* 10(3), 783-797.
- Al-Mansour, H.E., Al-Busairi, B.H., Baker, C.G.J. (2011). Energy consumption of a pilot-scale spray dryer. *Drying Technology* 29(16), 1901-1910.
- An, F., Li, Z., Ye, J., Wu, Z., Dong, P. (2007). Thin layer drying of fermentation spent liquor using corn bran adsorbent. *Drying Technology* 28(10), 1193-1200.
- ASHRAE (1998). Standard 139-1998 Method of testing for rating desiccant dehumidifiers utilizing heat for the regeneration process. Atlanta, ASHRAE.
- Åström, K.J., Hägglund, T. (2006). *Advanced PID Control*. ISA-Instrumentation, Systems and Automation Society, Research Triangle Park, NC27709.
- Atkins, M.J., Walmsley, M.R.W., Neale, J.R. (2010). Integration potential of milk powder plants using conventional heat recovery options. *Chemical Engineering Transactions* 21, 997-1002.
- Atuonwu, J.C., Straten, G. van., Deventer, H.C. van., Boxtel, A.J.B. van. (2010). Modeling and energy efficiency optimization of a low temperature adsorption based food dryer. In *Proceedings of the International Drying Symposium*, Magdeburg, Germany, October 3 – 6, 2010, 423-431.
- Atuonwu, J.C., Straten, G. van., Deventer, H.C. van., Boxtel, A.J.B. van. (2011a). Model-based energy efficiency optimization of a low temperature adsorption dryer. *Chemical Engineering and Technology*, 34, 1723-1732.
- Atuonwu, J.C., Straten, G. van., Deventer, H.C. van., Boxtel, A.J.B. van. (2011b). Improving adsorption dryer energy efficiency by simultaneous optimization and heat integration. *Drying Technology*, 29, 1459-1471.
- Atuonwu, J.C., Jin, X., Straten, G. van., Deventer, H.C. van., Boxtel, A.J.B. van. (2011c). Reducing energy consumption in food drying: opportunities in desiccant adsorption and other dehumidification strategies. *Procedia Food Science*, 1, 1799-1805.
- Atuonwu, J.C., van Straten, G., van Deventer, H. C., van Boxtel, A.J.B. (2012a). A mixed integer formulation for multistage adsorption dryer design. *Drying Technology* 30, 873-883.
- Atuonwu, J.C., van Straten, G., van Deventer, H. C., van Boxtel, A.J.B. (2012b). On the controllability and energy performance sensitivity of heat-integrated desiccant adsorption dryers. *Chemical Engineering Science* 30, 134-147.
- Atuonwu, J.C., Straten, G. van., Deventer, H.C. van., Boxtel, A.J.B. van (2012c). Improving dryer controllability and energy efficiency, *Proceedings, European Symposium on Computer-Aided Process Engineering*, London, UK, 847-851.
- Baker, C.G.J. (2005). Energy efficient dryer operation — an update on developments. *Drying Technology* 23(9), 2071-2087.

- Baker, C.G.J., McKenzie, K.A. (2005). Energy consumption of industrial spray dryers. *Drying Technology* 23(1-2), 365-386.
- Baliban, R.C., Elia, J.A., Floudas, C.A. (2011). Optimization framework for the simultaneous process synthesis, heat and power integration of a thermo-chemical hybrid biomass coal and natural gas facility. *Computers and Chemical Engineering* 35(9), 1647-1690.
- Beccali, M., Butera, F., Guanella, R., Adhikari, R.S. (2003). Simplified models for the performance evaluation of desiccant wheel dehumidification. *International Journal of Energy Research*, 27(1), 17-29.
- Berghel, J., Renström, R. (2004). Controllability of product moisture content when non-screened sawdust is dried in a spouted bed. *Drying Technology*, 22, 507-519.
- Bristol, E. H. (1966). On a new measure of interaction for multivariable process control. *IEEE Transactions on Automatic Control* AC-11, 133-134.
- Boxtel, A.J.B. van., Boon, M.A., Deventer, H.C. van., Bussmann, P.J. (2012). Zeolites for reducing drying energy usage. In: E. Tsotsas, A.S. Mujumdar (eds.) *Modern Drying Technology Vol. 4: Energy Savings*, pp. 163-198., Wiley VCH, Weinheim, Germany.
- Brunauer, S., Deming, L., Deming, W., Teller, E. (1940). On the Theory of the van der Waals Adsorption of Gases. *Journal of the American Chemical Society*.
- Carrington, C.G., Sun, Z.F., Bannister, P. (2000). Dehumidifier batch drying – effect of heat losses and air leakage. *International Journal of Energy Research* 24, 205-214.
- Cao, Y., Rossiter, D. (1997). An input pre-screening technique for control structure selection. *Computers and Chemical Engineering* 21, 563-569.
- Chakraborty, R., Mukhopadhyay, P., Bera, M., Suman, S. (2011). Infra-red-assisted freeze drying of tiger prawn: parameter optimization and quality assessment. *Drying Technology* 29, 508-519.
- Chang, J., Yu, C. (1992). Relative disturbance gain array. *AIChE Journal* 38, 521-534.
- Chi, C.W., Wasan, D. (1970). Fixed bed adsorption drying. *AIChE Journal* 16,23-31
- Chou, S.K., Chua, K.J. (2001). New hybrid drying technologies for heat sensitive products. *Trends in Food Science and Technology* 12, 359-369.
- Chung, J.D., Lee, D.Y. (2009). Effect of desiccant isotherm on the performance of desiccant wheel. *International Journal of Refrigeration* 32, 720-726.
- Chung, J.D., Lee, D.Y., Yoon, S.M. (2009). Optimization of desiccant wheel speed and area ratio of regeneration to dehumidification as a function of regeneration temperature. *Solar Energy* 83, 625-635.
- Clements, S., Wilkins, M., Beyzh, M. (2012). Airline carbon costs take off as EU emissions regulations reach for the skies. *Standard and Poor's Global Credit*. <http://www.environmentalfinance.com/download.php?files/pdf/4d663c478efb8/Airline%20Carbon%20Costs%20take%20Off.pdf>, Accessed 5/3/2012.
- Dandamrongrak, R., Mason, R., Yong, G. (2003). The effect of pretreatments on the drying rate and quality of dried bananas. *International Journal of Food Science and Technology* 38, 877-882.



- De Antonellis, S., Joppolo, C.M., Molinaroli, L. (2010). Simulation, performance analysis and optimization of desiccant wheels. *Energy and Buildings* 42, 1386-1393.
- De Antonellis, S., Joppolo, C.M., Molinaroli, L., Pasini, A. (2011). Simulation and energy efficiency analysis of desiccant wheel systems for drying processes. *Energy* 37(1), 336-345.
- Deventer, H.C. van., Heijmans, R.M.H. (2001). Drying with superheated steam. *Drying Technology* 19(8), 2033-2045.
- Djaeni, M., Bartels, P.V., Sanders, J.P.M., Straten, G. van., Boxtel, A.J.B. van. (2007a). Multistage zeolite drying for energy efficient drying. *Drying Technology* 25 (6), 1053-1067.
- Djaeni, M., Bartels, P.V., Sanders, J.P.M., Straten, G. van., Boxtel, A.J.B. van. (2007b). Process integration for food drying with air dehumidified by zeolites. *Drying Technology* 25(1), 225-239.
- Djaeni, M., Bartels, P.V., Asselt, C.J. van., Sanders, J.P.M., Straten, G. Van., Boxtel, A.J.B. van. Assessment of a two-stage zeolite dryer for energy efficient drying. *Drying Technology* 2009, 27, 1205-1212.
- Djaeni, M., Bartels, P.V., Sanders, J.P.M., van Straten, G., van Boxtel, A.J.B. (2008). Computational fluid dynamics for multistage adsorption dryer design. *Drying Technology*, 26(4), 487-502.
- Djaeni, M., Straten, G. van., Bartels, P.V., Sanders, J.P.M., Boxtel, A.J.B. van. (2009a). Energy efficiency of multistage adsorption drying for low-temperature drying. *Drying Technology* 27(4), 555-564.
- Djaeni, M., Bartels, P., Sanders, J., Straten, G. van., Boxtel, A.J.B. van. (2009b). Energy efficient multistage zeolite drying for heat-sensitive products. PhD Thesis, Wageningen University, the Netherlands.
- Dobruskin, V. Kh. (1998). Micropore volume filling. A condensation approximation approach as a foundation to the Dubinin–Astakhov equation. *Langmuir* 14 (14), 3840–3846.
- Dong, H.C., Lin, C.Y., Chang, C.T. (2008). Simultaneous optimization approach for integrated water allocation and heat exchange networks. *Chemical Engineering Science* 63(14), 3664-3678.
- Duan X., Zhang M., Mujumdar A.S., Wang R. (2010). Trends in microwave-assisted freeze drying of foods. *Drying Technology* 28, 444-453.
- Dufour, P. (2006). Control engineering in drying technology: review and trends. *Drying Technology* 24, 889-904.
- Doymaz, I. (2007). The kinetics of forced convective air-drying of pumpkin slices. *Journal of Food Engineering* 79, 243-248.
- Duran, M.A, Grossmann, I.E. (1986). Simultaneous optimization and heat integration of chemical processes. *AIChE Journal* 32(1), 123-138.
- Eicker, U., Schürger, U., Köhler, M., Ge, T., Dai, Y., Li, H., Wang, R. (2012). Experimental investigations on desiccant wheels. *Applied Thermal Engineering* 42, 71-80.

- Engell, S., Triewiler, J.O. Völker, M., Pegel, S. (2004). Tools and indices for dynamic I/O-controllability assessment and control structure selection, in: Seferlis, P., Georgiadis, M.C. (Eds.), *The Integration of Process Design and Control*. Elsevier, Amsterdam, pp. 430-463.
- Ertas, A., Azizul, H.A.K.M., Kiris, I. (1997). Low temperature peanut drying using liquid desiccant system climatic conditions. *Drying Technology* 15, 1045-1060.
- Europe's Energy Portal: Natural Gas Industry – End-user energy prices for industrial consumers. Accessed from <http://www.energy.eu/#Industrial-Gas> on 3/3/2012.
- Ferreira, D., Magalhaes, R., Taveira, P., Mendes, A. (2011). Effective adsorption equilibrium isotherms and breakthroughs of water vapor and carbon dioxide on different adsorbents. *Industrial and Engineering Chemical Research* 50, 10201-10210.
- Francesconi, J.A., Oliva, D.G, Mussati, M.C., Aguirre, P.A. (2009). Simultaneous flowsheet optimization and heat integration of a bioethanol processor for PEM fuel cell system. *Computer Aided Chemical Engineering* 27(C) 1791-1796.
- Getty, R.J., Armstrong, W.P. (1964). Drying air with activated alumina under adiabatic conditions. *Industrial and Engineering Chemistry Process Design and Development* 3 (1) , pp. 60-65.
- Gong, Z, Stanovský, Mujumdar, A.S. (2011). Energy audit of a fibreboard production line using simprosys software. *Drying Technology* 29, 408-418.
- Grabowski, S., Marcotte, M., Poirier, M., Kudra, T. (2002). Drying characteristics of osmotically pretreated cranberries – energy and quality aspects. *Drying Technology* 20(10), 1989-2004.
- Harshe, Y.M., Utikar, D.P., Ranade, V.V., Deepak, P. (2005). Modeling of rotary desiccant wheels. *Chemical Engineering and Technology* 28(12), 1473-1479.
- Hauer, A, Fischer, F. (2011). Open adsorption system for energy efficient dish washer. *Chemie Ingenieur Technik* 83(1-2), 61-66.
- Hodali, R., Bougard, J. (2001). Integration of a desiccant unit in crops solar drying installation: Optimization by numerical simulation. *Energy Conversion and Management* 42(13), 1543-1558.
- Holmström, K., Göran, A.O., Edvall, M.M. (2009). User's guide for TOMLAB/KNITRO V6. TOMLAB Optimization, Seattle, WA.
- Horvath, M., Mizsey, P. (2009). Decomposability of the control structure design problem of recycle systems. *Industrial Engineering Chemistry Research* 48, 6339-6345.
- Hovd, M., Skogestad, S. (1992). Simple frequency dependent tools for control system analysis, structure selection and design. *Automatica*, 28, 989-996.
- Islam, M.R., Ho., J.C., Mujumdar, A.S. (2003). Convective drying with time-varying heat input: Simulation results. *Drying Technology* 21(7), 1333-1356.
- Jia, X., Clements, S., Jolly, P. (1993). Study of heat pump assisted microwave drying. *Drying Technology* 11(7), 1583-1616.
- Jin, X., Sman, R.G.M. van der., Boxtel, A.J.B. van. (2011). Evaluation of the free volume theory to predict moisture transport and quality changes during broccoli drying. *Drying Technology* 29(16), 1963-1971.

- Kaiser, S., Antonijevic, D., Tsotsas, E. (2002). Formation of fouling layers on a heat exchanger element exposed to warm, humid and solid loaded air streams. *Experimental Thermal and Fluid Science* 26, 291-297.
- Kemp, I.C. (2005). Reducing dryer energy use by process integration and pinch analysis, *Drying Technology* 23(9), 2089-2104.
- Kemp, I.C., Fyhr, B.C., Laurent, S., Roques, M.A., Groenwold, C.E., Tsotsas, E., Sareno, A.A., Bonazzi, C.B., Bimbenet, J. Kind, M. (2001). Methods for processing experimental drying kinetics data. *Drying Technology* 19(1), 15-34.
- Kiranoudis, C.T., Maroulis, Z.B., Marinos-Kouris, D. (1995). Design and production planning for multiproduct dehydration plants. *Computers and Chemical Engineering* 5, 581-606.
- Kiranoudis, C.T., Maroulis, Z.B., Marinos-Kouris, D., Tsamparlis, M. (1997). Design of tray dryers for food dehydration. *Journal of Food Engineering* 32(3), 269-291.
- Kiranoudis, C.T. (1998). Design of batch grape dryers. *Drying Technology* 16(1-2), 141-162.
- Knaebel, K.S. Adsorbent selection. Accessed on 6/8/2011 from <http://www.adsorption.com/publications/AdsorbentSel1B.pdf>
- Kodama, A., Hirayama, T., Goto, M., Hirose, T., Critoph, R.E. (2001). The use of psychrometric charts for the optimization of a thermal swing desiccant wheel. *Applied Thermal Engineering* 21, 1657-1674.
- Kritsula, P.M. (1969). Automatic air drying units without heaters. *Coke Chemistry (USSR)* (11) 46-48.
- Krokida, M.K., Karathanos, Z., Maroulis, B. and Marinos-Kouris, D. (2003). Drying kinetics of some vegetables. *Journal of Food Engineering* 2003, 59(4), 391-403.
- Krokida, M.K., Bisharat, G.I. (2004). Heat recovery from dryer exhaust air. *Drying Technology* 22(7), 1661-1674.
- Kudra, T. (2004). Energy aspects in drying. *Drying Technology* 22(5), 917-932.
- Kudra, T., Mujumdar, A.S. *Advanced Drying Technologies*, 2nd Ed CRC Press: Boca Raton, FL, 2009.
- Kudra, T. (2012). Energy performance of convective dryers. *Drying Technology*, 30(11-12), 1190-1198.
- Kumar, A., Daoutidis, P. (2002). Nonlinear dynamics and control of process systems with recycle. *Journal of Process Control* 12, 475-484.
- La, D., Dai, Y.J., Li, Y., Wang, R.Z., Ge, T.E. (2010). Technical development of rotary desiccant dehumidification and air conditioning: a Review. *Renewable and Sustainable Energy Reviews* 14(1), 130-147.
- Laurijssen, J., De Gram, F.J., Worrell, E., Faaij, A. (2010). Optimizing the energy efficiency of conventional multi-cylinder dryers in the paper industry. *Energy* 35, 3738-3750.
- Lazzarin, R.M., Longo, G.A., Piccininni, F. (1992). Sorption dehumidification and heat recovery: Applications in industrial processes. *Heat Recovery Systems and CHP*, 12(5), 397-405.
- Langrish, T.A.G. (1998). The controllability assessment of flowsheeting options involving parallel-flow dryers. *Chemical Engineering Journal* 70(3), 221-229.

- Langrish, T.A.G., Harvey, A.C. (2000). A flowsheet model of a well-mixed fluidized bed dryer: applications in controllability assessment and optimization. *Drying Technology* 18, 185-198.
- Li, Z., Kobayashi, N., Watanabe, F., Hasatani, M. (2002). Sorption drying of soya bean seeds with silica gel. *Drying Technology* 20(1), 223-233.
- Likos, W.J., Lu, N. (2002). Water vapor sorption behavior of smectite-kaolinite mixtures. *Clay and Clay Materials*, 50(5), 553-561.
- Lowell, S., Shields, J. (1991). Powder surface area and porosity, 3<sup>rd</sup> ed., Chapman and Hall, London.
- Luz, G.R., Conceição, W.A.D., Jorge, L. M. M., Paraiso, P.R. Andrade, C.M.G. (2010). Dynamic modeling and control of soyabean meal drying in a direct rotary dryer. *Food and Bioproducts Processing* 88, 90-98.
- Madhiyanon, T., Adirekrut, S., Sathitruangsak, P., Soponronnarit, S. (2007). Integration of a rotary desiccant wheel into a hot-air drying system: Drying performance and product quality studies. *Chemical Engineering and Processing* 46, 282-290.
- Marfil, P.H.M., Santos, E.M., Telis V.R.N. (2008). Ascorbic acid degradation kinetics in tomatoes at different drying conditions. *LWT – Food Science and Technology* 41, 1642-1647.
- MarketResearch.com. (2012). Global dried food market to 2014. Accessed 29/6/ 2012 from <http://www.marketresearch.com/Datamonitor-v72/Global-Dried-Food-2892111/>.
- Menshutina, N.V., Gordienko, M. G., Voynovskiy, A. A., Kudra, T. (2004). Dynamic analysis of drying energy consumption. *Drying Technology* 22(10), 2281 – 2290.
- Milner, W.M. (1979). Surface drying fresh citrus with dehumidified air. Paper, American Society of Agricultural Engineers.
- Milner, W.M. (1983). Energy storage via desiccants for food/agricultural applications. *Energy in Agriculture* 2 (C), 341-354.
- Mishkin, M., Saguy I., Karel M. (1983). Minimizing ascorbic acid loss during air drying with a constraint on enzyme inactivation for a hypothetical foodstuff. *Journal of Food Processing and Preservation* 7, 193-210.
- Moore, J.D., Serbezov, A. (2005). Correlation of adsorption equilibrium data for water vapour on F-200 activated alumina. *Adsorption* 11, 65-75.
- Moraitis, C.S., Akiritidis, C.B. (1997). Energy saving in industrial drying plants by partial recovery of the latent heat of the exhaust air. *Drying Technology* 15(6-8), 1931-1940.
- Morari, M., Grimm, W., Oglesby, M.J., Prosser, I.D. (1985). Design of resilient processing plants-VII. Design of energy management system for unstable reactors-new insights, *Chemical Engineering Science* 40, 2, 187-198.
- Mujumdar, A.S. (1997). *Drying Fundamentals*. In: Baker, C.G.J. (ed.), *Industrial Drying of Foods*, 1<sup>st</sup> ed., Chapman and Hall, London.
- Mujumdar, A.S. (2004a). Research and development in drying: Recent trends and future prospects., *Drying Technology* 22(1-2), 1-26.

- Mujumdar, A.S. (2004b). Guide to industrial drying principles, equipment and new developments, in: International Workshop and Symposium on Industrial Drying, Mumbai, India.
- Mujumdar, A.S. (2007a). Principles, classification and selection of dryers. In: Mujumdar, A.S. (ed.), Handbook of Industrial Drying, 3rd ed., Taylor and Francis.
- Mujumdar, A.S. (2007b). An overview of innovation in industrial drying: current status and R and D needs. *Transp. Porous Med.* 66, 3-18.
- Nagaya, K., Li, Y., Jin, Z., Fukumuro, M., Ando, Y., Akaishi, A. (2006). Low temperature desiccant based food drying system with airflow and temperature control. *J. Food Engineering*, 75, 71-77.
- Namsanguan, Y., Tia, W., Devahastin, S., Soponronnarit, S. (2004). Drying kinetics and quality of shrimp undergoing different two-stage drying processes. *Drying Technology* 22(4), 759-778.
- Nastaj, J., Ambrozek, B. (2009). Modeling of drying of gases using solid desiccants. *Drying Technology* 27(12), 1344-1352.
- Niederlinski, A. (1971). A heuristic approach to the design of multivariable systems. *Automatica* 7, 691-701.
- Ogura, H., Mujumdar, A.S. (2000). Proposal for a novel chemical heat pump dryer. *Drying Technology* 18(4 and 5), 1033-1053.
- Ogura, H., Ishida, H., Kage, H., Mujumdar, A.S. (2003). Enhancement of energy efficiency of a chemical heat pump-assisted convective dryer. *Drying Technology* 21(2), 279-292.
- Ogura, H., Yamamoto, T., Otsubo, Y., Ishida, H., Mujumdar, A.S. (2005). A control strategy for a chemical heat pump dryer. *Drying Technology* 23, 1189-1203.
- Ortega, M.G., Castano, F., Vargas, M., Rubio, F.R. (2007). Multivariable robust control of a rotary dryer: analysis and design. *Control Engineering Practice* 15, 487-500.
- Osorio-Revilla, G., Gallardo-Velazquez, T., Lopes-Cortes, S., Arellano-Cardenas, S. (2006). Immersion drying of wheat using AL-PILC, zeolite, clay and sand as particulate media. *Drying Technology* 24, 1033-1038.
- Park, I., Knaebel, K.S. (1992). Adsorption breakthrough behavior: unusual effects and possible causes. *AIChE Journal* 38(6), 660-670.
- Papalexandri, K.P., Pistikopoulos, E.N. (1998). A decomposition-based approach for process optimization and simultaneous heat integration: application to an industrial process. *Transactions IChemE* 76(A), 273-286.
- Patel, J., Uygun, K., Huang, Y. (2008). A path constrained method for integration of process design and control. *Computers and Chemical Engineering* 32, 1373-1384.
- Perkins, J.D. and Walsh, S.P.K. (1996). Optimization as a tool for design/control integration. *Computers and Chemical Engineering* 20(4), 315-323.
- Phongpipatpong, M., Douglas, P.L. (2003). Synthesis of rice processing plants, II: MINLP Optimization, *Drying Technology* 21(9), 1611-1629.

- Pinaga, F., Carbonell, J.V., Pena, J.L., Miquel, J.J. (1984). Experimental simulation of solar drying of garlic using an adsorbent energy storage bed. *Journal of Food Engineering* 3(3), 187-203.
- Plachenov, T.G. (1965). New trends in sorption technique: Report at the general meeting of the Department of General and Technical Chemistry, Academy of Sciences, USSR., *Bulletin of the Academy of Sciences, USSR Division of Chemical Science* 14(6), 939-944.
- Puschner, H. (1964). *Wärme durch Mikrowellen* (in German). Philips Tech Bibl., Eindhoven.
- Raghavan, G.S.V., Rennie, F.J., Sunjka, P.S., Orsat, V., Phaphuangwittayakul, W., Terdtoon, P. (2005). Overview of new technologies for drying biological materials with emphasis on energy aspects. *Brazilian Journal of Chemical Engineering* 22(2), 195-201.
- Rahman, S.M.A., Mujumdar, A.S. (2008). A novel atmospheric freeze drying system using a vibrio-fluidized bed with adsorbent. *Drying Technology* 26(4), 393-403.
- Ratti, C., Crapiste, G.H. (1995). Determination of heat transfer coefficient during drying of foodstuffs. *Journal of Food Process Engineering* 18, 41-53.
- Ratti C. (2001). Hot air and freeze-drying of high-value foods: a review., *Journal of Food Engineering* 49, 311-319.
- Reay, D. (1984). Energy surveys: Case study of a fluid bed dryer, *Uniquist Continuing Education Symposium: Industrial Drying Operations* 6.1 – 6.13, University of Queensland.
- Ricardez-Sandoval, L.A., Budman, H.M., Douglas, P.L. (2009). Integration of design and control for chemical processes: a review of the literature and some recent results. *Annual Reviews in Control* 33, 158-171.
- Robinson, J.W. (1992). Improve dryer control. *Chemical Engineering Progress* 28-33.
- Roubinet, M. (1969). Dehumidification of air through solid adsorbents., *Review Pratique du Froid* 22 (274), 19-25.
- Salagnac, P., Dutournie, P., Glouannec, P. (2008). Optimal operating conditions of microwave-convective drying of a porous medium. *Industrial and Engineering Chemistry Research* 47, 133-144.
- Sander, A., Kardum, J.P. (2009). Experimental validation of thin-layer drying models. *Chemical Engineering and Technology* 32(4), 590-599.
- Seyhan, F.G., Evranuz, Ö. (2000). Low temperature mushroom (*A bisporus*) drying with desiccant dehumidifiers. *Drying Technology* 18(1-2), 433-445.
- Simo, M., Sivashanmugam, S., Brown, C.J., Hlavacek, V. (2009). Adsorption/desorption of water and ethanol on 3A zeolite in near-adiabatic fixed bed. *Industrial and Engineering Chemistry Research* 48, 9247-9260.
- Sivill, L., Ahtilla, P. (2009). Energy efficiency improvement of dryer section heat recovery systems in paper machines – A case study. *Applied Thermal Engineering* 29(17-18), 3663-3668.
- Skogestad, S., Morari, M. (1987). Effect of disturbance directions on closed-loop performance. *Industrial Engineering Chemistry Research* 26 2029-2035.

- Skogestad, S. (1996). A procedure for SISO controllability analysis-with application to design of PH neutralization processes. *Computers and Chemical Engineering* 20, 373-386.
- Spets, J., Ahtila, P. (2004). Reduction of organic emissions by using a multistage drying system for wood-based biomasses, *Drying Technology* 22(3), 541-561.
- Stoeckli, F. (1998). Recent developments in Dubinin's theory. *Carbon* 36(4), 363-368.
- Straten, G. van., Boxtel, A.J.B. van. (1996). Progress in process operation by goal oriented advanced control. *Annual Reviews in Control* 20, 209-223.
- Strumillo, C., Jones, P.L., Zylla, R. (1995). Energy aspects in drying. In *Handbook of Industrial Drying*, 2nd Ed, Mujumdar, A.S., Eds., Marcel Dekker, New York.
- Strumillo, C., Zbicinski, I., Liu, X.D.. (1995). Thermal drying of biomaterials with porous carriers. *Drying Technology* 13(5-7), 1447-1462.
- Tadayyon, A., Hill, G.A., Ingledew, W.M., Sokhasanj, S. (1997). Contact-sorption drying of penicillium bilaii in a fluidized bed dryer. *Journal of Chemical Technology and Biotechnology* 68(3), 277-282.
- Tahat, M.A., Babus, R.F., O'Callaghan, P.W., Probert, S.D. (1995). Performance of an integrated thermochemical heat pump/energy store. *Thermochimica Acta* 255, 39-47.
- Thibodeaux L.J. (1996). *Environmental Chemodynamics: Movement of chemicals in air, water and soil*, 2<sup>nd</sup> ed.; John Wiley and Sons, NY.
- Thoruwa, T.F.N., Johnstone, C.M., Grant, A.D., Smith, J.E. (2000). Novel low-cost CaCl<sub>2</sub> based desiccants for solar crop drying applications. *Renewable Energy* 19(4), 513-520.
- Tippayawong, N., Tantakitti, C., Thavornun, S. (2008). Energy efficiency improvements in longan drying practice. *Energy* 33(7), 1137-1143.
- Tirawanichakul, S., Tirawanichakul, Y., Sniso, E. (2008). Paddy dehydration by adsorption: Thermo-physical properties and diffusion model of agricultural residues. *Biosystems Engineering* 99(2), 249-255.
- Tival, H.L. (1927). U.S. Patent No. 1,630,985.
- Trelea, I.C., Tystram, G., Courtois, F. (1997). Optimal constrained nonlinear control of batch processes: application to corn drying. *Journal of Food Engineering* 31, 403-421.
- Tutova, E.G., Fel'dman, R. I. (1976). Influence of contact mass exchange on the process of dehydration in a vacuum. *Journal of Engineering Physics* 30, 702-705.
- Ülku, S., Caakicoglu, F. (1991). Energy recovery in drying applications. *Renewable Energy* 1(5-6), 695-698.
- Vineyard, E.A., Sand, J.R., Durfee, D.J. (2000). Parametric analysis of variables that affect the performance of a desiccant dehumidification system. *ASHRAE Transactions* 106, 87-94.
- Vreuls, H.H.J., Zijlema, P.J. (2009). The Netherlands: list of fuels and standard CO<sub>2</sub> emission factors. SenterNovem report to the Ministry of VROM (Spatial Planning, Housing and the Environment, Utrecht, the Netherlands).

- Wachiraphansakul, S., Dehavastin, S. (2007). Drying kinetics and quality of okara dried in a jet spouted bed of sorbent particles. *LWT – Food science and Technology*, 40(2), 207-219.
- Wang, W.C., Calay, R.K., Chen, Y. (2011). Experimental study of an energy efficient hybrid system for surface drying. *Applied Thermal Engineering* 31, 425-431.
- Wang, H.G., Senior, P.R. Mann, R., Yang, W.Q. (2009). Online measurement and control of solids moisture content in fluidized bed dryers. *Chemical Engineering Science*, 64, 2893-2902.
- Watts, K.C., Bilanski, W.K., Menzies, D.R. (1987). Simulation of adsorption drying of corn, wheat, barley and oats using sodium bentonites. *Canadian Agricultural Engineering* 29(2), 173-178.
- Witnantakit, K., Prachayawarakorn, S., Nathakaranakule, A., Soponronnarit, S. (2006). Paddy drying using adsorption technique: Experiments and simulation. *Drying Technology* 24(5), 609-617.
- Witnantakit, K., Prachayawarakorn, S., Nathakaranakule, A., Soponronnarit, S. (2009). Multipass sorption drying of paddy using rice husk adsorbent. *Drying Technology* 27(2), 226-236.
- Yang, X., Xu, W., Ding, J., Zhao, Y. (2005). Theoretical and experimental studies on low temperature adsorption drying of ginger. *Journal of Thermal Science* 15(1), 71-78.
- Ye, J., Luo, Q., Li, X., Xu, Q., Li, Z. (2008). Sorption drying of soybean seeds with silica gel in a fluidized bed dryer. *International Journal of Food Engineering* 4, 3
- Yeomans, H., Grossmann, I.E. (1999). A systematic modeling framework of superstructure optimization in process synthesis. *Computers and Chemical Engineering* 23, 709-735.
- Yiqing, L., Xigang, Y., Fenglian, D. (2010). Synthesis and heat integration of thermally coupled complex distillation system. *International Journal of Energy Research* 34, 626-634.
- Younes, A., Wongrat, W., Elkamel, A., Douglas, P.L., Lohi, A. (2010). Generalized disjunctive programming for synthesis of rice drying processes. *Industrial and Engineering Chemistry Research* 49, 2312-2325.
- Yuan, Z., Chen, B., Zhao, J. (2011). An overview on controllability analysis of chemical processes. *AIChE Journal* 57, 1185-1201.
- Yuan, Z., Chen, B., Sin, G., Gani, R. (2012). State of the art and progress in optimization-based simultaneous design and control for chemical processes. *AIChE Journal* 58(6), 1640-1659.
- Zhai, C. (2008). Performance modeling of desiccant wheel design and operation. PhD Thesis, Carnegie Mellon University.
- Zhang, L., Niu, J.L. (2002). Performance comparisons of desiccant wheels for air dehumidification and enthalpy recovery. *Applied Thermal Engineering* 22, 1347-1367.



## Nomenclature

$A$	Heat exchange area	$(\text{m}^2)$
$b$	Langmuir sorption constant	$(-)$
$C_p$	Specific heat capacity	$\text{Jkg}^{-1}\text{K}^{-1}$
$E$	Kinetic parameters	$\text{JKmol}^{-1}$
$\Delta H_v$	Latent heat of vaporization	$\text{Jkg}^{-1}$
$F$	Mass flowrate	$\text{kgs}^{-1}$
$f$	Recycle fraction	$(-)$
$g$	Acceleration due to gravity	$\text{ms}^{-2}$
$h$	Volume heat transfer coefficient	$\text{Wm}^{-3}\text{K}^{-1}$
$k$	Drying rate constant	$\text{s}^{-1}$
$M$	Number of adsorbents	$(-)$
$\mu$	Kinetic friction coefficient	$(-)$
$m$	Mass of desiccant wheel	$\text{kg}$
$M_{ax}$	Mass hold-up air on heat exchanger cold side	$\text{kg}$
$M_{ay}$	Mass hold-up air on heat exchanger hot side	$\text{kg}$
$N$	Number of drying stages	$(-)$
$N_p$	Vitamin C concentration	$(\% \text{ of inlet value})$
$N_K$	Number of cold streams	$(-)$
$N_L$	Number of hot streams	$(-)$
$n$	Wheel speed	$\text{rpm}$
$P$	Pressure	$\text{Pa}$
$r$ (Chapter 7)	Wheel radius	$\text{m}$
$r_1$	Adsorbent/drying air flow	$\text{kgkg}^{-1}$
$r_2$	Regeneration air/adsorbent flow	$\text{kgkg}^{-1}$
$RH$	Relative humidity	$(-)$
$\rho$	Density	$\text{kgm}^{-3}$
$s$	Regeneration air to adsorbent flow ratio	$\text{kgkg}^{-1}$
$T$	Temperature	$\text{K}$

$T_Q$	Load torque of wheel	Nm
$U$	Heat exchanger coefficient	$W^2K^{-1}$
$V$	Volume hold up	m <sup>3</sup>
$v$	Flow configuration choice	(-)
$W$	Heat exchanger existence	(-)
$X$	Moisture content	kgkg-1 db
$X_{zmax}$	Adsorbent capacity	kgkg-1 db
$Y$	Absolute humidity	kgkg-1 db
$y$	Adsorbent choice discrete variable	(-)
$Z$	Recycle existence	(-)

Bold symbols refer to vectors given in equations 2.3-2.17 & 2.22-2.29, Chapter 2; the bold-face symbols have same meanings when in normal font

### Subscripts

$a$	Air	$in$	Input, inlet
$A$	Adsorber	$j$	Drying stage number
$ads$	Adsorption	$k$	Cold stream number
$amb$	Ambient	$\ell$	Hot stream number
$atm$	Atmospheric	$out$	Output, outlet
$c$	Cold stream	$p$	Product
$calc$	Calculated	$r$	Regenerator heater
$d$	Dryer heater	$R$	Regenerator
$D$	Dryer	$rec$	Recovered
$dpt$	Dew point	$s$	Solid
$e$	Equilibrium	$sat$	Saturation
$evap$	Moisture evaporated	$SHR$	Simultaneous heat recovery
$h$	Hot stream	$w$	Water Zeolite (chapter 2 & 3);
$i$	Adsorbent number	$z$	Adsorbent (other chapters)

# Appendices

## Appendix A

**Table A1. Model parameters p**

$b_0$	$5.62 \times 10^{-8}$	$E_0$	$7.524 \times 10^6$	$C_{pz}$	$8.36 \times 10^2$	$k_0$	$4.04 \times 10^{-2}$
$C_{pa}$	$1 \times 10^3$	$E_1$	$-5.124 \times 10^7$	$R$	$8.314 \times 10^3$	$\mu_a$	$1 \times 10^{-3}$
$C_{pv}$	$1.93 \times 10^3$	$H_{ads}$	$3.2 \times 10^6$	$\rho_a$	1.2	$P_{atm}$	$1.01 \times 10^5$
$C_{pw}$	$4.18 \times 10^3$	$\Delta H_v$	$2.5 \times 10^6$	$\rho_z$	$1.2 \times 10^3$	$X_{z \max}$	0.1896

## Appendix B

### Kinetic, Equilibria and sorption properties of adsorbents and dried product

The sorption heat associated with 1kg of water adsorbed (or desorbed) for zeolite, alumina and silica gel respectively (Djaeni et al., 2007a; Kodama et al., 2001; Tahat et al., 1995) is approximately

$$H_{adsi} = [3200 \quad 2900 \quad 2300] \quad j \in J \quad (B1)$$

The maximum adsorbent loadings for each of the alternatives are as follows:

For zeolite (van Boxtel et al., 2012)

$$X_{zeA1j} = \frac{0.1896 b_{1j} P_{v1j}}{1 + b_{1j} P_{v1j}} \quad (B2)$$

where,

$$b_{1j} = 5.62 \times 10^{-8} \exp\left(5.124 \times 10^7 / RT_{aA1j}\right) \quad (B3)$$

$$P_{v1j} = \frac{Y_{aAij} P_{atm}}{0.62198 + Y_{aA1j}} \quad (B4)$$

For activated alumina (Moore and Serbezov, 2005),

$$X_{zeA2j} = 0.1736 \exp\left(-RT_{aA2j} \ln(1/RH_{aA2j})/7606\right) + 0.3252 \exp\left(-RT_{aA2j} \ln(1/RH_{aA2j})/862\right) \quad (B5)$$

For silica gel (Nastaj and Ambrozek, 2009),

$$X_{zeA3j} = 0.275 \exp\left[-(RT_{aA3j} \ln(RH_{aA3j})/3443.4)^2\right] + 0.073 \exp\left[-(RT_{aA3j} \ln(RH_{aA3j})/10931)^2\right] \quad (B6)$$

The drying behavior of pumpkin within the range of operation (Krokida et al., 2003; Doymaz, 2007) is used in simulating product drying. The equilibrium moisture content and drying constant are respectively given by

$$X_{pej} = 5 \times 10^{-7} \exp(3796.777/T_{adj})(RH/1 - RH)^{1.2848} \quad (B7)$$

$$k = \frac{\pi^2 D_{eff}}{4L^2} \quad (B8)$$

where effective diffusivity  $D_{eff}=3.88 \times 10^{-10}$  and slab half-thickness  $L$  is taken as 5mm.

### Appendix C

The vitamin C concentration  $N_p$  is derived thus,

$$\frac{dN_p}{dt} = \frac{1}{M_p} (F_p N_{pin} - F_p N_p) - \psi N_p \quad (C1)$$

where the degradation constant  $\psi$  (per hour) is given (Mishkin et al., 1983) by

$$\psi = 60 \exp(a_1 X_p + a_2 T^{-3} + a_3 X_p^3 + a_4 X_p^2 T^{-1} + a_5 X_p T^{-2} + a_6 X_p^3 T^{-3} + a_7) \quad (C2)$$

The constants are as follows (Mishkin et al., 1983):  $a_1=17.94$ ,  $a_2=-2.245 \times 10^8$ ,  $a_3=-33.33$ ,  $a_4=5921$ ,  $a_5=-1.585 \times 10^6$ ,  $a_6=4.711 \times 10^8$ ,  $a_7=-2.339$

$N_{pin}$ , the vitamin C concentration of the product at the inlet is taken as 100% and then, the concentration  $N_p$  after drying normalized with respect to the inlet value.

The heat recovery streams are described by

$$\frac{dT_x}{dt} = \frac{F_{aR}(C_{pa} + Y_{amb} C_{pv})(T_{amb} - T_x) + (UA/2)(T_y - T_{amb} + T_{aR} - T_x)}{M_{ax}(C_{pa} + Y_{amb} C_{pv})} \quad (C3)$$

$$\frac{dT_y}{dt} = \frac{F_{aR}(C_{pa} + Y_{aR} C_{pv})(T_{aR} - T_y) - (UA/2)(T_y - T_{amb} + T_{aR} - T_x)}{M_{ay}(C_{pa} + Y_{aR} C_{pv})} \quad (C4)$$

where heat exchanger coefficient  $U=200W/m^2K$  (Langrish, 1998);  $T_x$  and  $T_y$  are the heat exchanger outlet temperatures on the cold and hot stream sides respectively. The process state variable equations are defined in Atuonwu et al. (2011a), also in Chapter 2 of this thesis.

### Appendix D

Table D1. Process input, output and state variables and their nominal steady-state values (zeolite 4A used as adsorbent)

<i>Input</i>	<i>Description</i>	<i>Value</i>	<i>States</i>	<i>Description</i>	<i>Value</i>
$T_{aRin}$	Regenerator air temp. (°C)	400	$X_p$	Product outlet moisture (kg/kg)	0.05
$T_{ain}$	Drying air temp. (°C)	50	$T_p$	Product outlet temp. (°C)	50
$F_{aA}$	Drying air flow (kg/h)	$5.3 \times 10^4$	$X_{zA}$	Adsorber zeolite moisture (kg/kg)	0.1664
$F_z$	Zeolite flow (kg/h)	$4.12 \times 10^3$	$T_{zA}$	Adsorber zeolite temp. (°C)	50
$F_{aR}$	Regenerator air flow (kg/h)	$3.71 \times 10^3$	$X_{zR}$	Regenerator zeolite moisture (kg/kg)	0.0868
			$T_{zR}$	Regenerator zeolite temp. (°C)	170
			$Y_{Ad}$	Drying air abs. humidity (kg/kg)	0.0106
			$T_{aout}$	Drying air temp. (°C)	32
			$Y_{aA}$	Adsorber air abs. humidity (kg/kg)	0.0038
			$T_{aA}$	Adsorber air temp. (°C)	50
			$Y_{aR}$	Regenerator air abs. humidity (kg/kg)	0.0982
			$T_{aR}$	Regenerator air temp. (°C)	170

### Appendix E

Table E1. Sensor and equipment specifications

<b>Sensor/equipment</b>	<b>Specification</b>	<b>Supplier</b>
<b>Thermocouple</b>	Range: -100 to 1100°C	Labfacility LTD., UK
<b>Temperature and relative humidity transmitters</b>	Temperature: range -20 – 80°C; accuracy: 0.2°C at 20°C; Relative humidity: range 0-100%; accuracy $\pm 1\%$ (at 0-90%), $\pm 1\%$ (at 90-100%)	VAISALA, Finland
<b>Hot wire anemometer flowmeter</b>	Range: 0-20 m/s, operating temperature -40 to 85°C	SCHMIDT Feintechnik, Germany
<b>Dryer</b>	Tray dimensions 0.3m x 0.3m, height 0.4m	Ebbens Engineering Netherlands
<b>Zeolite wheel</b>	Thickness 0.2m, diameter 0.25m, adsorption to regeneration area ratio 3:1, zeolite mass in wheel 7.5kg (zeolite type 4A)	Ebbens Engineering Netherlands
<b>Heater</b>	Based on electric heating coil	Ebbens Engineering Netherlands

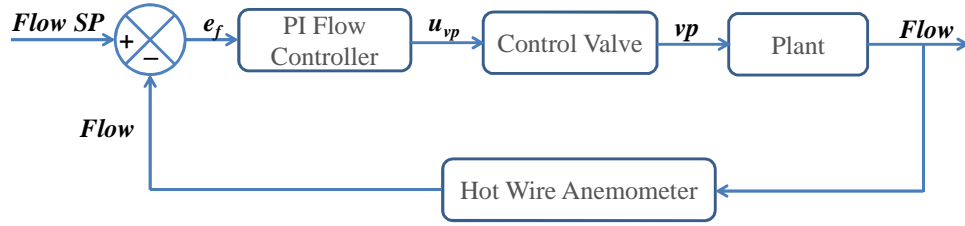


Fig. E1(a) Flow control loop: one for the adsorber or dryer air and one for the regenerator air

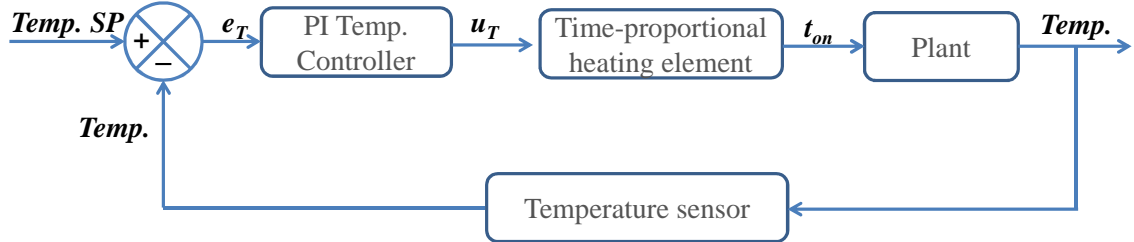


Fig. E1(b) Temperature control loop: one for the adsorber or dryer air and one for the regenerator air

The PI control algorithm for each loop of Fig. E1 is given by

$$u = K_c \left( e(t) + \frac{1}{T_i} \int_0^t e(t) dt \right) \quad (\text{E1})$$

where  $u$  is the controller output (% valve opening for 7(a) and % time ON  $t_{on}$ , for 7(b)) while  $e(t)$  is the error signal, that is the difference between the desired output (set-point  $SP$ ) and the instantaneous process variable in time  $t$ . The controller parameters are the proportional gain  $K_c$  and the integral time  $T_i$ . For good performance, the controllers are tuned using the relay auto-tuning using a modified Ziegler-Nichols method where the system is subjected to oscillating set-point changes by relay action and the  $K_c$  and  $T_i$  parameters iteratively adjusted until it gives a good response. At the end of the iterative tuning procedure, the controller parameters are returned as  $K_c=1$ ,  $T_i=0.01$  minutes for the dryer inlet (or adsorber outlet) flow control and  $K_c=13$ ,  $T_i=0.1$  minutes for the corresponding temperature control.

For the reference experiment with the wheel detached, the regeneration air flows and temperatures were set at zero and ambient respectively by putting the loops on manual. With the wheel inserted, the dryer flow and inlet temperature controller parameter settings remain unchanged. For the regeneration flow control,  $K_c=1$ ,  $T_i=0.01$  minutes while for the temperature control, we have a P-only controller with  $K_c=100$ .

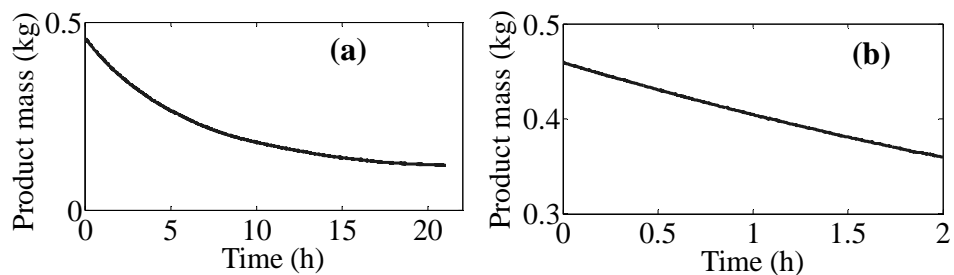


Fig. E2. Drying kinetics of the wet product under the nominal operating conditions: total drying curve (a) and first two hours (b) showing constant-rate conditions

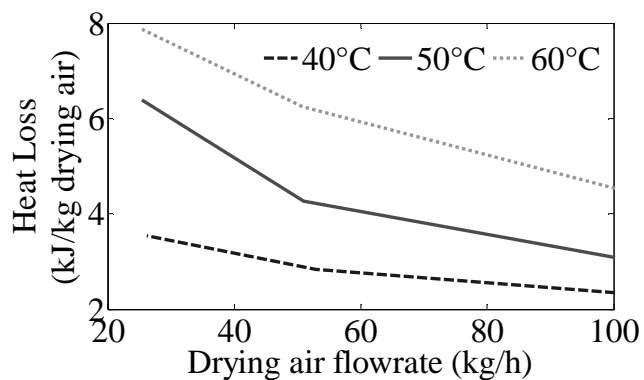


Fig. E3. Specific heat loss at different drying air flowrates. At 50°C, and 50kg/h (nominal conditions), specific heat loss=4.3kJ/kg of air, translating to 215 kJ/h





## Summary

The significant contribution of drying to industrial energy consumption and the low drying temperature requirement for heat-sensitive products has created a need to develop innovative low-temperature energy-efficient drying processes which must also be controllable. Conventional dryers with air as drying medium are characterized by low energy efficiencies in the order of 20-60% and improvements are continuously being sought after. By coupling an adsorbent dehumidifier to a conventional dryer whereby ambient air is dehumidified before contacting the wet product, some new features are introduced with potentials for improving energy efficiency. The reduction in air humidity is accompanied by sorption heat release with the combined effect enhancing drying capacity. On the other hand, extra energy is consumed in regenerating used adsorbents but this also creates opportunities for beneficial heat integration. The challenge entails exploiting these features to improve energy efficiency by appropriate design and operational strategies while limiting drying temperatures and maintaining a controllable, operable system.

In this work, we employ a systems approach to tackle the challenge. To facilitate this, an energy sensitivity-relevant generalized model of an adsorption dryer which considers the drying behavior of specific food products has been developed for a single-stage drying system with zeolite as adsorbent. Two approaches are used in optimizing the system. In the first, a sequential optimization approach is used where the drying process is optimized, followed by pinch analysis to optimally recover sensible and latent heat from the process exhausts whose conditions are determined by the drying process optimization. In the second, the drying process is simultaneously optimized with heat recovery using a pinch location technique whereby the inlet conditions to the heat exchange system are not determined a priori unlike in conventional pinch analysis. It has been shown that by optimizing regeneration air inlet temperature and flowrate, drying air and adsorbent flowrate, energy consumption is reduced significantly. Compared to a conventional dryer operating at the same drying temperature, a sequentially-optimized system reduces energy consumption by 20% without heat integration and 45% after heat integration while a simultaneously optimized system achieves a 55% reduction.

To explore energy efficiency improvement possibilities, multistage adsorption drying was considered. Here, the exhaust air from each dryer is passed through an adsorbent system to re-dehumidify and so recover sensible, latent heat and drying capacity which is then used for drying in subsequent stages. Rather than fixing the type of adsorbent in each stage which is the norm, a superstructure of alternatives was formulated in which adsorbent choice per-stage and product to air flow configuration are discrete decision variables. Combined with the same continuous variables used in the single-stage optimization case, this leads to a mixed integer nonlinear programming problem. For an adsorbent search space consisting of zeolite, silica gel

and alumina in a two-stage system, results indicate an optimal choice of zeolite as the first-stage adsorbent and silica-gel in the second-stage with counter-current flow between drying air and product. Compared to an equivalent two-stage conventional dryer, energy consumption is reduced by 59% without heat integration and 65% with subsequent heat integration while simultaneous heat integration optimization yields a 70% reduction with the same adsorbent choices and flow configuration.

For a generalized solution, the adsorbent search space is extended to obtain another superstructure that lumps all possible adsorbent behaviors, into a general isotherm structure consisting of the 5 classes of adsorbents by the standard BET classification. When optimized, the adsorbent properties that promote energy efficiency are identified to include high sorption capacities, regeneration to adsorption rate constant ratio and surface heterogeneity. The derived knowledge should guide adsorbent selection in energy-efficient drying applications. Overall, adsorbents requiring high-temperature regeneration are chosen in the first stage so the exhaust temperature is high enough to sufficiently regenerate the second-stage adsorbent. Those with higher sorption capacities at lower humidity are chosen for ambient air dehumidification while those more effective at higher vapour pressures take priority for exhaust air dehumidification. Also, the adsorbent flowrate pattern show the first stage adsorbent system is optimized for dehumidification and hence, drying capacity while the second stage by virtue of its higher flowrate behaves like an enthalpy wheel optimized for heat recovery. Optimization thus matches adsorbent choices and operating conditions to the characteristics of the drying system to maximally exploit the strengths of the adsorbent system and ensure a synergistic operation. All energy optimization problems for one-stage and two-stage systems were solved subject to constraints on the temperature ( $\leq 50^{\circ}\text{C}$ ) and moisture content (0.05 kg/kg) of the product.

Controllability analysis is important to explore options to control the adsorption dryer to reject disturbances and track desired set-points. This is done using tools like relative gain array, Niederlinski index, process condition number, single input effectiveness, closed-loop disturbance gain and disturbance condition number. Apart from the traditional control inputs like drying air temperature and flow in conventional systems, extra degrees of freedom like regeneration temperature, flow and adsorbent flowrate provide other control options. The analysis reveals some promising input-output combinations to include regeneration temperature-product moisture; drying temperature-product temperature combination and air flowrate-product moisture; regeneration temperature-product temperature combination. Others are regeneration air flowrate-product moisture; drying temperature-product temperature combination and drying air flowrate-product moisture; adsorbent flowrate-product temperature combination. For corresponding inputs, adsorption dryers have higher steady-state gains than equivalent conventional dryers as dehumidification leads to sorption heat release so the combined effect drives the output moisture and temperature further than would be possible without dehumidification. In terms of disturbance rejection, the adsorbent system is shown to

improve system moisture and temperature resilience to ambient air disturbances by introducing regulation properties which depend on the adsorbent properties like adsorption heat, sorption characteristics and operating conditions. At the same time, the regeneration energy is less sensitive to these disturbances than the energy input of a conventional dryer. Overall, the energy efficiency sensitivity of adsorption dryers to ambient disturbances is reduced compared to conventional dryers.

Integration of controllability aspects into energy-efficient drying system design would be enhanced if a relationship is established between the two variables. This is achieved in this work using energy balances and process resiliency analysis. From the process gain matrix, the dryer energy efficiency is reliably calculated with conditions for simultaneous controllability improvement established. By incorporating a drying rate modifying system such as a desiccant dehumidifier as an add-on, these conditions are shown to be achievable due to the extra dehumidification which can be manipulated using the additional degrees of freedom introduced by the sorption system. Specifically, the condition for energy efficiency improvement on addition of the adsorbent system is derived from component and system energy balances on the bases of which a new performance indicator for desiccant dehumidifiers is proposed. Known as the adsorber-regenerator net energy efficiency *ARNEE*, this indicator is better-suited to the specifics of the use of desiccant dehumidifiers in drying operations than pre-existing indicators. The desiccant is shown to be effective in improving energy performance without heat recovery only if the *ARNEE* is greater than the efficiency of the stand-alone dryer. The result is thus valuable in providing short-cut means of making decisions as to the dehumidifier specifications required to improve the performance of existing convective dryers.

The modeling approach detailed in the foregoing was extended to include practical batch drying systems and systems with significant heat losses. For batch dryers, product moisture has no steady-state and so is replaced for gain matrix calculations by drying rate which is steady under constant rate drying regimes. Using the gain matrix, the dryer temperature drop due to water evaporation is decoupled from heat loss effects providing a viable alternative for reliable instantaneous energy efficiency calculation even for non-adiabatic processes where the use of measured temperature drops is grossly inaccurate. The approach is tested on two experimental case studies with significant heat losses. First, literature data for a continuous fluidized-bed dryer is used. Finally, a zeolite wheel-assisted batch dryer with associated proportional-integral (PI) control system is designed in the current study and used for step tests in drying constant drying rate materials. For a reference, the wheel was detached to reduce the system to a conventional one and the experiments repeated to indicate the effects of the wheel on system performance. In all cases, the established relationship between controllability and energy efficiency was confirmed.



## Samenvatting

Droogprocessen zijn verantwoordelijk voor een aanzienlijk aandeel in het totale industriële energieverbruik. Conventionele drogers met lucht als droogmedium worden gekarakteriseerd door een lage energie-efficiëntie van tussen de 20 en 60%, en dit geldt zeker voor het drogen van warmtegevoelige producten bij lage temperatuur. Er wordt voortdurend gezocht naar optimalisaties en innovaties die moeten leiden tot energie-efficiënte lage-temperatuur droogprocessen, die bovendien goed regelbaar moeten zijn. Het koppelen van een absorptie luchtontvochtiger aan een conventionele droger - waardoor de omgevingslucht wordt ontvochtigd alvorens in contact te komen met het natte product – biedt nieuwe mogelijkheden om de energie-efficiëntie te verbeteren. Het terugbrengen van de luchtvochtigheid door absorptie gaat gepaard met warmteontwikkeling en dit gecombineerde effect leidt tot een verhoogde droogcapaciteit. Daar staat tegenover dat extra energie nodig is voor het regenereren van de absorbentia, maar dit biedt ook additionele mogelijkheden voor warmte integratie. De uitdaging bestaat eruit om met adequaat ontwerp en uitgekende integratie- en regelstrategieën deze mogelijkheden optimaal te benutten om de energie-efficiëntie van lage temperatuur droogprocessen te verhogen in een goed regelbaar systeem.

In dit proefschrift wordt een systeembenadering gebruikt om dit probleem aan te pakken. Hiertoe is een gegeneraliseerd model van een absorptiedroger ontwikkeld, met speciale aandacht voor de energie. Het model heeft betrekking op een enkeltraps droogstelsel met zeoliet als absorbens. Twee benaderingen zijn gekozen om het systeem te optimaliseren. De eerste is een sequentiële aanpak, waarin eerst het droogproces wordt geoptimaliseerd. Vervolgens wordt een pinch-analyse gebruikt om voelbare en latente warmte uit de uitlaatluchtstromen optimaal terug te winnen. De condities van deze stromen worden bepaald door de voorafgaande optimalisatie van de droger. De tweede methode is een simultane optimalisatie: droogproces en warmteterugwinning worden gelijktijdig geoptimaliseerd. Er wordt een pinch locatie techniek gebruikt waarbij in tegenstelling tot de gebruikelijke pinch-analyse de inlaatcondities van de warmtewisselaars niet *a priori* worden vastgelegd. Aangetoond is dat het energieverbruik aanzienlijk wordt verminderd door debiet en temperatuur van de regeneratielucht, het debiet van de drooglucht en de transportsnelheid van het absorbens te optimaliseren. Vergeleken met een conventionele droger met dezelfde droogluchttemperatuur bespaart een sequentieel geoptimaliseerd systeem 20% energie zonder warmte integratie en 45% met warmte integratie, terwijl bij simultane optimalisatie een besparing van 55% wordt bereikt.

Om verdere verbeteringen in energie-efficiëntie te bereiken is ook gekeken naar meertraps absorptiedrogen. In deze systemen wordt de uitlaatluchtstroom van elke droogtrap door een absorber geleid om deze te ontvochtigen, waardoor voelbare en

latente warmte wordt herwonnen en de droogcapaciteit van de lucht wordt hersteld voor gebruik in de volgende trap. In plaats van de normale praktijk om het type absorbens in elke trap vooraf vast te leggen, is een superstructuur van alternatieve opties geformuleerd waarin de keus van het absorbens per trap en de configuratie van productstroom en luchtdebiet discrete beslissingsvariabelen zijn. In combinatie met dezelfde continue variabelen als in het enkeltraps proces leidt dit tot een mixed integer niet-lineair programmeringsprobleem. Als zeoliet, silicagel en alumina als mogelijk adsorbens worden beschouwd, en meestroom en tegenstroom van drooglucht en product als mogelijke configuraties, blijkt bij een tweetrapsproces dat zeoliet de optimale keus is voor de eerste trap en silicagel voor de tweede, terwijl tegenstroom naar voren komt als de optimale configuratie. Vergeleken met een equivalente conventionele tweetraps droger vermindert bij sequentiële optimalisatie het energieverbruik zonder warmte integratie met 59% en met warmte integratie met 65%, terwijl simultane optimalisatie resulteert in een reductie van het energieverbruik met 70% bij dezelfde keuze van absorbentia en stromingsconfiguratie.

Om de oplossingsmethode te generaliseren wordt de absorbens zoekruimte uitgebreid zodat een andere superstructuur wordt verkregen waarin het gedrag van alle mogelijke absorbentia wordt samengenomen in een algemene isotherm structuur, bestaande uit 5 klassen van absorbentia volgens de standaard BET classificatie. Na optimalisatie kunnen de absorbenseigenschappen worden geïdentificeerd die energie-efficiëntie bevorderen. Dit zijn: hoge absorptie capaciteit, een hoge verhouding van de snelheidsconstanten van regeneratie en absorptie, en een grote oppervlakte heterogeniteit. De verkregen kennis kan dienen om richting te geven aan de selectie van absorbentia ten behoeve van energie-efficiënte droogtoepassingen. Samengevat kunnen in de eerste trap het beste absorbentia worden gekozen die een hoge regeneratietemperatuur nodig hebben, zodat de uitgaande luchtstroom een temperatuur heeft die hoog genoeg is om het absorbens van de tweede trap te kunnen regenereren. Absorbentia met een hoge absorptiecapaciteit bij lagere vochtigheid zijn het meest geschikt voor het ontvochtigen van de omgevingslucht, terwijl voor het ontvochtigen van de uitlaatlucht de voorkeur gegeven wordt aan absorbentia die een hogere effectiviteit hebben bij hogere dampspanningen. Het gevonden patroon van de absorbens transportsnelheid laat zien dat de eerste trap geoptimaliseerd wordt voor ontvochtigen, en dus droogcapaciteit, terwijl de tweede trap zich als gevolg van de hogere transportsnelheid gedraagt als een enthalpiewiel dat is geoptimaliseerd voor warmteterugwinning. Optimalisatie stemt aldus de keuzes voor absorbentia en bedrijfscondities af op de karakteristieken van het droogsysteem, teneinde de sterke kanten van het absorptiesysteem te benutten en een synergistische bedrijfsvoering te verzekeren. Alle optimalisatieproblemen voor het ééntraps- en tweetrapsstelsel werden opgelost met randvoorwaarden voor de droogluchttemperatuur ( $<50\text{ }^{\circ}\text{C}$ ) en het eindvochtgehalte van het product ( $0,05\text{ kg/kg}$ ).

Een regelbaarheidsanalyse is belangrijk om de opties te verkennen voor regeling van de absorptiedroger gericht op het onderdrukken van verstoringen en het volgen van

gewenste instelwaarden. Dit is gedaan door gebruik te maken van methodes zoals de relatieve versterkingsmatrix (relative gain array), Niederlinski index, procesconditiegetal, effectiviteit van een enkele input, en verstoringsconditiegetal. Behalve de gebruikelijke gemanipuleerde variabelen zoals de droogluchttemperatuur en het debiet in conventionele systemen, zijn er extra graden van vrijheid bij absorptie droogsystemen voor de keuze van de stuurvariabelen, zoals de regeneratietemperatuur, het regeneratiedebiet en de absorbens transportsnelheid. De analyse brengt veelbelovende input-output combinaties aan het licht, waaronder de combinaties regeneratie temperatuur – product vochtgehalte; drooglucht temperatuur – product temperatuur cq. luchtdebiet – product vochtgehalte; en regeneratietemperatuur – product temperatuur. Andere combinaties zijn regeneratie luchtdebiet – product vochtgehalte; droogtemperatuur – producttemperatuur cq. droogluchtdebiet – product vochtgehalte; en absorbens transportsnelheid – product temperatuur. Voor overeenkomstige sturingen hebben absorptiedrogers hogere statische versterkingen dan equivalente conventionele drogers, aangezien ontvochtiging leidt tot het vrijkomen van sorptiewarmte, zodat het gecombineerde effect het vochtgehalte en de temperatuur aan de uitgang verder opstuwt dan mogelijk was geweest zonder ontvochtiging. In termen van storingsonderdrukking wordt aangetoond dat het absorptiesysteem de weerstand van vocht en temperatuur tegen fluctuaties in omgevingsluchtvariabelen verbetert, door het inbrengen van reguleringseigenschappen in afhankelijkheid van absorbens eigenschappen zoals absorptiewarmte, sorptiekarakteristiek en bedrijfscondities. Tegelijkertijd is de regeneratie-energie minder gevoelig voor deze verstoringen dan de energie input van een conventionele droger. Concluderend kan worden gesteld dat de gevoeligheid van de energie-efficiëntie voor verstoringen in omgevingscondities voor absorptiedrogers geringer is dan voor conventionele drogers.

Het meenemen van regelbaarheidsaspecten in het ontwerpproces van energie-efficiënte droogsystemen zou bevorderd worden indien een relatie kon worden gelegd tussen regelbaarheid en energie-efficiëntie. Dit wordt gerealiseerd in dit proefschrift door energiebalansen te combineren met proces responsie analyse. Het blijkt dat de drogerefficiëntie betrouwbaar kan worden berekend uit de versterkingsmatrix van het proces. Tevens worden voorwaarden afgeleid voor verbetering van de regelbaarheid. Door in het ontwerp een systeem toe te voegen waarmee de droogsnelheid wordt gewijzigd, zoals een absorptie ontvochtiger, blijkt aan deze voorwaarden te kunnen worden voldaan, als gevolg van de extra ontvochtiging die kan worden gemanipuleerd door het benutten van de extra graden van vrijheid die het sorptiesysteem met zich meebrengt. Meer specifiek gezegd, worden de voorwaarden voor verbetering van de energie-efficiëntie bij toevoegen van een absorptiesysteem afgeleid uit component en systeem energiebalansen. Op basis hiervan wordt een nieuwe prestatie indicator voor absorptie-ontvochtigers voorgesteld, met de naam *ARNEE* (absorber-regenerator net energy efficiency). Deze indicator is beter geschikt voor de specifieke kenmerken van de toepassing van absorptie ontvochtigers in droogprocessen dan de bestaande indicatoren. Aangetoond wordt dat het sorptiesysteem alleen effectief is in het

verbeteren van de energie-efficiëntie indien de *ARNEE* groter is dan de efficiëntie van de standaard droger. Dit is een waardevol resultaat omdat het een korte route biedt voor het nemen van beslissingen over de specificaties van de ontvochtiger die vereist zijn om de prestaties van conventionele drogers te verbeteren.

De modelbenadering die hierboven is beschreven werd uitgebreid naar praktische batchgewijze droogsystemen en naar systemen met aanzienlijke warmteverliezen. In batchgewijze drogers heeft het productvochtgehalte geen stationaire toestand. Deze variabele is in de versterkingsmatrixberekeningen vervangen door de droogsnelheid die in perioden met constante droogsnelheid wel stationair is. Door gebruik te maken van de versterkingsmatrix kan de temperatuurval over de droger als gevolg van de verdamping worden losgekoppeld van het effect van warmteverliezen. Dit biedt een bruikbaar alternatief voor betrouwbare berekening van de momentane energie-efficiëntie, zelfs voor niet-adiabatische processen waar het gebruik van het gemeten temperatuurverschil erg onnauwkeurig is. Deze methode is experimenteel getest voor twee gevallen met aanzienlijke warmteverliezen. In het eerste geval zijn experimentele gegevens van een continue fluid-bed droger uit de literatuur gebruikt. Het tweede geval betreft een eigen experiment. Hiertoe is een batchgewijze droger met zeoliet-wiel ontworpen, en voorzien van een regelsysteem met PI regelaars. Met dit systeem zijn stapresponsies gemeten bij het drogen van materiaal gedurende de periode van constante droogsnelheid. Als referentie is hetzelfde gedaan met een systeem waarvan het zeoliet-wiel was losgekoppeld, zodat het systeem wordt teruggebracht tot een conventioneel systeem, om een idee te krijgen van de effecten van het absorptiewiel op de systeemprestaties. In alle gevallen werd de vastgestelde relatie tussen regelbaarheid en energie-efficiëntie bevestigd.



## **Tori sharp sharp for dis akada work**

Food wen we dey chop and de things wen dem dey make for factori dey get water inside wey fit make dem spoil quick quick and wey make dem too heavy for transport. Sake of dat, e dey important to dry dem. E good make we find ogbonge tekinologi for dry dem sake of say e dey take plenti energi kate kate in de patricula for product dem wey no like plenti heat. E still dey good make e dey easy to kontrol de kondition like temperature wen dis tekinologi dey work make kasala nor go burst wen person dey use am. Normal dryer wey dey market now dey use air take blow pass de wet product so tey e go drive de water komot. De wahala wey dey dia be say e dey take too much energi to komot tikene water. If you use dis dryer komot water, de energi wey dey inside de water wey u fit komot go dey be dat kind 20 to 60% of de energi wey you put inside (we call am energi efficienci). Dat wan nor too jell so we want make am beta. If we use one tekinologi wen oyibo dem dey call adsorbent take komot water for de air before we blow am pass de wet product, na im be say de air go dry sotey e go get plenti power to komot water from de product. So we no go too spend energi again. We dey call dis tekinologi adsorption dryer. Anyway sha, anoda wahala wey dey dia be say we still need energi to take use hot air komot water wey de adsorbent dey kollekt. De good thing again be say, e kom be like say we go fit kollekt back some of dis energi. E kom dey important make we sabi well well how to take use all dis beta thing so tey de wahala wey dey inside go kom small and we go dey use tikene energi komot plenti water and make de air no go too hot to spoil de thing wey we dey dry.

Na some kind mathematics wen dem dey call optimization we take do de thing wey we don talk before. Na im make we kom make something for komputer wey dem dey call model to show us how we fit take dey change as dem take dey use energi for de adsorption dryer. Na two ways we take do am. For one, we try make de adsorption dryer work gabadaya. Later, we kom check weda we fit still kollekt back some energi from de yama yama air wey kom out from de dryer. For de oda one we put both de adsorption dryer and de heat kollekting togeda for one big model to take find how de whole thing go take work. We kom see say if we use beta temperature and flow, we go komot around 20% from de energi wey de normal dryer dey use, if we nor kollekt back yama yama heat. If we later kollekt de heat na im be say we go komot 45%. But for de method wey we put everything togeda, we even komot 55%.

Dat one nor reach at all at all. Na im make we try konnect different adsorption dryer togeda sotey de air wey kom out from one we use am again for anoda one. If we do am we fit still kollekt some energi wey for kpafuka if we no konnect dem togeda. We kom make anoda model wey we use take find which kind adsorbent beta pass to use for each stage so tey tikene energi fit komot big water. We no just chose any adsorbent wen we like. Na optimization we use take find de adsorbent wey be say na im beta pass. We first say make we choose from three adsorbent wen dem dey call

zeolite, silica gel and alumina. We kom see say na zeolite beta for de first stage but for de second stage, na silica gel get power pass. We still see say e beta make de air wey dem take dey dry flow opposite de product wen we dey dry. De ting wen we see if we konnect adsorption dryer togeda be say we komot 59% of de energi of normal dryer if we no kolekt back yama yama heat. If we kolekt am later, we komot 65%. If we kom kolekt am de same time wen we dey make de thing work gabadaya, na im be say we go even komot 70% from de energi wen normal dryer dey use.

Wetin we kom see be say e no too jell to choose from only three adsorbent dem. Na im we kom make model wen we fit use find de kind way wey we want make de adsorbent behave wey be say we no fix any adsorbent. We kom find out say e beta pass make we use adsorbent wey need plenti heat to remove de water wey im kollekt for de first stage sake of say de hot air wen kom out of am go fit komot de water wey dey for de adsorbent wey dey second stage. Sake of dat, e kom good make de adsorbent wey dey de second stage no need plenti heat. Again, we kom see say e beta pass to use adsorbent wey dey kollekt plenti water from air wen tikene water dey for first stage and de one wey dey kollekt plenti water only wen water dey jabrata for de air wey dey second stage. De reason be say de first stage dey use normal air wen dey environment whereas, de second stage dey use de air wey kom out from de first dryer wey be say e get water jabrata wen u compare am to de normal air. Wetin we go say last last for dis matter be say optimization na one kind ogbonge way to take choose de kind stuff to use for all de parts of ur dryer sotey de whole thing go work well well pass as e go be if u just use komon sense take do am. For all de optimization dem we make sure say de temperature of de product wey we dey dry no pass 50°C and make de weight of de water wey remain after we don dry be 0.05 kg inside 1kg product.

To dry any product or to make anything for factori, e good make we keep de plant wey we dey operate for beta kondition wey good for de plant, product, environment and wey go make us use tikene money to run am. Dis kondition dem fit be something like beta temperature and those kind things dem. For some plant dem, e no easy at all at all to maintain de kondition sake of say de plant no get beta kontrol or e fit be say disturbances like weda wey dey change anyhow or quality wey change anyhow dey. E good make we get something wen we go dey set and tune make de thing work well well. E kom dey important make we sabi how easy e be to maintain de beta kondition. And de name wey oyibo take describe dis thing na im be kontrollability. To check de kontrollability e get some numbers like relative gain array gbogbotigbo wen we use. At de end we see say some new way to take kontrol de water wey dey inside de product and de temperature dey wey no dey normal dryer. Dis one na becos of de adsorbent tekinology wen we konnect to de normal dryer. De extra thing wey we fit take kontrol how de product dey behave na de speed wen de adsorbent take dey move, de speed wey de air wey komot water from de adsorbent take dey flow and de temperature of dis same air. We kom see say de adsorbent self dey make de temperature and water wey dey inside de air wen we take dey dry steady pass de air wey dey environment even if de weda dey change anyhow. Dis na becos d adsorbent

dey behave one kind wey be say as de kondition of de air change imself go bahave anoda way take try komot de change to get back de kondition wey dey before.

Anoda matter be say e go good make we join de method wey we take reduce energi wen we dey use take dry with de kontrollability matter. We do dis one with some kind method wen dem dey call energi balance and process resiliency analysis. Energi balance be say we check de energi wen enter every part of de adsorption dryer and de one wey lost and de one wey we use take dry. We fit use de model wen we get from hia take find how we fit reduce energi wen we dey use. Process resiliency analysis be say we go change de things dem wey we go fit take kontrol how de product de behave, and kom see how de product kondition self take respond. If we divide de respond by de change wey we give de thing we take dey kontrol, we go get wetin dem day call “process gain”. From dia we kom know how we go take dey set our dryer to make sure say we get beta beta product and use tikene energi for dey dry things.

One thing wey kom surprise us be say we kom see say kontrollability for dryer and energi wen we dey use take dry, dey related to each oda nor be small. We kom still see say de adsorbent fit help take make both de kontrollability beta and de energi we use small pass if we no use adsorbent. De only thing wey dey dia be say de adsorbent stuff need to meet some kondition sha before dat one go happen. Dis kondition we give am name wen we call “adsorber-regenerator net energi efficienci *ARNEE*”. To reduce energi wen we dey use, de adsorbent stuff on e own suppose get *ARNEE* wey big pass de how good wey de dryer on e own take dey use energi (wey we call dryer energi efficienci). As *ARNEE* depend on de adsorbent stuff, dis result go help person wey wan buy adsorbent stuff wey e wan konnect for normal dryer to know which kind one e go buy and which kondition dem go take dey run am make e money no go lost.

De energi and kontrollability work wen we dey do since na for dryer wen e be say product and air dey enter inside and komot every time. Dis one dem call am “continuous dryer”. We still assume say heat no too lost. For real life sha, heat fit lost wella. We fit still use batch dryer where we just put de product once (not everytime) like say we put something for fire, den kom dey blow air pass am. Sake of dis, we kom combine energi and kontrollability matter for batch dryer dem and continuous dryer wey heat loss dey too much to take get one big model wey tell us how de energi we use for dry relate to kontrollability. We kom see say we fit use de process gain (wey relate to kontrollability) take kalkulate de energi efficienci korekt korekt even when heat loss plenti well well. But when we use normal temperature wen we measure take kalkulate de energi efficiency as plenti people dey do am before, de answer nor correct at all at all. Na im be say dis method wey we take kalkulate energi efficiency na real ogbonge method. To show sey dis method dey work for real life, we test am for one kind real dryer wen some people don describe for book before and anoda one wey we sef kom build ourself, both de one wey get adsorbent and de one wey no get. For all of dem we see say our model korekt gidigba. Na Baba God give me life take do all dis work dem so I throway salute for am well well pass anybody.



## Acknowledgements

I wish to express my immense gratitude to the Dutch Ministry of Economic Affairs for funding the work under Project EOSLT07043 of its Energy Research Program. I am also highly indebted to my Promoter, Gerrit van Straten and supervisors, Ton van Boxtel and Henk van Deventer for the opportunity given me to participate in the project on the basis of which this work has been produced. Thanks for keeping faith with me through the ups and downs of the period. I am also grateful for providing me excellent directions through the long, narrow, uncertain path of PhD research. Your inputs have made the completion of the thesis possible and for this, I am grateful.

Special thanks also to other members of staff of the Biomass Refinery and Process Dynamics Group (formerly Systems and Control Group) who have contributed in no small measure to the successful completion of the project. To my fellow PhD students, Xin, Ellen, Nurul, Jimmy, Jan, Emmanuel and of course, Teresa of the Product Design and Quality Group who was part of the broader project, I say thank you for the nice time and co-operation we had. Gerard, thanks for the nice discussions on modeling and optimal control. Kees, I am most grateful for your help with the experimental set-up and providing useful practical insights. Karel and Rachel, thanks for your incisive lectures and hands-on exercises on Physical Modeling which no doubt proved helpful in the course of the work. Kudos also to the indefatigable Marja Portengen for ensuring all the administrative aspects of my work here was well taken care of. I am also highly grateful to Joop van der Belt of Ebbens Engineering for his diligence in constructing the experimental set-up used in this work.

To the Nigerian community in Wageningen, I say special thanks. I am grateful for helping make my stay here in Wageningen more interesting. The parties, incisive discussions and sometimes fierce arguments have been worth the while. *I hail una oh!*

I would also appreciate the Christian community in Wageningen, particularly those of the International Christian Fellowship ICF and the Amazing Grace Parish AGP. You have no doubt helped in *oiling the wheels of the soul so the body does not grind to a halt!* Special thanks to Farai Maphosa and family, Johan Velema and family and many others whom time and space would not permit me to list. I am very grateful!

And how can I forget members of my family back home in Nigeria? You have provided the springboard from which I have leapt to higher heights. The heights attained including this PhD thesis would not have been possible without you. Special thanks to my mum, Favour Atuonwu, brother, Eze and sisters Ebere, Chinyere, Nnenna, Joy, nephews Chukwuemeka and Onyedikachi and nieces, Onyekachi, Chima, Onyinyechi and Miriam, brother-in-law, Musa and sister-in-law Chinenye. I am most grateful for all your encouragements.

Finally, my thanks go to friends too numerous to mention and all who at one time or the other, consciously or unconsciously, contributed directly or indirectly to the *vast pool of knowledge from which this work is drawn.*



## About the author

James Chibuzo Atuonwu was born on May 15, 1980 in Benin City Nigeria. He had his high school education at the Edokpolor Grammar School, Benin City and thereafter proceeded to the University of Benin, Nigeria where he obtained a Bachelor's degree in Electrical and Electronic Engineering (First Class Honours) in 2005. After brief stints with the PZ Industries PLC, Aba and the Nigerian Breweries PLC, Lagos both in Nigeria as an intern, he joined the University of Benin as a Graduate Assistant Lecturer in 2006 teaching *Process Instrumentation*. He then proceeded to Cranfield University, the UK, where he bagged a Master's degree in Process Systems Engineering with specialization in Process Control in 2008, courtesy of the "Petroleum Technology Development Fund" scholarship award of the Nigerian Government. Between 2009 and 2013, he has been researching on improving the energy efficiency of dryers at the Systems and Control Group, Wageningen University, the Netherlands which has culminated in this PhD thesis. Simultaneously, he has been involved in teaching activities on the courses *Control Engineering and Process Control* and *Dynamic Systems Modeling*. He has at various times served as reviewer for the international journals *Drying Technology*, *Science for the Total Environment* and *Chemical Engineering Science*.





## List of Publications

### Peer-reviewed International Journals

1. Atuonwu, J.C., Straten, G. van., Deventer, H.C. van., Boxtel, A.J.B. van (2012). On the controllability and energy sensitivity of heat-integrated desiccant adsorption dryers. *Chemical Engineering Science* 80, 134-147.
2. Atuonwu, J.C., Straten, G. van., Deventer, H.C. van., Boxtel, A.J.B. van (2012). A mixed integer formulation for energy efficient multistage adsorption dryer design. *Drying Technology* 30(8), 873-883.
3. Atuonwu, J.C., Straten, G. van., Deventer, H.C. van., Boxtel, A.J.B. van (2011). Model-based energy efficiency optimization of a low-temperature adsorption dryer, *Chemical Engineering and Technology*, 34, 1723-1732.
4. Atuonwu, J.C., Straten, G. van., Deventer, H.C. van., Boxtel, A.J.B. van (2011). Improving adsorption dryer energy efficiency by simultaneous optimization and heat integration, *Drying Technology* 29(12), 1459-1471.
5. Atuonwu, J.C., Straten, G. van., Deventer, H.C. van., Boxtel, A.J.B. van (2011). Optimizing energy efficiency in drying by zeolite adsorption and process integration, *Chemical Engineering Transactions* 25, 111-116.
6. Atuonwu, J.C., Cao, Y., Rangaiah, G.P., Tade, M.O. (2010). Identification and predictive control of a multistage evaporator. *Control Engineering Practice* 18(12), 1418-1428.
7. Atuonwu, J.C., Straten, G. van., Deventer, H.C. van., Boxtel, A.J.B. van. Synergistic process design: reducing drying energy consumption by optimal adsorbent selection. *Submitted*.
8. Atuonwu, J.C., Straten, G. van., Deventer, H.C. van., Boxtel, A.J.B. van. Improving dryer controllability and energy performance by process modification. *Submitted*.
9. Atuonwu, J.C., Straten, G. van., Deventer, H.C. van., Boxtel, A.J.B. van. On dryer controllability and energy performance: generalized modeling and experimental validation. *Submitted*.

### Peer-reviewed International Conferences

1. Atuonwu, J.C., Straten, G. van., Deventer, H.C. van., Boxtel, A.J.B. van (2012). Improving dryer controllability and energy efficiency. *Proceedings, European Symposium on Computer-Aided Process Engineering (ESCAPE 22)*, London, UK, 847-851.
2. Atuonwu, J.C., Straten, G. van., Deventer, H.C. van., Boxtel, A.J.B. van (2012). Reducing drying energy consumption by adsorbent property optimization in

- multistage systems. *Proceedings, 11<sup>th</sup> International Symposium on Process Systems Engineering (PSE 2012)*, Singapore, 1146-1150.
3. Atuonwu, J.C., Straten, G. van., Deventer, H.C. van., Boxtel, A.J.B. van (2012). Reducing drying energy consumption by multistage adsorption dryer combinatorial optimization. *International Drying Symposium IDS 2012*, November 11-15, Xiamen, China.
  4. Atuonwu, J.C., Jin, X., Straten, G. van., Deventer, H.C. van., Boxtel, A.J.B. van. (2011). Reducing energy consumption in food drying: opportunities in desiccant adsorption and other dehumidification strategies. *Procedia Food Science, International Conference on Engineering & Food*, Athens, Greece, 1, 1799-1805.
  5. Atuonwu, J.C., Straten, G. van., Deventer, H.C. van., Boxtel, A.J.B. van (2010). Modelling & energy efficiency optimization of a low temperature adsorption based food dryer, *International Drying Symposium IDS 2010*, October 3-10, Magdeburg, Germany.
  6. Atuonwu, J.C., Cao, Y., Rangaiah, G.P., Tade, M.O. (2009). Nonlinear Model Predictive Control of a Multistage Evaporator System using Recurrent Neural Networks. Proc., *IEEE Conference on Industrial Electronics & Applications*, Xian, China, 1662-1667.

## Other Conferences

1. Atuonwu, J.C., Straten, G. van., Deventer, H.C. van., Boxtel, A.J.B. van (2012). Controllability and energy performance of the drying process. *Book of Abstracts, 31<sup>st</sup> Benelux Meeting on Systems and Control*, Heijden, the Netherlands, 107.
2. Atuonwu, J.C., Straten, G. van., Deventer, H.C. van., Boxtel, A.J.B. van (2011). On the dynamic operability of adsorption dryers. *Book of Abstracts, 30<sup>th</sup> Benelux Meeting on Systems and Control*, Lommel, Belgium, 92.
3. Atuonwu, J.C., Straten, G. van., Deventer, H.C. van., Boxtel, A.J.B. van (2010). Optimization of the adsorption drying process for energy efficiency and product quality. *Netherlands Process Technology Symposium (NPS 2010)*, Veldhoven, the Netherlands.

## Overview of Completed Training Activities

Course	Graduate School/Institute	Year
<b>Discipline-specific Activities</b>		
Physical Modeling	SENSE	2009
Reaction Kinetics in Food Science	VLAG	2009
Model Predictive Control	EECI – Paris	2009
Design Methods for Control Systems	DISC	2010
NPS 2010 Symposium, the Netherlands	OSPT	2010
IDS 2010 Conference, Germany	DECHEMA	2010
PRES 2011 Conference, Italy	AIDIC	2011
Benelux 2011 Conference, Belgium	DISC	2011
ESCAPE 2012 Conference, UK	IChemE	2012
PSE 2012 Conference, Singapore	NUS	2012
Benelux 2012 Conference, the Netherlands	DISC	2012
<b>General Courses</b>		
Scientific writing	CENTA	2009
VLAG Student Week	VLAG	2009
Effective Behavior in Professional surroundings	WGS	2011
Career Perspectives	WGS	2012
<b>Optional</b>		
Updating Research Proposal	SCO	2009
GPROMS Modeling	PSE – London	2010
Lecturing	ESD & PS	2011
Internal Training in LABVIEW	SCO	2012
Participation in SCO Meetings	SCO	2009 – 2013